THERMAL EFFECTS OF UNDERGROUND CARPARK STRUCTURE A COMPARATIVE STUDY OF UNDERGROUND CAR PARK CONCRETE BUILDINGS IN DUBAI - UNITED ARAB EMIRATES

دراسة التأثير الحراري على التصميم الإنشائي لمبنى مواقف السيارات أسفل الارض في الامارات العربية المتحدة

by

OLA OMAR

Dissertation submitted in fulfilment

of the requirements for the degree of

MSc STRUCTURAL ENGINEERING

at

The British University in Dubai

February 2020

DECLARATION

I warrant that the content of this research is the direct result of my own work and that any use made in it of published or unpublished copyright material falls within the limits permitted by international copyright conventions.

I understand that a copy of my research will be deposited in the University Library for permanent retention.

I hereby agree that the material mentioned above for which I am author and copyright holder may be copied and distributed by The British University in Dubai for the purposes of research, private study or education and that The British University in Dubai may recover from purchasers the costs incurred in such copying and distribution, where appropriate.

I understand that The British University in Dubai may make a digital copy available in the institutional repository.

I understand that I may apply to the University to retain the right to withhold or to restrict access to my thesis for a period which shall not normally exceed four calendar years from the congregation at which the degree is conferred, the length of the period to be specified in the application, together with the precise reasons for making that application.

Signature of the student

COPYRIGHT AND INFORMATION TO USERS

Abstract

The underground car park buildings considered as an ideal solution for the parking spaces in urban area, and it is more commonly used when the land values are high. So, the main intention to have a durable and economical building along it service life. Particularly these types of buildings are vulnerable to the structural distress related to the restrained volumetric change due to the shrinkage and thermal change during the parking operation, many of the designers and owners avert to have a separation in the underground structure, especially when the water table is very high. But Ignoring the thermal effects with the structure stiffness characteristic can lead to premature deterioration and cracking because of the generated forces.

This study intent to show the importance of thermal analysis of underground car park concrete building, by conduct a comparative study between three models of three floors underground car park building, with length around 147 m and width around 38 m.

The first model analyzed the building for the gravity load only, and the second model analyzed the building for gravity load and thermal change in absence of expansion joints, while the third model analyzed for the gravity load and thermal change in present of expansion joints.

The analysis of the three models shows how the thermal change of underground parking structure affect members internal forces with unexpected amount, which at some extend are not considered in the design by most of the designers. The forces produced from the strain forces (thermal changes) must be well studied as it is different than the forces produced from the gravity loads, generally these forces affect the connection design, specially between the walls and slabs or columns and slabs, and how this effect is reduced by the presence of expansion joints.

The comparisons between the three models covered the comparisons of structural elements forces (columns, Slabs and the walls), in addition to the comparison of the whole building maximum drifts and maximum displacements, and the columns shear forces which produced specially on the columns in both directions due to the horizontal movements of the slabs due to the thermal changes. These forces and results record in a manifest the maximum in the model analyzed for thermal stresses with full building length (without expansion joints), while the presence of the expansion joint results in structure with less slab stresses, wall stresses, building drift and displacement, member forces which in-turn lesser section properties and reinforcement hence leading to economical design of the structure.

أثر التغير في الحرارة على مبنى المواقف تحت الارض

تعتبر مواقف السيارات تحت الأرض حلاً مثاليًا لمواقف السيارات في المناطق الحضرية ، وهي أكثر شيوعًا عندما تكون قيم الأراضي مرتفعة. لذلك ، فإن الهدف الرئيسي هو الحصول على مبنى دائم واقتصادي .

هذا النوع من المباني على وجه الخصوص عرضة للاجهادات الناتجة من التغير الحجمي المقيد للخرسانة بسبب الانكماش والتغير الحراري أثناء تشغيل المواقف ، حيث يتجنب العديد من المصممين والمالكين استخدام الفواصل الانشائية في الطوابق اسفل الأرض، خاصةً عندما تكون المياه الجوفية مرتفعة. لكن تجاهل التأثيرات الحرارية مع صلابة العناصر الانشائية كالجدران , يمكن أن يؤدي إلى تدهور مبكر وتشقق العناصر بسبب القوى المتولدة.

تهدف هذه الدراسة إلى إظهار أهمية التحليل الحراري للمبنى الخرساني لموقف السيارات تحت الأرض ، من خلال إجراء دراسة مقارنة بين ثلاثة نماذج لمبنى مواقف سيارات تحت الارض ، بطول حوالي 147 م وعرضها حوالي 38 متر.

في النموذج الأول يتم تحليل المبنى لحمل الجاذبية فقط ، اما في النموذج الثاني فتم تحليل المبنى لحمل الجاذبية والتغير الحراري في غياب الفواصل التمدد ، في حين تم تحليل النموذج الثالث لحمل الجاذبية والتغيير الحراري مع وجود الفواصل الانشاية .

توضح المقارنة بين النماذج الثلاثة كيف تكون التأثيرات الحرارية على العناصر الانشائية ، والتي في بعض الاحيان لا يتم أخذها بعين الاعتبار خلال التصميم مثل قوى القص على الاعمدة ، وكيف يتم تقليل هذا التأثير من خلال وجود فواصل التمدد.

Dedication

To my Father soul.....

To my beloved Daughters NOUR and ZAINA .....

To my love MOHAMMAD .....

To my Mother for her endless love and prays .....

To my brothers and sisters .....

OLA RATEB OMAR

Feb -2020

Acknowledgement

I would like to thank Almighty **ALLAH** for giving me the strength and the determination to do my research. His continuous grace and mercy were with me throughout my life and ever more during the tenure of my research.

Now, I would like to thank deeply and appreciate my Daughters **NOUR,** for all the time taken from her, and my baby **ZAINA**.

I owe thanks to a very special person, my husband, **MOHAMMAD** for his continued and unfailing love, support and understanding during my pursuit that made the completion of thesis possible. You were always around at times I thought that it is impossible to continue, you helped me to keep things in perspective.

I owe thanks to my Mother for her continuous prays, and to my brothers Mohammad and Ahmad, and my sisters Rasha , Rola and Tasneem , and to my brother Ahmad Shawqi , for his support .

I express my deep and sincere gratitude to my supervisor Dr. Abid Abu Tair for his support and patience.

Table of content

List of Tables

List of Figueres

List of Symbols

a	The solar absorption coefficient	
G	The global radiation striking the surface.	
I_b	The direct radiation	
I_d	The diffuse radiation	
I_t	The global radiation	
Ig	The radiation that is reflected from another surface	
σ	The Stefan-Boltzmann constant = 5.67x 10^{-6}	$W/(m^2 \cdot K^4)$
T_s	The absolute temperature (K) of the surface	°C
T_{air}	The temperature in the surrounding air	°C
h_c	The convection heat transfer coefficient	$W/(m^2 \cdot °C)$
T_{max}	The maximum daily temperature	°C
T_{min}	The minimum daily temperature	°C
h_{max}	The time corresponding to the maximum temperature	
h_{min}	The time corresponding to the minimum temperature	
ρ	The density	(Kg/m^3)
c	The specific heat capacity	$(J/ (kg \cdot {}^oC))$
$\partial T/\partial t$	The change in temperature over time	$({}^oC/s)$
k	The thermal conductivity of concrete	$(W/ (m \cdot {}^oC))$
q_v	The heat generated in the concrete due to hydration, which considered negligible for hardened concrete	
q	The rate of heat transferred per unit area	(W/m^2)
q_s	The fluxed heat from incident solar radiation,	
q_c	The convection heat transfer	
q_r	The long-wave radiation heat transfer.	
T_i	The temperature at layer *i*	
h_i	The height of layer *i*	
h	The section thickness	
*x*i	The layer *I* center coordinates from the gravity point.	
α	The thermal expansion coefficient	
T(y)	The temperature at coordinate y	
E_c	The concrete modulus of elasticity	
A	The cross-sectional area	
I	The moment of inertia for the section	
ψ_x	The curvature in the horizontal direction	
ψ_y	The curvature in the vertical direction	
I_y	The moment of inertia around the y-axis	
I_x	The moment of inertia around the x-axis.	
T_m	The mean Temperature during The normal construction season.	

T_w	The Temperature exceeded the average only 1% of the time during the summer months	
T_c	The Temperature equal or exceeded the average 99 % of the time during the winter months	
e_{th}	The coefficient of thermal expansion	
L	The length subjected to the thermal change.	
ΔT	The temperature change	
M_{th}	The movement factor	
r	ratio of stiffness factor of column to stiffness factor of beam	
Kc	Column stiffness factor	in^3
Kb	beam stiffness factor	in^3
h	column height	in
L	beam length	in
Ic	moment of inertia of the column	in^4
Ib	moment of inertia of the beam	in^4
Mf	fixed-end moment at The beam-column joint due to gravity Load	
ζ	The interpolation coefficient	
s	The average crack spacing	
$\Delta\varepsilon s$	The change in steel strain	
$\Delta\sigma s$	The steel stress	
M22	First order factored moment at a section about 2-axis	N.mm
M33	First order factored moment at a section about 3-axis	N.mm
$\varkappa$	Curvature	

1. INTRODUCTION

All the concrete structures are affected by the different types of action during its life time, one of these loads are the restrained forces due to the thermal change, the effect of the thermal change lead to concrete deterioration , it is produced once the tensile strength of the concrete is exceeded by this load and cause the appearance of the cracks in concrete sections .

Underground parking structures generally are not designed for the thermal effects, as the common belief that the underground structures are not affected by the thermal changes, where as the intention of most designers to eliminate the presence of an expansion joints, to avoid the problems caused by the presence of the expansion joints due to the execution, earth pressures and the high water table, and affect the building durability, but the facts that these type of buildings are vulnerable to the structural distress related to the restrained volumetric change due to the shrinkage and thermal change during the parking operation, so Ignoring the thermal effects with the structure stiffness characteristic can lead to premature deterioration and cracking because of the generated forces.

1.1 Research Significance

A concrete structure under sequential thermal changes exhibits a volume change that will affect the entire structure due to the induced self-staining forces, subsequently affecting the structural system performance and durability. The thermal properties of concrete are complicated compared with most materials, since it is composite material with different constituent properties and extreme variability of the strain and resulting forces, and

"*At present, there is no universally accepted design approach to accommodate building movements caused by temperature or moisture changes*" **(ACI 224.3R-8).**

Underground car-parking structures should be designed to accommodate the volume change considering the affecting of temperature change of unheated structures along with the higher relative humidity, ground water, the lateral load from surrounding soil and the loads from the structure above, and this study highlights the importance of considering the volume change with the design criteria of such structures.

The study highlights the rationale reason to consider the thermal effects on the underground structures starting from the thermal effect specification, the concrete properties the main elements of the volume changes and how it is affecting the buildings.

The comparative study of the models of the same building showing how the applying of the thermal change on the building will affect the building elements forces , which might be missed during the design or at the best it is recovered by the minimum reinforcement defined by code for the thermal effects.

1.2 Research Objective

The main objective of this study to improve that the volume change restrained forces are affecting the underground car park structure, even though it is not exposed directly to the sun heating through the below Themes of discussion:

1- Define the volume change restrained forces resultant from the shrinkage, creep and the thermal changing.

2- Referring to the criteria of estimating the distance between building expansion joints (**The national academy of science (1974)**) Figure 4.4, with zero temperature change the minimum distance between the expansion joints equal to 182.88 m, which modified after use the factors defined by **ACI 224.3R-8** to be around 49.5 m.

3- When the standard **ACI 224.3R-8** defined the distance between the expansion joints, the shrinkage and temperature reinforcement required defined on **ACI 318-11** based on this distance , once this distance is exceeded, the required steel need to be revisited to maintain the tension forces produced in the elements due to the volume changes.

4- The importunacy of the induced straining action from the volumetric change affect, shown clearly in the load combinations in **ACI318-14**, as important as the dead load.

5- Cracks induced from thermal change created in the connections between the slabs and retaining walls, since the walls are very stiff and restrict the slab to freely moving under the temperature variation, in addition to the distribution of the walls in the plane, which have great factor for increasing the cracks,

6- The support conditions of columns and the foundation (hinge or fixed) have major effect on the slab horizontal movement due to the temperature change.

7- The model shall be studied with two steps , first study the structure in service conditions without cracks and without reduce the sections stiffness to design the slab without crack

in the service condition, and in the ultimate condition the section will be reduced to design the columns and walls .

1.3 Research Overview

In order to achieve the objectives of the research, the important points of the literature review have been addressed in the chapters as necessity to solidify the knowledge about the thermal effects on the concrete structures.

Chapter 2 of this study defines the concept of the thermal stress, by define the thermal effects and how it is affected the concrete structures. In addition to the thermal action concept and type of thermal stresses.

While chapter 3 shows the concrete properties, to assert the complicity for the thermal effects including the material components and the property affecting the thermal stresses.

Chapter 4 define the concept of the volume change forces and the thermal differences effects, in addition to the expansion joints criteria, then the crack induced by the volume change and the deflection induced by the temperature.

Chapter 5 described the analytical models used in the analysis using ETABS software including the criteria considered during the study in relation to the objectives of the research, while chapter 6 showing the comparative results of the three models.

2. THERMAL STRESSES

Thermal stresses in concrete defined as the stresses resulting when the concrete structure is exposed to a temperature change in the presence of constraints. Thermal stresses are also defined as a mechanical stresses produced from the internal forces caused by a constraint part attempting to expand or contract.

The type of the constraints produced the thermal stresses in concrete are two types, the internal constrains, within the concrete material itself because the concrete compositions expands or contracts by different amounts, however it should remain continuous. And the external constrains that prevent the entire structural system to expand and contract when the temperature changes are occurred.

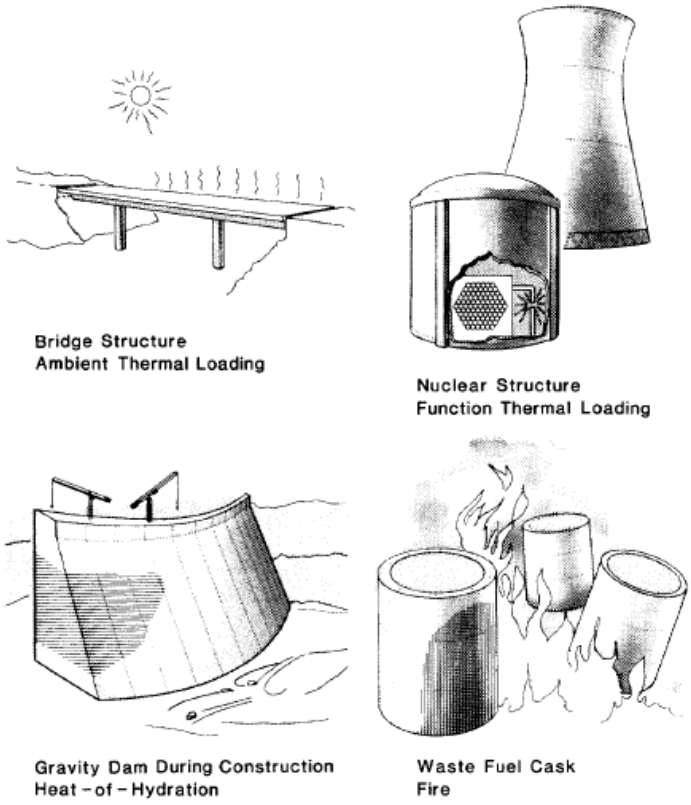

Figure 2.1 Type of the thermal loads on different concrete structures (Vecchio 1987)

2.1 Thermal input factors

All the concrete structures are affected by the temperature in different ways Figure 2.1, showing types of thermal loads affecting the concrete structures, the stresses caused by the temperature can be either by the Eigen stresses produced from the nonlinear temperature distribution or by preventing the structure form the moving due to the constraint.
Below the description of the thermal loads factors that affect the structure and lead to the thermal stresses.

2.1.1 Solar Radiation

The solar radiation defined as energy emitted from the sun (**Larsson, Svensson 2013**) There are three types of light in the solar radiation, ultraviolet, visible and infra-red light. that differ by the short wavelength.
The earth is struck by an average amount of solar radiation between 1320 to 1410 W/m² per year on surface called Solar constant, which depends on the distance between the earth and the sun (**Larson 2012**), as the radiation flux decreases with distance.
The global or total radiation is the solar radiation reaches the earth's surface after losing some parts that's absorbed or scattered during the light passing through the atmosphere, the amount of reached radiation depends on the humidity, how far the radiation has gone through the atmosphere, the air particles and the amount of clouds.
The total amount of total radiation absorbed by a surface close to the ground is calculated by Equation 2.1 as:

$$q_s = a \cdot G \qquad \text{(Eq. 2.1)}$$

where;

a is the solar absorption coefficient
G is the global radiation striking the surface.

Kirchhoff's law expresses the relation between the heat radiation with longer wave and the surface absorptivity which equal to the emissivity of the material, and this relation is not valid when the surface is sunlit, as the sunlight is of shorter wavelengths. Then the absorptivity is depending on the texture and the color of the surface. The dark surface is absorbing more solar radiation than a light surface, hence, the concrete solar absorptivity is varying over time as the color is changing when it became older. many studies had been performed to measure the concrete solar absorptivity by measuring the solar reflectivity of the surface, because for the

opaque material the solar reflectivity is equal to the solar radiation which is not absorbed, where the solar absorption factor of concrete found between 0.3 to 0.6 (**Larson 2012**) .

In defining the incident global solar radiation I_h on a horizontal surface, Equation. 2.2 shall be used as

$$G = I_h = I_b + I_d \quad \text{(Eq. 2.2)}$$

As, I_b is the direct radiation, and I_d is the diffuse radiation.

Also, an inclined surface is affected by reflected radiation either from the ground or the other buildings.

The global radiation I_t on a inclined surface is calculated as

$$G = I_t = I_b + I_d + I_g \quad \text{(Eq. 2.3)}$$

The total radiation I_t which reaches the ground is either direct radiation I_b, diffuse radiation I_d or radiation that is reflected from another surface I_g.

The main reasons that the direct radiation reaches the earth surface without being disturbed and its intensity are:

- Latitude and altitude
- Time of the day and year
- Inclination of the surface

The diffuse radiation I_d, refers to all radiation that scattered with atmosphere, during the way between the sun and earth surface.

The magnitude of the total global radiation varies between seasons, for the clear day in summer it will be around 1000 W/m², while in cloudy day between 300-400 W/m².

When the solar radiation strikes the earth surface without being scattered by the atmosphere, it is called a Direct solar radiation which is defined as beam radiation and expressed by;

$$I_b = I_{b,n} \cos(\theta) \quad \text{(Eq. 2.4)}$$

$I_{b,n}$ is the direct radiation on a surface perpendicular to the sun, and θ is the angle between the beam radiation on the surface and normal to the surface, as shows in Figure 2.2.

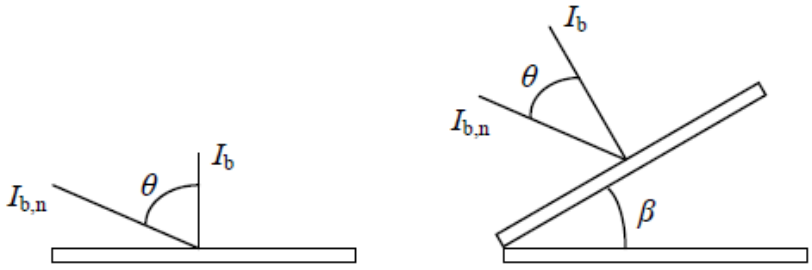

*Figure 2.2 The incidence angle θ for a horizontal and a tilted surface with the slope β (**Larson 2012**)*

2.1.2 Long wave heat radiation

The heat transfer by solar radiation to the concrete surface consists of short wavelengths radiation. when the materials have a temperature above the absolute zero, it will release a long length wave radiations. The transfer of the energy by radiation will not require a medium material like the thermal conductivity.

The emissive power defined as the rate of thermal energy release per unit area, which is originated from the radiation emitted by a surface, and the upper limit is called a blackbody radiation.

$$E_b = \sigma T_s^4 \quad \text{(Eq. 2.5)}$$

Where;

σ is the Stefan-Boltzmann constant = 5.67x 10^{-8} W/(m²·K⁴)

T_s is the absolute temperature (K) of the surface.

The heat flux releases by a real surface, E_s, is the blackbody radiation which reduced by the emissivity ε.

$$E_s = \varepsilon \sigma T_s^4 \quad \text{(Eq. 2.6)}$$

However, along wave radiation also received by a surface like the building, or cloud and the resulting energy absorbed or released to the surrounding calculated by

$$q_r = E_s - E_{sur} = \varepsilon \sigma (T_s^4 - T_{sur}^4) \quad \text{(Eq. 2.7)}$$

2.1.3 Convection

Heat convection transfer occurs between the concrete and the in-motion fluid, when both have different temperatures, it is described as the energy transfer occurring within the air because of the molecular motion. In this paper the convective heat transfer is regarded by the air, and concrete.

The velocity of the fluid close to the bonding surface between the concrete and the air is very low, so convection is dominated by diffusion, and going away from the surface the moving velocity may increase and the bulk fluid motion contribution will increase accordingly this action called advection.

Air temperature is the most important factor for convection, where the temperature variation described through sinusoidal cycles for 1 day and 1 year. The first cycle is 24-hour cycle, where

the temperature variation will be for the day and night, the second cycle is for 365 days cycle, where it described the temperature variation between the winter and summer.

These cycles will affect the concrete structure, due to its low thermal conductivity, by produce an internal stresses based on the structure geometry and size.

The flows are described by two convection classifications, either the flow forced by external source it called Forced convection, or the free or natural convection which caused by the forces produced from the temperature variation in the air. The convection can be either purely free, or purely forced or combination of the two. The convection heat model expressed in equation 2.8,

$$q_c = h_c\,(T_s - T_{air}) \qquad \text{(Eq. 2.8)}$$

Where; T_s is the surface temperature, T_{air} is the temperature in the surrounding air and h_c is the convection heat transfer coefficient in W/(m² · °C).

The convection coefficient depends on the boundary layers' conditions, which are influenced by the roughness of the surface and the nature of the fluid motion. the heat transfer coefficient for walls and slabs can be approximated by

$$h_c = 6 + 4V \qquad \text{if V} \leq 5 \text{ m/s} \qquad \text{(Eq. 2.9a)}$$

$$h_c = 7.4V^{0.78} \qquad \text{if V} > 5 \text{ m/s} \qquad \text{(Eq. 2.9b)}$$

The rate of convection heat between the concrete and the surrounding environment governed by the air temperature, so the air temperature must be measured with regular intervals, and the approximate air temperature during a day expressed by.

$$\text{T} = A \sin\left(2\pi\ \frac{t-b_1}{2b_2}\right) + B \qquad \text{(Eq. 2.10)}$$

$$\text{T} = A \sin\left(2\pi\ \frac{t+12-b_1-b_2}{2(24-b_2)}\right) + B$$

(Eq. 2.11)

Where;

$$\text{A} = \frac{T_{max} - T_{min}}{2} \qquad \text{(Eq. 2.12)}$$

$$\text{B} = \frac{T_{max} + T_{min}}{2} \qquad \text{(Eq. 2.13)}$$

$$b_1 = \frac{h_{max} + h_{min}}{2}$$

(Eq. 2.14)

$$b_2 = h_{max} - h_{min} \quad \text{(Eq. 2.15)}$$

Where;

T_{max} is the maximum daily temperature.

T_{min} is the minimum daily temperature.

h_{max} is the time corresponding to the maximum temperature.

h_{min} is the time corresponding to the minimum temperature.

When the temperature rises during the day Eq. 2.10 to be used, while if the temperature drops during the night Eq. 2.11 to be used.

2.2 Heat Transfer

The temperature gradient is the uneven temperature distribution of the concrete cross section due to the cooling and heating takes place in the concrete structure surface at its serviceability state, this difference on the temperature will produce an energy which will flow to the structure part with low temperature. Fourier's law described the three- dimensional heat flow as

$$\rho c \frac{\partial T}{\partial t} = k \left(\frac{\partial^2 T}{\partial x^2} + \frac{\partial^2 T}{\partial y^2} + \frac{\partial^2 T}{\partial z^2} \right) + q_v \quad \text{(Eq. 2.16)}$$

Where;

ρ	the density	(Kg/m³).
c	the specific heat capacity	(J/ (kg·ºC))
$\partial T / \partial t$	the change in temperature over time	(ºC/s)
k	the thermal conductivity of concrete	(W/ (m·ºC))
$\partial^2 T/\partial x^2$, $\partial^2 T/\partial y^2$, $\partial^2 T/\partial x^2$	the second spatial derivatives (thermal conductions) of temperature in the x, y and z directions	
q_v	the heat generated in the concrete due to hydration, which considered negligible for hardened concrete.	

The equation 2.16 material properties shall be described in chapter 3, and the boundary conditions of the three-dimensional heat transfer are described as follow,

$$k \left(\frac{\partial T}{\partial x} n_x + \frac{\partial T}{\partial y} n_y + \frac{\partial T}{\partial z} n_z \right) - q = 0 \quad \text{(Eq. 2.17)}$$

Where;

q	the rate of heat transferred per unit area (W/m²).
n_y, n_y, n_z	the direction cosines of the unit outward vector normal to the boundary surface.
$\partial T/\partial x$, $\partial T/\partial y$, $\partial T/\partial z$	the temperature change in the x, y and z directions.

The total heat transferred rate from the surrounding environment to the concrete consists of three different parts;

$$q = q_s + q_c + q_r \quad \text{(Eq. 2.18)}$$

where;

q_s is the fluxed heat from incident solar radiation,

q_c is the convection heat transfer

q_r is the long-wave radiation heat transfer.

The main factors governed the convection are the wind speed and the air temperature, while the long-wave heat radiation is dominated by the temperature of the surroundings as well as the cloud-cover.

2.3Thermal stress and action

The movements produced in the concrete structure from the spatial and time variation in temperatures these movements occur either transverse or longitudinal movement due to the non-uniformity of the temperature distribution.

The average temperature T_{avg} and linear temperature differential ΔT components, can be calculated for a one-dimensional distribution as (**Larsson, Oskar 2013**)

$$T_{avg} = \frac{1}{h} \sum T_i h_i \quad \text{(Eq. 2.19)}$$

$$\Delta T = \frac{12}{h^2} \sum (T_i x_i h_i) \quad \text{(Eq. 2.20)}$$

where;

T_i is the temperature at layer *i*,

h_i is the height of layer *i*,

h is the section thickness,

x_i is the layer *I* center coordinates from the gravity point.

The difference between the actual temperature, linear temperature differential and the average temperature for each point at the section defined as the non- linear temperature T_{nl}.

$$T_{nl} = T - T_{avg} - \Delta T \quad \text{(Eq. 2.21)}$$

The average temperature calculated by the integral over the cross section T_{avg} .

$$T_{avg} = \frac{1}{A} \int_A T(x, y) dA \quad \text{(Eq. 2.22)}$$

Where $T_{(x,y)}$ is the temperature of the section dA , and A cross section, and the linear temperature ΔT will be calculated over the section in two directions by :

$$\Delta T_x = \frac{12}{b^2} \int_A T\,(x,y)xdA \qquad \text{(Eq.2.23)}$$

$$\Delta T_y = \frac{12}{h^2} \int_A T\,(x,y)ydA \qquad \text{(Eq.2.24)}$$

Where;

ΔT_x the temperature gradient in the horizontal direction,

ΔT_y the temperature gradient in the vertical direction,

b,h the cross section dimensions (width and height),

x,y the center of gravity coordinates (horizontal and vertical).

To simplify the average temperature and linear differential over any section, a one-dimensional distribution approach can be used. the difference between the actual temperature and the combined average temperature and linear differential is the principle of nonlinear component in two-dimensional calculation, which is considered same in the one-dimensional cases.

The temperature variations in concrete lead to the volume change of the material, either expand or contract depends on the temperature change types, in addition to the uneven temperature distribution , the movements become different on the structure parts, as the Average temperature component can produce a longitudinal movement along the elements, while the linear temperature differential will affect the element cross section. A significant contribution of the structure movements will be produced from the non-linear temperature, if the structure does not have any restraint, so it will induced a self-equilibrating stresses only, while if the structure has restrained by the support or connections, so the continuous stresses will be induced with cracking the section.

2.4 Type of Thermal Stresses

The thermal stress produced in the concrete structure due to the restrained thermal expansion can be identified by two components, primary thermal stresses and continuity thermal stresses, figure 2.3.

The Primary thermal stresses were induced in the section when the non-linear thermal gradient exists, the self-equilibrating in cross section, the primary stress a rise from the incompatibility between the two requirements of remaining the plane of the cross section and the section expand with amount proportional to the local temperature raised figure 2.3a (**Vecchio 1987**).

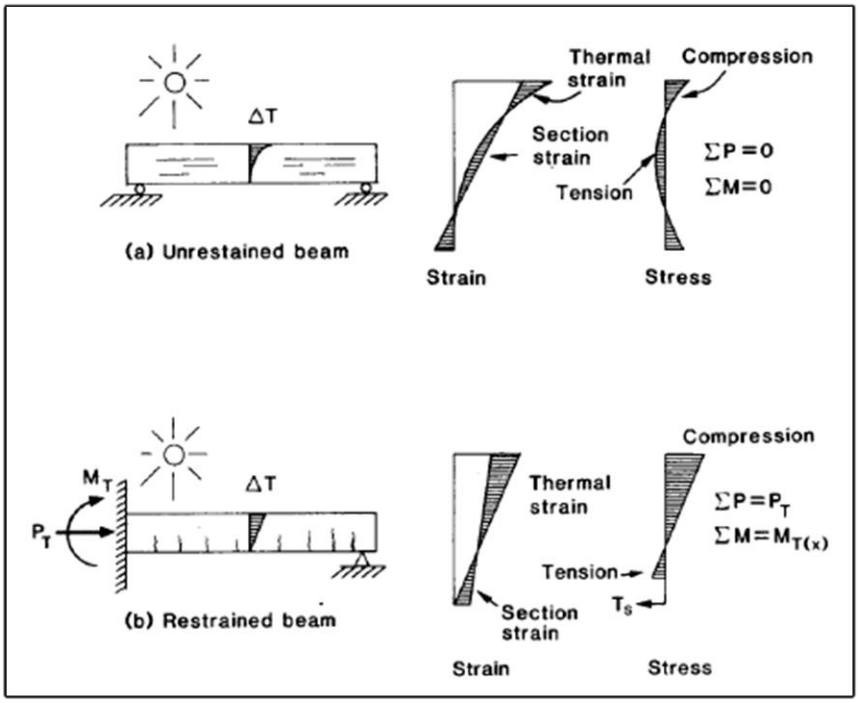

*Figure 2.3 Type of Thermal Stresses: (a) Primary Thermal stress, (b) Continuity Thermal stress (**Vecchio 1987**)*

The continuity thermal stresses are the induced stresses in indeterminate structures, where it results from the deflections and rotation of restrained element subjected to thermal deformations, figure 2.3b.

From the two types in most instances, the continuity thermal stresses play a major role for the structure distress, as it is greater than the primary stresses.

The thermal stresses tend to be self-relieving in the concrete structure, unlike the other mechanical stresses, and the amount of this stress governed by the stiffness of the members, if the stiffness of the section is reduced , the induced thermal bending moments will be relaxed.

So, the analysis of the thermal stress cannot be estimated by a conventional method of structural analysis, many studies had been carried out for the thermal stresses in the concrete structure.
The first establishment of the analytical method to determine the primary thermal stress in concrete cross section by **Priestley 1981**, where he developed a general uncracked section subjected to arbitrary vertical temperature distribution, and ended up with excellent agreement between the theory and the results of box girder bridge. **Thurston 1978**, also agreed with his study, even with the modification in theory he made of. Generally, all the methods held for the primary mothed sounds the same, and considering the assumption of the tensile strength, temperature distribution and any other behavioral characteristics.
On other hands, various methods have been conducted for the continuity thermal stresses, in general, these methods attempt to understand the section reduced stiffness affect in the determining of moment distribution for the thermally loaded section. hence this way is very complicated, as many of the section properties shall be affected after the cracking, the prediction of the continuity thermal stresses compromised by many factors such, concrete tension ,mechanical load interactions , nonuniformly cracked member , tension stiffening effects after cracking and nonlinear thermal gradients .

2.5 Thermal behavior in the longitudinal direction

The thermal behavior in the longitudinal direction of the building highly depends on the support conditions, in the simply supported structure the internal restrained due to the section geometry will affecting the structure, while the external restraint will not affect , figure 2.4 shows how the simply supported beam affected by the internal restrained when it subjected to non-uniform temperature distribution.

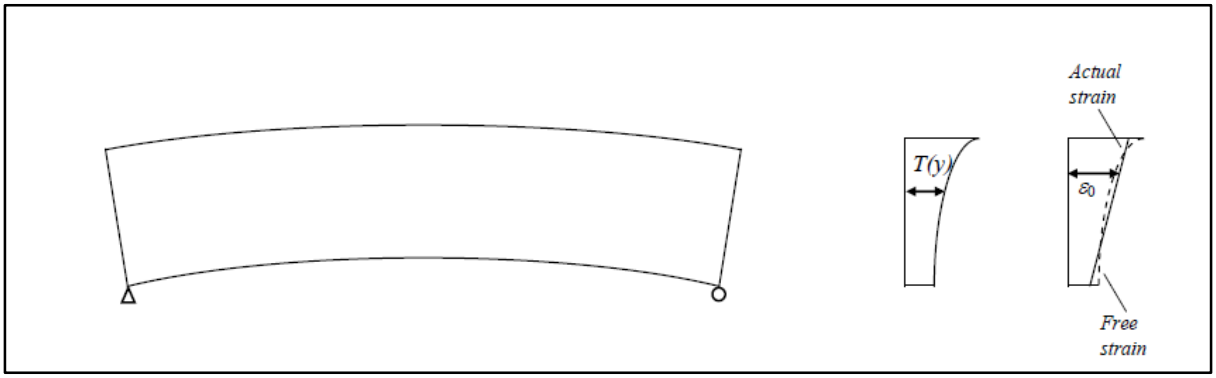

*Figure 2.4 Simply supported beam subjected to a thermal load (**Oskar 2012**)*

The free strain in the longitudinal direction of the structure **(Elbadry and Ghali (1995)**), such a beam at any location with coordinate y (Equ. 2.25) and the stress required to restrain the free strain (Equ. 2.26)

$$\varepsilon_f = \alpha T(y) \quad \text{(Eq.2.25)}$$

$$\sigma_{restraint} = -E\ \alpha T(y) \quad \text{(Eq.2.26)}$$

Where;

α is the thermal expansion coefficient

$T_{(y)}$ is the temperature at coordinate y

E is the concrete modulus of elasticity

The Moment and axial force produced from the restraint stress are:

$$N = \int \sigma_{restraint}\ dA \quad \text{(Eq.2.27)}$$

$$M = \int \sigma_{restraint}\, y dA \quad \text{(Eq.2.28)}$$

When the opposite forces are equal the artificial restraint is removed. the resulting strain at any location shall be:

$$\varepsilon = \varepsilon_0 + \psi y \quad \text{(Eq.2.29)}$$

Where, ϵ_0 is the axial strain at the center and Ψ is the curvature, and it is produced as follow:

$$\varepsilon_0 = -\frac{N}{EA} \quad \text{(Eq.2.30)}$$

$$\psi = -\frac{M}{EI} \quad \text{(Eq.2.31)}$$

When the Equs. 2.26 – 2.28 are substituted into Equ. 2.30 and Equ 2.31; the statically determinate structure axial strain and curvature can be obtained by;

$$\varepsilon_0 = \frac{\alpha}{A}\int T(y) b dy \quad \text{(Eq.2.32)}$$

$$\psi = \frac{\alpha}{I}\int T(y) b y dy \quad \text{(Eq.2.33)}$$

Where;

A is the cross-sectional area

I is the moment of inertia for the section

The stress distribution in the concrete section induced from the difference between the free strain and the actual strain expressed by:

$$\sigma = E\ (\varepsilon_0 + \psi y - \alpha T(y)) \quad \text{(Eq.2.34)}$$

The resultant of these stresses must be zero, so these stresses are self-equilibrating. When the different temperature components are defined, the axial strain and curvature simplified as;

$$\varepsilon_0 = \frac{\alpha}{A}(T_{avg} - T_0) \quad \text{(Eq.2.35)}$$

$$\psi = \frac{\alpha}{I}\,\Delta T \qquad \text{(Eq.2.36)}$$

where;

T_0 is the initial temperature of the structure

T_{avg} is the average temperature

ΔT is the linear temperature differential.

Fig. 2.5 shows force method analysis for statically indeterminate reactions and bending moments due to temperature rise in a three-span continuous beam. For given span arrangement, the amount of resultant forces such as the continuity moments and reactions are related directly to the flexural rigidity (EI) and the statically determinate curvature (ψ) of the beam members, the internal forces analysis due to the temperature variation is affected by the calculation of the section axial strain (ε_0) and curvature (Ψ), and it is remain same when $T_{(y)}$ either linear or nonlinear over the cross section . (**Elbadry and Ghali 1995**).

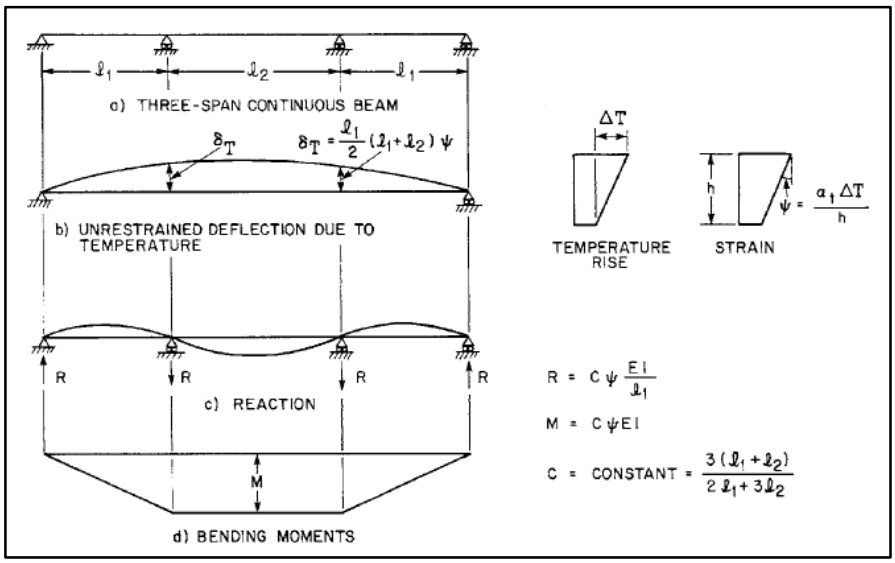

*Figure 2.5 Statically indeterminate reactions and bending moments due to temperature rise in three-span continuous beam. (**Elbadry and Ghali 1995**)*

As shown in Fig 2.5 the continuity reactions and moments shall be;

$$R = \frac{c\alpha E}{l}\int T(y)bydy \qquad \text{(Eq.2.37)}$$

$$M = c\alpha E \int T(y)bydy \qquad \text{(Eq.2.38)}$$

Where;

c is the multiplier constant according to Figure 2.5

l is the span length.

The axial strain and curvatures for the cross section that the temperature distribution is affecting the horizontal and vertical directions are;

$$\varepsilon_0 = \frac{\alpha}{A}\iint T(x,y)dxdy \quad \text{(Eq.2.39)}$$

$$\psi_x = \frac{\alpha}{I_x}\iint T(x,y)ydxdy \quad \text{(Eq.2.40)}$$

$$\psi_y = \frac{\alpha}{I_y}\iint T(x,y)xdxdy \quad \text{(Eq.2.41)}$$

Where;

ψ_x is the curvature in the horizontal direction

ψ_y is the curvature in the vertical direction

I_x is the moment of inertia around the y-axis

I_y is the moment of inertia around the x-axis.

So, the self-equilibrating stresses induced in the cross-section is,

$$\sigma_{x,y} = E\,(\varepsilon_0 + \psi_x y + \psi_y x - \alpha T(x,y)) \quad \text{(Eq.2.42)}$$

3. FUNDAMENTALS OF CONCRETE

The concrete compositions result in the complexity of concrete as a material with the effect of the thermal forces. This chapter covers the concrete properties that affect the thermal stress produced from the temperature change, the concrete behavior subjected to the restraint forces, the principle of heat transfer in concrete, the Effect of thermal stresses on the behavior of concrete structures and the design consideration of thermal stresses during the design of the concrete structure as per the code requirements.

The chapter also illustrate the cracking behavior in concrete resulted from the thermal affect.

3.1 Background

Concrete known as the most manufactured man-made material commonly used on earth and has been used for a long time. As some buildings related to few hundred years B.C have been found made of material similar to concrete (**Larsson, Svensson 2013**).

Concrete is a very important material used extensively in different type of engineering construction covering the buildings, bridges, roads, and dams, from the structural applications, to pavers, Krebs, pipes, and drains. it considered as an attractive materials for the wide range of structural applications, Because of its distinctive properties of efficiency, strength, stiffness, and the economy. Nevertheless, the nature of concrete for the volume change due to the shrinkage, creep and the thermal loading is recognized as a major disadvantages of concrete, furthermore the low tensile strength, with restrained conditions leads to the thermal cracking of concrete structures, which compromise the structure integrity , aesthetics and the durability.

The Concrete is a composition of cementitious materials, aggregate (coarse and fine) and water mixed with designed percentage, in addition to the admixture/ additives to obtain specific properties of the concrete mixed as used. Hence, the concrete properties are controlled by the properties of the hydrated cement paste and the aggregate. Figure 3.1 shows the basic concrete composition.

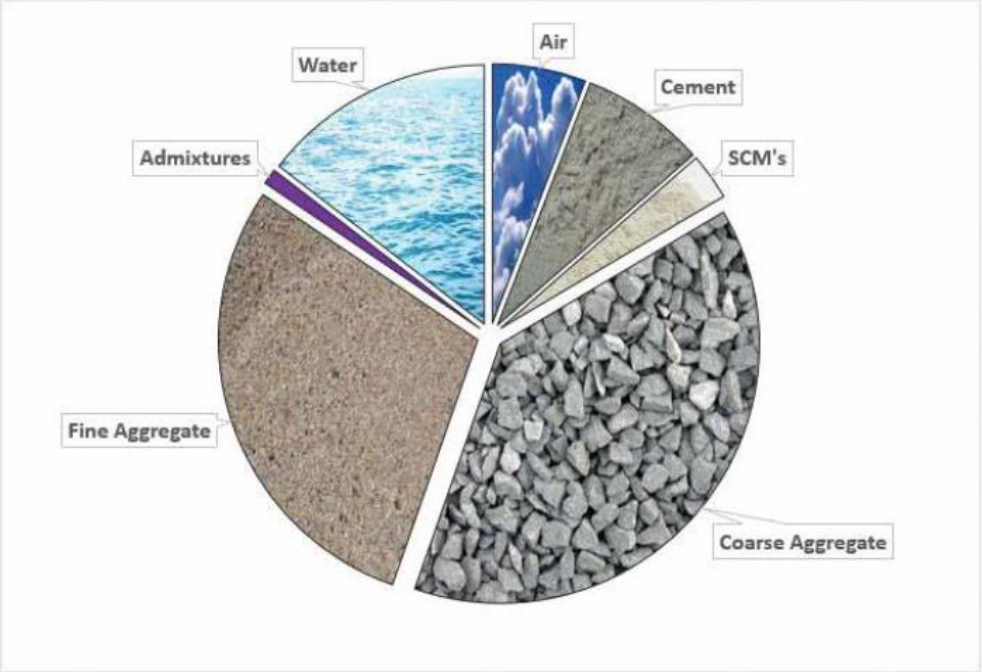

*Figure 3.1 Typical concrete composition (*https://www.constructioncanada.net*)*

3.2 Concrete Components

3.2.1 Cement

The primary component of concrete is cement that works as a hydraulic bonding agent. Cements distinguish by its ability to harden in reaction with water. The cements come from burning the limestone in special ovens together with clay.

The Portland cements constituting compounds are: Tricalcium Aluminate (C_3A), Dicalcium Silicate (C_2S), Tricalcium Silicate (C_3S) and Tetracalcium Aluminoferrite (C_4AF).

The most important components considered as it responsible for the cement strength Amongst these components are the ones containing the silicates (C_3S & C_2S).

3.2.2 Water

The water/ cement ratio, showing the relation between the amount of water to the cement amount during the mix design, which affect the fresh concrete placement at site.

3.2.3 Aggregate

The main part of the concrete volume is the aggregate with all rock material size (course and fine aggregates), the concrete mix with all grain size that covers as much empty spacing between the large aggregates will have high strength.

3.2.4 Admixtures

The admixtures used in the concrete mixed design to modify the properties of the concrete mix, for example the accelerator and the retarders for harden the concrete rabidly or slowly.

3.3 Concrete Thermal properties

The thermal effects stresses in concrete structure are depends on the concrete thermal properties, as it is an important aspect for the concrete durability, since the Concrete is a material used in different climatic regions for all kinds of structures.

Reference to equation (2.16) which specified the thermal diffusivity of concrete material, this section describe the concrete properties governed the thermal diffusivity of concrete, in addition to table 3.1 which presents the concrete thermal properties based on different studies and for different concrete aggregate types (**ACI 207.2R-5**).

3.3.1 Density

The concrete density is an important term of the thermal diffusivity of the concrete in equation (2.16), which dominated by the density of the main concrete components, since the Aggregate is the most concrete components mass, due to that the concrete density is affected mostly by the aggregate, the common value of the concrete density is $\rho = 2400$ *Kg/m³*. (***Larsson 2012***).

3.3.2 Thermal Conductivity

Thermal conductivity defined as the ability of the material to conduct the heat, the thermal conductivity of the concrete depends on the density and the concrete compositions, in addition to the moisture content of the concrete.

The thermal conductivity found be varied between 1.6 and 3.6 W/ (Kg. ºC) depending on the aggregate and moisture content, as well as the temperature level.

If the thermal conductivity is low, it means larger temperature differentials, once it is underestimated, the temperature differentials may be exaggerated (***Larsson 2012***).

3.3.3 Thermal Expansion Coefficient

Thermal expansion coefficient describes the tendency of the concrete to volume change in response to the thermal change, simply it is related to the concrete thermal deformation, which depends on changing the energy particles at different temperatures. however, the thermal expansion is complicated in concrete as a high internal stresses produced due to the differential expansion of its components.

The parameters affect this coefficient include the aggregates, cement type, water-cement ratio, the mixing design, temperature, the concrete age and the relative humidity

The thermal coefficient of concrete governed by the thermal coefficient of the cement paste which varies between about 11 x 10^{-6} and 20 x 10^{-6} per °C and the aggregate thermal coefficient even the cement coefficient is higher than the thermal coefficient of the Aggregate in addition to the elastic properties and the volumetric proportions of the cement and aggregate, furthermore the aggregate restrains the cement paste thermal deformation, so the thermal stress will be produced .

The concrete thermal coefficient is positive always with average value of 7 x 10^{-6} to 14 x 10^{-6} per °C based on the aggregate type used.

3.3.4 Young's Modulus

Young's modulus of concrete is an important mechanical property developed rapidly at early stage and related to the concrete stiffness; therefore, it is very important to understand its development at early age to determine the restrained stress at that stage.

The development of Young's modulus of early age is more rapid than the compressive strength of the concrete, but afterward the compressive strength development becomes more rapid (**SON 2017**).

3.3.5 Compressive strength

The concrete compressive strength considered as the most intensively studied property, as it is very important in the structural analysis of the elements. The concrete considered as a material

with high compressive strength, which mean if the internal stresses produced in compression terms which will be utilized by the compressive properties of concrete.

The concrete is defined as non- linear material when a significant uniaxial compression applied, Figure 3.2. shows the concrete behavior under the compression, the ultimate strain Up to 30 % the concrete behaves linearly, between the 70 − 90 % of the ultimate strain the tangent modulus is gradually decreased to reach the peak value of the stress-strain curve, the material starts to soften, where the strain is increased even though the stress is reduced. The softening will continue until reaches the ultimate strain.

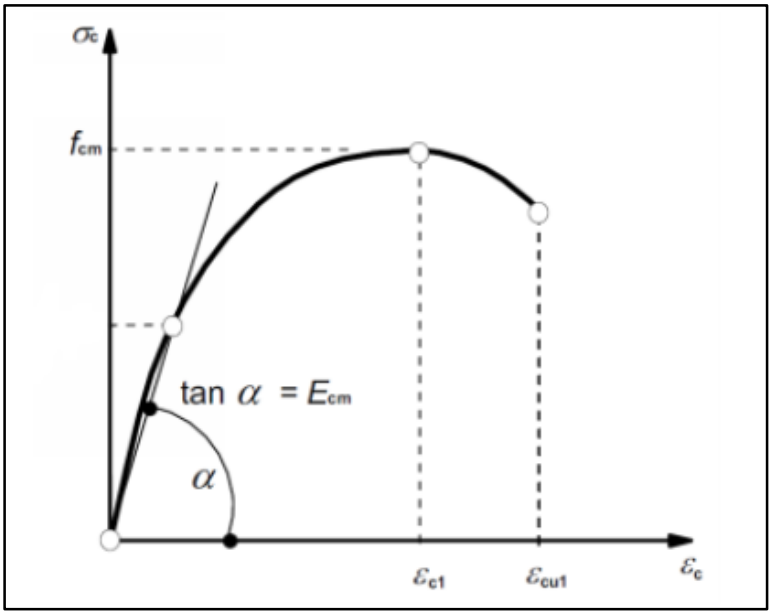

*Figure 3.2 Concrete subjected to uniaxial compression (**Brattstrom & Hagman 2017**)*

3.3.6 Tensile Strength

The tensile strength defined as the ability of the concrete to withstand the Tensile Stress without failure, it is assumed that in conventional reinforced concrete design concrete has no tensile strength. But when the internal thermal volume change tensile stress produced, the tensile strength will be the most important consideration for prediction of cracks initiation, as when the tensile strength reached the concrete strength, the crack will be produced, need to be identified in the time to the critical volume change. Normally the compressive strength of the concrete is specified, it is desirable to relate the tensile strength to the compressive strength.

Aggregate type and properties affect the concrete tensile strength, it has found that when the concrete made from crushed coarse aggregate will withstand without cracking in the drop of temperature compared with the rounded coarse aggregate concrete.

The concrete age at which it attains the compressive strength will affect the relationship between the tensile and compressive strength, as the older the concrete, the larger tensile strength for specific compressive strength (**ACI 207.2R-5**).

Splitting test is the most used test for determining the concrete tensile strength, in this test the specimen failure forced to be occur within the narrow band of it rather than occur the weakest section, when the failure occurs in the center section, the strength will be indicated as higher than the actual strength.

The actual tensile strength is not specified exactly, (**Kwak & Filippou 1990**) highlight that the tensile strength of concrete generally less than 20 % of the compressive strength. While (**ACI 207.2R-5**) assumed conservatively the tensile strength for normal weight concrete to be 6.7 psi (/1.8 MPa). For the dried concrete surface, the tensile strength shall be lower than this value to predict cracks initiating at the surface.

The critical volume change controlled by the strength of concrete, which may occur either in the first 7 days of placing the concrete or in the first 3 to 6 months depending on the peak temperature. The critical volume change will occur in the first week, if the initial cooling potential cracks exceed the seasonal temperature drop potential cracks.

Structure	Coarse aggregate type	Temperature,	Coefficient of expansion		Thermal conductivity	Specific heat,	Density	Diffusivity
		°F (°C)	millionths/°F (millionths/°C)		Btu/ft·h·°F (kJ/m·h·°C)	Btu/lb·°F (kJ/kg·°C)	lb/ft³ (kg/m3³)	ft²/h ([m²/h] × 10–³)
			1-1/4 in. (37.5 mm) max.	4-1/2 in. (114 mm) max.				
Hoover	Limestone and granite	50 (10)	5.3 (9.5)	4.8 (8.6)	1.70 (10.6)	0.212 (0.887)	156.0 (2500)	0.051 (4.7)
		100 (38)			1.67 (10.4)	0.225 (0.941)		0.047 (4.4)
		150 (66)			1.65 (10.3)	0.251 (1.050)		0.042 (3.9)
Grand Coulee	Basalt	50 (10)	4.4 (7.9)	4.6 (8.3)	1.08 (6.74)	0.219 (0.916)	158.1 (2534)	0.031 (2.9)
		100 (38)			1.08 (6.74)	0.231 (0.967)		0.029 (2.7)
		150 (66)			1.09 (6.78)	0.257 (1.075)		0.027 (2.5)
Friant	Quartzite granite and rhyolite	50 (10)	____	____	1.23 (7.66)	0.216 (0.904)	153.8 (2465)	0.037 (3.4)
		100 (38)			1.23 (7.66)	0.230 (0.962)		0.035 (3.2)
		150 (66)			1.24 (7.70)	0.243 (1.017)		0.033 (3.1)
Shasta	Andesite and slate	50 (10)	____	4.8 (8.6)	1.32 (8.20)	0.219 (0.916)	156.6 (2510)	0.039 (3.6)
		100 (38)			1.31 (8.16)	0.233 (0.975)		0.036 (3.3)
		150 (66)			1.31 (8.16)	0.247 (1.033)		0.034 (3.2)
Angostura	Limestone	50 (10)	4.0 (7.2)	____	1.49 (9.29)	0.221 (0.925)	151.2 (2423)	0.045 (4.2)
		100 (38)			1.48 (9.20)	0.237 (0.992)		0.041 (3.8)
		150 (66)			1.46 (9.08)	0.252 (1.054)		0.038 (3.5)
Kortes	Granite gabbros and quartz	50 (10)	5.2 (9.4)	4.5 (8.1)	1.61 (10.0)	0.208 (0.870)	151.8 (2433)	0.050 (4.6)
		100 (38)			1.60 (9.96)	0.221 (0.925)		0.047 (4.4)
		150 (66)			1.59 (9.87)	0.234 (0.979)		0.044 (4.1)
Hungry Horse	Sandstone	50 (10)	6.2 (9.7)	5.7 (9.4)	1.72 (10.1)	0.217 (0.895)	150.1 (2425)	0.053 (4.6)
		100 (38)			1.71 (10.0)	0.232 (0.937)		0.049 (4.4)
		150 (66)			1.69 (9.87)	0.247 (0.983)		0.046 (4.2)
Monticello	Sandstone, metasiltsone, quartzite, and rhyolite	50 (10)	5.2 (9.4)	____	1.57 (9.79)	0.225 (0.941)	151.3 (2454)	0.046 (4.3)
		100 (38)			1.55 (9.67)	0.237 (0.992)		0.043 (4.0)
		150 (66)			1.53 (9.54)	0.250 (1.046)		0.040 (3.7)
Anchor	Andesite, latite, and limestone	50 (10)	5.6 (10.1)	4.5 (8.1)	1.14 (7.11)	0.227 (0.950)	149.0 (2388)	0.034 (3.2)
		100 (38)			1.14 (7.11)	0.242 (1.013)		0.032 (3.0)
		150 (66)			1.15 (7.15)	0.258 (1.079)		0.030 (2.8)
Glen Canyon	Limestone, chert, and sandstone	50 (10)	____	____	2.13 (13.3)	0.217 (0.908)	150.2 (2407)	0.065 (6.0)
		100 (38)			2.05 (12.8)	0.232 (0.971)		0.059 (5.5)
		150 (66)			1.97 (12.3)	0.247 (1.033)		0.053 (4.9)
Flaming Gorge	Limestone and sandstone	50 (10)	____	____	1.78 (11.1)	0.221 (0.925)	150.4 (2411)	0.054 (5.0)
		100 (38)			1.75 (10.9)	0.234 (0.979)		0.050 (4.6)
		150 (66)			1.73 (10.8)	0.248 (1.038)		0.046 (4.3)
Yellowtail	Limestone and andesite	50 (10)	____	4.3 (7.7)	1.55 (9.67)	0.226 (0.946)	152.5 (2444)	0.045 (4.2)
		100 (38)			1.52 (9.46)	0.239 (1.000)		0.042 (3.9)
		150 (66)			1.48 (9.20)	0.252 (1.054)		0.039 (3.6)
Dworshak	Granite gneiss	100 (38)	____	5.5 (9.9)	1.35 (8.41)	0.220 (0.920)	154 (2467)	0.040 (3.9)
Ilha Solteira	Quartzite and basalt	100 (38)	____	6.9 (12.5)	1.73 (10.8)	0.220 (0.920)	159 (2552)	0.049 (4.6)
Itaipu	Basalt	101 (38)	____	4.3 (7.8)	1.06 (6.61)	0.233 (0.975)	158 (2537)	0.029 (2.7)
Theodore Roosevelt Modification	Granite	50 (10)	4.3 (7.7)	____	1.71 (10.7)	0.234 (0.979)	148.7 (2380)	0.049 (4.6)
		100 (38)			1.73 (10.9)	0.248 (1.037)		0.047 (4.4)
		150 (66)			1.70 (10.6)	0.260 (1.088)		0.044 (4.1)
Olivenhain	Granodiorite	100 (38)	5.4 (9.7)		0.94 (5.86)	0.210 (0.880)	147.4 (2360)	0.030 (2.8)

*Table 3.1 Concrete Thermal properties (**ACI 207.2R-5**)*

3.4 Restraint Actions

Any concrete element is restrained to some degree, where the restrained can comes from the support or the element itself. The concrete elements restraints are either internal or external restraint, the internal restraint comes from the component of the elements and the stress produced internally like the bonds between the concrete and steel reinforcement, while the external restraint produced from external surface contact (***ACI 318 -14***).

The structure freedom to move described in term of the degree of restraint R, where it represents the structure extent to be prevented from the moving in relation to the structure supports. Equation 3.1. so, it is obtained in a range of $0 \leq R \leq 1$, on other word, without restraint, partial restraint, or fur full restraint.

$$R = 1 - \frac{\varepsilon_{obtained}}{\varepsilon_{free}} \qquad \text{(Eq. 3.1)}$$

3.4.1 Internal restraint

The internal restraint produced when the different component within the structural elements subjected to different strains, so conducting that one-part restraining and affect another, by increasing the internal stressed which will lead to crack the concrete section.

For example, the bond between the concrete and steel reinforcement will restraint the concrete to shrink, so the total strain of the concrete section will be affected by this internal restraint, as shows in Figure 3.3.

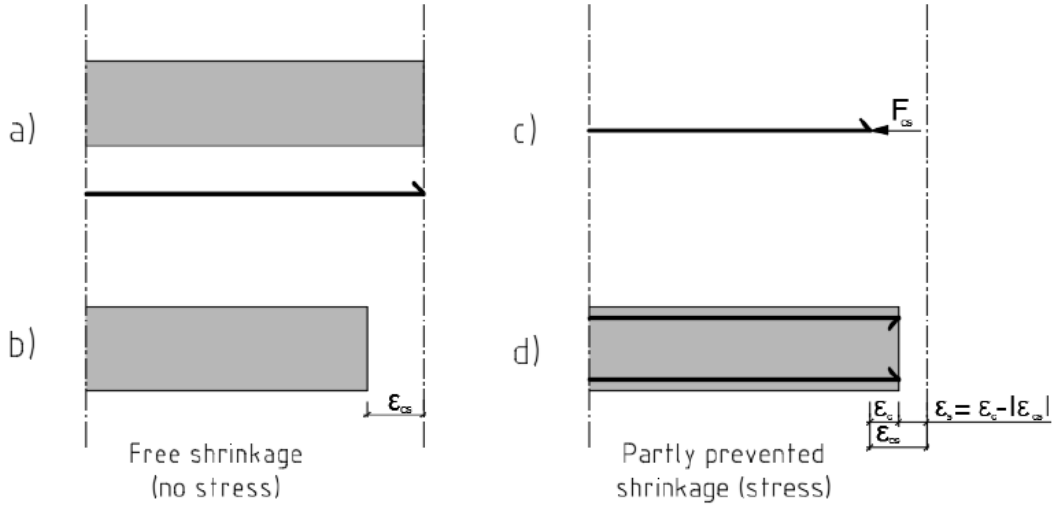

*Figure 3.3 Reinforced prismatic member subjected to shrinkage, (**Brattstrom & Hagman 2017**)*

- Sketch (a) shows both the concrete and the steel subjected to zero loading.

- Sketch (b) assuming no interaction between the concrete and the steel, so concrete shrink freely with no stress εcs.
- Sketch (c) the reinforcement and concrete are coupled together, as the steel compressed to the same concrete length by the force Fcs.
- Sketch (d) the affected force removed, so the reinforcement elongates subsequently the concrete will be subjected to a tensile force of the same magnitude as Fcs.

Assuming the full bond between the concrete and reinforcement, the concrete stress calculated can be calculate as Equation 3.2

$$\sigma c = \frac{F_{Cs}}{A_{I,ef}} \qquad \text{where } AI,ef = Ac,ef + (\alpha e - 1) \qquad \text{(Eq. 3.2)}$$

So, the steel stress could be calculated by, Equation 3.3

$$\sigma s = \frac{-F_{Cs}}{A_S} + \alpha e \cdot \sigma c \qquad \text{(Eq. 3.3)}$$

Assuming the strain of concrete and reinforcement to be equal, so the reinforced concrete member strain can be expressed by Equation 3.4

$$\varepsilon cm = \frac{1}{E_S}\left(\frac{-F_{Cs}}{A_S} + \alpha e \cdot \sigma c\right) \qquad \text{(Eq. 3.4)}$$

The restraint force due to imposed strain may also be expressed by Equation 3.5

$$\sigma_s \cdot A_s = \sigma_c \cdot A_c,ef \qquad \text{(Eq.3.5)}$$

3.4.2 External restraint

The external restraint produced from the restraining action caused by the connections or the support of the concrete elements, the degree of restraints depends on the stiffness of the member and the stiffness of the connected members as well as the boundary conditions type, Figure 3.4 illustrates different type of the restraint degree over the concrete member height, where the this members is restrained with fixed edge at the bottom. Figure 3.4 shows the restraint percentage decreases over the member height.

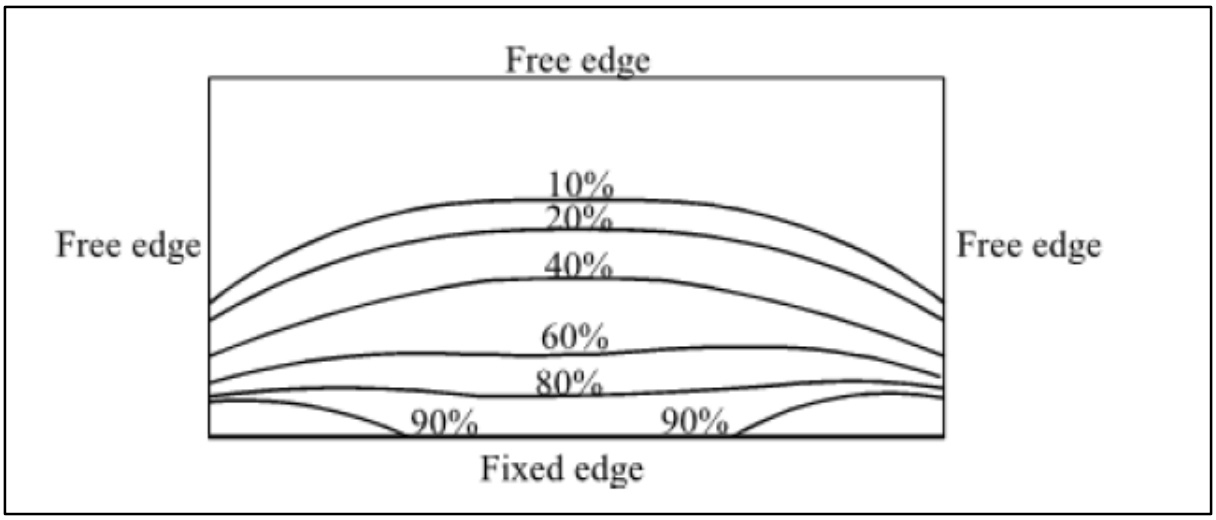

*Figure 3.4 The restraint degree in a concrete member restrained along its base, (**Brattstrom & Hagman 2017**)*

The difference of the restraint degree is highly dependent on the ratio between the length and the height of the element section, the L/H-ratio (**Brattstrom & Hagman 2017**). The relation is Inverse relationship, when the ratio is high, the variation is less over the height of the mid-section. The compression stress will be produced at the top of the member when the L/H ratio is very low (**ACI 318 14**).

The concrete member will be allowed for the volume change. only if one or two edges are restraint, however the situation will be worse when the two opposite sides are restraint and further measures must be considered.

3.4.3 Strains Types

The Strains have two types depending on the stress dependency, stress-dependent and stress-independent strain. The stress-dependent strain comes as a result of the external load causing the deformation.

Base on Hook's law, the initial elastic stain can be obtained followed by the strain (time dependent strain) due to creep, since the creep is considered as proportional elastic strain, Hence the total strain determined by Equation 3.6

$$\varepsilon = \varepsilon el\ (1 + \varphi) \qquad \text{(Eq. 3.6)}$$

While the stress-independent strain is caused by any factors that do not introduce stresses, such as volume changes due to thermal action (Equation 3.7) or shrinkage (Equation 3.8) .

When the concrete member is free to move, the stresses will not be raised within the members. If there is some degree of restraint, so the stresses will occur and thus introduce stress dependent strains (**Brattstrom & Hagman 2017**).

The cracks in the concrete section are always produced once the stresses become sufficiently large in the sense that the tensile strength of the concrete is exceeded, cracking will occur (**Brattstrom & Hagman 2017**).

$$\varepsilon T = \Delta T \cdot \alpha T \quad \text{(Eq. 3.7)}$$

$$\varepsilon cs(t) = \varepsilon cd\,(t) + \varepsilon ca\,(t) \quad \text{(Eq. 3.8)}$$

3.5 Effect of thermal forces on the behavior of concrete structures

In the examination of the statically indeterminate structure loaded with temperature gradient, at the time of crack initiation, it was found that the cracked reinforced section force deformation at the force-controlled stress case is differs from the corresponding force deformation-controlled stress case, refer Figure 3.5 (***Jokela***) .

If the stress case is force controlled case, like the external load increasing continually, the related moments curvature will also increase. accordingly, the steel percentage will be increased. But if the state of stress controlled by the deformation, like the stress results from the restrained deformations, the moments produced in the cracked cross section will be reduced directly at the preliminary stage of crack initiation, since the concrete tension is not acting. So, the determination of the moment produced by the thermal stress should consider for concrete cracked section.

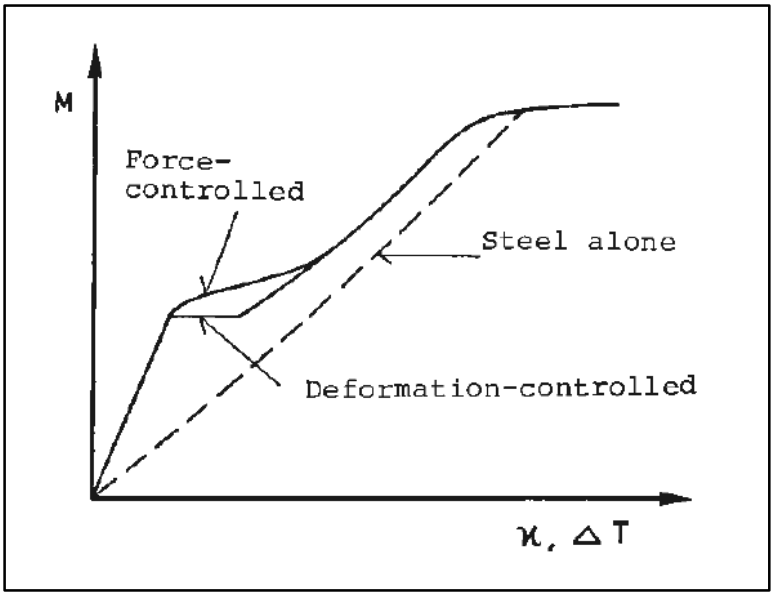

*Figure 3.5 Difference between curves M – ϰ or M - ΔT in principle under force-controlled and deformation-controlled load of the concrete section (**Jokela**)*

The relationship M - ϰ is examined before and after the formation of the section first crack. The thermal stresses and the corresponding deformation can be assumed are the same prior and

immediately after the first cracking, where in the reinforcement elongation in both cases will be large (Figure 3.6).

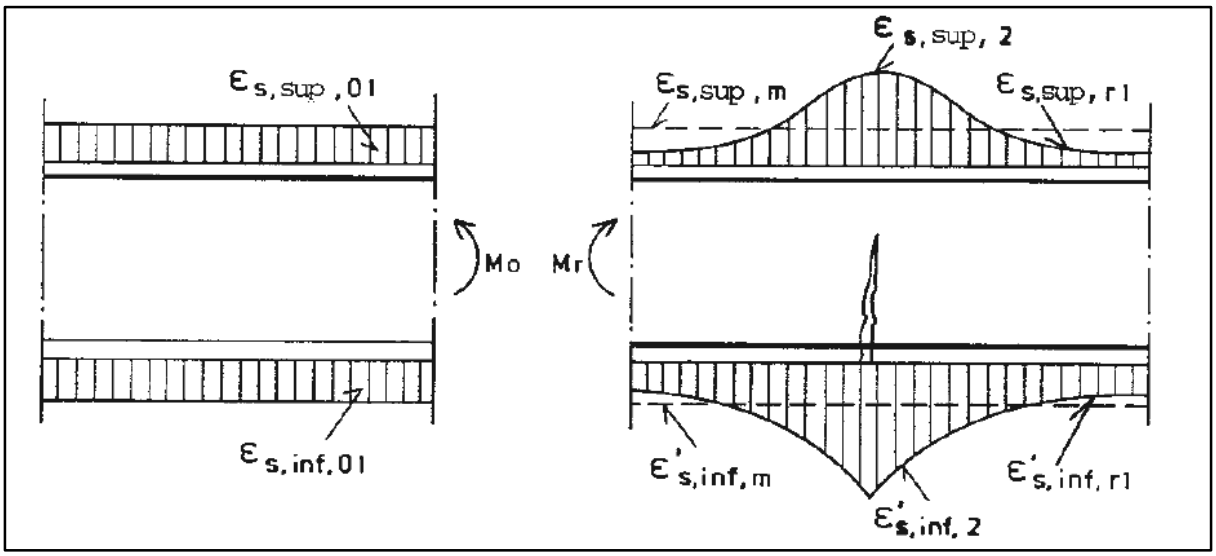

Figure 3.6 Steel Reinforcement Elongations prior to and subsequent to crack formation

When the structure is subject to the thermal stresses, the next crack cannot be formed until the thermal stresses is increased to the point that coincide with the cracking force , this mechanism will be repeated until the full cracks pattern of the whole structure become stable, then only the restraint force exceed the cracking forces. Figure 3.7

The cracking performance considered as the ideal case, since the concrete tensile strength must be constant, but this not the case, as the cracking moments are slightly increase after the crack formation.

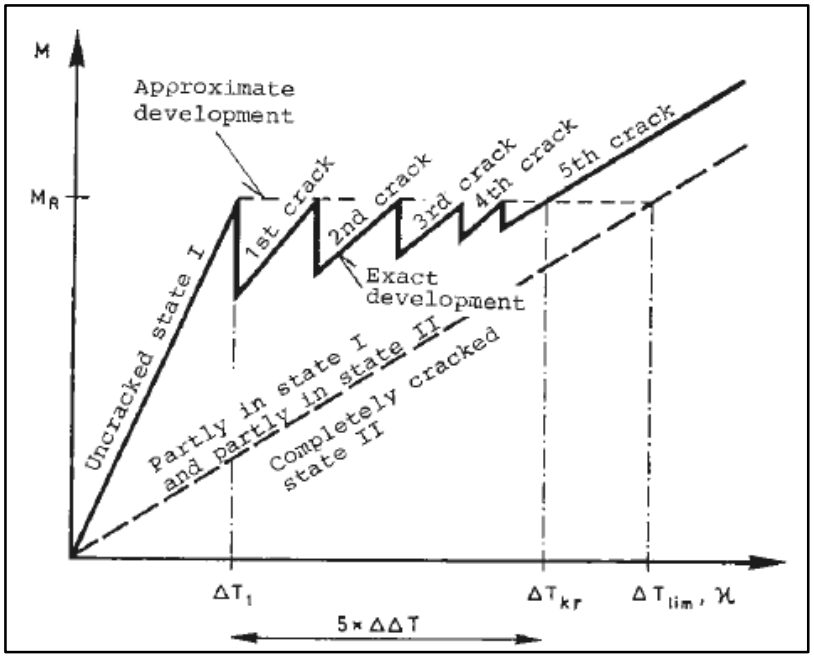

Figure 3.7 M – ϰ curve in the state of restraint stress

4. VOLUME CHANGE

A concrete structure under sequential thermal changes exhibits a volume change that will affect the entire structure due to the induced self-staining forces, subsequently affecting the structural system performance and durability.

The thermal properties of concrete considered as complicated comparing with most materials, since it is composite material with different constituent properties and extreme variability of the strain and resulting forces.

The forces and deformations result from the volume changes of a restraints structure, can greatly affect the structural strength, the connections between the elements and the service load behavior, on other hands, the prediction of these forces is not possible comparing with the prediction of the gravity load stress. Subsequently the assumption of conservative volume change forces during the design stage leads to impractical and costly design.

Underground carparking structures should be designed to accommodate the volume change considering the affecting of temperature change of unheated structures along with the higher relative humidity, ground water, the lateral load from surrounding soil and the loads from the structure above.

This chapter covers the review of the related research of the volume change due to the temperature change of the concrete structures mainly the underground car parks and the effect on the structural durability by go through the crack mitigation. the review is extended to cover the needed of the expansion joints in the underground car park and the effect of the volume change on the structural elements stiffnesses. the following reviews covers the historical researches, adopted method, conclusions and the recommendations of each subject related to the thermal effect of underground car park structure.

4.1 Background

Volume change is defined as a dimensional change in structural elements due to forces relate to shrinkage, Creep, elastic shortening, differential settlements and temperature change in the Concrete structure, the restrained stress resulted from the volume change considered as a major problem of the parking structure durability (**ACI 362.1R-97**), the change due to the creep and shrinkage will shorten the structural element , and it is result will be culminated in the first 3

years of the structure age as shown in table 4.1 (**ACI 435R-95)**, while the temperature variation affect will be either shorten or elongate the structural element, and for the whole structure

lifetime, even these self-staining mechanism are slow , but are powerful enough to induced cracks and affecting the elements stiffness.

Creep, shrinkage ratios	Concrete Age					
	2 months	3 months	6 months	1 year	2 years	> 5 years
C_t / C_U	0.48	0.56	0.68	0.77	0.84	1.00
$(\varepsilon_{sh})_t / (\varepsilon_{sh})_u$ -M.C.	0.46	0.60	0.77	0.88	0.94	1.00
$(\varepsilon_{sh})_t / (\varepsilon_{sh})_u$ -S.C.	0.36	0.49	0.69	0.82	0.91	1.00

M.C. = Moist Cured

S.C. = Steam Cured

*Table 4.1_ Creep and shrinkage ratios from age 60 days to the indicated concrete age (**ACI 435R-95**)*

ACI 224.4R-13 contribute the volume change factors on typical slab Table 4.2, which shows within the first year of the project most of the slab shortening comes from the concrete shrinkage.

Volume change factor	Percentage contribution of total shortening
Shrinkage	70
Creep	12
Temperature	18
Total	100

*Table 4.2_Contributions to slab shortening (**ACI 224.4R-13**)*

The difference between the volume change effects and other loads effects (gravity, wind…etc.), that the substantial Forces created from the restrained movements is a self-staining force , these deformations and forces have important effect on the service load behavior ,the connections between the attached elements and the strength of the elements. (**ACI 362.1R-97 , Elbadry and Ghali 1995**). The volume change restraint will cause different stress from the gravity loads which related directly to the building length, for example the columns in the moment resistance frame will have moments , shears and deflection , while the beams and slabs will have a tension stresses , the magnitude of these stress must be considered in the design stage (**PCI Design Handbook 2010**). However, there is no specific design approach accepted universally to accommodate the building movement caused by the temperature change , but most of the

studies consensus on the importance of considering the induced forces from the volume change in the design, **ACI 362.1R-97** adopted a clear notification to consider the volume change of the below grade parking structure because of the great chance of the problems due to the ground water and higher relative humidity, the lateral load from the above structure and the

surrounded soil , as well as the temperature changes , especially when the underground parking structure extended partially above the grade or the slab exposed to the direct sun. **ACI 224.3R-8** and (**Pfeiffer & Darwin 1987**) agreed about the main variables influence the volume change in the reinforced concrete structure, that includes The reinforcement percentage , The footing restrains, Structural geometry, Insulation, cooling and heating provision , Magnitude of intermediate cracks, Material properties (Aggregate, cement, mix proportion and admixture) and the Construction sequence and curing procedure.

ACI 318-14 does not differentiate the forces effects from volume change and gravity loads, however **ACI 318-14** requires a realistic assessment of the effect of volume change forces specially in the structure element deflection, while (**PCI Design handbook 2010)** is the first research provides a procedure to estimate the volume change forces in the prestressed - precast structures since 1977 (**Klein and Lindenberg 2009**), depending on determining the strains induced from volume change (shrinkage, creeps and thermal change including daily and seasonally changes) movements and forces from **ACI 209R-924** equations, then developed a reasonable criteria of reducing the stains to base a prediction of volume change movements called equivalent shortening, shrinkage and creep equivalent shortening comes from reducing the computed creep and shrinkage strains by factor of 4.0, and the temperature effects strains reduced by 1.5. (**Klein and Lindenberg 2009**) summarize the PCI procedure for evaluating the Volume change movements and forces as follow:

1. Determine the maximum seasonal temperature change.
2. Determine the annual average ambient relative humidity.
3. Determine the volume-change strains caused by creep and shrinkage as influenced by the following:
    - concrete type (normal weight or lightweight)
    - curing conditions
    - age at erection
    - volume-to-surface ratio
    - relative humidity
    - concrete strength and level of prestress
4. Determine the design temperature strain.
5. Evaluate the need for and location of expansion joints.
6. Determine the expansion-joint width and movement.

7. Estimate equivalent volume-change strains (reduced by K factors) for analyzing volume change forces.
8. Estimate fixity of column bases.
9. Calculate volume-change-restraint forces based on frame analysis or approximate methods.
10. Proportion members based on calculated forces.

Design for volume-change forces is quite complicated, due to the extreme variability of concrete strain and the resulting forces. In addition to the shortage of the actual data on volume-change effects concrete buildings. The material properties of concrete, thermal exposure, and structural response increase the challenge to predict volume-change forces with accuracy comparable with the prediction of gravity load forces. treating the volume change forces as an external force can lead to non-reasonable design decisions. This complication comes from the effect of the volume changes forces on the elements , and when these forces are factored with gravity loads as per the ACI 318 requirements to determine the needed reinforcement, and when the stress are greater than expected , the designer will going to enhance the section strength by either increasing the section dimensions or add the reinforcement which will not address the exact requirements of the volume change.

In order to estimate the prediction of the volume change forces **(Iqbal 2007)** had confirmed the unpredictability of volume-change response, through conducting an extensive field campaign in several precast concrete parking structures measuring the thermal movements, during **(Iqbal 2007)** study the temperature displacement of 10 parking facilities buildings were monitored, (**Klein and Lindenberg 2009**) figured out the ratio of actual to predicted joint movement from (**Iqbal 2007)** study Figure 4.1, which shows that the reduction factor in the thermal expansion equation can be considered to calculate the free displacements produced by temperature, since the actual movements are generally less than predicted movements**. (Tobias, Hugo, Eduardo and Alejandro 2012)** presented the result of the actual measurements of underground car park thermal movement over a period of 5 years. The obtained results confirmed the behavior of non-air- conditioned parking building that undergo temperature cycles above the monthly average temperature, by indicating the temperature strains derived

from the displacement measurements as a function of temperature. **(Aboumoussa & Iskander 2003)** also agreed that the volume change response is unpredictable, by determining the Apparent coefficients of thermal expansion (ACTE) of the concrete structure (annually, seasonally and daily apparent), through involved the instrumentation and monitoring of an

expansion joint provided in a four-story concrete car park recorded hourly over the period of one year. As ACTE depends on the type and amount of restraint imposed on the concrete structure.

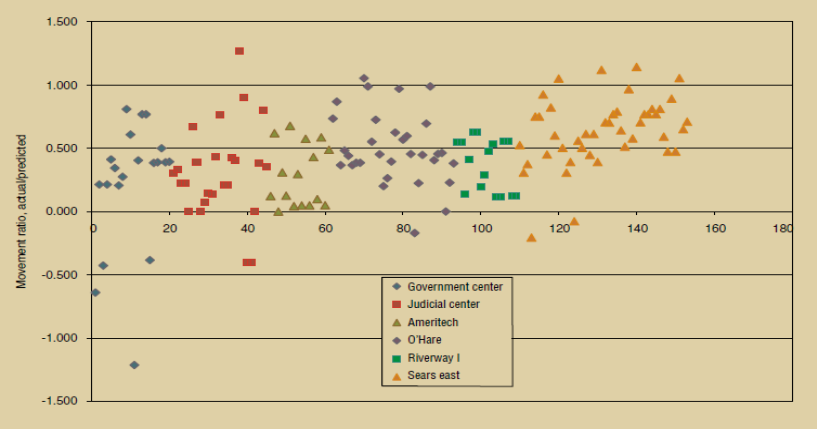

*Figure 4.1 _ This plot of the ratio of actual to predicted joint movements in precast concrete parking structures illustrates the extreme variability of volume-change movement (**Klein and Lindenberg 2009**).*

The volume changes restraint forces affect the various concrete structural system differently, for the cast in place and post tension systems the restraint forces inducing cracks along the length of the element, while it is affecting the members connections in the precast system.

ACI362.1R97 summarize the effects of the volume change restrains on each system in Table 4.3. The detrimental effects of the strains produced by the volume change should be avoided by relieving such restraint through considering a detailing methods to design the members and connections to resist the restraining force. This can be achieved by designing the structure taking in consideration the rigidity of the structure or by flexible connection design, so these developed forces are linked to the stiffness and flexibility of the structure and the connection type.

Volume change can be controlled by allowing the concrete structure to receive the induced strains and react flexibly without affecting the structure integrity or serviceability. (**The national academy of science 1974)** , it is highly recommended to use a fixable or ductile

connections in the Precast structure , while Expansion joints can be used in the Cast in situ and post tension system, in addition to use Pour strip during the construction stage to allow the concrete slab to release the early age volume changes due to the shrinkage and creep.

Volume change type	Structural system		
	Cast-in-place non-prestressed concrete	Precast pretensioned concrete	Cast-in-place post-tensioned concrete
Elastic shortening	**None**	**None**	**Full**
Shrinkage	**Partial[1]**	**Partial[2]**	**Full**
Creep	**None[3]**	**Partial**	**Full**
Temperature change	**Partial[1]**	**Full[4]**	**Full**

Notes: 1) Cracks in the concrete slabs and beams absorb a significant amount of movement, resulting in a reduction of the volume change effects on the structural frame.
2) Shrinkage of topping placed over precast elements primarily results in cracking of the topping over joints in the precast elements.
3) Primary effect of weep is increased deflection of beams or slabs which may affect drainage. Creep can also affect precast and post-tensioned member deflection.
4) May be "partial" under some conditions, with connection details absorbing part of the volume change movement.

*Table 4.3 _Relative effect of volume changes on structural frames (**Table 2.2- ACI 362.1R97**)*

4.2 Shrinkage and creep

The most important concrete properties at the early stage are the shrinkage and creep which come under the category of time- dependent volume change, many studies and research focus on the cracks produced because of these properties at early stage. Shrinkage phenomenon is the reduce of the concrete volume due to curing of the concrete on ambient air after the placing, the volume shall be reduced due to the loses of the internal moisture. And the creep phenomenon is produced when the concrete element subjected to the compressive stress permanently which caused by the own weight of the member as well as the external loads , so at the time of load application an elastic shortening is undergo , and then the creep of concrete material cause a long term shortening . the volume change effect due to shrinkage and creep practically cannot be separated as they occur simultaneously.

The effect of shrinkage and creep is applicable one the vertical elements as the horizontal element such as the columns to relieve the load caused by the slab shortening , so the equivalent volume change used in the design shall be produced by dividing the computed volume change by reduction factor Kl . As shown in table 4.1, the shrinkage and creep rate is decreased over time, as around 30% to 50 % of this volume change occurred in the first 30 days of the structure age.

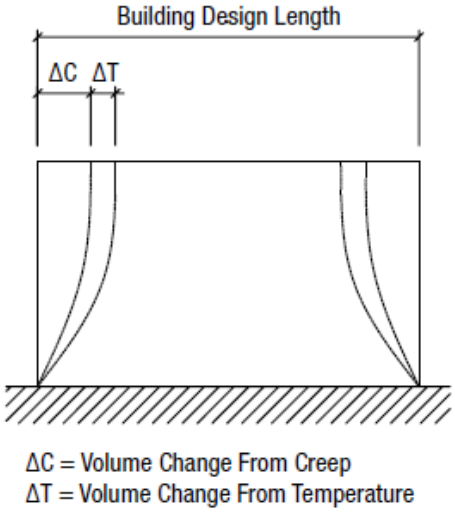

Figure 4.2_ Volume change from creep and temperature.

4.3 Thermal volume change Effects

The accurate determination of the concrete building stresses and movements due to the temperature change is complicated and depends on several factors, include the nature of temperature changes, building geometry, structural systems, moisture conditions, the material properties, and internal thermal control.

The effect of the thermal volume changes during the structure service related to instantaneous and long-term temperature differentials **ACI 224.3R-08,** the long-term effect related to the large temperature difference either daily or seasonally. the effect of thermal dilatation had been studied by **(Borst and. Peeters 1989**) through developing an algorithm and models for analyzing the concrete structure either reinforced or not, for thermal change considering the changes in elastic properties with temperatures change. (**Ahmed 2011**) present analytical investigation of the effect of daily and seasonal temperature change on multi story concrete structure ,and compare the compare the result on each member and highlight the effect of the columns to footing connection effects either fixed or hinge , which agreed with most of the research and the result of **(Sabouni and Sydnaoui 2016**) study which conduct a comparison for different building cases including the column- footing fixing detail.

The deformations resulted from the thermal change affecting the structural building appearance and durability by induced cracks, as well as the strength of the structural elements to withstand the design loads. In concrete structure the element is cracking to resist the induced stresses

comes from restrained the temperature movement by the lateral stability system. Movement induced from the thermal volume change can be estimated simply form multiplying the building length and the design temperature change with average coefficient of thermal expansion CTE of concrete, which is on the order of 0.1% per 100°C (0.055% per 100°F) (**Iskander, Parikh, Aboumoussa 2012**) .This coefficient reflects the aggregate and cement paste average thermal coefficient, since it comprise around 70% of the concrete total volume.(**Iqbal 2007**) in his study conduct to measure the movement produced from the thermal effect in full parking structures, his study shows the value of the thermal coefficient in parking structure is larger than the used in the literature, so the thermal actions study needs to be considered as indirect action and variable. **The national academy of science (1974)** discussed the variation of the expansion coefficient in further detail, and highlight the minimum factors affecting the expansion joint design and location by computing the temperature change required for the design. The temperature variation.

causing the stresses and the displacement is difficult to be estimated as it is not the same temperature during the construction stage and is not the same for all parts of the structures. However, the report provides a guideline to compute the design Temperature change from the formula:

$$\Delta T = (T_W - T_m) \text{ or } (T_m - T_c) \qquad \text{(Eq. 4.1)}$$

Whichever is greater, where,

T_m = The mean Temperature during the normal construction season.

T_w = The Temperature exceeded the average only 1% of the time during the summer months

T_c = The Temperature equal or exceeded the average 99 % of the time during the winter months

The general expression to calculate the thermal movement magnitude either expansion or contraction is

Thermal change is

$$\Delta L = e_{th}\, L \Delta T\, M_{th} \qquad \text{(Eq. 4.2)}$$

Where:

e_{th} is the coefficient of thermal expansion.

L is the length subjected to the thermal change.

ΔT is the temperature change,

M_{th} is the movement factor (equal to 0.0 for a fully restrained element and 1.0 for an unrestrained element).

(Eq. 4.2) shows how the building material used is factor of the magnitude of unrestrained thermal movement, the coefficient of thermal expansion of concrete is not a constant. since concrete is not homogeneous or an elastic material.

The concrete's thermal coefficient (e_{th}) reflects Its elastic modulus E_c which is varies with stress level, and the stress-strain relation is nonlinear. the value of e*th* is estimated for concrete to be 5.5 microstrains /°F (10 microstrains/°C) with an upper bound of 7.5 microstrains/°F (12 microstrains/°C) for unheated structures (**Iqbal 2007**). (**The national academy of science (1974)**, recommended an e*th* value of 6.0 microstrains/°F (11 microstrains/°C) for the expansion joint design. but **PCI Design Handbook 2010** reduced this value by 50% for heated structures and 25% for unheated, considering the thermal lag in the computing design strains for temperature, as well as reducing the temperature strains by a factor of 1.5 when computing thermal shortenings.

The main factors impact the concrete thermal response of completed concrete structure are the aggregate and cement paste thermal coefficient, thermal lag and the Concrete cracking.

- Aggregate, aggregates comprise around 70% of the total concrete volume, so the concrete coefficient value eth is a weighted average of the coefficients of thermal expansion of its component mainly aggregates and cement paste. the coefficient of thermal expansion of concrete has direct relation with the amount of the cement past, and revers relation with the aggregate size.
- Thermal lag is another factor considered to impact the concrete thermal coefficient mainly for closed building and subjected to cooling and heating loads, which was

  quantify by using the National Bureau of Standard (NBS) temperature test cycle. The NBS cycle simulates a 60 °F (34 °C) swing in outdoor temperature over a 24-hour period, with the outdoor temperature varying from 45 to 105 °F (7 to 41 °C), while inside temperature is maintained at approximately 72 °F (22 °C). Tests have shown that the thermal lag for an 8 in. (200 mm) thick normal weight concrete wall subjected to the NBS model varies between 3.0 to 4.5 hours (**Iqbal 2007**).

The movement of a cast-in-place concrete frame subjected to a thermal change depends on the stiffness of its elements and support restraints. The dominant factors impact the frame stiffness

are, the columns size, the clear height and degree of base fixity, the high stiffer frames have less movement under thermal changes, but the stress will be very high.

The main challenge in analysing the thermal effects, the type of thermal effects must be distinguished between different types, accordingly, characterize the structural response.

like the concrete and reinforcing steel strain, influence of cracking, component stiffness, and degree of fixity of end and boundary restraints.

4.4 Expansion joints

(**The national academy of science (1974)** described the expansion joint as an isolation joints provided within the building to permit the separated segments of the structural system to expand and contract in response to temperature changes without adversely affecting the building serviceability or structure integrity. Expansion joint also provide relief from cracking because of contraction of the structure.

The building dimensions and configurations are obviously the overriding parameters regarding the needing of the expansion joint since the problem of expansion raised for the substantial building length and complex building configuration. Subsequently, the design of the expansion joint should be influenced by the structural frame type, the columns connection to the footing and the structural frame stiffness against the lateral displacement.

The spacing between the building expansion joints is dictated by the amount of movement that can be tolerated, and the permissible stresses or capacity of the members, spacing was followed a rule of thumb which have been developed according to **ACI 224.3R-08** , Table 4.4. shows the rules that depend on the type of structure, so it generally quite conservative.

Author	Spacing
Lewerenz (1907)	75 ft (23 m) for walls.
Hunter (1953)	80 ft (25 m) for walls and insulated roofs, 30 to 40 ft (9 to 12 m) for uninsulated roofs.
Billig (1960)	100 ft (30 m) maximum building length without joints. Recommends joint placement at abrupt changes in plan and at changes in building height to account for potential stress concentrations.
Wood (1981)	100 to 120 ft (30 to 35 m) for walls.
Indian Standards Institution (1964)	45 m (≈ 148 ft) maximum building length between joints.
PCA (1982)	200 ft (60 m) maximum building length without joints.
ACI 350R-83	120 ft (36 m) in sanitary structures partially filled with liquid (closer spacings required when no liquid present).

*Table 4.4_Expansion joint spacings (**ACI 224.3R-08**)*

Expansion joints are used to limit the concrete structure member forces caused by thermally induced volume changes when the structure is restrained, in practice, all buildings are restrained to some degree. The width of the Joints varies 1 to 6 in. (25 to 152 mm) or more, and typical width used is 2 in. (51mm). when the joint width is wider, the use of joints is to accommodate additional differential movement that might cause by seismic loading or settlement. Joints should divide the entire building above the level of the foundation, and covered Expansion joints should be covered which might be empty of filled.

Figure 4.3 Car park expansion joint

In addition to the rule of thumb expressed in table 4.4, many studies had been conducted for the expansion joint spacing**, Martin and Acosta (1970**) in their study of one-story concrete buildings present a term for the maximum spacing of expansion joints, by studying a frame structure subject to temperature changing, were the joint spacing found as a function of the frame members stiffness and length, as well as the seasonal temperature changes at the building site. The design temperature change considered as the difference between the extreme values of the normal daily maximum and minimum temperatures, in addition to the extra drop in temperature of about 30°F (17°C), to specify the concrete drying shrinkage.

In **Martin and Acosta (1970**) study a specific values of shrinkage equivalent temperature drop were provided, so the joint spacing was controlled by the contraction instead of expansion since the additional volume change was produced because of the drying shrinkage.

Varyani and Radhaji (1978) present in their study the calculating method of the expansion joints based on the analysis and design of the symmetrical frame corner columns to resist the gravity load and thermally induced combination , where the joint spacing is related to the relative stiffness of the beams and column of first floor frame , the extreme temperature change

with shrinkage allowance. This procedure is applicable in single and multi-story building with rectangular column layout, which is somehow more general than **Martin and Acosta (1970)** method but had similar approach.

The National Academy of Sciences in their technical report .65 (1974) for selecting expansion joint spacing adopted two methods ,initially determine the pacing by the empirical basis, in accordance to Figure 4.4, which provide maximum building spacing in the bases of the design temperature change (ΔT) from the change of exterior temperatures, this procedure is applicable in both single and multi-story structural concrete frames , which considered the building configuration and stiffness, if the building is heated or unheated and the columns to footings connections, most of federal agencies relied on this method for heated and unheated building, without having any experimental or theoretical justification the upper and lower bounds.

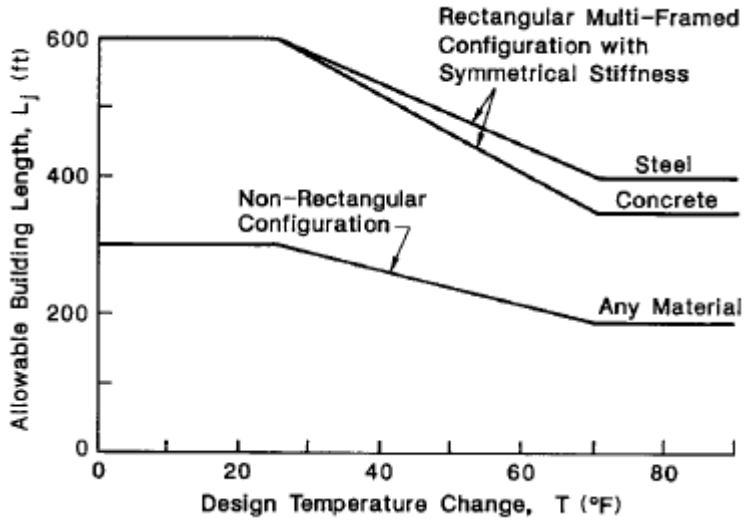

*Figure 4.4_ Expansion joint criteria for most federal agencies (**The national academy of science (1974)**)*

4.4.1 Martin and Acosta (1970) method

This method presents the calculation of the maximum spacing of expansion joints in approximately equal spans one story beam-column frames.it is based on presuming
That the factor of safety for gravity load will also covers the effects of temperature change. Martin and Acosta developed an expression for expansion joint spacing by considering this premise to frames structures analysis to the thermal design.
To remove the need for specific temperature calculations in design, **Martin and Acosta** try to find an adequate factor of safety in the building design to withstand the applied lateral, gravity, and thermally induced loads. Since the thermal loading has a short-term nature like the wind load, the thermal load was addressed in this study in the same way as **ACI 318-63** addressed wind loads. Accordingly, the maximum equivalent temperature load is represented by:

$$T = 0.2DL + 0.44LL \qquad \text{(Eq. 4.3)}$$

Which mean that temperature loads should not exceed the effect of 20% of the dead load plus 44% of the live load.
The design magnitude of the temperature change, ΔT, was taken as two thirds of the difference between the extreme values of the normal daily maximum and minimum temperatures, T_{max} and T_{min}. the two-thirds factor arbitrarily chosen as the building would be somewhere in

between the at the maximum or minimum daily temperature. The coefficient of thermal expansion α used in **Martin and Acosta** study is 5.5 X 10 in./in.per °F (9.9 x 10 -6 mm/mm per °C).
As previously mentioned, **Martin and Acosta** had considered the concrete shrinkage as equivalent temperature differential, they had considered about 30°F, to obtain the total design temperature change in the temperature analysis.

$$\Delta T = \frac{2}{3}(T_{max} - T_{min}) + 30°F \qquad \text{(Eq .4.4)}$$

In this equation (Eq. 4.4) ΔT represents the combination of a temperature drop with shrinkage, although ΔT is used to proportion expansion joints.

Martin and Acosta developed an expression for maximum expansion joint spacing, by analyze the structure based on the equation (Eq. 4.3), Lj in ft.

$$Lj = \frac{112{,}000}{R\,\Delta T} \qquad \text{(Eq. 4.5)}$$

Which:

$$R = 144 \frac{I_c}{h^2} \left(\frac{1+r}{1+2r}\right) \qquad \text{(Eq. 4.6)}$$

r = ratio of stiffness factor of column to stiffness factor of beam = Kc/Kb;
Kc = column stiffness factor = Ic/h in^3;
Kb = beam stiffness factor Ib /L in^3;
h = column height, in.; L= beam length, in.;
Ic = moment of inertia of the column, in^4 ;
Ib = moment of inertia of the beam, in^4

The resulting length between joints, Lj, given by Eq. (4.6) for typical values of R is given in Fig. 4.4

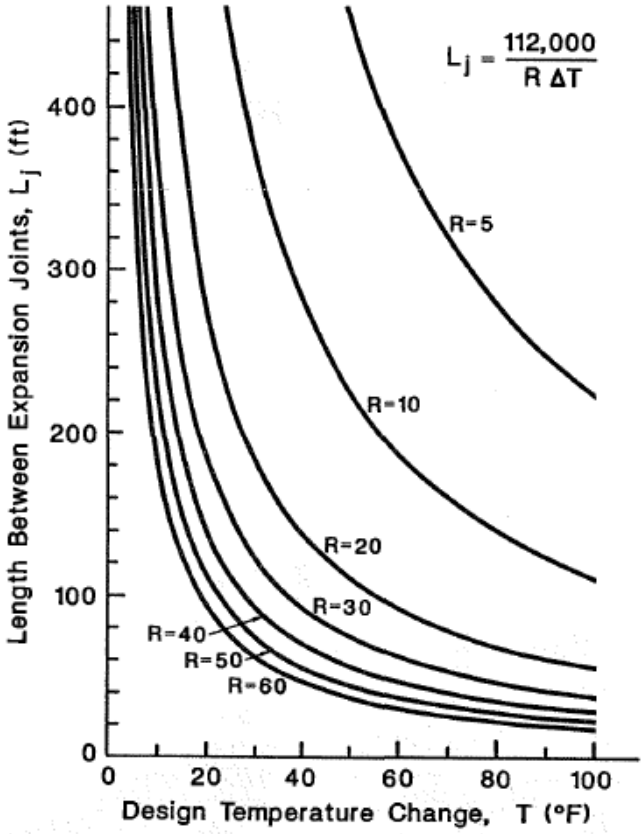

*Figure 4.5_ Length between expansion joints vs. design temperature change, ΔT (**Martin & Acosta 1970**) (1 ft = 0.305 m., 1°F = 1℃)*

Martin and Acosta study limit the expansion joint spacing with the maximum allowable lateral deflection δ to 1/180 of the column height hc. T_o avoid the damage of the exterior walls, so the maximum imposed lateral deflection on a column is taken as:

$$\delta = \frac{1}{2}\, \alpha\ L_j\, \Delta\, T \qquad \text{(Eq. 4.7)}$$

This leads to the limitation on L_j of

$$L_j \leq \frac{200\, h}{\Delta T} \qquad \Delta T \text{ in } °F \qquad \text{(Eq. 4.8)}$$

This Eq. (4.8) assumes that the floor lateral deflection induced by a temperature change is not significantly restrained by the columns. Where This assumption is realistic since the lateral stiffness of the supporting columns generally less than the in-plane stiffness of a floor system .so, the columns have little effect on δ.

4.4.2 Varyani and Radhaji (1978) method

Varyani and Radhaji (1978) present in their study the calculation of the maximum distance between the expansion joints a procedure for symmetrical beam- column frame buildings either single or multi story building. They had used the same Thermal loads produced from the temperature differential that used by **Martin and Acosta (1970)**, also two-thirds of the difference between maximum and minimum daily temperatures factor was used, but they select temperatures from the single day on which the difference between the maximum and minimum temperatures is the greatest. The moments due to thermal loading are calculated at the corner columns at the building, considering the maximum biaxial bending produced in columns.it has found that the first story beams and columns only are substantially affected by temperature change. Then the effect of temperature above the first story is dissipated. Therefore, the first two stories of multistory buildings only are assumed to be critical in the analysis.

The designing of the corner columns for the thermal change, by calculate the column moment induced by the temperature ,based on trial selection of the expansion joint spacing L_j, and design the column for the factored axial load and the biaxial bending due to gravity load, when the final joint spacing is selected , definitely the column design is adequate for the combination of the gravity load and thermal loading, otherwise the columns reinforcement shall increase to covered the increased moments for the selected joint spacing L_j.

The moment at the base of corner columns presented by Varyani and Radhaji through expressions for, M_g (base), in several different single bay frames due to the gravity load, as shown in Fig. 4.6 , the moment at the corner column base induced from temperature loading M_T(base) also presented in Fig. 4.7 and below expressions.

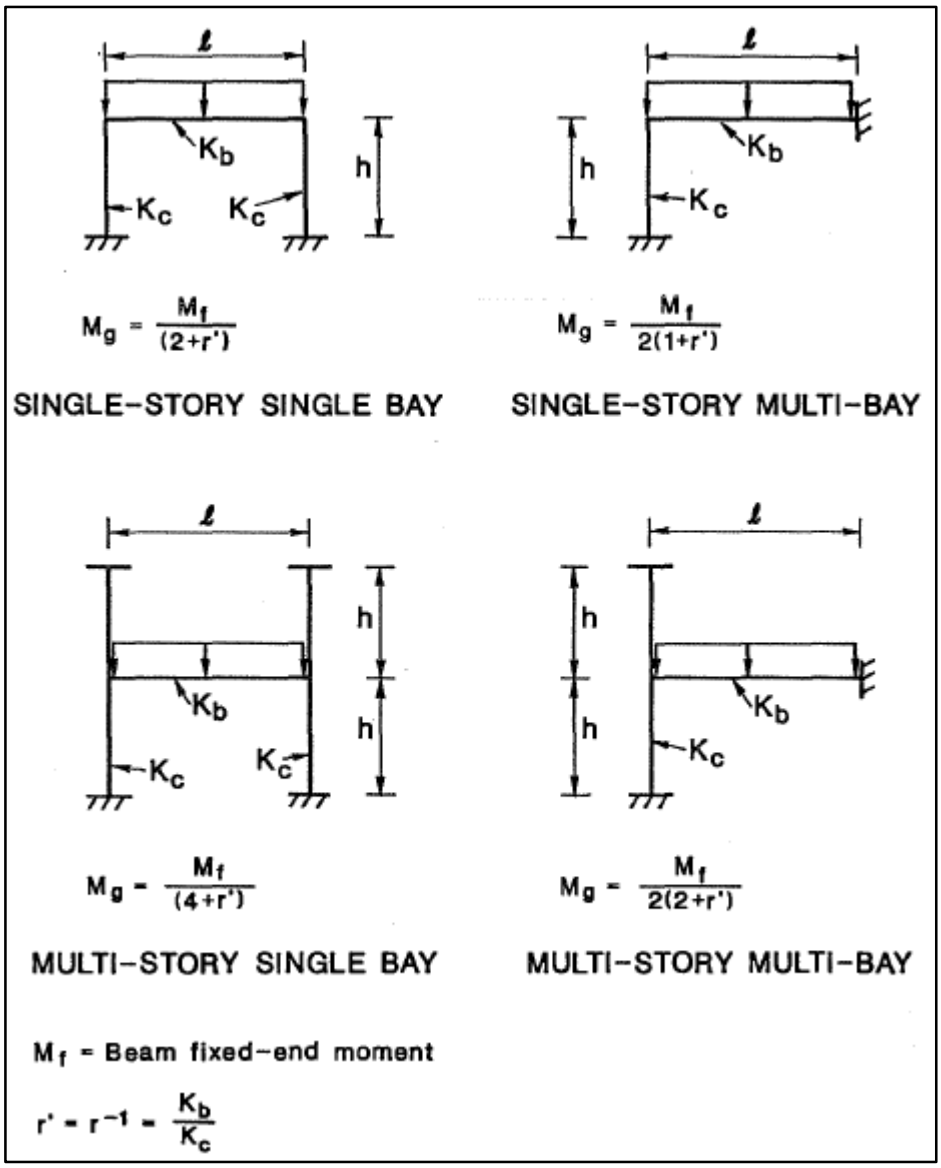

*Figure 4.6_ Moments at base of corner columns due to gravity using one bay substitute frame (**Varyani & Radhaji 1978**)*

Single story, single bay: $M_g\,(base) = \frac{M_f}{(2+r')}$ (Eq. 4.9)

Single story, multi-bay: $M_g\,(base) = \frac{M_f}{2(1+r')}$ (Eq. 4.10)

Multi-story, single bay: $M_g\,(base) = \frac{M_f}{(4+r')}$ (Eq.4.11)

Multi-story, multi-bay: $M_g\,(base) = \frac{M_f}{2(2+r')}$ (Eq. 4.12)

Where, M_f is the fixed-end moment at the beam-column joint due to gravity Load and

$r' = r^{-1} =$ Kb/Kc

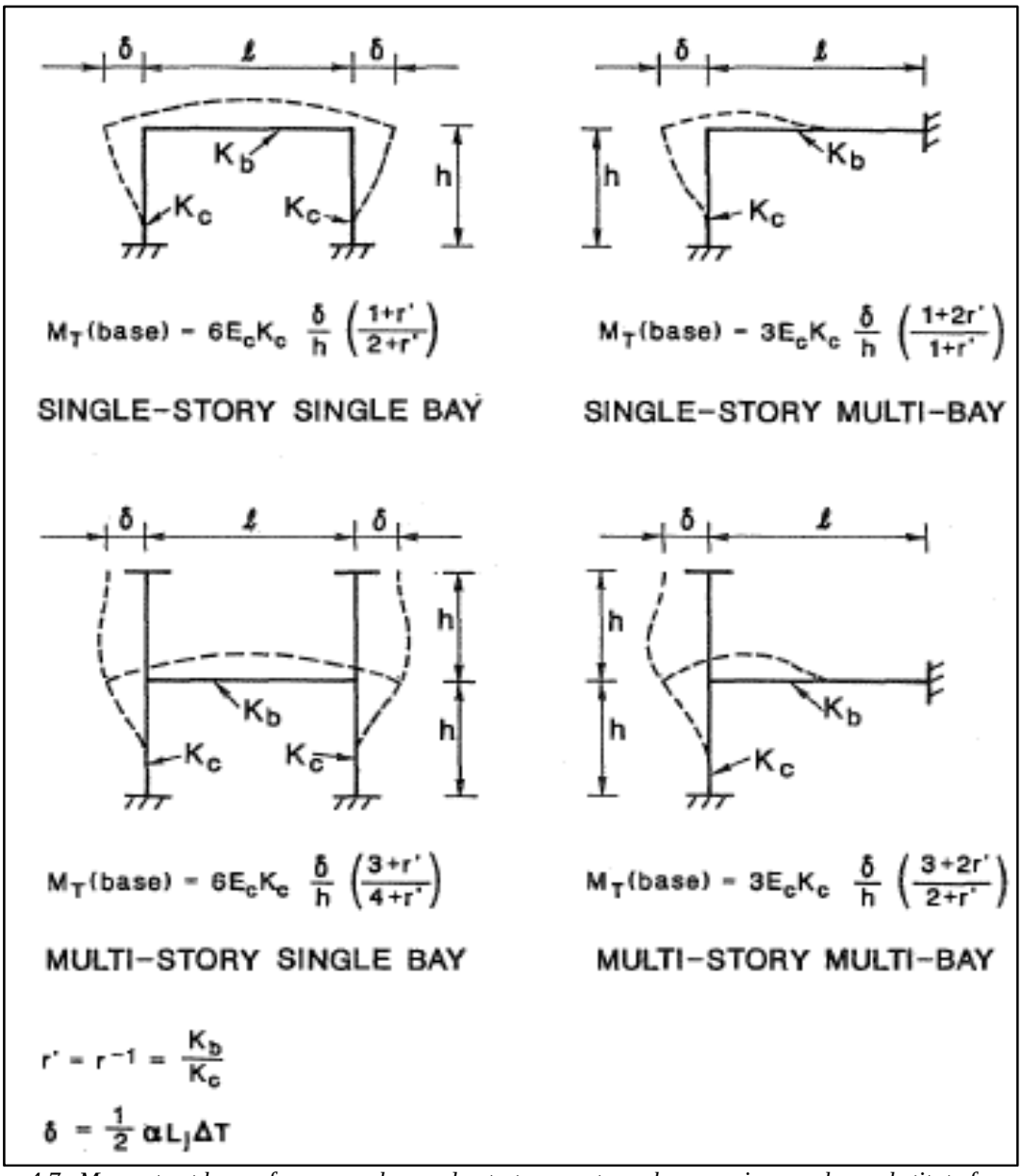

*Figure 4.7_ Moments at base of corner columns due to temperature change using one bay substitute frame, Lj. total length between expansion joints (**Varyani & Radhaj 1978**).*

Single story, single bay: $M_T\,(base) = 6E_cK_c\,\frac{\delta}{h}\left(\frac{1+r'}{2+r'}\right)$ (Eq. 4.13)

Single story, multi-bay: $M_T\,(base) = 3E_cK_c\,\frac{\delta}{h}\left(\frac{1+2r'}{1+r'}\right)$ (Eq. 4.14)

Multi-story. single bay: $M_T\,(base) = 6E_cK_c\,\frac{\delta}{h}\left(\frac{3+r'}{4+r'}\right)$ (Eq. 4.15)

Multi-story, multi-bay: $M_T\,(base) = 3E_cK_c\,\frac{\delta}{h}\left(\frac{3+2r'}{2+r'}\right)$ (Eq. 4.16)

Similar to **Martin and Acosta (1970), Varyani and Radhaji** use the factor to reduce the maximum temperature change as 2/3, and the equivalent temperature to the shrinkage considered to adjust the maximum fall in temperature (contraction) is 15°C (27 °F). While the equivalent temperature to the shrinkage considered to adjust the maximum rise in temperature (expansion) is 8 °C (14 °F). also, additional reduce considered to account many factors include the creep, and the effect of load duration and the loss of fixity due to soil movement.

$$\Delta T = \frac{1}{2}\left[-\frac{2}{3}(T_{max} - T_{min}) - 27\ °F\right] \quad \text{(Eq .4.17)}$$

$$\Delta T = \frac{1}{2}\left[\frac{2}{3}(T_{max} - T_{min}) - 14\ °F\right] \quad \text{(Eq .4.18)}$$

The expansion joint spacing L_j shall be;

Single story, single bay: $L_j = \frac{M_T h}{3E_c K_c \alpha \Delta T}\left(\frac{2+r'}{1+r'}\right)$ (Eq. 4.19)

Single story, multi-bay: $L_j = \frac{2M_T h}{3E_c K_c \alpha \Delta T}\left(\frac{1+r'}{1+2r'}\right)$ (Eq. 4.20)

Multi-story. single bay: $L_j = \frac{M_T h}{3E_c K_c \alpha \Delta T}\left(\frac{4+r'}{3+r'}\right)$ (Eq. 4.21)

Multi-story. multi bay: $L_j = \frac{2M_T h}{3E_c K_c \alpha \Delta T}\left(\frac{2+r'}{3+2r'}\right)$ (Eq. 4.22)

From the above expressions, it shows that **Varyani and Radhaji** study did not develop a general expression like **Martin and Acosta (1970)** for the expansion joint spacing L_j, but both methods had similar approach by considering the resistance of the first level frame to the thermal induced load to find out the expansion joint spacing. The temperature range suggested by **Martin and Acosta (1970)** should be applied rather than the recommended temperature range by **Varyani and Radhaji,** since it is considered as maximum temperature difference in a single day, however the seasonal changes logically are more appropriate.

The results obtained by **Varyani and Radhaji** are linked and sensitive to the beams and columns stiffnesses, and this method only focusing in the exterior / corner columns and beams did not consider the effect of the temperature change on interior beams and columns.

4.4.3 National Academy of Sciences (technical report .65) method

Due to the shortage of the design procedure for the expansion joint spacing accepted nationally , **the National Academy of Sciences (1974)** formulate the criteria developed by the federal constructions for the expansion joints spacing design in form of a graph shows in the figure 4.4, this figure expresses the allowable building length with relation of the temperature change. This relationship is applicable heated building with beam-column frames system, and the columns had a hinge connection at the base.

The criteria addressed in Figure 4.4 is based on an analytical study for the temperature change effects on two-dimensional elastic frames to the actual records of the movements along one-year study by the Public Buildings Administration (1943-1944).

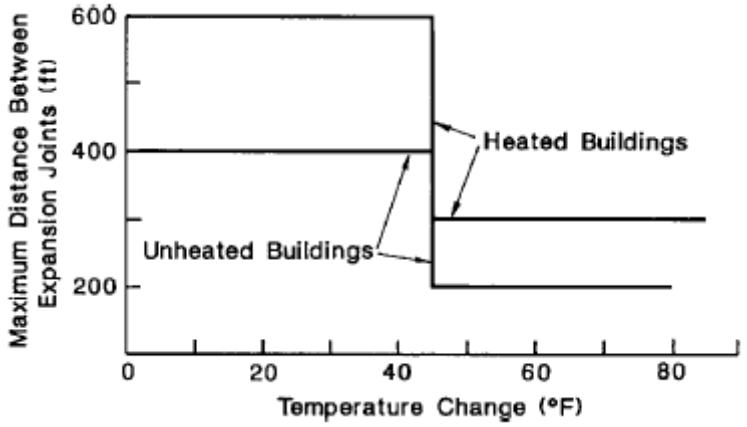

*Figure 4.8_ Expansion joint criteria of the Federal Construction Council (**The national academy of science (1974))***

The selection of the expansion joint spacing by federal agencies was relied on the criteria addressed in Figure 4.8. which provide the maximum distance between the expansion joint for heated and unheated structure, which is a function of the exterior temperature, the illustrated criteria reflect two assumptions: when the maximum difference between the maximum/minimum temperature and the mean annual temperature increases, the maximum allowable building length between joints must be decreased, and dimensions between joints can be increased for heated structures, because of ability to control the temperature inside the building. National Academy of Sciences (1974) Temperature change was taken as the maximum difference between the mean temperature during the normal construction season and

the extreme value during the summer or winter. The upper and lower bounds of 600 and 200 ft have no experimental or theoretical justification.

The figure 4.8 is adaptable to a wide range of building, by apply the modifications that matches with studied structure, the boundaries considered in both ways are clearly shows that at zero temperature change, the max allowable building length to be 600 ft (200 m) of the concrete building.

As stated above, for the structure not matching with Figure 4.8 assumptions, the following modifications should be applied to the joint spacings obtained from Fig. 4.8.

- If the building will be heated, but not air-conditioned, and has hinged column bases, use the length specified.
- If the building will be heated and air-conditioned, increase the allowable length by 15 percent.
- If the building will not be heated, decrease the allowable length by 33 percent.
- If the building will have fixed column bases, decrease the allowable length by 15 percent.
- If the building will have substantially greater stiffness against lateral displacement at one end of the structure, decrease the allowable length by 25 percent.
- When more than one of these conditions occur, the total modification factor is the algebraic sum of the individual adjustment factors that apply.

This empirical approach is not rational but are easy to use and produce realistic joint spacings. If this empirical method is not helpful and detailed analysis is required to determine the joint spacing, an analytical method defined by (**The national academy of science (1974).** can be used, which include the stress strain analysis of the structural frame under the temperature change. The Analytical Method can be used when the designer looking to increase the spacing length between expansion joints above the limits in the empirical approach, so a detailed analysis is required considering all the procedure to design the building against the thermal change effects. (**The national academy of science (1974)** suggested procedure for the design of the building to thermal change effect starting from understanding the basic of distributed stress within the structure and the ability of the structural member to resist this deformation and not exceed the member strength and cause structural failure accordingly, either by limit the potential deformation of the structure , or allow the building elements for substantial movement or compromise both together .The main factors affecting the location of the

expansion joints are the shape of the structure, the structure flexibility, the maximum movement desired within the joint and type of expansion joint seal, the expansion joint recommended to be located at the high point of the drainage system.

The expansion joint width can vary between 1 and 6 inches (25 and 150 mm), but typically a width of 2 in. (50 mm) is being used. As roughly estimated width can be from calculating the contraction or elongation of the structure under the temperature variation and based on the building length.

There are several type of expansion Joints, *double-column expansion joint*, which is more expensive than other types of expansion joints, but it allows the building to be separated into independent parts without supporting on the other part.

The *cantilevered expansion joint,* which provides architectural continuity. However, careful attention must be considered for the negative moment-reinforcing detailing and construction.

The lap-type sliding expansion joint, which provides architectural continuity also and can eliminates the possibility of differential deflection that may occur with a cantilever joint.

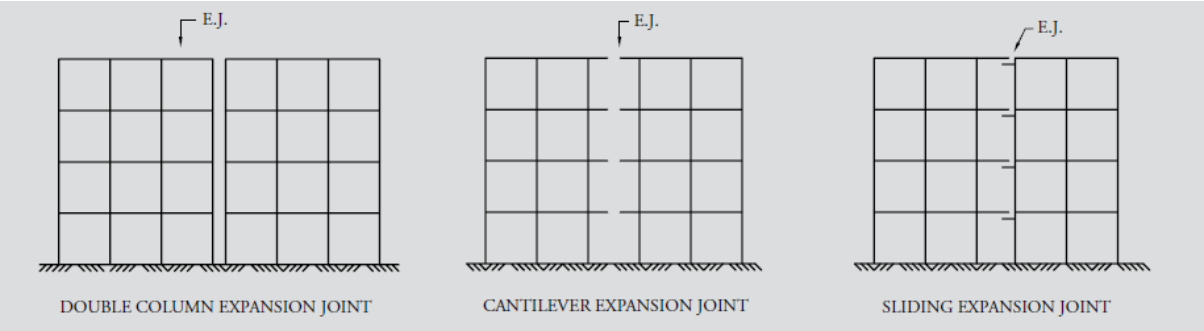

*Figure 4.9_ Expansion joint Types (**PCI 1997**)*

From the durability point of view, the need of the expansion joints should be minimizing by the design, as in certain cases it represents a potential pathway for moisture ingress into the slab.

Many researches addressed the topic of eliminating the expansion joint and its effect on the structural elements design, design the building without an expansion joints is desirable due as per the architectural and aesthetic appearance, and the additional expense incurred for construction and maintenance. (**Pooja & Karthiyaini 2017**) deals with design and analysis of structures of with different lengths (80m, 138m and 180m) with and without expansion joints,

And comparing the models for the produced stress at different levels and the overall changing in steel quantity on the structure after due to the temperature loads. Same approached had been conducted in (**Suchitra &Sai ramya 2017**) , but the study done For four different types of RC framed buildings and building shape (C, T, L and Rectangular) with and without expansion joints, and in each case the lateral displacement and quantity of steel had been compared and studied . While **(Aziz & Azeem 2018)** focus the behavior of long building for the gravity and seismic loads in addition to the temperature loading, in the presence and
absence of an expansion joint, two models had been studied for the same building with and without the expansion joint, with same loads applied (seismic, gravity, wind and thermal loads), and evaluate the story displacements, drifts, bending moments and steel consumption.

James M. Fisher, S.E (2005) highlight the difficulties associated with expansion joints construction , which includes firstly , the temperature changes during construction of the unheated structure may exceed the design temperature changes after the completion, which should considered by the designer, The construction of the expansion joint is difficult to be adjusted at the desired location, the erection tolerances to locate the expansion joint.

4.5 Cracks induced from thermal change:

The most common durability problems of the car park structure either above or below ground, is the response of the structural system to volume change (**ACI 362.1R-97**),

Since the result of volume change actions are the development of cracks. Which have main role to provide an access to the moisture and aggressive chemicals causing a concrete deterioration and it is aesthetically not accepted. For proper durability and serviceability, the reasonable predict of the volume change cracking will help at the design stage to mitigate or reduce these cracks.

the major causes of cracking in the concrete structure is the restrained movements the structural members will have a tensile stresses due to these restrained either it is Internal or external restraints which might exceed the tensile strength capacity of these members **ACI 224.3R-8**, Thermal variation in the concrete structure produce stresses that are enough to produce cracking, (**Elbadry and Ghali 1995)** investigated the stresses induced from the thermal changes and the cracks produced and effect on the section stiffness, the study used an analytical model to determine the effects of progressive reduction in stiffness due to developed cracks by the temperature change and the corresponding stresses in continuous structures. In addition to the mitigation of the cracks by determining the required reinforcement to control the cracks width up to specific limit. **(Aalami & Barth)** had recognized the causes of the cracks formation which related to the inadequate design and construction, or the restrained volume change and called as *Restraining cracks*, Restrain cracks generally do not impair the slab strength, and not necessarily lead to excessive deflection. And It might be caused by combining several factors together, when the vertical stiff elements (walls, elevator and columns) retrain the slab shortening. Depending on the length of the slab spans and the stiffness of the restraining elements, multiple restraint cracks may form.

(**Elbadry and Ghali 1995) and (Fritz Leonhardt 1987)** agreed about the importance of the tensile strength of concrete to control concrete cracking, because it is occurring when tensile stresses exceed the tensile strength of concrete. and the amount of normal force N_{cr} and bending moment M_{cr}, at which cracking of a section occurs, are directly proportional to the tensile strength of concrete f_{ct}. generally, the value of f_{ct} might be differ from section to section, and less than the determined value by testing the cylinder / cube sample of the same concrete, consequently the cracks do not form in the same level.

Cracking of the concrete section due to the thermal effects cannot be done separately, as it depends on the stress due to the temperature effect combined with the gravity loads, so iterative calculations are required to determine N and M in statically indeterminate structures. Which was addressed by (**Elbadry and Ghali 1995).** This study differentiates effects of cracking on internal forces, in the case of the external force- induced cracking the internal forces are not changed if the external force not changed , while the displacement induced cracking produced by Temperature variation, the member stiffness will be reduce, and the internal forces magnitude drops from the values existing before cracking. Fig. 4.10 (a) and (b) show the relation between the displacement D with axial force N in both cases, and the figures shows that the force is within the range of the first crack axial force N*cr1*.

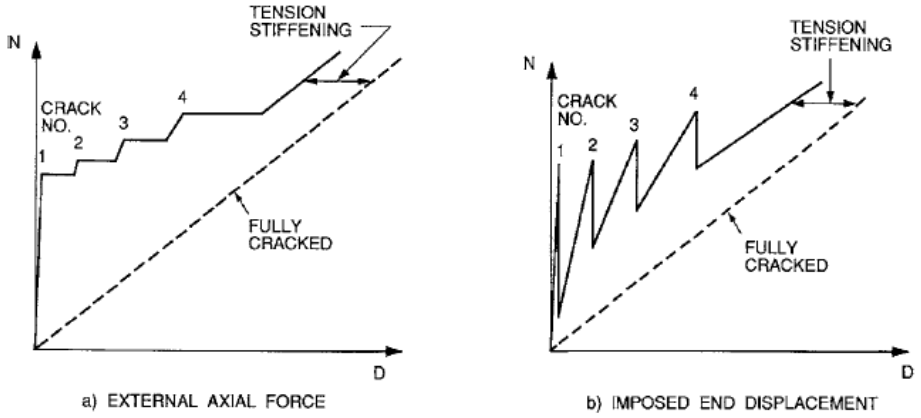

*Figure 4.10 _a Reinforced concrete member subjected to external axial force N or imposed end displacement D (**Elbadry and Ghali 1995**).*

Figures 4.11 and 4.12 illustrates the probable locations of restraint cracks in a two-way slab and one-way slab systems relative to the location of structural elements and discontinuities. Figure 4.11 shows the two-way concrete slab shortening toward the point of no movement or center of rigidity. The cracks occur along the length of the connection between the slab and walls, since the walls limits the shortening movements. Note that restraint may result in top, bottom, or through cracking of the slab. Figure 4.12 shows that the cracks in the one-way slab are parallel to the main flexural direction of the slab. restraint cracks in one-way slab system are dependent on the type of the used lateral load resisting system. Hence, the moment resistance frame induced the cracks to be transverse to the main flexural direction.

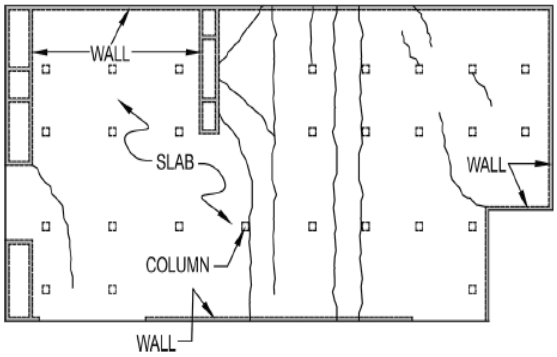

Figure 4.11_Illustration of restraint cracking in two-way slab.

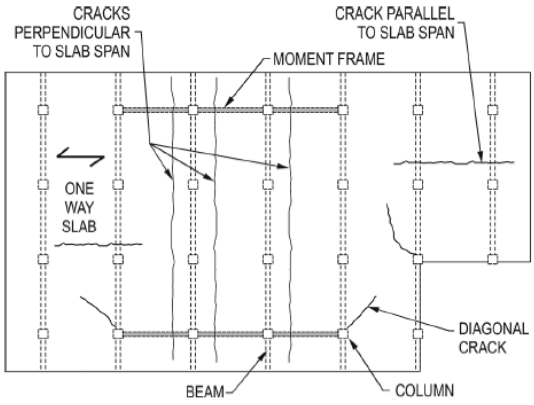

Figure 4.12 _Illustration of restraint cracking in one-way slab.

ACI 224.4R-13 defines two terms for the cracks in order to reduce the occurrence of these cracks in the parking structure , the first term is the Crack mitigation, means prevent the cracks occurring by eliminating or minimizing restraint at the design stage , such as design of the connection and the building layout . the other term is Crack control, which means that the cracks will be occurred, but it should be controlled in the location, the spacing or the width, this can be done by the joints and reinforcement detailing. **(Aalami & Barth)** specify the principle techniques to mitigate the cracks at design stage starting from the early design stage by planning the layout of the restraining members (walls & columns) to allow the slab to move freely by reduce the crack formation tendency Fig 4.13 ,shows the favorable and unfavorable arrangement of the column and walls to mitigate the cracks.

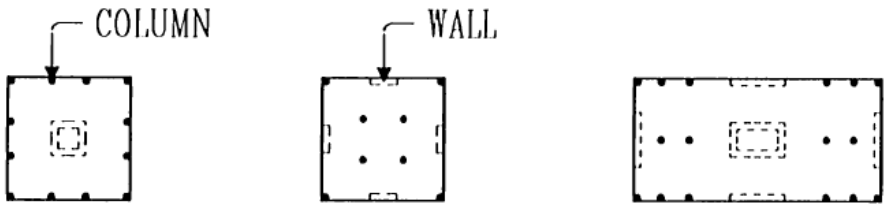

Figure 4.13a_ Favourable arrangement of restraining shear walls.

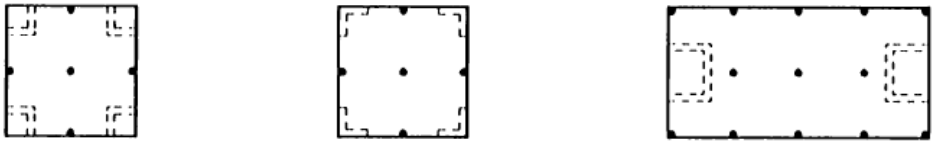

Figure 4.13b _Unfavorable arrangement of restraining shear walls.

structural separation is the other technique to release the stresses produced by thermal change and cause cracks, especially for the irregular slab geometry by using expansion joint. Allow the slab to undergo the early age shortening by using the pour strips helps is also highly recommended to mitigate the slabs cracks. **(Aalami & Barth)** considered also the releasing of the connections in the effective means of cracks mitigations, in which grouped into wall – slab release, slab – column release, slab joints and wall joints.

The Reinforcement for controlling the cracks is common approach by most of the reference of the thermal affects. (**Elbadry and Ghali 1995)** specified the sufficient amount of the reinforcement to limit the cracks width induced from both external force and displacement, by limiting the steel strain at a cracked section. The following equations express the reinforcement amount based on the assumption that the section is subjected to normal force N at reference point O and a bending moment M about an axis through O (Fig. 4.14).

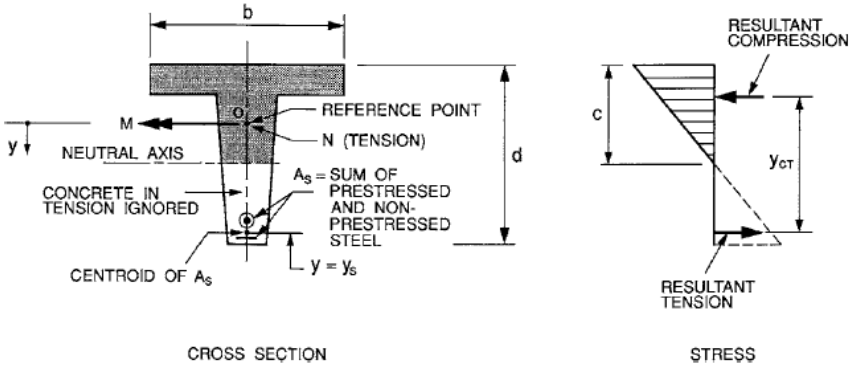

Figure 4.14_Stress distribution in cracked prestressed section; positive sign convention for N, M, and y.

Average crack width can be predicted by

$$w = s\zeta(\Delta\varepsilon_s) \quad \text{(Eq. 4.23)}$$

where s is the average crack spacing, ζ is the same interpolation coefficient used before to account for the tension stiffening effect, and $\Delta\varepsilon_s$ is the change in steel strain calculated for a transformed section ignoring concrete in tension. For a prestressed section, $\Delta\varepsilon_s$ is the change in steel strain after the decompression of concrete. The change in steel strain $\Delta\varepsilon_s$ and the corresponding change in steel stress $\Delta\sigma_s$ can be calculated as

$$\Delta\varepsilon_s = \frac{(M_s/y_{CT}) + N}{E_s A_s} \quad \text{(Eq.4.24)}$$

the change $\Delta\sigma_s$ in steel stress

$$\Delta\sigma_s = E_s\Delta\varepsilon_s \quad \text{(Eq. 4.25)}$$

The minimum area of steel required to limit crack width to a specified limit is

$$A_s = \frac{(M_s/y_{CT}) + N}{\Delta\sigma_s} \quad \text{(Eq. 4.26)}$$

ACI 318-14 define the minimum area of Deformed reinforcement to resist shrinkage and temperature stresses show in the table 4.5

Reinforcement type	f_y, **psi**	**Minimum reinforcement ratio**	
Deformed bars	< 60,000	0.0020	
Deformed bars or welded wire reinforcement	≥ 60,000	Greater of:	$\frac{0.0018 \times 60{,}000}{f_y}$
			0.0014

Table 4.5_Minimum ratios of deformed shrinkage and temperature reinforcement area to gross concrete area ***(ACI 318-14)***

4.6 Temperature-induced deflections:

The temperature changes affected the concrete structure element deflection, which may have adverse effects on serviceability of whole concrete structures. when these elements are restrained from deforming under the temperature change, the tensile stress induced in the elements, if these stresses are more than the concrete tensile strength , the restrained cracks will occur and consequent reduction in the member section flexural stiffness, so the section will be deformed for subsequent loading, hence the thermal effect should be considered during the design stage on estimating the section stiffness to the deflection .

ACI 435.7R-85 Conclude the effect of the temperature change on the concrete structure serviceability which induced the deflections, and adverse the Measures which should be taken at the design stages to alleviate these effects, the report provide a simplified Calculation procedures to estimate the deflection and section stiffness changed as a result of the temperature change for non-cracked section.

4.6.1 Thermal induced deflection:

The deflection of the simply supported and cantilever beam calculated in **ACI 435.7R-85** based on the inter-relation between the temperature, stiffness and the deflection.

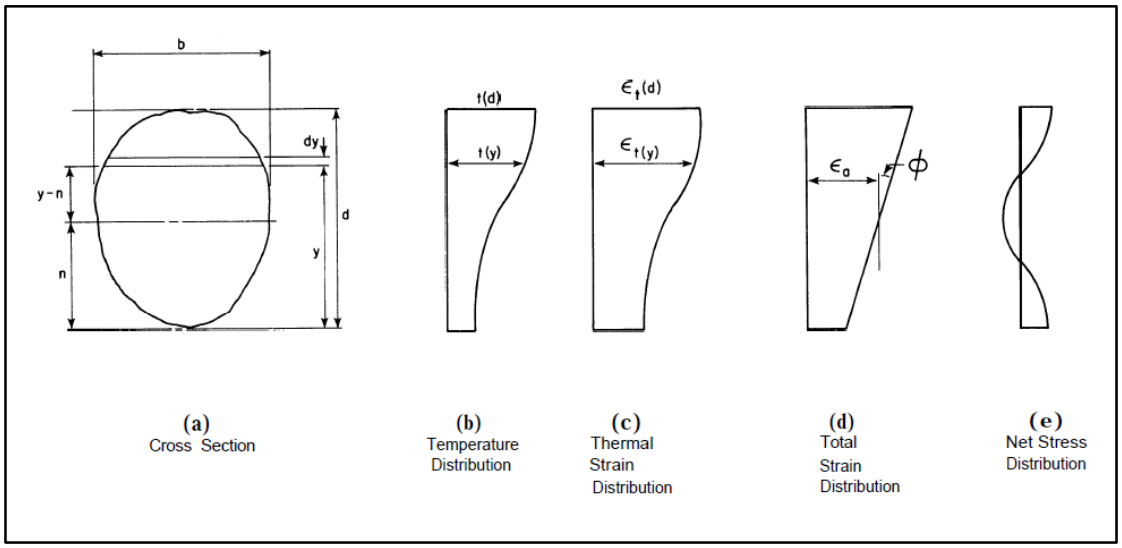

*Fig. 4.15_ Thermal stress and strain distribution on general cross section (**ACI435.7R-85**)*

Reference to Figure 4.15 for the Thermal stress and strain distribution on cross section,
With temperature distribution **t(y)** considered on the section, the Thermal strain at distance **y** from the bottom of the section shall be expressed by:

$$\varepsilon_t\ (y) = \alpha\ t(y) \qquad \text{(Eq. 4.27)}$$

The movement due to temperature t(y) shall be restrained, by applying a stress in the opposite direction to ε_t (y):

$$\sigma\ (y) = E_c\ \alpha\ t(y) \qquad \text{(Eq. 4.28)}$$

The net restraining axial force (P) and moment (M) are obtained by integrating the stress over the depth of the section:

$$P = \int_A\ \sigma\ dA = \int_0^h \alpha\ Ec\ t(y)\ b(y)\ dy \qquad \text{(Eq. 4.29)}$$

$$M = \int_A\ \sigma\ (y - n)\ dA = \int_0^h \alpha\ Ec\ t(y) b(y)(y - 2)\ dy \qquad \text{(Eq. 4.30)}$$

The total strains on the unrestrained cross section can be obtained by applying the net restraining axial force and the moment in another direction of the restraining force with assuming the plane section remain plane, the axial strain (ε_a) and curvature (Φ) are given by:

$$\varepsilon a\ = \frac{P}{A\ Ec} = \frac{\alpha}{A} \int_0^h\ t(y)\ b(y)\ dy \qquad \text{(Eq. 4.31)}$$

$$\Phi = \frac{M}{Ec\ I} = \frac{\alpha}{I} \int_0^h\ t(y) b(y)(y - n)\ dy \qquad \text{(Eq. 4.32)}$$

The net stress distribution on the cross section is given by:

$$\Phi n\ (y) = \frac{P}{A} \pm \frac{M\ (y-n)}{I}\ -\ E_c\ \alpha\ t(y) \qquad \text{(Eq. 4.33)}$$

If the temperature gradient varies linearly from 0 to Δt, the curvature is given by:

$$\Phi = \frac{\alpha\ \Delta\ t}{h} \qquad \text{(Eq. 4.34)}$$

For the uniform temperature gradient along the length of a member, the deflections of the simply supported beam (Δ_{ss}) is

$$\Delta_{ss} = \frac{\emptyset\, L^2}{8} = \frac{\alpha\, \Delta\, t}{h}\,\frac{L^2}{8} \qquad \text{(Eq. 4.35)}$$

and the deflection of the cantilever beams (Δ_{cant}) are calculated as

$$\Delta_{cant} = \frac{\emptyset\, L^2}{2} = \frac{\alpha\, \Delta\, t}{h}\,\frac{L^2}{2} \qquad \text{(Eq. 4.36)}$$

Deflection to span ratio is given

$$\frac{\Delta}{L} = \frac{\alpha\, \Delta\, t}{K}\,\frac{L}{h} \qquad \text{(Eq. 4.37)}$$

where k = 8 for simply supported and 2 for cantilever beams.

4.6.2 How the restraint to thermal movement effect the concrete member:

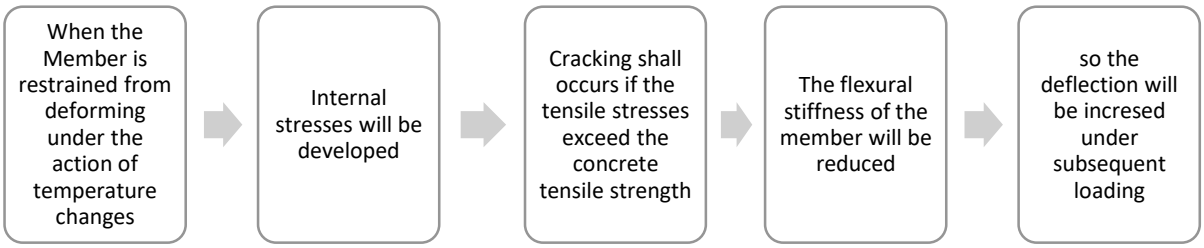

Figure 4.16_ the effect of the thermal movement in restraint concrete elements

Therefore, the Temperature effects should be considered when determining the member stiffness for deflection calculation, and the calculation of the effective moment of inertia should be based on the maximum moment condition **ACI 435R-16**.

(Priestley 1981) suggest considering the uncracked section during the calculation of the unrestrained thermal curvature, and to consider the moment of inertia linked to the expected distribution of cracking when calculating the thermal stresses and moments. And he highlighted the importunacy of solving the final strain distribution of cracked section as the cracking extent is a function of the thermal load. While using the estimated reduced stiffness due to thermal effect was presented by **(Mentes, Bhat and Ranni, 1980).** Which was based on considering

the effective moments of inertia and iterative procedure. **ACI 349.1R-07** adopt the same concept of considering the uncracked stiffness during the analysis of the mechanical loads. **ACI 349** calculation procedures considered Ig for uncracked sections for thermal stresses and for deflection calculation Icr for cracked sections.

Figure 4.17 shows how the moment will be increased due to the thermal effect in two span slabs along with the gravity load effect, since the bending moment diagram indicates the moment exceed the cracking moment Mcr on the negative moment region.

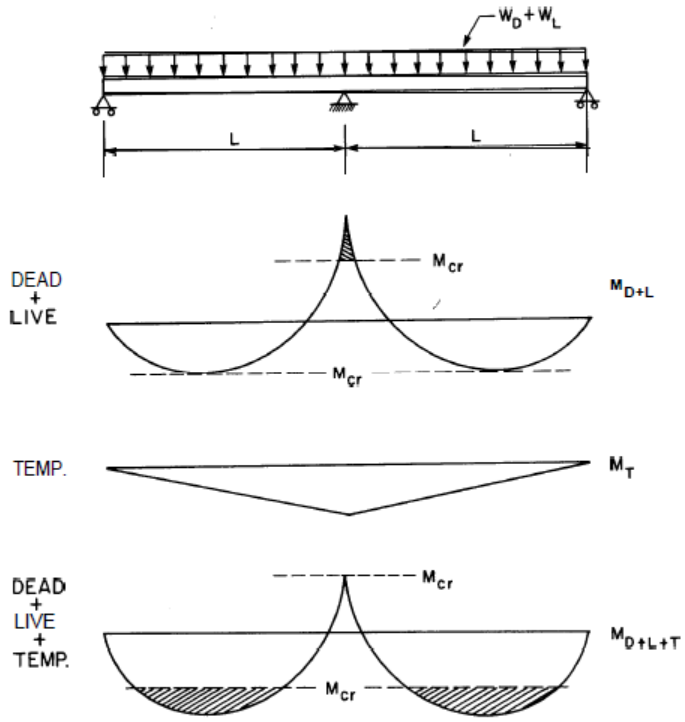

Figure 4.17_Effect of temperature gradient on bending moments in two-span slab

4.6.3 Control of deflection:

The concrete flexural member's deflection is controlled by the concrete section minimum thickness, the steel reinforcement ratio, and the limitation of span/deflection ratio.

4.6.3.1 Minimum thickness limitations

(**ACI 318-11**) provide the criteria of the one-way slab and the beams criteria, where the deflection of the one-way slab and beams is not required to be calculated, if the element thickness is matching these criteria as mentioned in the Table 4.6. the table values are applying only on the members not supporting or attached to the partitions or other items shall affected or likely damaged by excessive deflections.

Table 4.6 values are applicable directly on the members with normal weight concrete and reinforcement grade of 420, any other conditions the value to be modified as follows:

a) Lightweight concrete with density (Wc) in the range of 1440 to 1840 kg/m³, the values shall be multiplied by (1.65 – 0.0003Wc), but not less than 1.09.
b) If the reinforcement grade other than 420 MPa, the values shall be multiplied by (0.4 + fy/700).

Member	Minimum Thickness *h*			
	Simply Supported	one end continuous	Both ends continuous	Cantilever
	Members not supporting or attached to partitions or other construction likely to be damaged by large deflection			
Solid one-way slabs	L/20	L/24	L/28	L/10
Beams or ribbed one-way slabs	L/16	L/18.5	L/21	L/8

*Table 4.6_ Minimum Thickness of Non- Prestressed Beams or One- way slabs unless the Deflections are calculated (**ACI 318-14**).*

The values provided by **ACI 318-14** on table 4.3 have been modified by **ACI 435R-95** and developed in Table 4.7 which cover the exclusion mentioned in table 4.6 for the members supporting the elements that damaged by the deflections.

Member	Members not supporting or not attached to non-structural elements likely to be damaged by large deflections				Members supporting or attached to non-structural elements likely to be damaged by large deflection			
	Simply Supported	one end continuous	Both ends continuous	Cantilever	Simply Supported	one end continuous	Both ends continuous	Cantilever
Roof slab	L/22	L/28	L/35	L/9	L/14	L/18	L/22	L/5.5
Floor slab, and roof beam or ribbed roof slab	L/18	L/23	L/28	L/7	L/12	L/15	L/19	L/5
Floor beam or ribbed floor slab	L/14	L/18	L/21	L/5.5	L/10	L/13	L/16	L/4

*Table 4.7_ Minimum thickness of beams and one-way slabs used in roof and floor construction (**ACI 435R-95**)*

4.6.3.2 Tension steel reinforcement ratio limitations

The ratio of the tension reinforcement has an important role to minimize the concrete elements deflection, generally the steel reinforcement ratio limited in ranging between (0.25 ρ_b to 0.40 ρ_b) as recommended by **ACI 435R-95** in table 4.8.

Member	Cross section	Normal weight concrete	Lightweight concrete
Not supporting or not attached to non-structural elements likely to be damaged by large deflections	Rectangular	$\rho \leq 35\ \% \rho_b$	$\rho \leq 30\ \% \rho_b$
	"T' or box	$\rho_w \leq 40\ \% \rho b$	$\rho_w \leq 35\ \% \rho b$
Supporting or attached to non-structural elements likely to be damaged by large deflections	Rectangular	$\rho \leq 25\ \% \rho b$	$\rho \leq 20\ \% \rho b$
	"T' or box	$\rho_w \leq 30\ \% \rho b$	$\rho_w \leq 25\ \% \rho b$

*Table 4.8_ Recommended tension reinforcement ratios for non-prestressed one-way members so that deflections will normally be within acceptable limits (**ACI 435R-95**)*

ACI 318-14 limits the minimum steel ratio for temperature and shrinkage by for slabs where the reinforcements grade is grade 420 deformed bars or welded wire reinforcement are used 0.0018 of the concrete cross section.

4.6.3.3 Computed deflection limitations

The permissible deflection of one- way system defined in ACI 318-14 and these limits defined in table 4.9

Type of member	Deflection to be considered	Deflection Limitation
Flat roofs not supporting or attached to non-structural elements likely to be damaged by large deflections	Immediate deflection due to live load L	$\frac{L}{180}$
Floors not supporting or attached to non-structural elements likely to be damaged by large deflections	Immediate deflection due to live load L	$\frac{L}{360}$
Roof or floor construction supporting or attached to non-structural elements likely to be damaged by large deflections	That part of the total deflection occurring after attachment of non-structural elements (sum of the long-time deflection due to all sustained loads and the immediate deflection due to any additional live load)	$\frac{L}{480}$
Roof or floor construction supporting or attached to non-structural elements not likely to be damaged by large deflections		$\frac{L}{240}$

*Table 4.9_ Maximum permissible computed deflections (**ACI 318-14**)*

5. ANALYTICAL MODELS

5.1 Introduction

To obtain a better understanding of the thermal effect on underground car park concrete building, and the importance of designing this structure for strained effect (T) with or without the expansion joints, A three dimensional analysis of three models for underground car park structure assumed located in Dubai – UAE, were performed using the commercial finite element analysis software *ETABS.*

The study considered the effects of the lateral forces from the earth pressure taken by the shoring around the building, with no effect on the structure, as the volumetric strains caused by the thermal effects , such as expansion and contraction movements will result in complex soil – structure interactions, and it is out of the purpose of this study.

A simple linear static analysis of the three models subjected to the gravity loads and the strained forces as per ASCE 7-10 only , without any study of the seismic loading, to gain better understanding of the volume change response (movements and forces) of the underground building by comparing the three models and recommend the design consideration specially for this type of buildings.

5.2 Studied Structure

he studied Structure is a multi-story underground car park reinforced concrete building with a rectangular footprint measuring 140.55 m by 38.75 m, refer figure (5.1). the building has three typical floors only and totally under the ground parking level figure (5.2). The building structural system consists of reinforced concrete flat slab supported by rectangular reinforced concrete columns, and a retaining wall all around the building except the location of the in and out ramps which are excluded from the models.

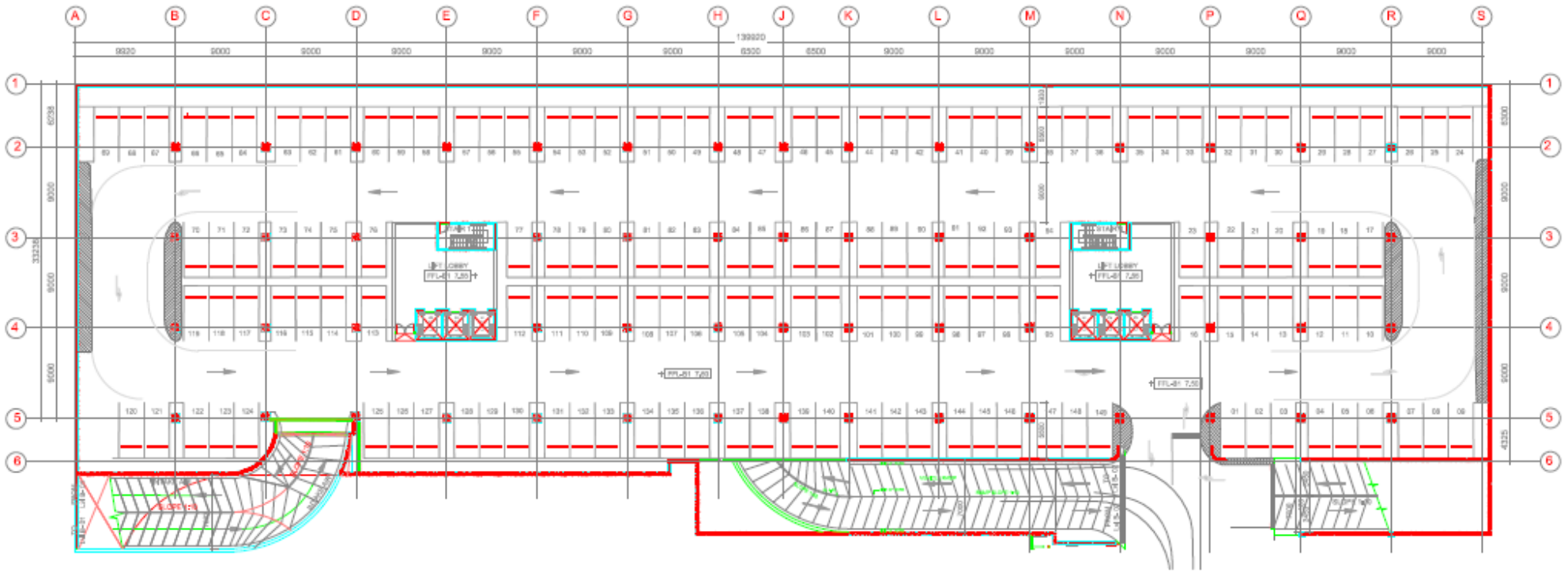

Figure 5.1_ Studied Underground car park building floor plan

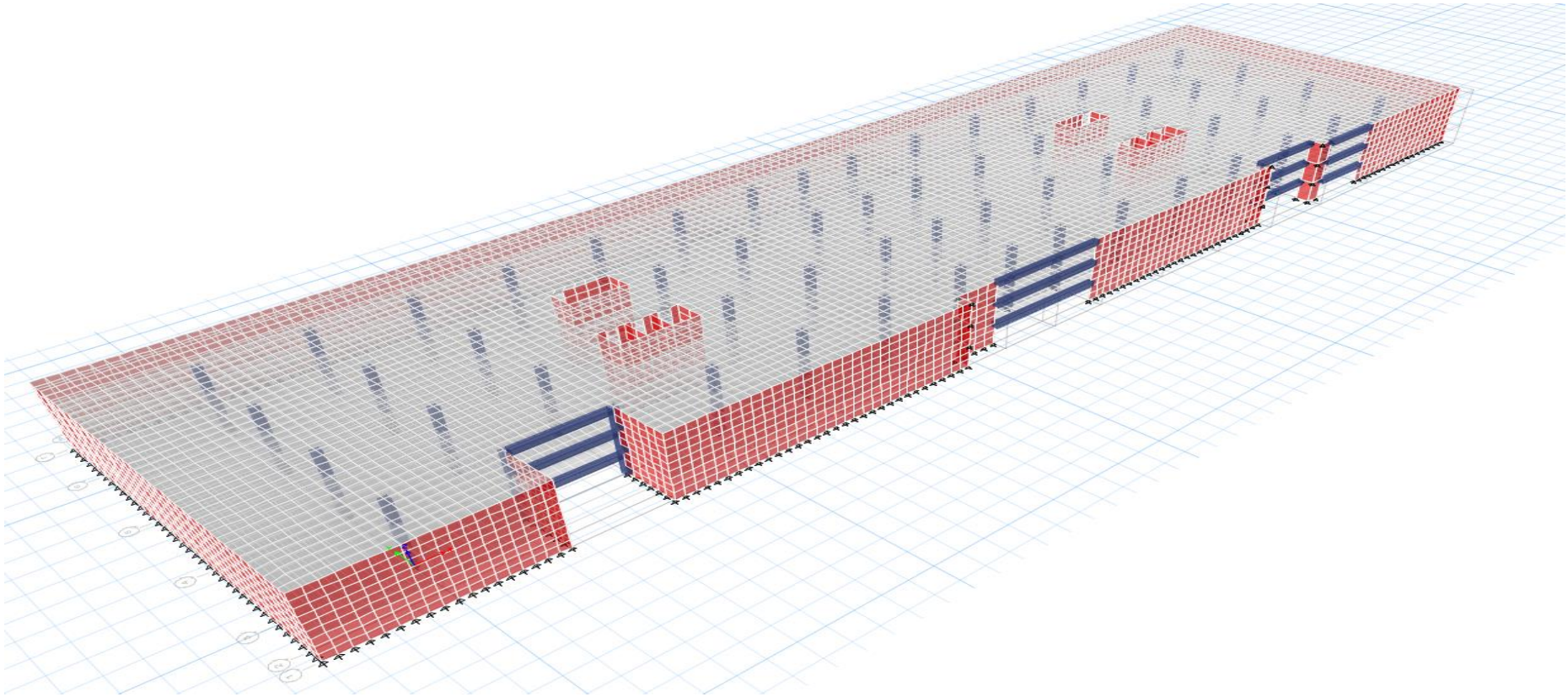

Figure 5.2_ Studied Underground car park building three-dimensional model

The preliminary data considered for the project models analysis are shown in table 5.1

	Property	Value	unit
1	Reinforcement Grade 60 (yield strength)	460	MPa
2	Concrete Grade C40 (compressive strength)	40	MPa
3	Concrete Modulus of elasticity	34000	MPa
4	Coefficient of Thermal Expansion	0.00001	1/C°
5	Specific weight of reinforced concrete	25	KN/m³

Table 5.1_ Models preliminary analysis Data

The Materials properties used in the studying the project are shown in table 5.2

S.No.	Property	Value	unit
1	Building Plan Dimensions	140.55 X 38.75	m
2	Number of Stories	3	
3	Floor Height	3.5	m
4	Columns size	600 X 600	mm
5	Beams Size	600 X 800	mm
6	Slab thickness	300	mm
7	Shear Wall thickness	300	mm
8	Retaining wall thickness	400	mm
9	Typical Spacing between columns	9	m

Table 5.2_ Materials Properties

5.3 The Studied Models

In order to investigate the thermal effects on underground car park structure, including the volume change forces, a three models for the same building was analyzed, and the analysis results are compared, to conclude the best design aim to be considered in the designing of similar buildings in future, the results of the stress on the slab and walls, and the forces on the columns shall be studied and compared with the results between the models.

The models specifications are defined as follow:

5.3.1 Model A

The three floors underground car park concrete building is taken as a complete single unit without the presence of an expansion joint, and subjected to the gravity loads (Dead Load including the structure own weight and finishing loads, and the live loads as per the load standard ASCE-7_10), considering the Self-Straining Forces resultant from the concrete shrinkage and creep only for period of three years and considering the temperature change is zero.

5.3.2 Model B

The three floors underground car park concrete building is taken as a complete single unit without the presence of an expansion joint, and subjected to the gravity loads (Dead Load including the structure own weight and finishing loads, and the live loads as per the load standard ASCE-7_10), and the Self-Straining Forces including the temperature loading , concrete shrinkage and creep within three years.

5.3.3 Model C

The three floors underground car park concrete building is divided, by introducing an expansion joint in the structure as it calculated as per ACI 224.3R-95, where it is located at the distance required by code of the building plan along the X direction, and there is no expansion joint along the y direction the distance between the expansion joint is following. The building is subjected to the gravity loads (Dead Load including the structure own weight and finishing loads, and the live loads as per the load standard ASCE-7_10), and the Self-Straining Forces including (temperature loading, concrete shrinkage and creep).

5.4 The Study assumptions and exclusions

The analytical models will be run for three models as described earlier while considering the below:

- The analysis of three models considered for the gravity loads as mentioned in section 5.5.1 and 5.5.2.
- The temperature changes studied based on the temperature readings of Dubai- UAE for the period between 1st Jan 2018 and 31st Dec 2019, from the National Center of Meteorology & Seismology (NCMS).
- The three models considered for the building as underground car park basements only.
- The earth pressure loading on the basements retaining walls of the three models, is not considered in the analysis of the models.
- The seismic loading is not considered in the analysis for three models.
- The Self-Straining Forces (T) will not applied fully in the model as ETABS doesn't have the option for the analysis for the creep and shrinkage forces, as the strain of creep and shrinkage will be calculated for our project as shown in section 5.5.3.1, and will not be applied in the model, as only the temperature change shall be applied.
- The concrete sections applied as cracked section, which performed in the models by adjust the modifier of the section as follows;
  - Columns section modifiers = 0.70
  - Beams section modifiers = 0.35
  - Slabs section modifiers = 0.25
  - Walls section modifiers = 0.35
- The type of support considered as hinge support for all models.
- The three models diaphragm considered as semi rigid diaphragm, to simulate the actual in-plane stiffness properties and behavior of the slab and to ensure that the slab in-plan deformation is take in place and to record the produced forces and stresses (**Computers and Structures, Inc. (CSI)**).

5.5 Applied loads

As described the models, below are the applied load on the models including the load combinations.

5.5.1 Dead Load

Dead loads consist of the weight of all materials of construction incorporated into the building including, but not limited to walls, floors, roofs, ceilings, stairways, built-in partitions, finishes, cladding, and other similarly incorporated architectural and structural items (**ASCE-7 _10**).

Since the building is car park, the applied dead load comes from the own weight of the concrete structure element and the finishing of the flooring, in this project the applied load on the slabs as a uniform load taken as

$$\underline{DL = 2.0\ KN/m^2}$$

5.5.2 Live load

The live load is the maximum loads expected by the intended use or occupancy but shall in no case be less than the minimum uniformly distributed unit loads required by the live load table defined in (**ASCE-7 _10)** standard, including any permissible reduction. Which is equal for garage building of Passenger vehicles only about 1.92 KN/m^2. in this project the applied Live load on the slabs as a uniform load taken as

$$\underline{LL = 3.5\ KN/m^2.}$$

5.5.3 Self-straining forces

Provision shall be made for anticipated self-straining forces arising from restrained dimensional changes due to temperature, moisture, shrinkage, creep, and similar effects **(ASCE-7 _10).** Which shows in all the load combination in term of **T**.

5.5.3.1 Shrinkage and creep forces

Following to the discussion earlier in section 4.1 from this study, and reference to the tables and figures for calculating the strain forces produced from creep and shrinkage of the studied building at the age of 3 years from the reference of **(PCI Design Handbook- 7th (2010)**).

(Refer to Appendix C for tables)

At 3 years age;

From Table C-1

Creep strain = $273\ x\ 10^{-6}$ in./in.

Shrinkage strain = $543\ x\ 10^{-6}$ in./in.

Reference to the climate data in reference A, the average humidity for the studied period = 69 %

From Table C-2

Correction Factors for Relative Humidity for creep = 1.08

Correction Factors for Relative Humidity for shrinkage = 1.014

The strain forces from Creep = $273\ x\ 10^{-6}\ x\ 1.08$

= $275\ x\ 10^{-6}$ in./in.

The strain forces from shrinkage = $543\ x\ 10^{-6}\ x\ 1.014$

= $550.6\ x\ 10^{-6}$ in./in.

The Total Strain forces = $825.6\ x\ 10^{-6}$ in./in.

5.5.3.2 Temperature changes

The temperature change for this project studied for the period of between 1st Jan 2018 and 31st Dec 2019, from the National Center of Meteorology & Seismology (NCMS), the temperature readings of this period shows in appendix A, and Figure 5.3 showing the temperature records , showing daily maximum and minimum value.

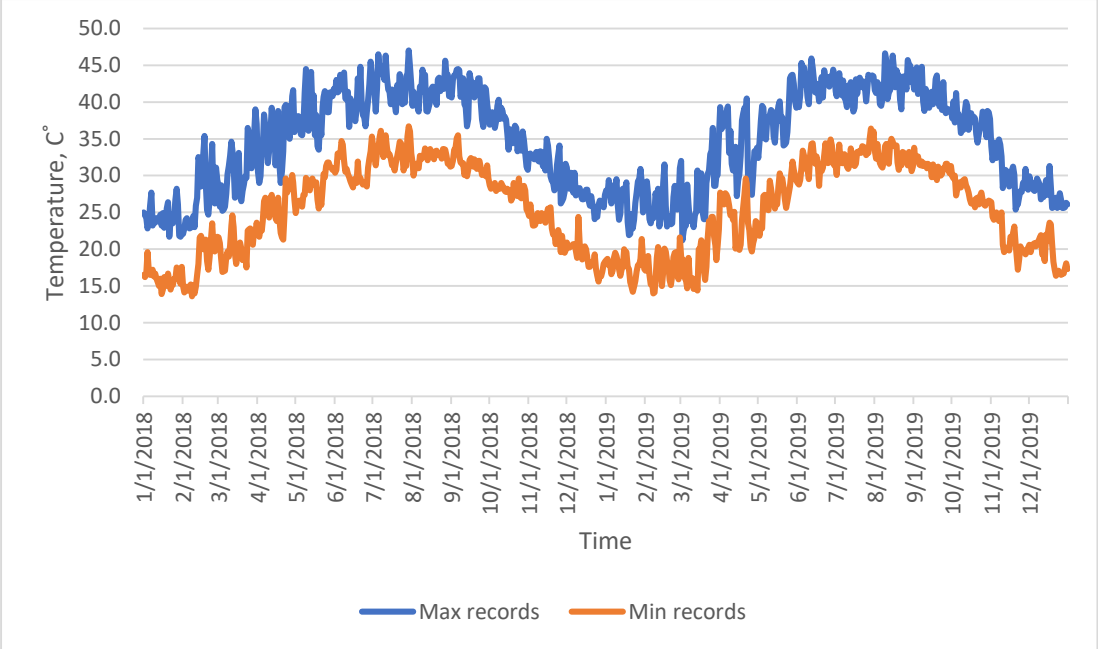

Figure 5.3_ The temperature records (maximum and minimum) for Dubai-UAE from the National Center of Meteorology & Seismology (NCMS) for the period from 1st Jan 2018 to 31st Dec 2019 (Appendix A).

The maximum recorded temperature on 29th July 2018 = 47˚C

The minimum recorded temperature on 8th February 2018 = 13.6 ˚C

Reference to equation 4.1;

$$\Delta T = (T_W - T_m) \text{ or } (T_m - T_c) \quad \text{(Eq. 4.1)}$$

T_m = The mean Temperature during the normal construction season
= 28 ˚C

T_w = The Temperature exceeded the average only 1% of the time during the summer months
= 41 ˚C

T_c = The Temperature equal or exceeded the average 99 % of the time during the winter months
= 20 ˚C

So,

ΔT = 21 ˚C

In the model the temperature difference applied in all the project elements is 25 ˚C

5.5.4 Load Combinations

Where applicable, the structural effects of load T shall be considered in combination with other loads **(ASCE-7 _10).**

- The ultimate load factor applied in the study for the loads include the temperature, reference to (**PCI Design Handbook- 7th (2010))** is

1.2 DL +1.6 LL + 1.2 TL

- The service load factor applied in the study for the loads include the temperature, is

1.0 DL +1.0 LL + 1.0 TL

5.6 Model C – Expansion joints distances

The expansion joints in this study was done based on the recommendation of National Academy of Sciences (technical report .65) which described earlier in section 4.3.3, figure 4.4 shows the recommended distance for the temperature change for both heated and unheated structure.

For this study the building considered as unheated, and the temperature change in˚F

ΔT = 21 ˚C = 69.8 ˚F

The recommended distance from figure 4.4 = 400 ft = 121.92 m

Since the building is unheated the distance shall reduced 33%

= 268 ft = 81.68 m

But the project has two expansion joints with distance in between almost 48 to 49 m.

6. RESULTS AND DISCUSSIONS

In this chapter, the result of the analyze models described in chapter 5 will present and compared between the models to show the effect of the temperature of underground car park under the exclusions mentioned earlier.

6.1 Model A Results

As described in the model A criteria, this model affected by the gravity load (dead and live loads) only, to consider the forces, drift, displacement, and reactions as a base to compare with.

6.1.1 Column axial forces

The maximum axial forces produced in model A as a result to the ultimate gravity loads of dead and live loads presents in figure 6.1, which shows the max amount in column C53 with amount of 4569.99 KN.

6.1.2 Slabs Max and Min Forces

The figures of the slab forces (figure 6.2 , 6.3) for model A showing the normal distribution of the slab forces due to the gravity loads, M_{max} , M_{min}, which shows the logic gravity distribution of the moments as negative in the column location and positive moment in the middle of span between the columns.

6.1.3 Wall Max and Min Forces

The figures of the wall forces (figure 6.4, 6.5) for model A showing the normal distribution of the wall forces due to the gravity loads, M_{max}, M_{min}, as the wall stresses is typical for all the basement walls.

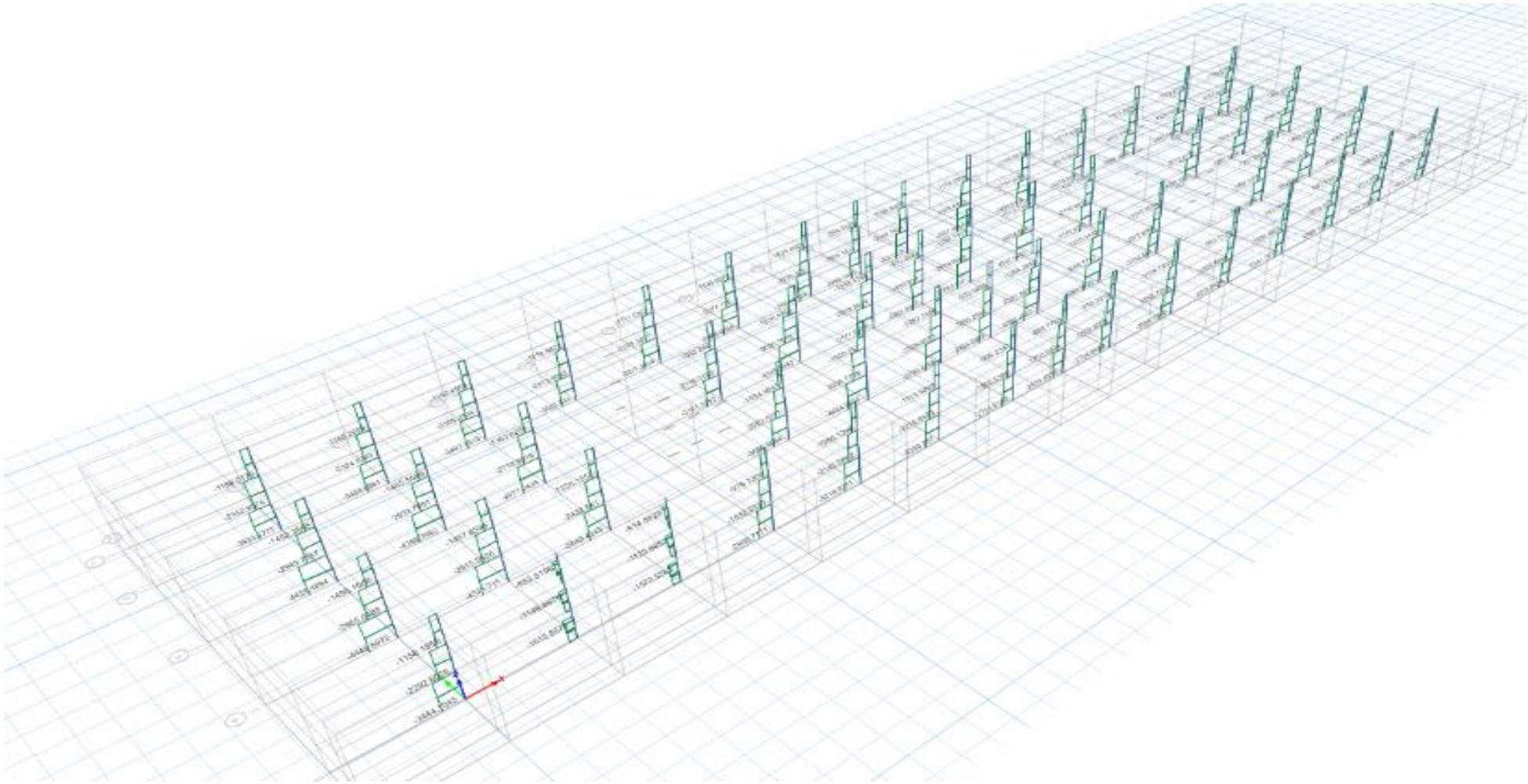

Figure 6.1_ Model A- Columns axial forces

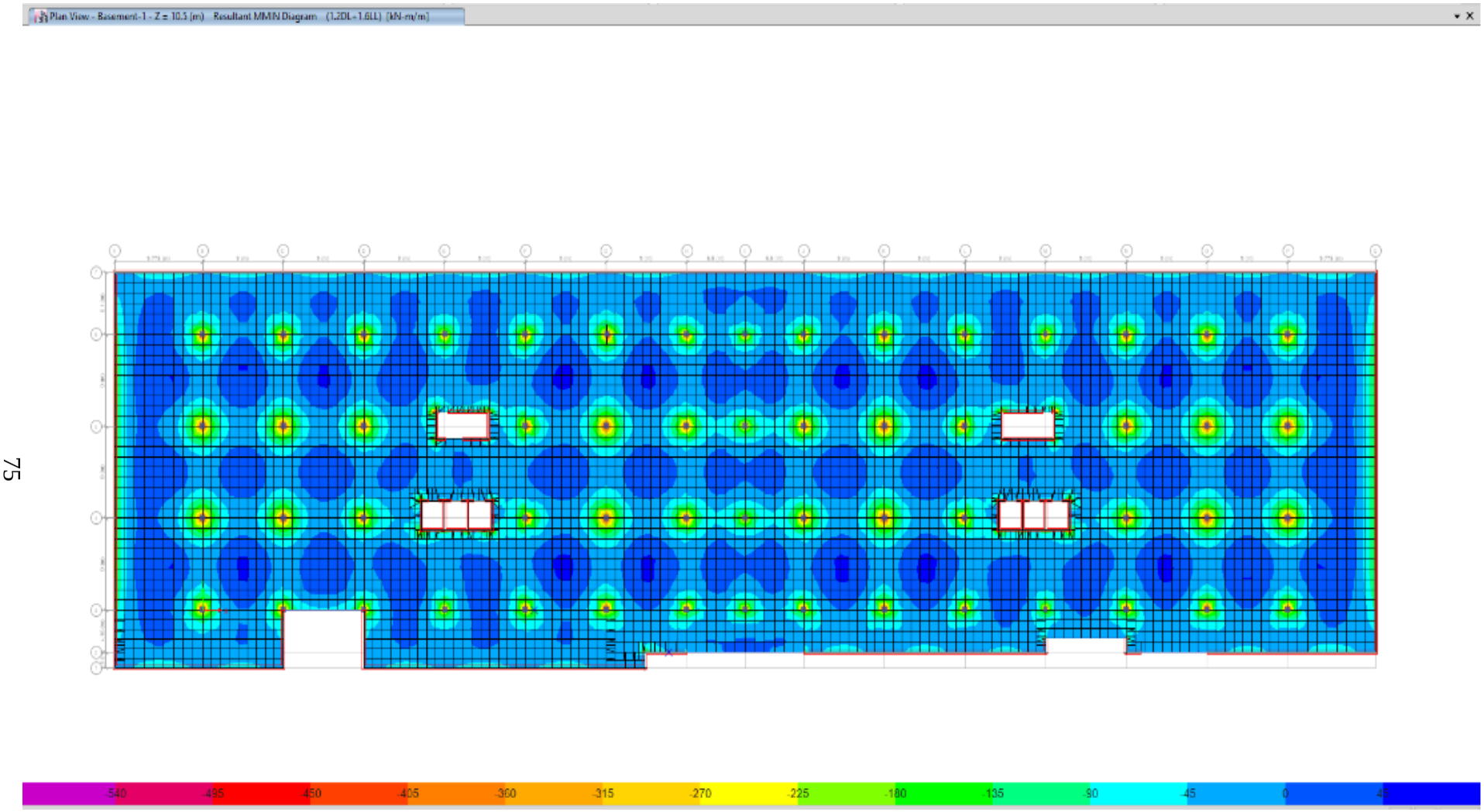

Figure 6.2_ Model A Basement 1 – M_{min} for ultimate loads

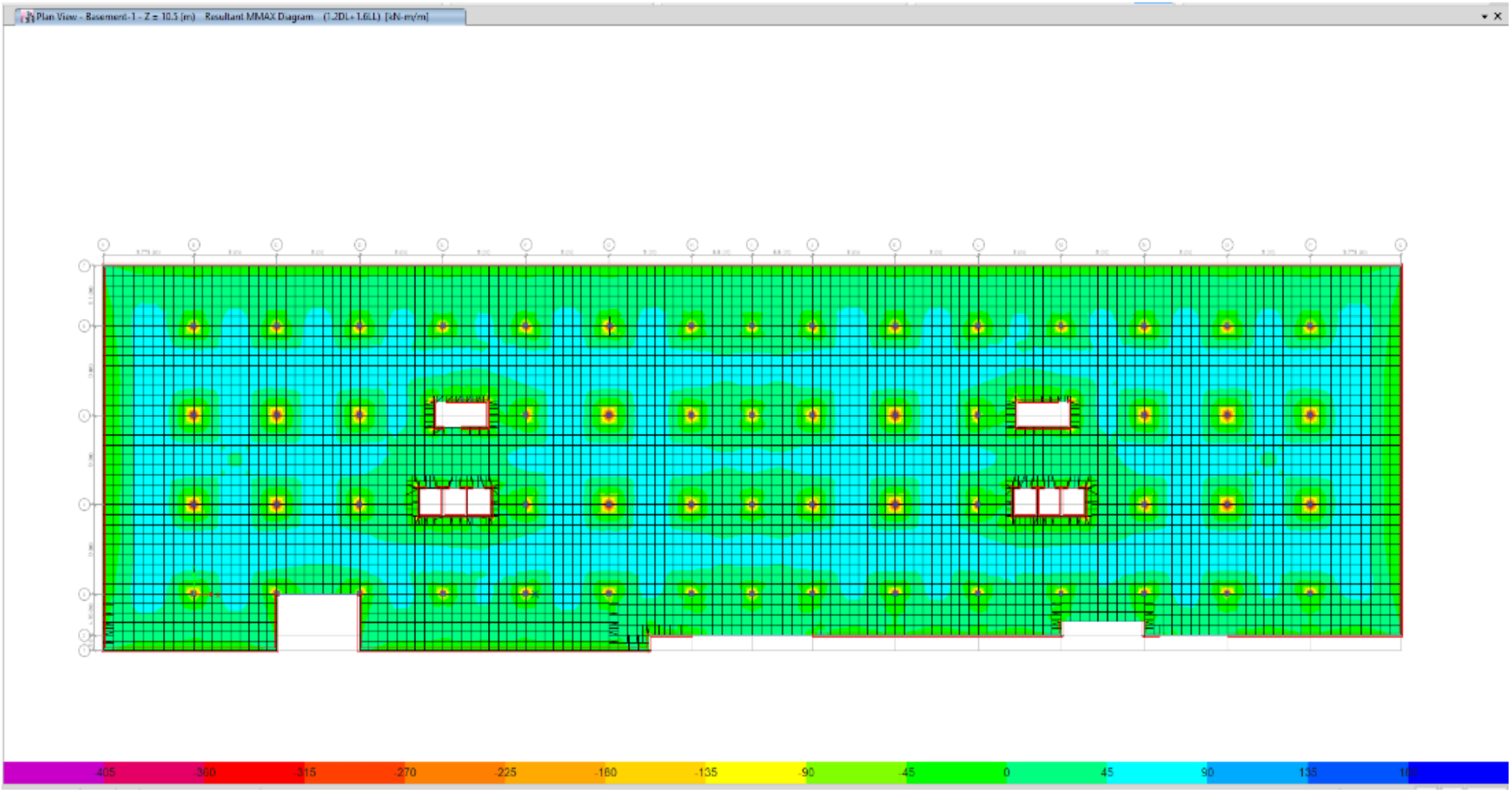

Figure 6.3_ Model A Basement 1 – M_{max} for ultimate loads

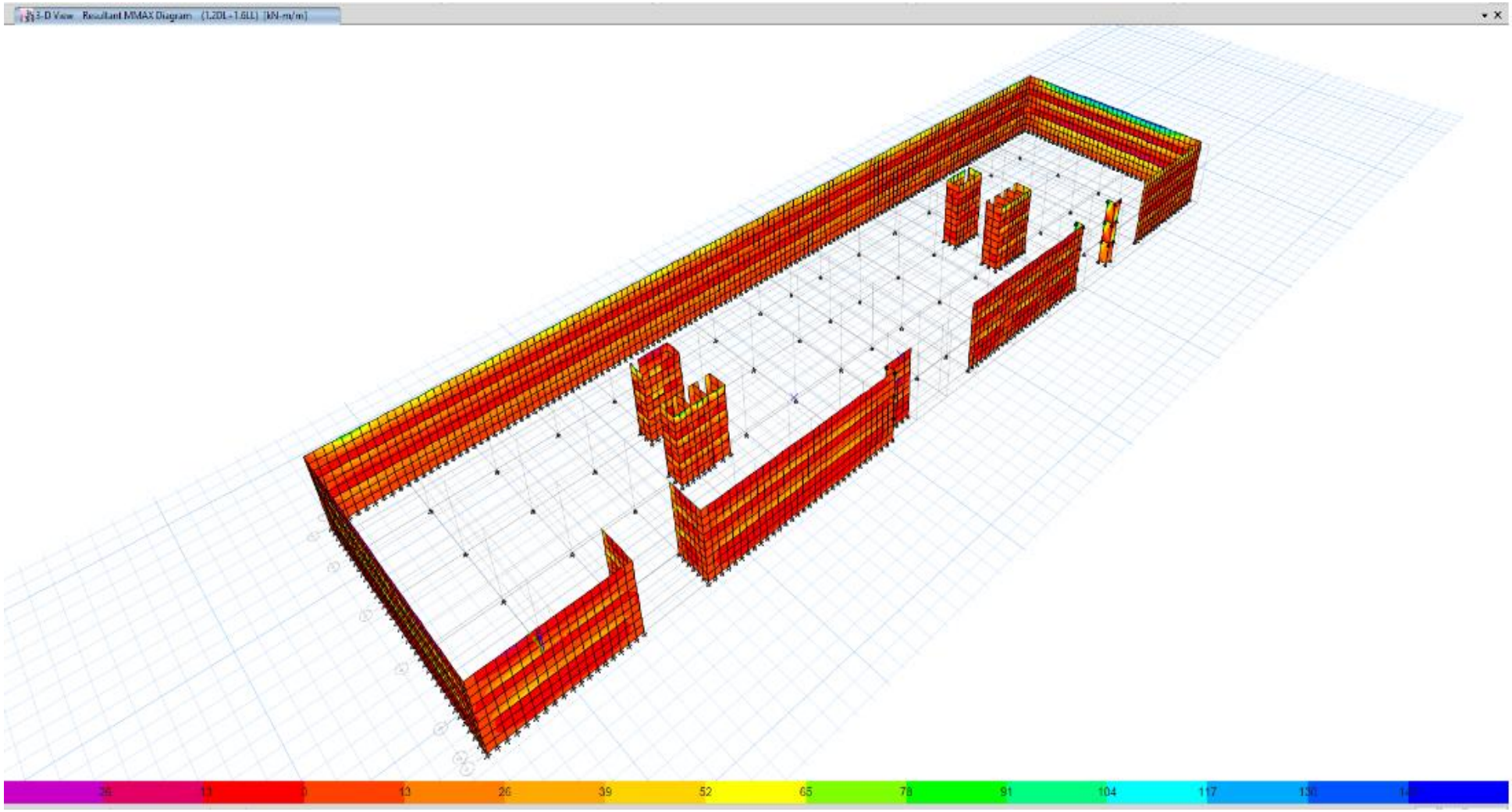

Figure 6.4_ Model A Wall forces – M_{max} for ultimate loads ultimate loads

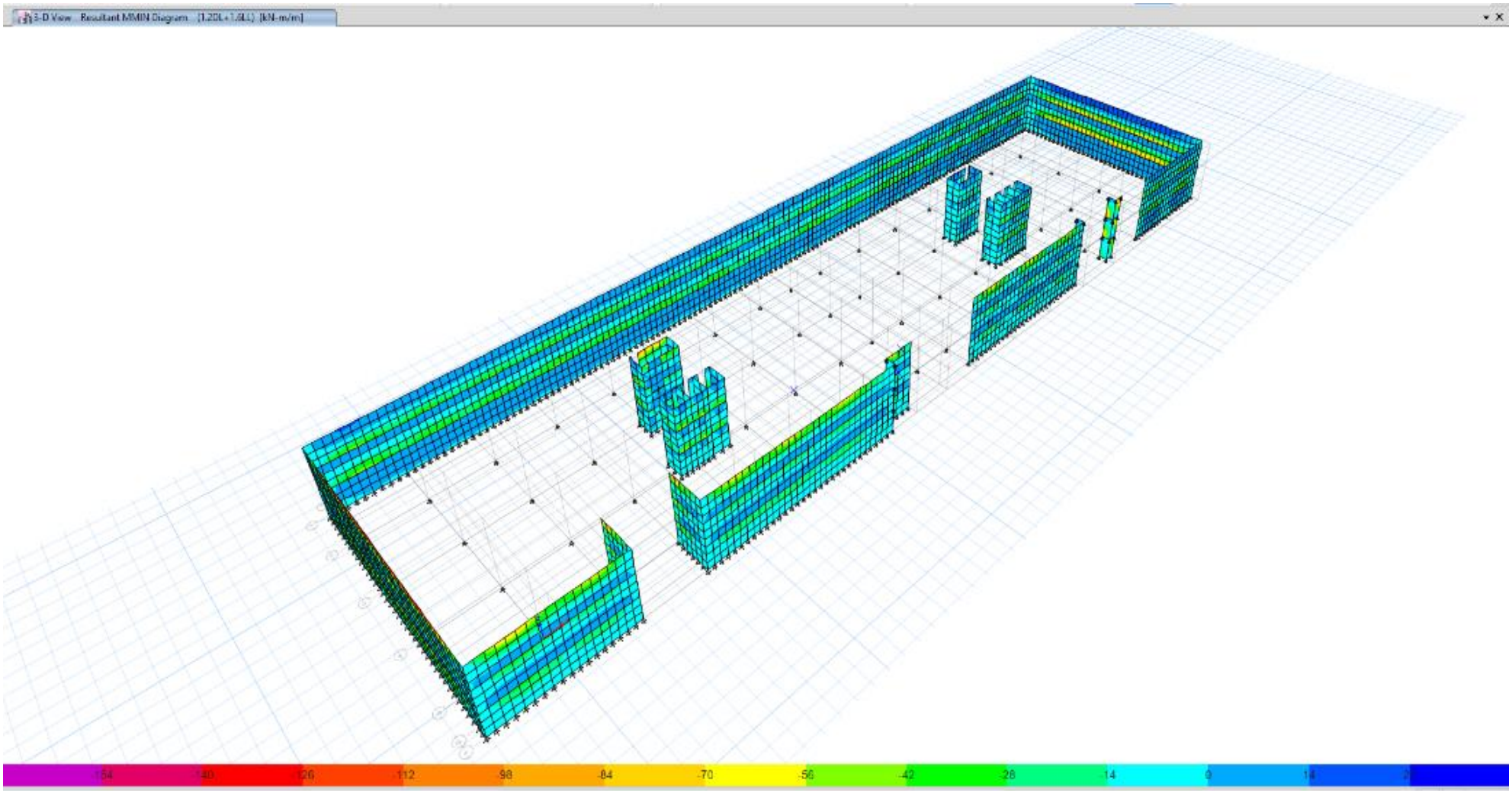

Figure 6.5_ Model A Wall forces – M_{min} for ultimate loads

6.2 Model B Results

In this model the temperature change applied in max and minimum effects, in run the project Etabs software will result the max load in the result from the load combination, the below graph shall show the effect of applying the temperature effect on long building.

6.2.1 Column axial forces

The maximum axial forces produced in model B as a result to the ultimate gravity loads of dead and live loads as well as the temperature change which presents in figure 6.6, the same column of model A had almost same axial force, column C53 with amount of 4571.39 KN.

6.2.2 Slabs Max and Min Forces

The figures of the slab forces for model B showing the distribution of the slab forces due to the gravity loads in addition to the temperature change in absence of expansion joints, M_{max} , M_{min}, which shows the distribution of the moments is not typical between the columns bay in the M_{max} as shows in figure 6.8 , while it is typical in the M_{min} as shows in figure 6.7.

6.2.3 Wall Max and Min Forces

The figures of the wall forces for model B showing that the wall force distribution is not typical in the floors and some area the M_{max} , M_{min}, become more at the middle of the wall as shown in figure 6.9 , and 6.10.

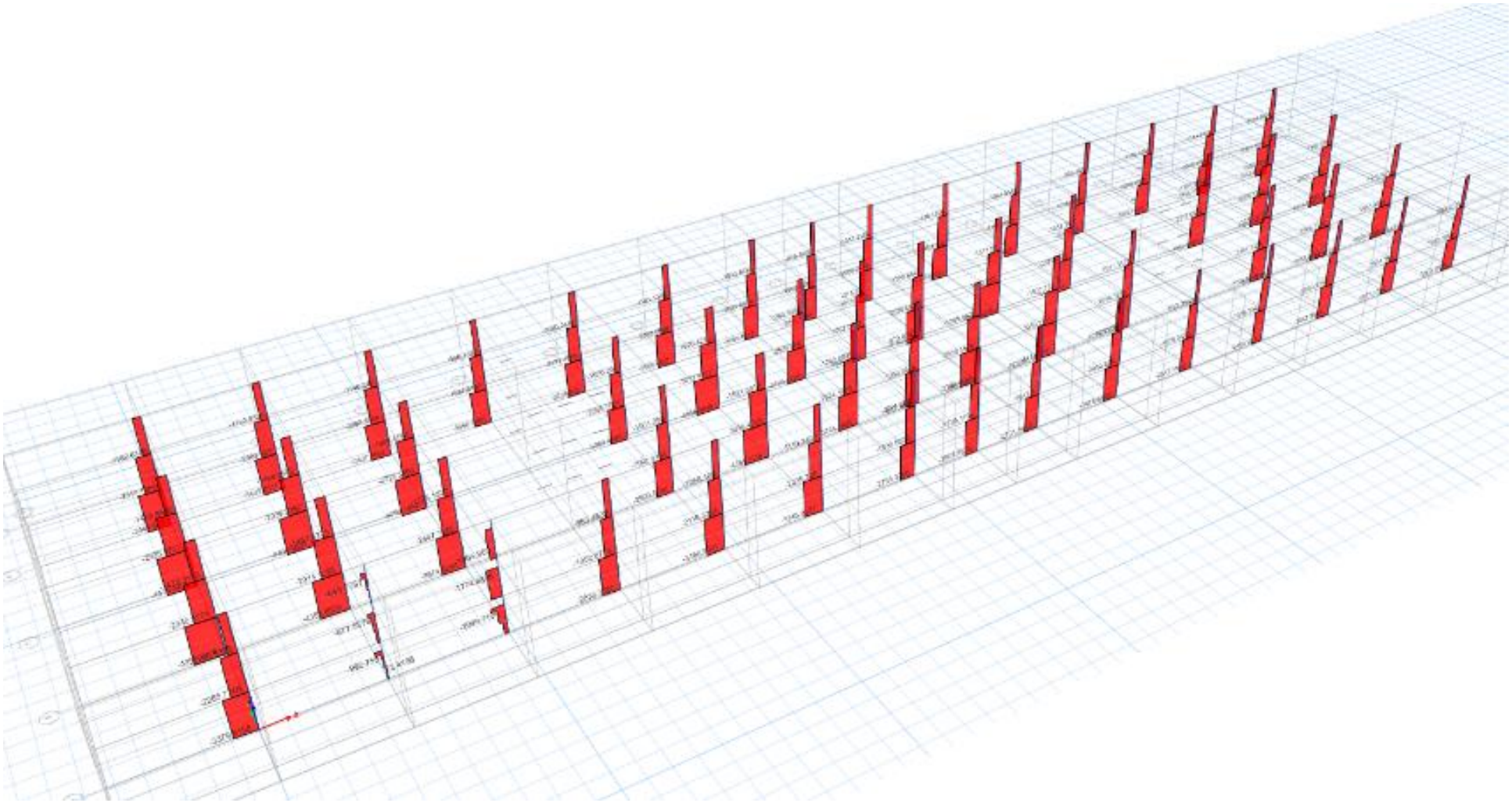

Figure 6.6_ Model B- Columns axial forces

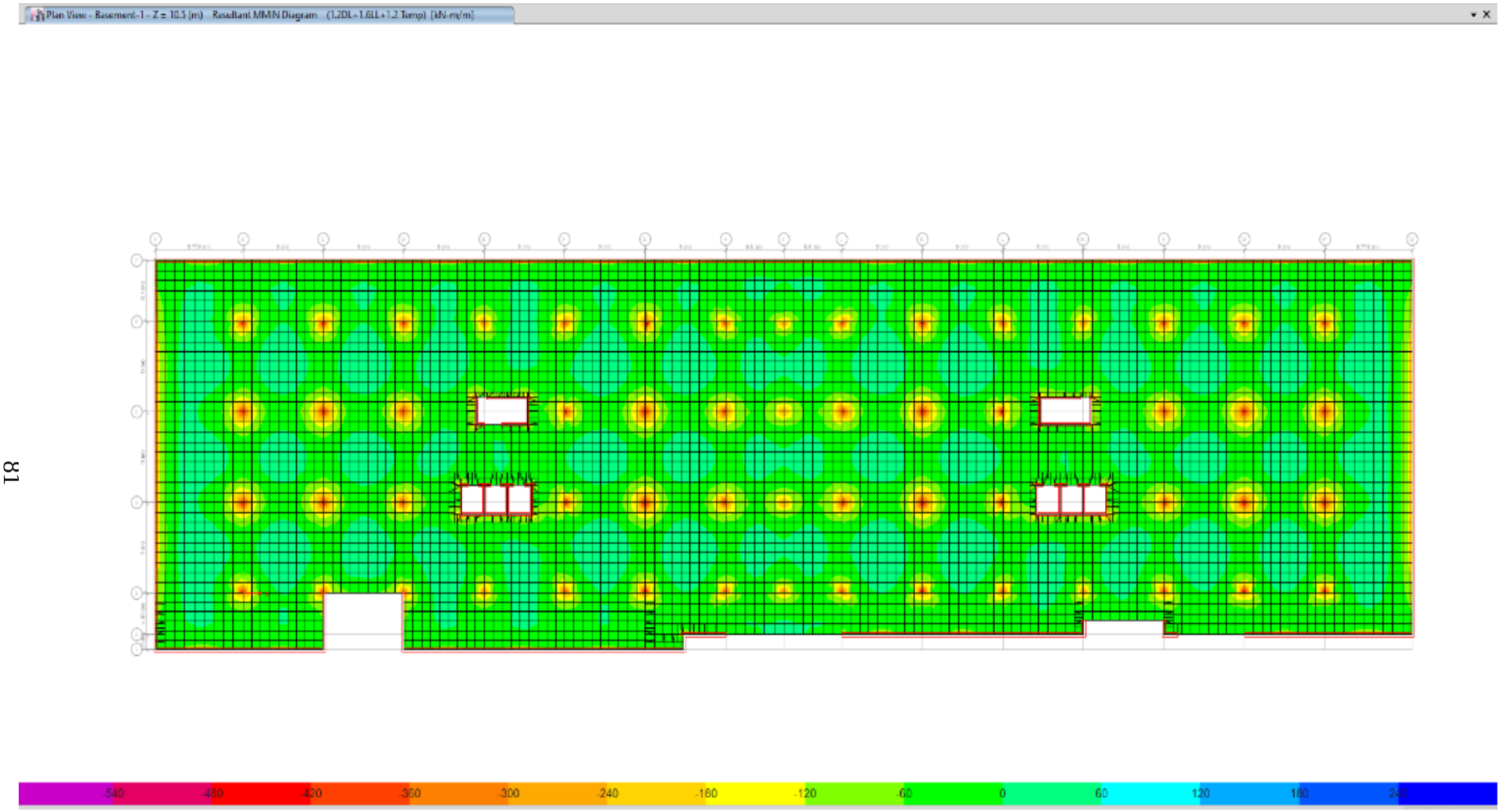

Figure 6.7_ Model B Basement 1 – M_{min} for ultimate loads

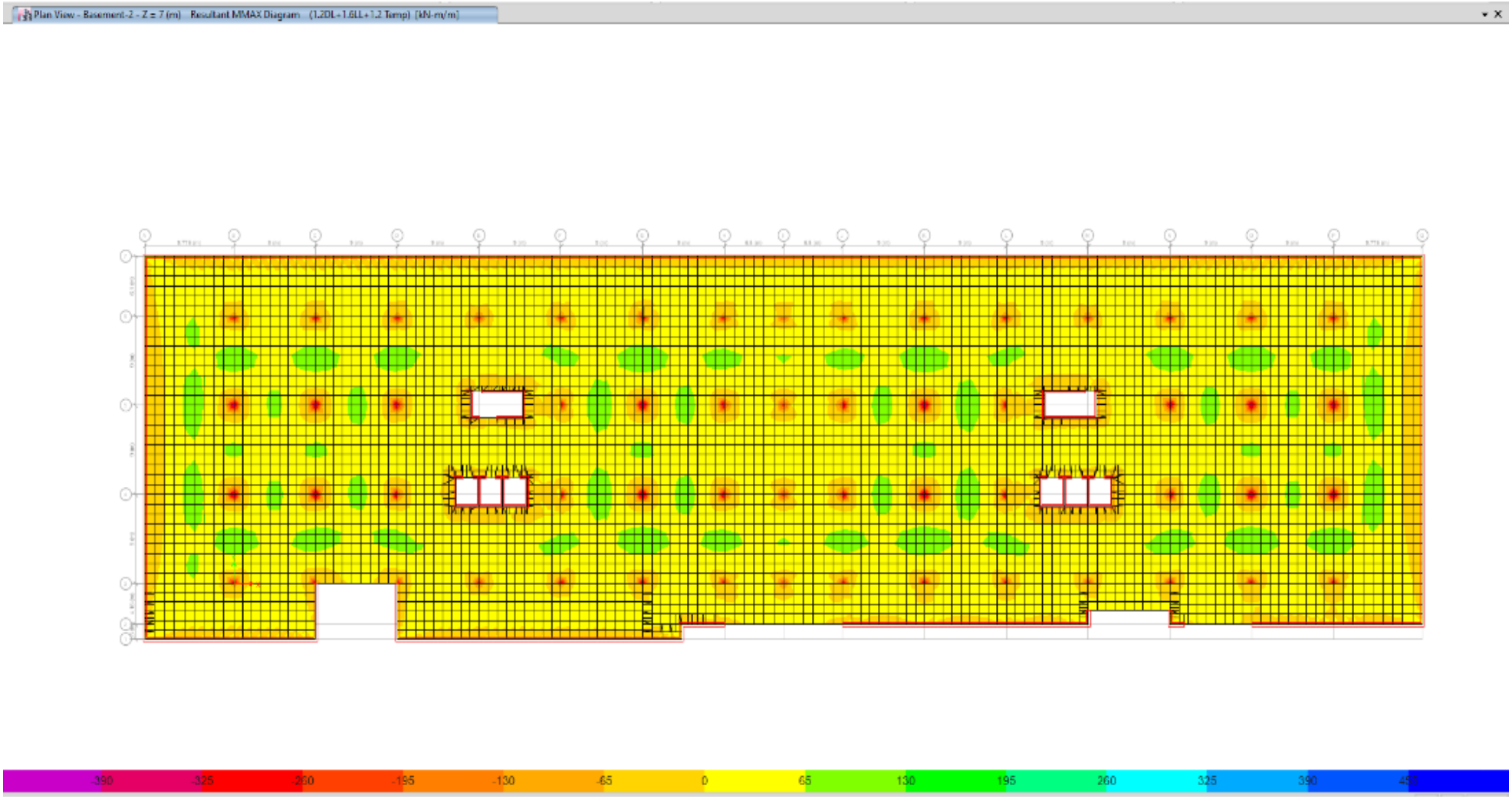

Figure 6.8_ Model B Basement 1 – M_{max} for ultimate loads

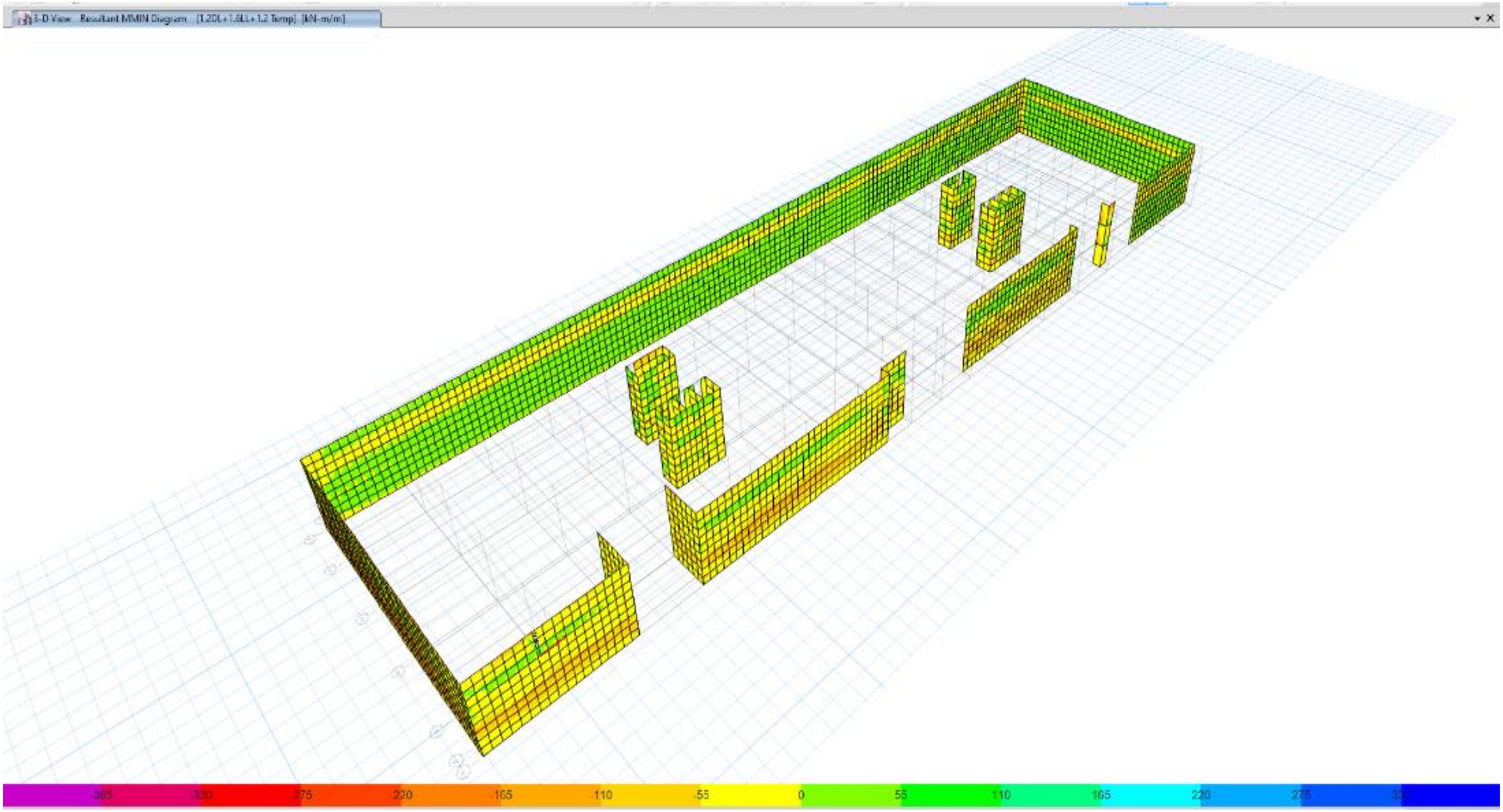

Figure 6.9_ Model B Wall forces – M_{min} for ultimate loads

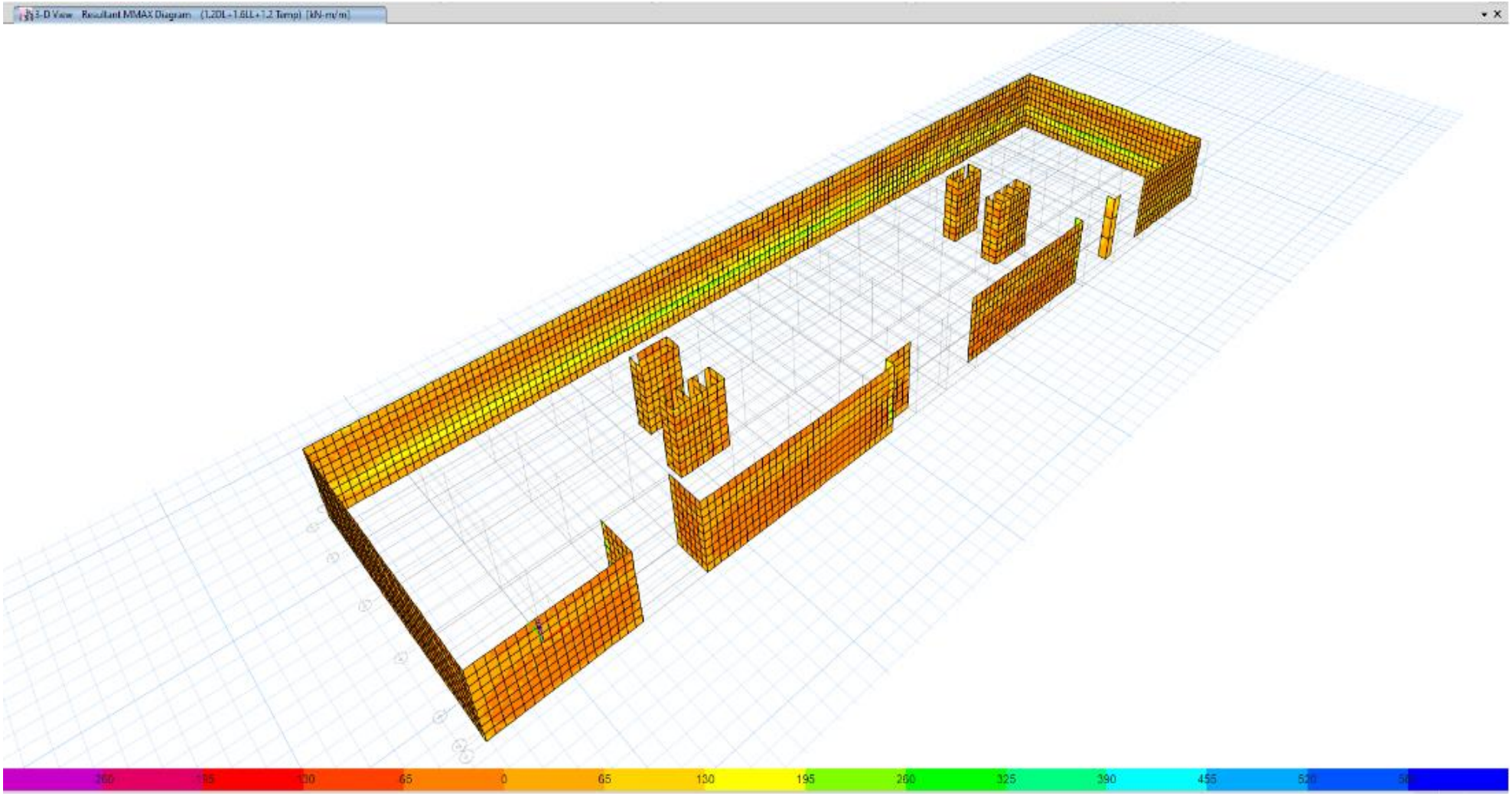

Figure 6.10_ Model B Wall forces – M_{max} for ultimate loads

6.3 Model C Results

In this model two expansion joint applied in the model in addition to the temperature change applied in max and minimum effects, the below graph shall show the effect of applying the temperature effect in the presence of the expansion joints.

6.3.1 Column axial forces

The maximum axial forces produced in model C as a result to the ultimate gravity loads of dead and live loads as well as the temperature change which presents in figure 6.11, the same column of model A and B had almost same axial force, column C53 with amount of 4535.25 KN.

6.3.2 Slabs Max and Min Forces

The figures of the slab forces for model C showing the distribution of the slab forces due to the gravity loads in addition to the temperature change in presence of expansion joints, M_{max}, M_{min}, which shows the distribution of the moments is almost typical between the columns bay in the M_{max} as shows in figure 6.12 , and the M_{min} as shows in figure 6.13.

6.3.3 Wall Max and Min Forces

The figures of the wall forces for model B showing that the wall force distribution is not typical in the floors and some area the M_{max}, M_{min}, become more at the middle of the wall as shown in figure 6.14 , and 6.15 but the force amount become less comparing the B model.

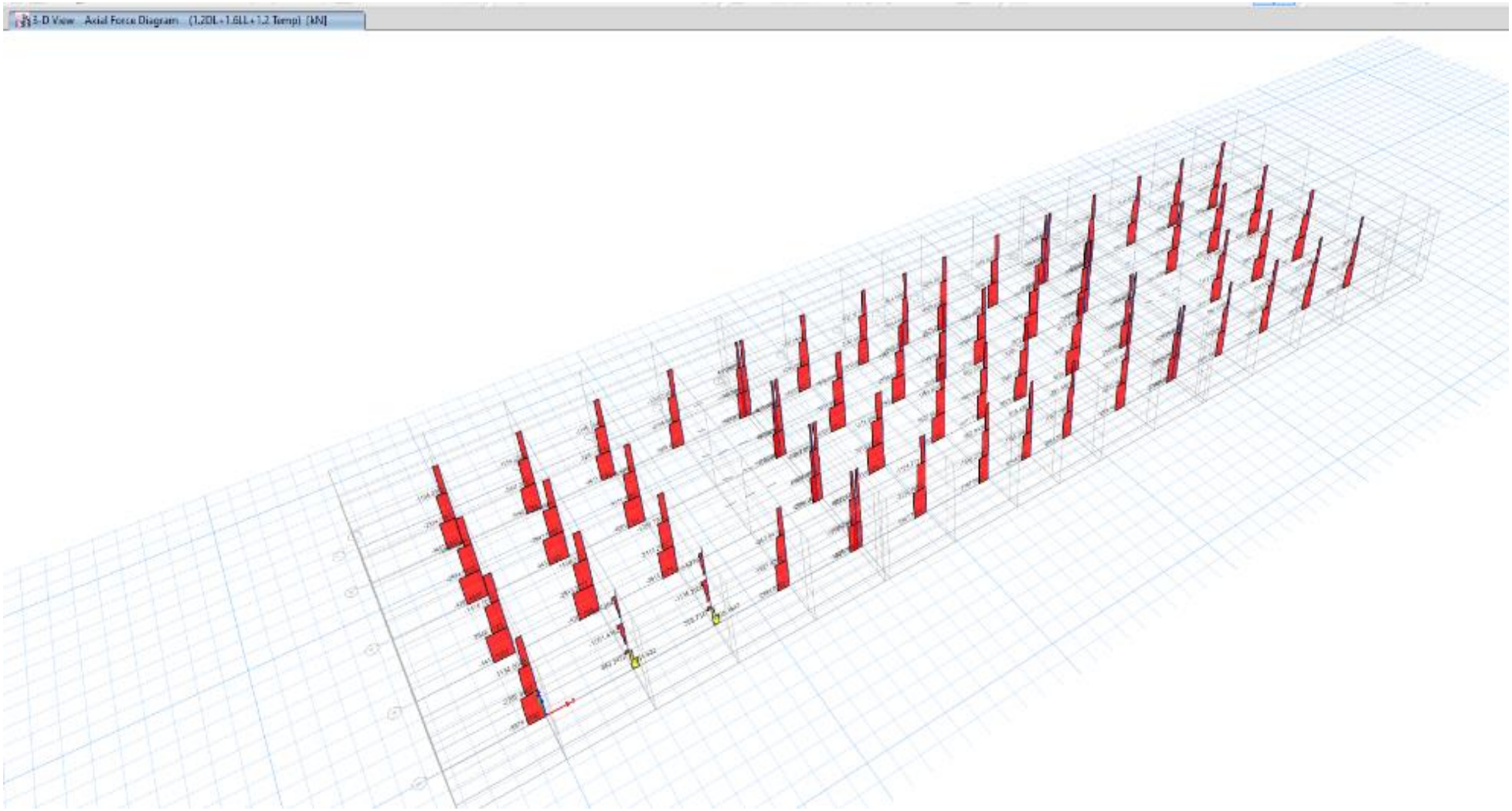

Figure 6.11_ Model C- Columns axial forces

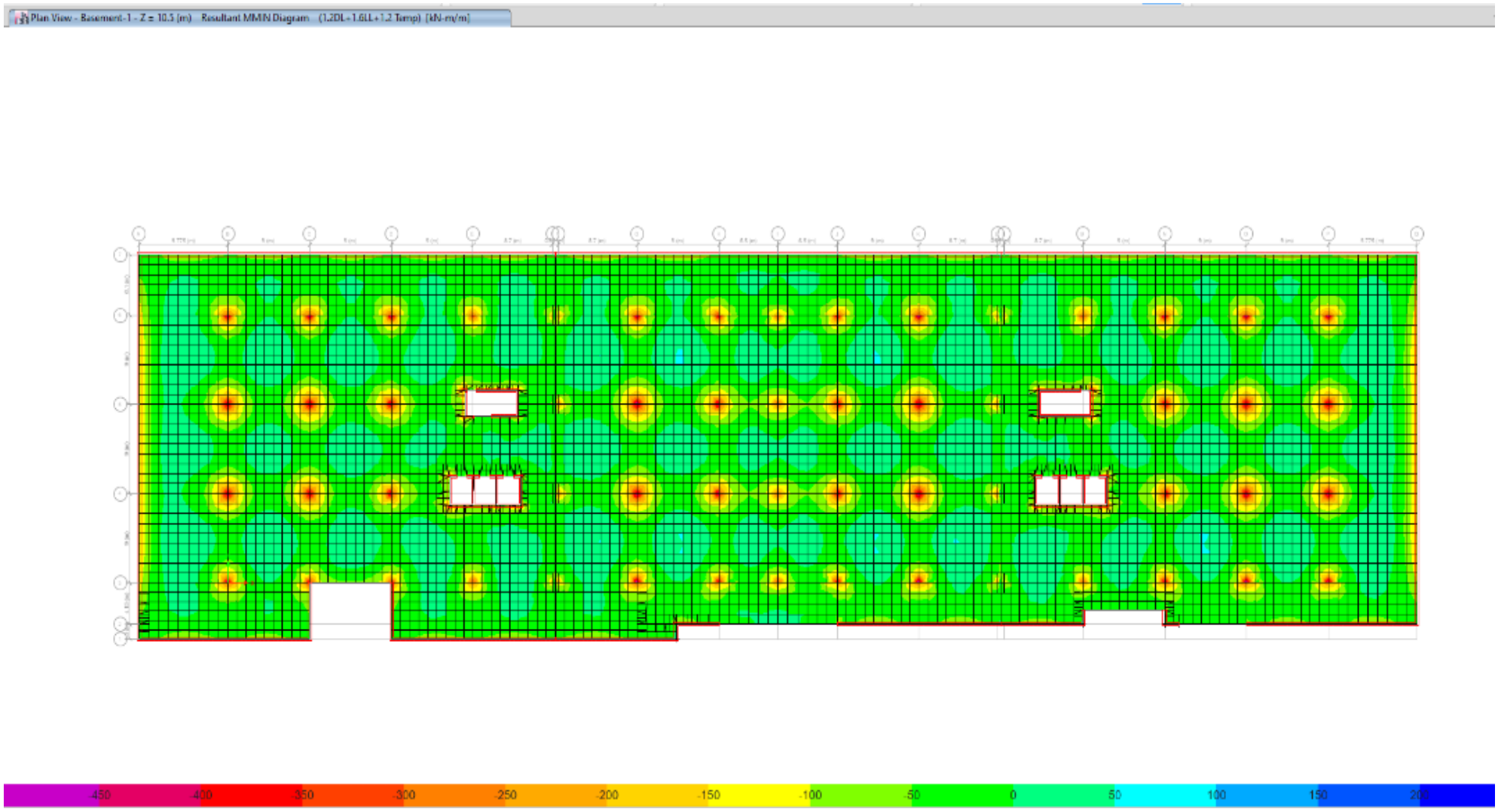

Figure 6.12_ Model C Basement 1 – M_{min} for ultimate loads

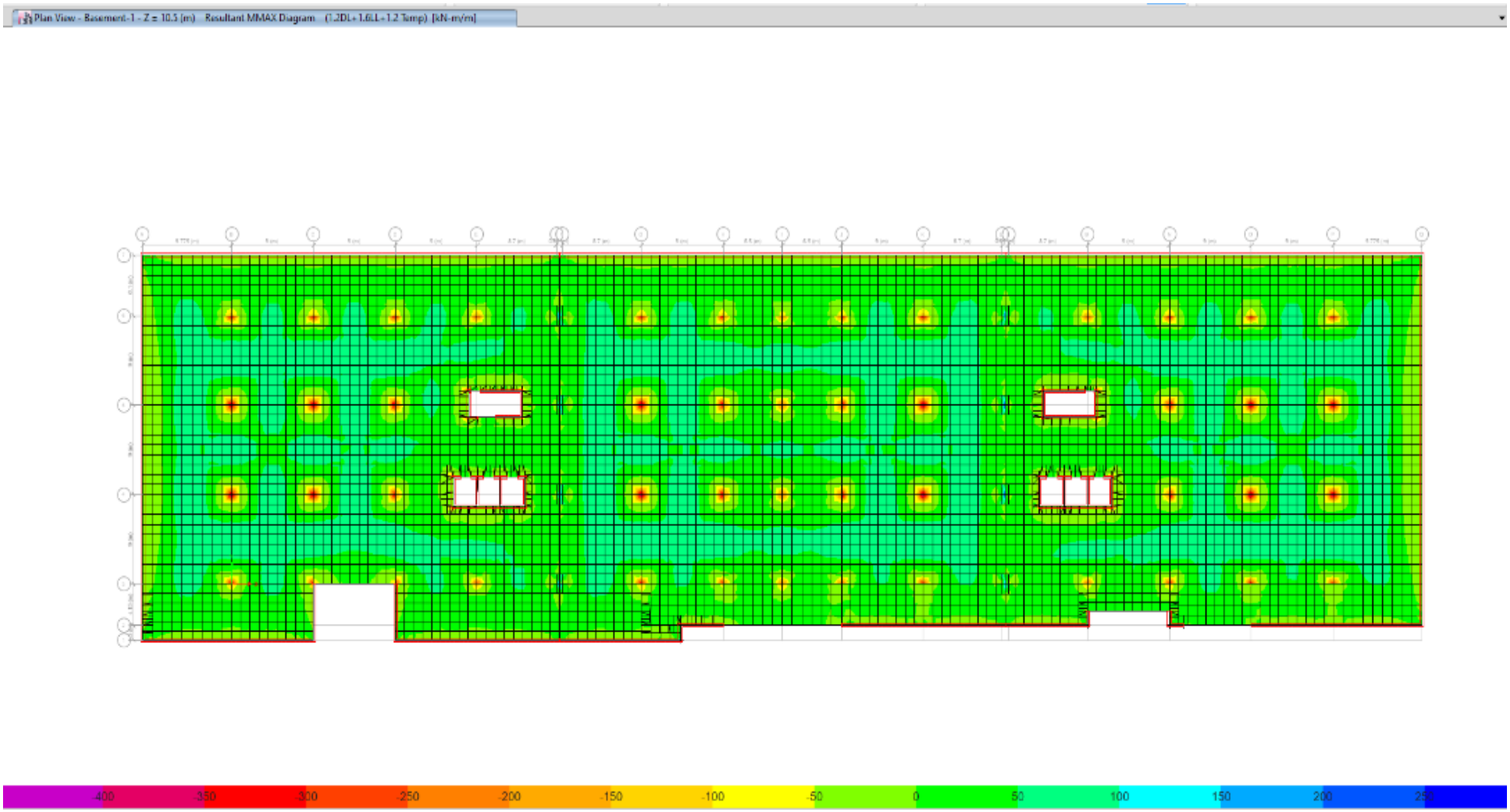

Figure 6.13_ Model C Basement 1 – M_{max} for ultimate loads

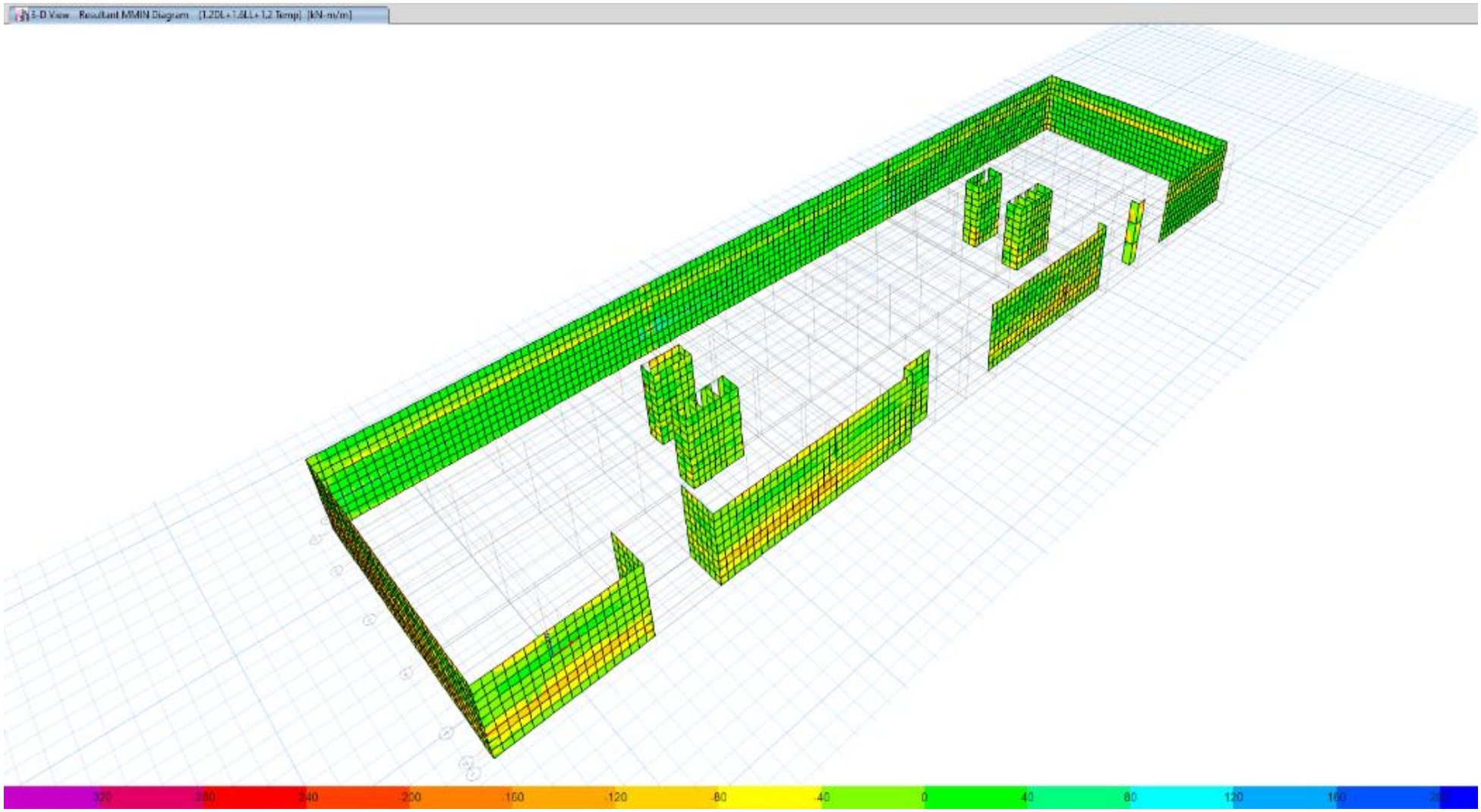

Figure 6.14_ Model C Wall forces – M_{min} for ultimate loads

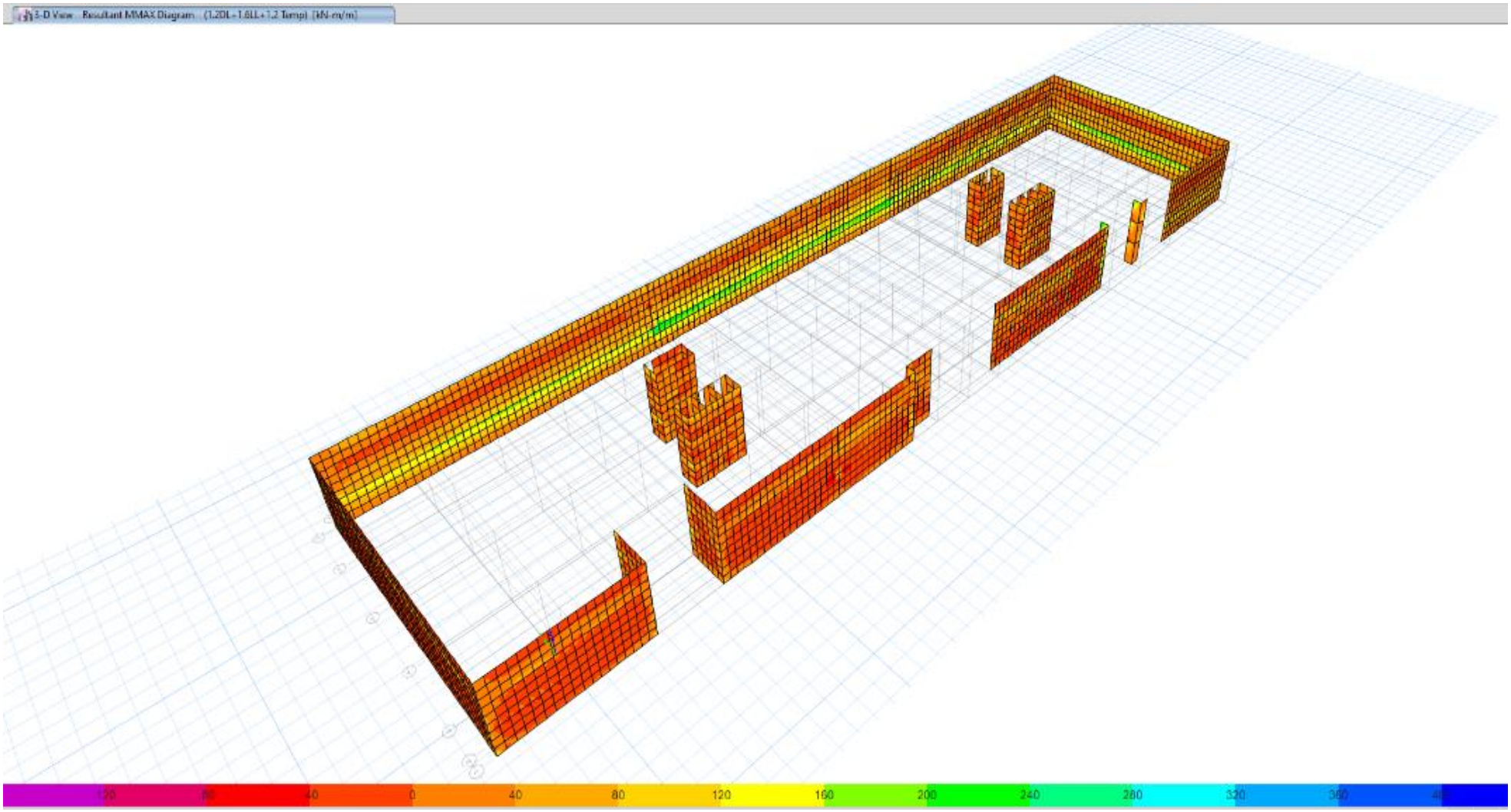

Figure 6.15_ Model C Wall forces – M_{max} for ultimate loads

6.4 Models comparisons:

Reference to the analysis of the three models based on this studied assumption and the results, the comparisons between the three model shall be presented to conclude the best design recommendations for designing such projects like studied project.
The comparison covered, the columns moments distribution, slab moments and the max displacement and drift (this comparison shall me for one element of each, the remain result in Appendix D).

6.4.1 The columns forces comparisons;

The difference of the result of the axial forces between model A , B and C , is not the max moment around the 2- axis (M_{22}) or the max moment around the 3- axis (M_{33}) in the total for each columns in the models , because it will found as max force for the same column in the three models is almost same, while the difference comes from the distribution of these forces between floors.
Figure 6.16, 6.17 and 6.18 shows the difference between model A, model B and model C M_{22} max result at elevation B.
The column located at grid 6- B shows the moment M_{22} at the top of B3 level in model A = -85.77 KN , while in model B shows = -236.99 KN and in model C shows = -226.0 KN , all are negative, and model B and C almost equal , but the amount around double or more the force in model A , which means that the column have to be designed for the moment produced from the temperature effect based on this moment , the same applied in the column located at grid 3-B also , while the middle columns are not affected much.

Figure 6.16_ Model A- Elevation B – M_{22} results

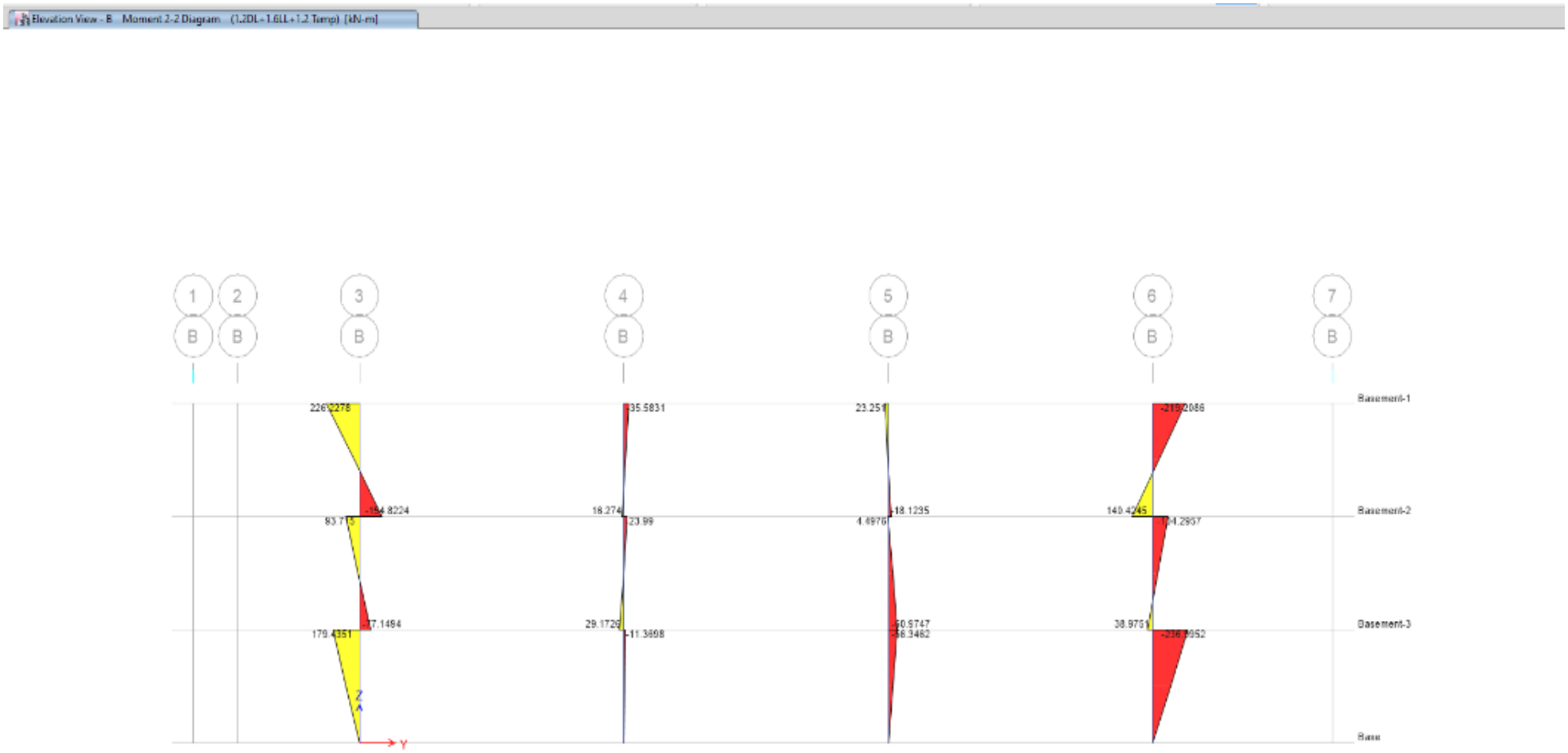

Figure 6.17_ Model B- Elevation B – M_{22} results

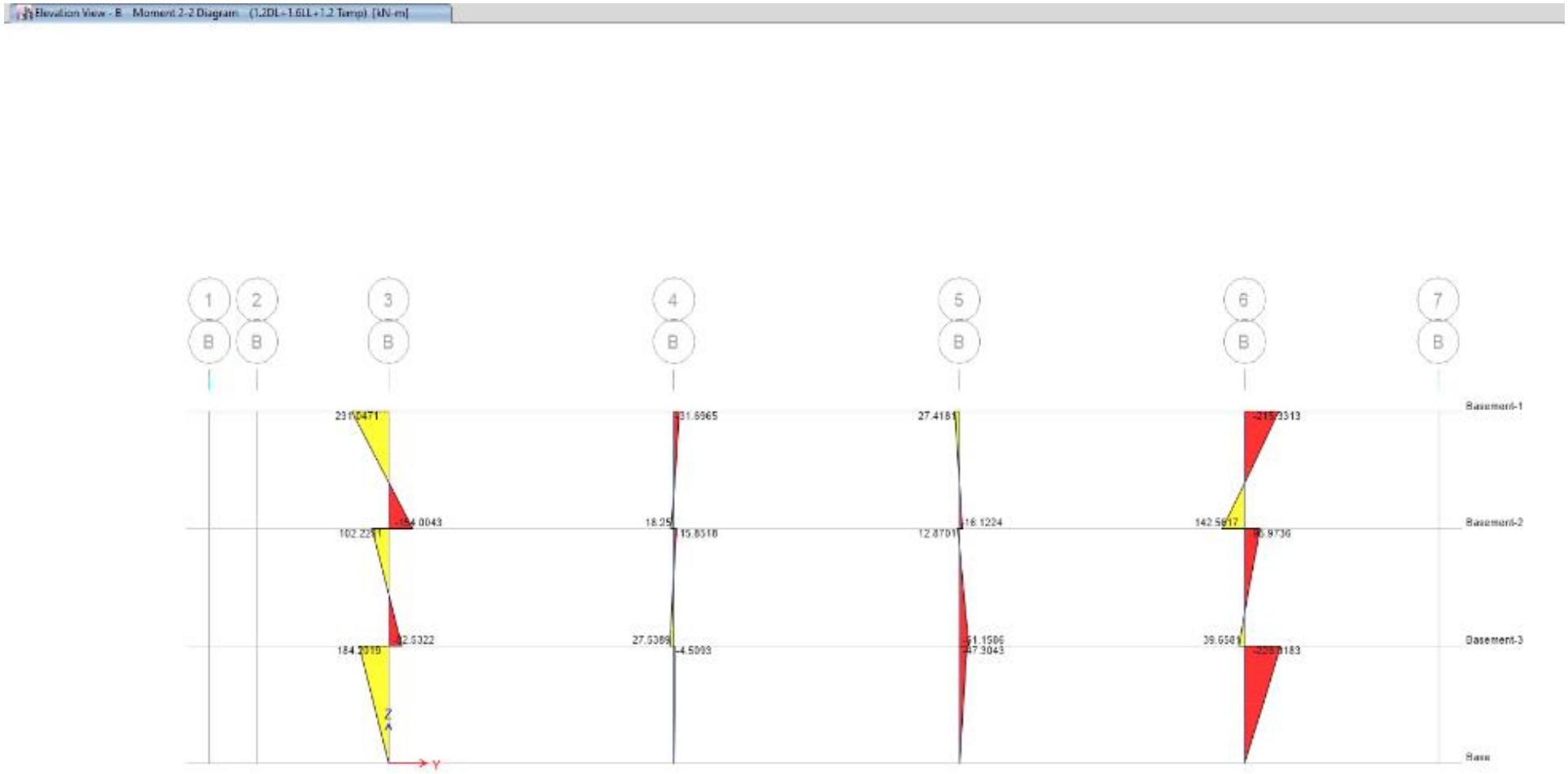

Figure 6.18 _ Model C- Elevation B – M_{22} results

6.4.2 The Slab forces comparisons.

From Figure 6.2 , 6.3 for model A , figure 6.7, 6.8 for model B and figure 6.12 , 6.13 for model C , the slab forces contours show the effect of the temperature change on the forces of the concrete slab (model B) comparing with the slab forces without the temperature effects (model A), and how the expansion joint reduced these forces in (model C).

6.4.3 The Wall forces comparisons.

From Figure 6.4 , 6.5 for model A , figure 6.9 , 6.10 for model B and figure 6.14 , 6.15 for model C , the wall forces contours showing the effect of the temperature change effects on the forces of the concrete wall (model B and model C) comparing with the slab forces without the temperature effects (model A), which need to be considered in the wall designing.

6.4.4 The max building Drift comparisons.

The story drift defined as a relative displacement of one level relative to above or below level, the max drift for the three models are compared through figure 6.19 for drift in X direction and figure 6.20 in Y direction.

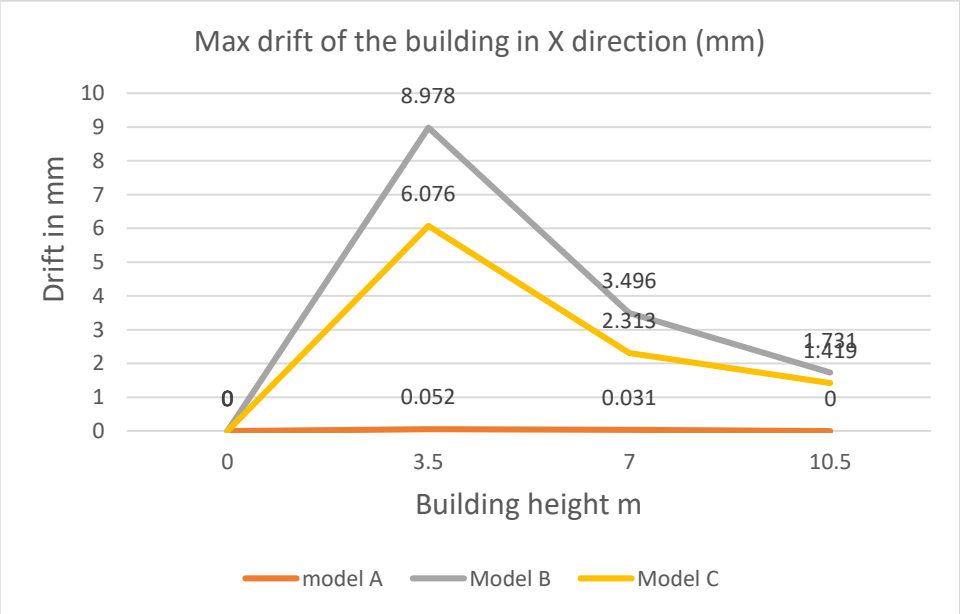

Figure 6.19_ MAX building drift in X direction

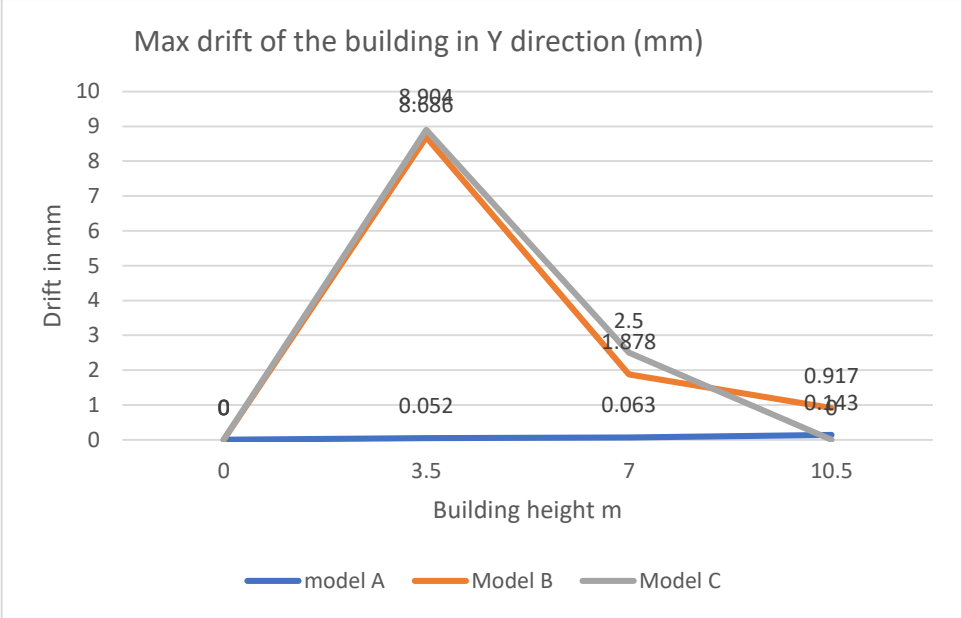

Figure 6.20_ MAX building drift in Y direction

The max building drift in both directions (X & Y) shows the maximum in model B where the temperature is applied in the long building , comparing with model A which the drift near zero this effect the design, the presence of the expansion joint reduce the drift .

6.4.5 The max building displacement comparisons;

The story displacement defined as an average displacement of one level with respect to the base of the structure. the average displacements for the three models are compared through figure 6.21 for displacement in X direction and figure 6.22 in Y direction.

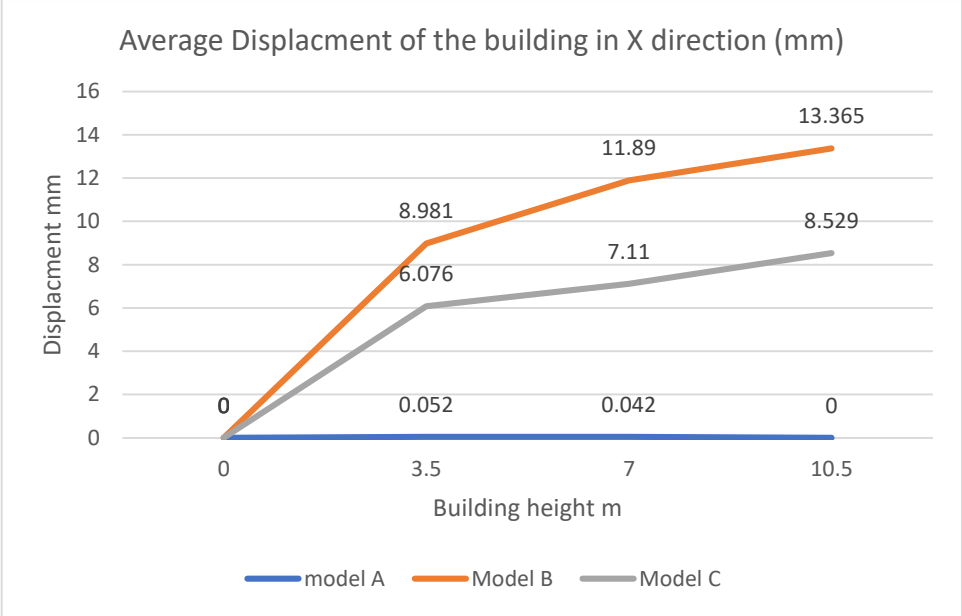

Figure 6.21_ Average building displacement in X direction

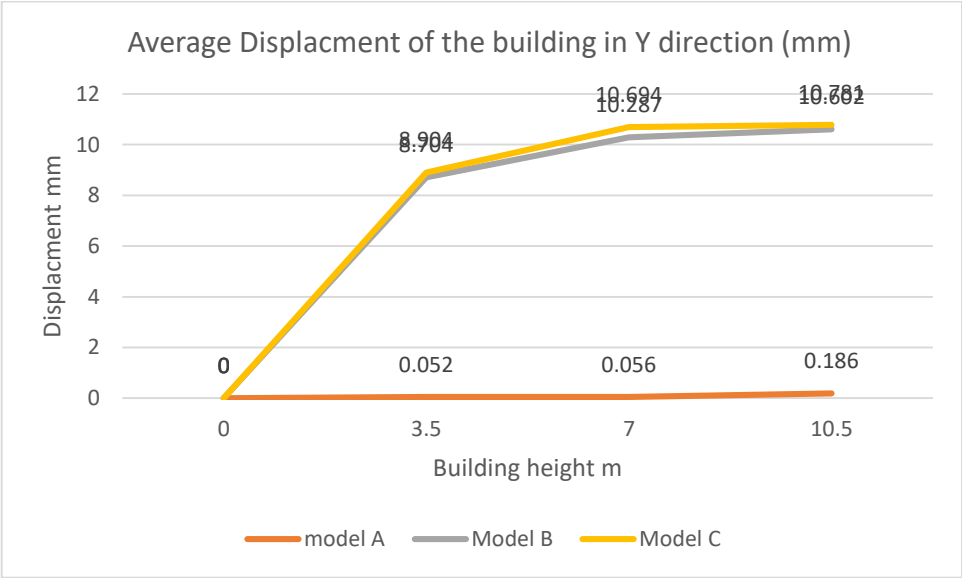

Figure 6.22_ Average building displacement in Y direction

The Average building displacements in both directions (X & Y) shows the maximum in model B where the temperature is applied in the long building , comparing with model A which the drift near zero this effect the design, the presence of the expansion joint reduce the displacement in X direction as it is applied in this direction.

6.4.6 The max columns shear forces (V2 and V3)

The horizontal movements of the slab due to the thermal change are transferring to the columns as shear forces in both direction , figure 6.23 and 6.24 , showing a comparison between the three models for the produced shear forces in the columns at the slab level due to the ultimate load.

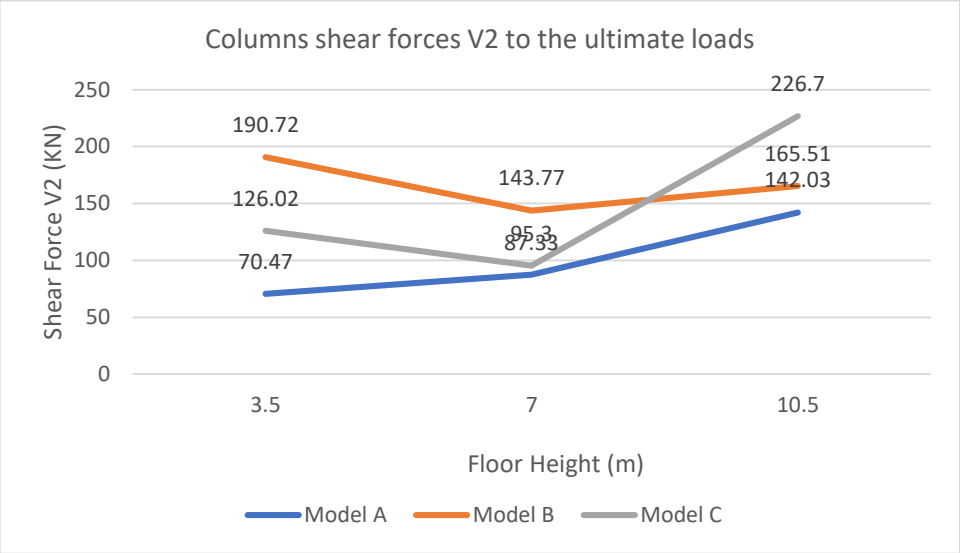

Figure 6.23_ Max column shear forces V2 (KN)

In figure 6.23 the shear forces produced at the column top due to the temperature change had higher value in Model B at basement 3 level where the shear force become 2.5 times the shear force produced Model A. at the same model C had the shear force increased from Model A but the increment around double the value.

At the second floor Model B and C have drop in the shear forces, while in Model A it is increased, then at Basement 1 the Model C result shows a huge increment comparing with the other models.

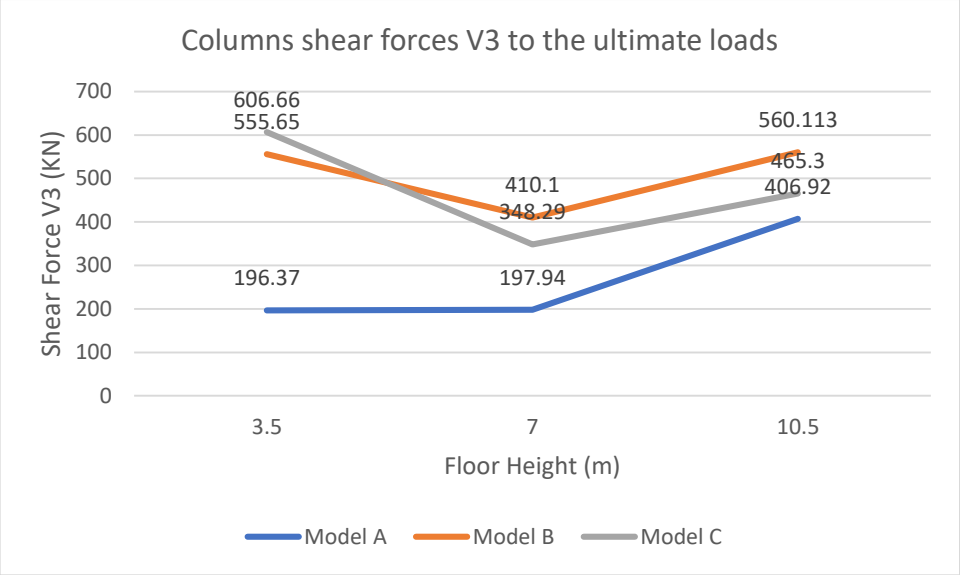

Figure 6.24_ Max column shear forces V3 (KN)

On other hand the shear forces on columns at the other direction V3 shown in Figure 6.24, model B and C had become almost the triple value of the Model A value at basement 3, and model C had greater value which is logic as the expansion joint reduce the restrain of the building along grid F and L . And the values of model B become more than model A and C in the basement 1 and 2.

From this analysis the thermal change increases the shear force on the columns which must be considered specifically at the design stage.

6.5 Conclusion

The results of applying the temperature change during the analysis of underground car park building with and without expansion joints are;

- The temperature changes to be applied during the design of the structure of underground car park, either with building above or not.
- The presence of the expansion joint results in structure with less slab stresses, wall stresses, building drift and displacement, member forces which in-turn lesser section properties and reinforcement hence leading to economical design of the structure.
- The presence of the expansion joint in the underground structure had a huge challenge for the structure durability, due to the underground condition of high-water table and earth pressure, hence studying the temperature change to be done for the structure with the full length.
- The forces produce from the strain forces (temperature change) must be well studied as it is different than the force reduced from the gravity load and will affect the connection design, specially between the wall and slab or columns and slabs.
- This study is the basic comparison for the temperature effect of underground car park structure with the assumption mentioned earlier, and it is missing the earth pressure effect with temperature in the structural design as well as the support type and the seismic analysis.

Appendix B

B-1 Model A ETABS summary report

ETABS® 2016
Integrated Building Design Software

Summary Report

Model File: model-A, Revision 0
1/30/2020

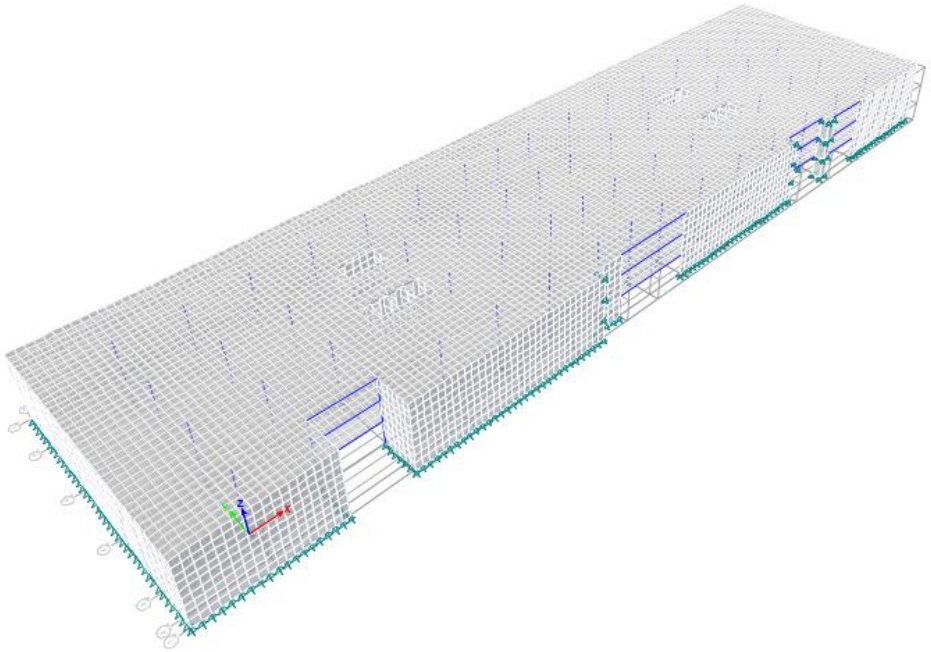

B-1-1 Structure Data

This chapter provides model geometry information, including items such as story levels, point coordinates, and element connectivity.

1.1 Story Data

Table B-1 – Model A Story Data

Name	Height mm	Elevation mm	Master Story	Similar To	Splice Story
Basement-1	3500	10500	No	None	No
Basement-2	3500	7000	No	None	No
Basement-3	3500	3500	No	None	No
Base	0	0	No	None	No

B-1-2 Loads

This chapter provides loading information as applied to the model.

2.1 Load Patterns

Table B-2 - Model A Load Patterns

Name	Type	Self Weight Multiplier
Dead	Dead	1
Live	Live	0

2.2 Load Cases

Table B-3 - Model A Load Cases - Summary

Name	Type
Dead	Linear Static
Live	Linear Static

B-1-3 Analysis Results

This chapter provides analysis results.

3.1 Structure Results

Table B-4 - Model A Base Reactions

Load Case/Combo	FX kN	FY kN	FZ kN	MX kN-m	MY kN-m	MZ kN-m	X m	Y m	Z m
Dead	0	0	195674.0063	2813455.4016	-11716198	-2.399E-06	0	0	0
Live	0	0	54433.1729	782841.663	-3275397	-8.253E-07	0	0	0
Service	0	0	250107.1792	3596297.0645	-14991594	-3.225E-06	0	0	0
1.2DL+1.6LL	0	0	321901.8841	4628693.1426	-19300072	-4.2E-06	0	0	0

Table B-5 - Model A Centers of Mass and Rigidity

Story	Diaphragm	Mass X kg	Mass Y kg	XCM m	YCM m	Cumulative X kg	Cumulative Y kg	XCCM m	YCCM m	XCR m	YCR m
Basement-1	D1	0	0	60.0106	14.3039	0	0	0	0		
Basement-2	D1	0	0	59.8182	14.3919	0	0	0	0		
Basement-3	D1	0	0	59.8182	14.3919	0	0	0	0		

Table B-6 - Model A Diaphragm Center of Mass Displacements

Story	Diaphragm	Load Case/Combo	UX mm	UY mm	RZ rad	Point	X m	Y m	Z m
Basement-1	D1	Dead	-0.002	-0.004	-1E-06	3747	60.0106	14.3039	10.5
Basement-1	D1	Live	0.0004086	-0.003	-1.954E-07	3747	60.0106	14.3039	10.5
Basement-1	D1	Service	-0.001	-0.007	-1E-06	3747	60.0106	14.3039	10.5
Basement-1	D1	1.2DL+1.6LL	-0.001	-0.01	-1E-06	3747	60.0106	14.3039	10.5
Basement-2	D1	Dead	-0.001	0.013	-3.198E-07	3749	59.8182	14.3919	7
Basement-2	D1	Live	0.0003079	0.005	-1.051E-07	3749	59.8182	14.3919	7
Basement-2	D1	Service	-0.0002091	0.018	-4.249E-07	3749	59.8182	14.3919	7
Basement-2	D1	1.2DL+1.6LL	-0.0001277	0.024	-1E-06	3749	59.8182	14.3919	7
Basement-3	D1	Dead	-1.521E-05	0.011	-1.325E-07	3751	59.8182	14.3919	3.5
Basement-3	D1	Live	0.0001233	0.004	-3.667E-08	3751	59.8182	14.3919	3.5
Basement-3	D1	Service	0.0001081	0.015	-1.691E-07	3751	59.8182	14.3919	3.5
Basement-3	D1	1.2DL+1.6LL	0.0001791	0.02	-2.176E-07	3751	59.8182	14.3919	3.5

3.2 Story Results

Table B-7 - Model A Story Max/Avg Displacements

Story	Load Case/Combo	Direction	Maximum mm	Average mm	Ratio
Basement-1	Dead	Y	0.133	0.044	3.059
Basement-2	Dead	X	0.031	0.004	7.533
Basement-2	Dead	Y	0.04	0.012	3.333
Basement-3	Dead	X	0.038	0.001	45.489
Basement-3	Dead	Y	0.039	0.004	9.419
Basement-1	Live	Y	0.047	0.015	3.111
Basement-2	Live	X	0.01	0.002	5.853
Basement-2	Live	Y	0.014	0.005	2.673
Basement-3	Live	X	0.013	0.0004096	31.433
Basement-3	Live	Y	0.011	0.002	7.071
Basement-1	Service	Y	0.18	0.059	3.072
Basement-2	Service	X	0.041	0.006	6.537
Basement-2	Service	Y	0.054	0.017	3.131

Story	Load Case/Combo	Direction	Maximum mm	Average mm	Ratio
Basement-3	Service	X	0.05	0.001	40.736
Basement-3	Service	Y	0.05	0.006	8.755
Basement-1	1.2DL+1.6LL	Y	0.235	0.076	3.075
Basement-2	1.2DL+1.6LL	X	0.053	0.008	6.479
Basement-2	1.2DL+1.6LL	Y	0.07	0.023	3.088
Basement-3	1.2DL+1.6LL	X	0.066	0.002	39.784
Basement-3	1.2DL+1.6LL	Y	0.065	0.008	8.61

Table B-8 - Model A Story Drifts

Story	Load Case/Combo	Direction	Drift	Label	X m	Y m	Z m
Basement-1	Dead	Y	2.9E-05	101	18	0	10.5
Basement-1	Live	Y	1.1E-05	101	18	0	10.5
Basement-1	Service	Y	4E-05	101	18	0	10.5
Basement-1	1.2DL+1.6LL	Y	5.2E-05	101	18	0	10.5
Basement-2	Dead	X	7E-06	88	-9.775	-5.65	7
Basement-2	Dead	Y	1.3E-05	102	18	-5.65	7
Basement-2	Live	X	2E-06	88	-9.775	-5.65	7
Basement-2	Live	Y	4E-06	102	18	-5.65	7
Basement-2	Service	X	9E-06	88	-9.775	-5.65	7
Basement-2	Service	Y	1.7E-05	102	18	-5.65	7
Basement-2	1.2DL+1.6LL	X	1.1E-05	88	-9.775	-5.65	7
Basement-2	1.2DL+1.6LL	Y	2.3E-05	102	18	-5.65	7
Basement-3	Dead	X	1.1E-05	2662	130.775	16	3.5
Basement-3	Dead	Y	1.1E-05	70	-9.775	33.1	3.5
Basement-3	Live	X	4E-06	2661	130.775	15	3.5
Basement-3	Live	Y	3E-06	70	-9.775	33.1	3.5
Basement-3	Service	X	1.4E-05	2662	130.775	16	3.5
Basement-3	Service	Y	1.4E-05	70	-9.775	33.1	3.5
Basement-3	1.2DL+1.6LL	X	1.9E-05	2662	130.775	16	3.5
Basement-3	1.2DL+1.6LL	Y	1.9E-05	70	-9.775	33.1	3.5

Table B-9- Model A Story Forces

Story	Load Case/Combo	Location	P kN	VX kN	VY kN	T kN-m	MX kN-m	MY kN-m
Basement-1	Dead	Top	48646.0366	-536.0359	-86.9564	-13110.1533	710674.173	-2911211
Basement-1	Dead	Bottom	64179.2395	-536.0359	-86.9564	-13110.1533	941991.7449	-3824635
Basement-1	Live	Top	17950.3553	-125.0001	-20.0183	-3718.256	261599.0348	-1076588
Basement-1	Live	Bottom	17950.3553	-125.0001	-20.0183	-3718.256	261669.0987	-1077025
Basement-1	Service	Top	66596.392	-661.036	-106.9747	-16828.4094	972273.2078	-3987799
Basement-1	Service	Bottom	82129.5948	-661.036	-106.9747	-16828.4094	1203660.8436	-4901660
Basement-1	1.2DL+1.6LL	Top	87095.8125	-843.2432	-136.377	-21681.3937	1271367.4632	-5215994
Basement-1	1.2DL+1.6LL	Bottom	105735.6559	-843.2432	-136.377	-21681.3937	1549060.6518	-6312802
Basement-2	Dead	Top	112440.6381	-564.1309	-19.4063	-9170.1492	1654432.4958	-6709547
Basement-2	Dead	Bottom	127973.8409	-564.1309	-19.4063	-9170.1492	1885513.642	-7623069
Basement-2	Live	Top	35867.2519	-131.5594	-1.5952	-2670.248	523441.5327	-2151512
Basement-2	Live	Bottom	35867.2519	-131.5594	-1.5952	-2670.248	523447.116	-2151973
Basement-2	Service	Top	148307.89	-695.6903	-21.0015	-11840.3972	2177874.0285	-8861059
Basement-2	Service	Bottom	163841.0928	-695.6903	-21.0015	-11840.3972	2408960.758	-9775041
Basement-2	1.2DL+1.6LL	Top	192316.3687	-887.4522	-25.8399	-15276.5758	2822825.4473	-11493876
Basement-2	1.2DL+1.6LL	Bottom	210956.2122	-887.4522	-25.8399	-15276.5758	3100131.756	-12590839

Story	Load Case/Combo	Location	P kN	VX kN	VY kN	T kN-m	MX kN-m	MY kN-m
Basement-3	Dead	Top	176438.2313	-379.1243	41.3783	-3832.4177	2597038.3685	-10521166
Basement-3	Dead	Bottom	191971.4342	-379.1243	41.3783	-3832.4177	2827906.7689	-11434041
Basement-3	Live	Top	53819.896	-90.2764	13.0121	-1344.6615	785060.2056	-3228944
Basement-3	Live	Bottom	53819.896	-90.2764	13.0121	-1344.6615	785014.6634	-3229260
Basement-3	Service	Top	230258.1274	-469.4007	54.3903	-5177.0792	3382098.5741	-13750110
Basement-3	Service	Bottom	245791.3302	-469.4007	54.3903	-5177.0792	3612921.4323	-14663301
Basement-3	1.2DL+1.6LL	Top	297837.7112	-599.3914	70.4732	-6750.3596	4372542.3711	-17791710
Basement-3	1.2DL+1.6LL	Bottom	316477.5547	-599.3914	70.4732	-6750.3596	4649511.5841	-18887665

3.3 Modal Results

Table B-10 - Model A Modal Periods and Frequencies

Case	Mode	Period sec	Frequency cyc/sec	Circular Frequency rad/sec	Eigenvalue rad²/sec²
Modal	1	0.111	9.021	56.6779	3212.3863
Modal	2	0.081	12.351	77.6025	6022.1462
Modal	3	0.075	13.352	83.8945	7038.2932
Modal	4	0.074	13.428	84.3706	7118.3903
Modal	5	0.066	15.259	95.8744	9191.9045
Modal	6	0.057	17.573	110.4163	12191.7487
Modal	7	0.057	17.623	110.7296	12261.043
Modal	8	0.054	18.583	116.7621	13633.3974
Modal	9	0.051	19.719	123.8956	15350.1094
Modal	10	0.045	22.351	140.4359	19722.2319
Modal	11	0.043	23.271	146.2139	21378.4991
Modal	12	0.043	23.347	146.6904	21518.0754

Table B-11 - Model A Modal Participating Mass Ratios (Part 1 of 2)

Case	Mode	Period sec	UX	UY	UZ	Sum UX	Sum UY	Sum UZ
Modal	1	0.111	0.0155	0.6097	0	0.0155	0.6097	0
Modal	2	0.081	0.0341	0.1421	0	0.0496	0.7518	0
Modal	3	0.075	0.6497	0.0269	0	0.6993	0.7788	0
Modal	4	0.074	0.004	0.0604	0	0.7034	0.8392	0
Modal	5	0.066	0.019	0.0676	0	0.7224	0.9068	0
Modal	6	0.057	0.0945	0.0273	0	0.8169	0.9341	0
Modal	7	0.057	0.0022	0.0057	0	0.8191	0.9398	0
Modal	8	0.054	0.0006	0.0019	0	0.8197	0.9417	0
Modal	9	0.051	0.0306	0.0028	0	0.8503	0.9445	0
Modal	10	0.045	0.0005	0.0165	0	0.8508	0.961	0
Modal	11	0.043	0.0096	0.004	0	0.8604	0.9649	0
Modal	12	0.043	0.0438	0.0007	0	0.9042	0.9656	0

Table B-12 - Model A Modal Participating Mass Ratios (Part 2 of 2)

Case	Mode	RX	RY	RZ	Sum RX	Sum RY	Sum RZ
Modal	1	0.1665	0.0034	0.1664	0.1665	0.0034	0.1664
Modal	2	0.0133	0.0061	0.4574	0.1798	0.0095	0.6238
Modal	3	0.0007	0.135	0.0076	0.1805	0.1445	0.6315
Modal	4	0.5227	3.572E-06	0.0087	0.7031	0.1445	0.6402
Modal	5	0.004	0.004	0.1256	0.7072	0.1484	0.7658

Case	Mode	RX	RY	RZ	Sum RX	Sum RY	Sum RZ
Modal	6	0.0004	0.0175	0.0032	0.7076	0.166	0.769
Modal	7	0.0347	0.0004	0.0011	0.7422	0.1663	0.77
Modal	8	0.0075	0.0034	0.0616	0.7497	0.1697	0.8316
Modal	9	0	0.0068	0.0778	0.7497	0.1765	0.9094
Modal	10	0.1422	0.0023	0.0021	0.892	0.1788	0.9115
Modal	11	0.0007	0.1922	0.0044	0.8927	0.371	0.9159
Modal	12	0.0056	0.2265	2.731E-05	0.8983	0.5975	0.916

Table B-13 - Model A Modal Load Participation Ratios

Case	Item Type	Item	Static %	Dynamic %
Modal	Acceleration	UX	98.31	90.42
Modal	Acceleration	UY	99.77	96.56
Modal	Acceleration	UZ	0	0

Table B-14 - Model A Modal Direction Factors

Case	Mode	Period sec	UX	UY	UZ	RZ
Modal	1	0.111	0.023	0.95	0	0.026
Modal	2	0.081	0.201	0.796	0	0.003
Modal	3	0.075	0.952	0.036	0	0.012
Modal	4	0.074	0.006	0.993	0	0.001
Modal	5	0.066	0.14	0.458	0	0.402
Modal	6	0.057	0.06	0.022	0	0.918
Modal	7	0.057	0.004	0.909	0	0.087
Modal	8	0.054	0.007	0.019	0	0.975
Modal	9	0.051	0.024	0.002	0	0.973
Modal	10	0.045	0.014	0.758	0	0.229
Modal	11	0.043	0.773	0.019	0	0.208
Modal	12	0.043	0.844	0.017	0	0.139

B-2 Model B ETABS summary report

Summary Report

Model File: model-B, Revision 0
1/30/2020

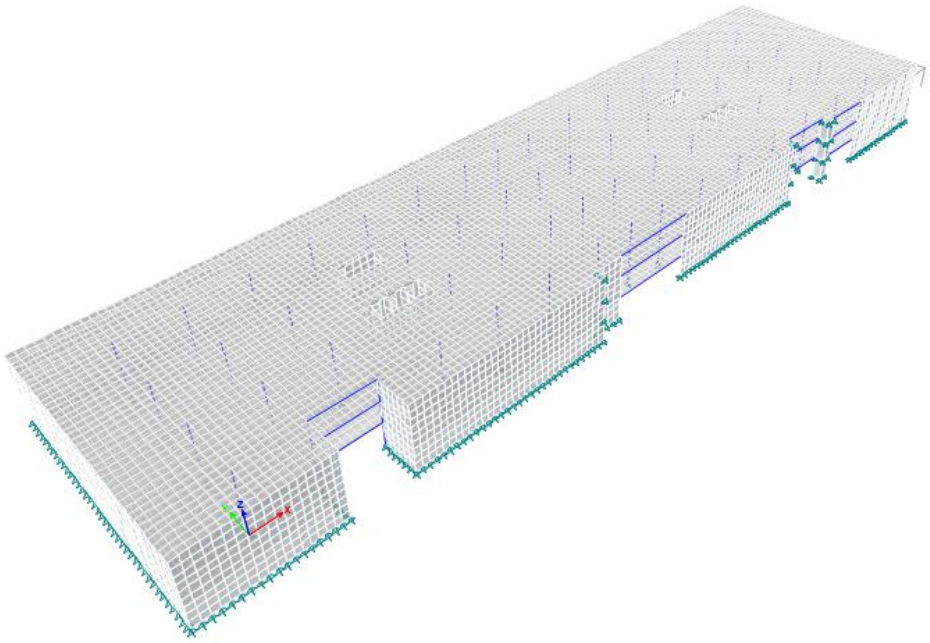

B-2-1 Structure Data

This chapter provides model geometry information, including items such as story levels, point coordinates, and element connectivity.

1.1 Story Data

Table B-15 - Model B Story Data

Name	Height mm	Elevation mm	Master Story	Similar To	Splice Story
Basement-1	3500	10500	No	None	No
Basement-2	3500	7000	No	None	No
Basement-3	3500	3500	No	None	No
Base	0	0	No	None	No

B-2-2 Loads

This chapter provides loading information as applied to the model.

2.1 Load Patterns

Table B-16 - Model B Load Patterns

Name	Type	Self Weight Multiplier
Dead	Dead	1
Live	Live	0
Temp	Other	0

2.2 Load Cases

Table B-17 - Model B - Load Cases - Summary

Name	Type
Dead	Linear Static
Live	Linear Static
temp	Nonlinear Static

B-2-3 Analysis Results

This chapter provides analysis results.

3.1 Structure Results

Table B-18 - Model B - Base Reactions

Load Case/Combo	FX kN	FY kN	FZ kN	MX kN-m	MY kN-m	MZ kN-m	X m	Y m	Z m
Dead	0	0	195674.0063	2813455.4016	-11716198	-2.126E-06	0	0	0
Live	0	0	54433.1729	782841.663	-3275397	-7.215E-07	0	0	0
temp Max	-4.755E-06	-1.007E-05	-1.749E-06	2.08E-05	-4.927E-06	-0.0002	0	0	0
temp Min	-4.755E-06	-1.007E-05	-1.749E-06	2.08E-05	-4.927E-06	-0.0002	0	0	0
Service	-4.75E-06	-1.017E-05	250107.1792	3596297.0646	-14991594	-0.0002	0	0	0
1.2DL+1.6LL+1.2 Temp	-5.699E-06	-1.221E-05	321901.8841	4628693.1427	-19300072	-0.0002	0	0	0

Table B-19 - Model B Centers of Mass and Rigidity

Story	Diaphragm	Mass X kg	Mass Y kg	XCM m	YCM m	Cumulative X kg	Cumulative Y kg	XCCM m	YCCM m	XCR m	YCR m
Basement-1	D1	0	0	60.0106	14.3039	0	0	0	0		
Basement-2	D1	0	0	59.8182	14.3919	0	0	0	0		
Basement-3	D1	0	0	59.8182	14.3919	0	0	0	0		

Table B-20- Model B Diaphragm Center of Mass Displacements

Story	Diaphragm	Load Case/Combo	UX mm	UY mm	RZ rad	Point	X m	Y m	Z m
Basement-1	D1	Dead	-0.001	-0.006	-1E-06	3753	60.0106	14.3039	10.5
Basement-1	D1	Live	0.0004257	-0.004	-1.914E-07	3753	60.0106	14.3039	10.5
Basement-1	D1	temp Max	-0.941	5.17	2.1E-05	3753	60.0106	14.3039	10.5
Basement-1	D1	temp Min	-0.941	5.17	2.1E-05	3753	60.0106	14.3039	10.5
Basement-1	D1	Service	-0.942	5.16	2E-05	3753	60.0106	14.3039	10.5
Basement-1	D1	1.2DL+1.6LL+1.2 Temp	-1.13	6.19	2.4E-05	3753	60.0106	14.3039	10.5
Basement-2	D1	Dead	-0.0004714	0.013	-3.213E-07	3755	59.8182	14.3919	7
Basement-2	D1	Live	0.0003237	0.004	-1.066E-07	3755	59.8182	14.3919	7
Basement-2	D1	temp Max	-0.868	4.879	1.7E-05	3755	59.8182	14.3919	7
Basement-2	D1	temp Min	-0.868	4.879	1.7E-05	3755	59.8182	14.3919	7
Basement-2	D1	Service	-0.868	4.896	1.7E-05	3755	59.8182	14.3919	7
Basement-2	D1	1.2DL+1.6LL+1.2 Temp	-1.042	5.877	2E-05	3755	59.8182	14.3919	7
Basement-3	D1	Dead	-1.146E-05	0.011	-1.339E-07	4747	59.8182	14.3919	3.5
Basement-3	D1	Live	0.0001271	0.004	-3.812E-08	4747	59.8182	14.3919	3.5
Basement-3	D1	temp Max	-0.475	3.479	5E-06	4747	59.8182	14.3919	3.5
Basement-3	D1	temp Min	-0.475	3.479	5E-06	4747	59.8182	14.3919	3.5
Basement-3	D1	Service	-0.475	3.494	4E-06	4747	59.8182	14.3919	3.5
Basement-3	D1	1.2DL+1.6LL+1.2 Temp	-0.57	4.194	5E-06	4747	59.8182	14.3919	3.5

3.2 Story Results

Table B-21- Model B Story Max/Avg Displacements

Story	Load Case/Combo	Direction	Maximum mm	Average mm	Ratio
Basement-1	Dead	Y	0.13	0.042	3.121
Basement-2	Dead	X	0.031	0.004	7.67
Basement-2	Dead	Y	0.04	0.012	3.367
Basement-3	Dead	X	0.038	0.001	42.792
Basement-3	Dead	Y	0.039	0.004	9.764
Basement-1	Live	Y	0.046	0.014	3.233
Basement-2	Live	X	0.01	0.001	6.575
Basement-2	Live	Y	0.014	0.005	2.697
Basement-3	Live	X	0.013	0.0004314	29.84
Basement-3	Live	Y	0.011	0.002	7.304
Basement-1	temp Max	X	13.365	0.952	14.046
Basement-1	temp Max	Y	10.426	2.624	3.973

Story	Load Case/Combo	Direction	Maximum mm	Average mm	Ratio
Basement-2	temp Max	X	11.893	0.806	14.749
Basement-2	temp Max	Y	10.233	2.777	3.685
Basement-3	temp Max	X	8.93	0.508	17.562
Basement-3	temp Max	Y	8.654	2.481	3.488
Basement-1	temp Min	X	13.365	0.952	14.046
Basement-1	temp Min	Y	10.426	2.624	3.973
Basement-2	temp Min	X	11.893	0.806	14.749
Basement-2	temp Min	Y	10.233	2.777	3.685
Basement-3	temp Min	X	8.93	0.508	17.562
Basement-3	temp Min	Y	8.654	2.481	3.488
Basement-1	Service	X	13.251	0.939	14.111
Basement-1	Service	Y	10.363	2.64	3.925
Basement-2	Service	X	11.922	0.807	14.779
Basement-2	Service	Y	10.261	2.794	3.673
Basement-3	Service	X	8.978	0.507	17.694
Basement-3	Service	Y	8.686	2.482	3.5
Basement-1	1.2DL+1.6LL+1.2 Temp	X	15.889	1.125	14.123
Basement-1	1.2DL+1.6LL+1.2 Temp	Y	12.429	3.17	3.921
Basement-2	1.2DL+1.6LL+1.2 Temp	X	14.31	0.968	14.783
Basement-2	1.2DL+1.6LL+1.2 Temp	Y	12.316	3.355	3.672
Basement-3	1.2DL+1.6LL+1.2 Temp	X	10.778	0.609	17.706
Basement-3	1.2DL+1.6LL+1.2 Temp	Y	10.426	2.979	3.5

Table B-22- Model B Story Drifts

Story	Load Case/Combo	Direction	Drift	Label	X m	Y m	Z m
Basement-1	Dead	Y	2.9E-05	101	18	0	10.5
Basement-1	Live	Y	1E-05	101	18	0	10.5
Basement-1	temp Max	X	0.000505	2772	-5.4306	33.1	10.5
Basement-1	temp Max	Y	0.000279	70	-9.775	33.1	10.5
Basement-1	temp Min	X	0.000505	2772	-5.4306	33.1	10.5
Basement-1	temp Min	Y	0.000279	70	-9.775	33.1	10.5
Basement-1	Service	X	0.000495	2772	-5.4306	33.1	10.5
Basement-1	Service	Y	0.000262	70	-9.775	33.1	10.5
Basement-1	1.2DL+1.6LL+1.2 Temp	X	0.000592	2772	-5.4306	33.1	10.5
Basement-1	1.2DL+1.6LL+1.2 Temp	Y	0.000313	70	-9.775	33.1	10.5
Basement-2	Dead	X	7E-06	88	-9.775	-5.65	7
Basement-2	Dead	Y	1.3E-05	102	18	-5.65	7
Basement-2	Live	X	2E-06	88	-9.775	-5.65	7
Basement-2	Live	Y	4E-06	102	18	-5.65	7
Basement-2	temp Max	X	0.001001	2766	-6.5167	33.1	7
Basement-2	temp Max	Y	0.000538	2751	-9.775	31.0667	7
Basement-2	temp Min	X	0.001001	2766	-6.5167	33.1	7
Basement-2	temp Min	Y	0.000538	2751	-9.775	31.0667	7
Basement-2	Service	X	0.000999	2766	-6.5167	33.1	7
Basement-2	Service	Y	0.000536	2751	-9.775	31.0667	7
Basement-2	1.2DL+1.6LL+1.2 Temp	X	0.001198	2766	-6.5167	33.1	7
Basement-2	1.2DL+1.6LL+1.2 Temp	Y	0.000644	2751	-9.775	31.0667	7
Basement-3	Dead	X	1.1E-05	2662	130.775	16	3.5
Basement-3	Dead	Y	1.1E-05	70	-9.775	33.1	3.5
Basement-3	Live	X	4E-06	2661	130.775	15	3.5
Basement-3	Live	Y	3E-06	70	-9.775	33.1	3.5
Basement-3	temp Max	X	0.002551	2350	-9.775	16	3.5
Basement-3	temp Max	Y	0.002473	3595	64.8333	33.1	3.5

Story	Load Case/Combo	Direction	Drift	Label	X m	Y m	Z m
Basement-3	temp Min	X	0.002551	2350	-9.775	16	3.5
Basement-3	temp Min	Y	0.002473	3595	64.8333	33.1	3.5
Basement-3	Service	X	0.002565	2350	-9.775	16	3.5
Basement-3	Service	Y	0.002482	3595	64.8333	33.1	3.5
Basement-3	1.2DL+1.6LL+1.2 Temp	X	0.00308	2350	-9.775	16	3.5
Basement-3	1.2DL+1.6LL+1.2 Temp	Y	0.002979	3595	64.8333	33.1	3.5

Table B-23- Model B Story Forces

Story	Load Case/Combo	Location	P kN	VX kN	VY kN	T kN-m	MX kN-m	MY kN-m
Basement-1	Dead	Top	48644.4304	-552.1058	-77.4141	-12095.0785	710713.524	-2910929
Basement-1	Dead	Bottom	64177.6333	-552.1058	-77.4141	-12095.0785	941997.6977	-3824409
Basement-1	Live	Top	17949.3183	-129.1354	-15.8659	-3300.0627	261614.8683	-1076452
Basement-1	Live	Bottom	17949.3183	-129.1354	-15.8659	-3300.0627	261670.399	-1076904
Basement-1	temp Max	Top	18263.0419	28936.5661	-1758.6961	-107534.8619	-78534.4792	-1397189
Basement-1	temp Max	Bottom	18263.0419	28936.5661	-1758.6961	-107534.8619	-72379.043	-1295911
Basement-1	temp Min	Top	18263.0419	28936.5661	-1758.6961	-107534.8619	-78534.4792	-1397189
Basement-1	temp Min	Bottom	18263.0419	28936.5661	-1758.6961	-107534.8619	-72379.043	-1295911
Basement-1	Service	Top	84856.7906	28255.3249	-1851.9761	-122930.003	893793.913	-5384571
Basement-1	Service	Bottom	100389.9935	28255.3249	-1851.9761	-122930.003	1131289.0537	-6197224
Basement-1	1.2DL+1.6LL+1.2 Temp	Top	109007.876	33854.7357	-2228.7177	-148836.0287	1177198.6429	-6892066
Basement-1	1.2DL+1.6LL+1.2 Temp	Bottom	127647.7195	33854.7357	-2228.7177	-148836.0287	1462215.0241	-7867431
Basement-2	Dead	Top	112428.0029	-575.6461	-23.2962	-9229.07	1654525.4571	-6708467
Basement-2	Dead	Bottom	127961.2058	-575.6461	-23.2962	-9229.07	1885620.218	-7622029
Basement-2	Live	Top	35862.1754	-134.7478	-2.8635	-2685.1075	523473.7157	-2151086
Basement-2	Live	Bottom	35862.1754	-134.7478	-2.8635	-2685.1075	523483.7378	-2151558
Basement-2	temp Max	Top	26099.0178	51318.6407	-11945.1247	-898810.3455	-109812.7804	-1801518
Basement-2	temp Max	Bottom	26099.0178	51318.6407	-11945.1247	-898810.3455	-68004.8438	-1621903
Basement-2	temp Min	Top	26099.0178	51318.6407	-11945.1247	-898810.3455	-109812.7804	-1801518
Basement-2	temp Min	Bottom	26099.0178	51318.6407	-11945.1247	-898810.3455	-68004.8438	-1621903
Basement-2	Service	Top	174389.1961	50608.2468	-11971.2844	-910724.523	2068186.3924	-10661072
Basement-2	Service	Bottom	189922.399	50608.2468	-11971.2844	-910724.523	2341099.112	-11395490
Basement-2	1.2DL+1.6LL+1.2 Temp	Top	223611.9055	60675.9971	-14366.6866	-1093943	2691213.1571	-13653721
Basement-2	1.2DL+1.6LL+1.2 Temp	Bottom	242251.7489	60675.9971	-14366.6866	-1093943	3018712.4296	-14535212
Basement-3	Dead	Top	176422.7734	-384.0742	27.2777	-4893.4725	2597184.3382	-10519816
Basement-3	Dead	Bottom	191955.9763	-384.0742	27.2777	-4893.4725	2828102.0906	-11432707
Basement-3	Live	Top	53813.2908	-92.3193	8.2064	-1705.4809	785112.5761	-3228382
Basement-3	Live	Bottom	53813.2908	-92.3193	8.2064	-1705.4809	785083.8538	-3228705
Basement-3	temp Max	Top	29355.0198	67568.9354	-40683.9268	-3199880	-83943.7652	-1826539
Basement-3	temp Max	Bottom	29355.0198	67568.9354	-40683.9268	-3199880	58449.9786	-1590048
Basement-3	temp Min	Top	29355.0198	67568.9354	-40683.9268	-3199880	-83943.7652	-1826539
Basement-3	temp Min	Bottom	29355.0198	67568.9354	-40683.9268	-3199880	58449.9786	-1590048
Basement-3	Service	Top	259591.084	67092.5418	-40648.4427	-3206479	3298353.1491	-15574737
Basement-3	Service	Bottom	275124.2869	67092.5418	-40648.4427	-3206479	3671635.923	-16251460
Basement-3	1.2DL+1.6LL+1.2 Temp	Top	333034.6171	80474.1224	-48774.8487	-3848457	4272068.8093	-19981037
Basement-3	1.2DL+1.6LL+1.2 Temp	Bottom	351674.4606	80474.1224	-48774.8487	-3848457	4719996.6491	-20793234

3.3 Modal Results

Table B-24- Model B Modal Periods and Frequencies

Case	Mode	Period sec	Frequency cyc/sec	Circular Frequency rad/sec	Eigenvalue rad²/sec²
Modal	1	0.11	9.079	57.0466	3254.3115
Modal	2	0.081	12.404	77.9359	6074.0082
Modal	3	0.075	13.372	84.018	7059.0264
Modal	4	0.073	13.787	86.6249	7503.8817
Modal	5	0.065	15.294	96.0951	9234.2675
Modal	6	0.057	17.604	110.6081	12234.1621
Modal	7	0.053	18.84	118.3777	14013.2735
Modal	8	0.051	19.561	122.903	15105.1431
Modal	9	0.051	19.757	124.1365	15409.8605
Modal	10	0.044	22.59	141.9381	20146.4167
Modal	11	0.043	23.38	146.9034	21580.595
Modal	12	0.043	23.515	147.7479	21829.4393

Table B-25- Model B Modal Participating Mass Ratios (Part 1 of 2)

Case	Mode	Period sec	UX	UY	UZ	Sum UX	Sum UY	Sum UZ
Modal	1	0.11	0.0164	0.6062	0	0.0164	0.6062	0
Modal	2	0.081	0.034	0.1421	0	0.0504	0.7483	0
Modal	3	0.075	0.652	0.0244	0	0.7024	0.7727	0
Modal	4	0.073	0.0008	0.0678	0	0.7033	0.8405	0
Modal	5	0.065	0.0186	0.0659	0	0.7218	0.9063	0
Modal	6	0.057	0.0972	0.0228	0	0.8191	0.9291	0
Modal	7	0.053	0.0006	0.0011	0	0.8197	0.9302	0
Modal	8	0.051	0.0001	0.0113	0	0.8198	0.9415	0
Modal	9	0.051	0.0305	0.0022	0	0.8503	0.9437	0
Modal	10	0.044	0.0005	0.0166	0	0.8508	0.9603	0
Modal	11	0.043	2.404E-05	0.0044	0	0.8508	0.9647	0
Modal	12	0.043	0.0539	5.83E-06	0	0.9046	0.9647	0

Table B-26- Model B Modal Participating Mass Ratios (Part 2 of 2)

Case	Mode	RX	RY	RZ	Sum RX	Sum RY	Sum RZ
Modal	1	0.1654	0.0036	0.1702	0.1654	0.0036	0.1702
Modal	2	0.0192	0.006	0.4573	0.1846	0.0095	0.6275
Modal	3	0.0028	0.1352	0.0072	0.1874	0.1447	0.6347
Modal	4	0.5111	0.0002	0.0061	0.6985	0.1449	0.6407
Modal	5	0.0036	0.0039	0.1253	0.7021	0.1488	0.766
Modal	6	0.0027	0.0182	0.003	0.7048	0.167	0.769
Modal	7	0.0048	0.0034	0.0657	0.7095	0.1703	0.8347
Modal	8	0.0386	2.018E-06	0.0001	0.7482	0.1704	0.8349
Modal	9	0.0001	0.0067	0.0745	0.7483	0.177	0.9093
Modal	10	0.1407	0.0028	0.0021	0.889	0.1798	0.9114
Modal	11	0.0001	0.0442	0.0047	0.8891	0.224	0.9161
Modal	12	0.0064	0.3775	0.0006	0.8955	0.6015	0.9167

Table B-27- Model B Modal Load Participation Ratios

Case	Item Type	Item	Static %	Dynamic %
Modal	Acceleration	UX	98.34	90.46
Modal	Acceleration	UY	99.77	96.47
Modal	Acceleration	UZ	0	0

Table B-28- Model B Modal Direction Factors

Case	Mode	Period sec	UX	UY	UZ	RZ
Modal	1	0.11	0.025	0.951	0	0.024
Modal	2	0.081	0.197	0.8	0	0.003
Modal	3	0.075	0.953	0.034	0	0.013
Modal	4	0.073	0.002	0.997	0	0.002
Modal	5	0.065	0.132	0.431	0	0.436
Modal	6	0.057	0.06	0.013	0	0.927
Modal	7	0.053	0.007	0.022	0	0.971
Modal	8	0.051	0	0.972	0	0.028
Modal	9	0.051	0.023	0.005	0	0.972
Modal	10	0.044	0.017	0.772	0	0.211
Modal	11	0.043	0.376	0.035	0	0.59
Modal	12	0.043	0.943	0.014	0	0.043

B-3 Model C ETABS summary report

Summary Report

Model File: model-C , Revision 0
1/30/2020

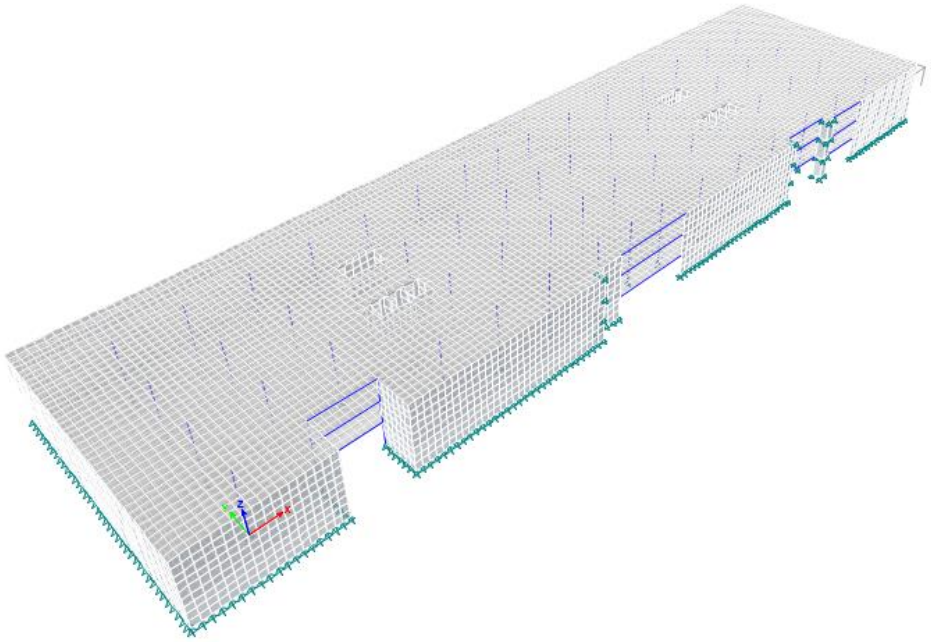

B-3-1 Structure Data

This chapter provides model geometry information, including items such as story levels, point coordinates, and element connectivity.

1.1 Story Data

Table B-29- Model C Story Data

Name	Height mm	Elevation mm	Master Story	Similar To	Splice Story
Basement-1	3500	10500	No	None	No
Basement-2	3500	7000	No	None	No
Basement-3	3500	3500	No	None	No
Base	0	0	No	None	No

B-3-2 Loads

This chapter provides loading information as applied to the model.

2.1 Load Patterns

Table B-30- Model C - Load Patterns

Name	Type	Self Weight Multiplier
Dead	Dead	1
Live	Live	0
Temp	Other	0

2.2 Load Cases

Table B-31- Model C Load Cases - Summary

Name	Type
Dead	Linear Static
Live	Linear Static
temp	Nonlinear Static

B-3-3 Analysis Results

This chapter provides analysis results.

3.1 Structure Results

Table B-32- Model C - Base Reactions

Load Case/Combo	FX kN	FY kN	FZ kN	MX kN-m	MY kN-m	MZ kN-m	X m	Y m	Z m
Dead	0	0	195674.0063	2813455.4016	-11716198	-2.126E-06	0	0	0

Load Case/Combo	FX kN	FY kN	FZ kN	MX kN-m	MY kN-m	MZ kN-m	X m	Y m	Z m
Live	0	0	54433.1729	782841.663	-3275397	-7.215E-07	0	0	0
temp Max	-4.755E-06	-1.007E-05	-1.749E-06	2.08E-05	-4.927E-06	-0.0002	0	0	0
temp Min	-4.755E-06	-1.007E-05	-1.749E-06	2.08E-05	-4.927E-06	-0.0002	0	0	0
Service	-4.75E-06	-1.017E-05	250107.1792	3596297.0646	-14991594	-0.0002	0	0	0
1.2DL+1.6LL+1.2 Temp	-5.699E-06	-1.221E-05	321901.8841	4628693.1427	-19300072	-0.0002	0	0	0

Table B-33- Model C - Centers of Mass and Rigidity

Story	Diaphragm	Mass X kg	Mass Y kg	XCM m	YCM m	Cumulative X kg	Cumulative Y kg	XCCM m	YCCM m	XCR m	YCR m
Basement-1	D1	0	0	60.0106	14.3039	0	0	0	0		
Basement-2	D1	0	0	59.8182	14.3919	0	0	0	0		
Basement-3	D1	0	0	59.8182	14.3919	0	0	0	0		

Table B-34- Model C - Diaphragm Center of Mass Displacements

Story	Diaphragm	Load Case/Combo	UX mm	UY mm	RZ rad	Point	X m	Y m	Z m
Basement-1	D1	Dead	-0.001	-0.006	-1E-06	3753	60.0106	14.3039	10.5
Basement-1	D1	Live	0.0004257	-0.004	-1.914E-07	3753	60.0106	14.3039	10.5
Basement-1	D1	temp Max	-0.941	5.17	2.1E-05	3753	60.0106	14.3039	10.5
Basement-1	D1	temp Min	-0.941	5.17	2.1E-05	3753	60.0106	14.3039	10.5
Basement-1	D1	Service	-0.942	5.16	2E-05	3753	60.0106	14.3039	10.5
Basement-1	D1	1.2DL+1.6LL+1.2 Temp	-1.13	6.19	2.4E-05	3753	60.0106	14.3039	10.5
Basement-2	D1	Dead	-0.0004714	0.013	-3.213E-07	3755	59.8182	14.3919	7
Basement-2	D1	Live	0.0003237	0.004	-1.066E-07	3755	59.8182	14.3919	7
Basement-2	D1	temp Max	-0.868	4.879	1.7E-05	3755	59.8182	14.3919	7
Basement-2	D1	temp Min	-0.868	4.879	1.7E-05	3755	59.8182	14.3919	7
Basement-2	D1	Service	-0.868	4.896	1.7E-05	3755	59.8182	14.3919	7
Basement-2	D1	1.2DL+1.6LL+1.2 Temp	-1.042	5.877	2E-05	3755	59.8182	14.3919	7
Basement-3	D1	Dead	-1.146E-05	0.011	-1.339E-07	4747	59.8182	14.3919	3.5
Basement-3	D1	Live	0.0001271	0.004	-3.812E-08	4747	59.8182	14.3919	3.5
Basement-3	D1	temp Max	-0.475	3.479	5E-06	4747	59.8182	14.3919	3.5
Basement-3	D1	temp Min	-0.475	3.479	5E-06	4747	59.8182	14.3919	3.5
Basement-3	D1	Service	-0.475	3.494	4E-06	4747	59.8182	14.3919	3.5
Basement-3	D1	1.2DL+1.6LL+1.2 Temp	-0.57	4.194	5E-06	4747	59.8182	14.3919	3.5

3.2 Story Results

Table B-35- Model C - Story Max/Avg Displacements

Story	Load Case/Combo	Direction	Maximum mm	Average mm	Ratio
Basement-1	Dead	Y	0.13	0.042	3.121
Basement-2	Dead	X	0.031	0.004	7.67
Basement-2	Dead	Y	0.04	0.012	3.367
Basement-3	Dead	X	0.038	0.001	42.792
Basement-3	Dead	Y	0.039	0.004	9.764
Basement-1	Live	Y	0.046	0.014	3.233
Basement-2	Live	X	0.01	0.001	6.575
Basement-2	Live	Y	0.014	0.005	2.697
Basement-3	Live	X	0.013	0.0004314	29.84
Basement-3	Live	Y	0.011	0.002	7.304
Basement-1	temp Max	X	13.365	0.952	14.046
Basement-1	temp Max	Y	10.426	2.624	3.973
Basement-2	temp Max	X	11.893	0.806	14.749
Basement-2	temp Max	Y	10.233	2.777	3.685
Basement-3	temp Max	X	8.93	0.508	17.562
Basement-3	temp Max	Y	8.654	2.481	3.488

Story	Load Case/Combo	Direction	Maximum mm	Average mm	Ratio
Basement-1	temp Min	X	13.365	0.952	14.046
Basement-1	temp Min	Y	10.426	2.624	3.973
Basement-2	temp Min	X	11.893	0.806	14.749
Basement-2	temp Min	Y	10.233	2.777	3.685
Basement-3	temp Min	X	8.93	0.508	17.562
Basement-3	temp Min	Y	8.654	2.481	3.488
Basement-1	Service	X	13.251	0.939	14.111
Basement-1	Service	Y	10.363	2.64	3.925
Basement-2	Service	X	11.922	0.807	14.779
Basement-2	Service	Y	10.261	2.794	3.673
Basement-3	Service	X	8.978	0.507	17.694
Basement-3	Service	Y	8.686	2.482	3.5
Basement-1	1.2DL+1.6LL+1.2 Temp	X	15.889	1.125	14.123
Basement-1	1.2DL+1.6LL+1.2 Temp	Y	12.429	3.17	3.921
Basement-2	1.2DL+1.6LL+1.2 Temp	X	14.31	0.968	14.783
Basement-2	1.2DL+1.6LL+1.2 Temp	Y	12.316	3.355	3.672
Basement-3	1.2DL+1.6LL+1.2 Temp	X	10.778	0.609	17.706
Basement-3	1.2DL+1.6LL+1.2 Temp	Y	10.426	2.979	3.5

Table B-36- Model C - Story Drifts

Story	Load Case/Combo	Direction	Drift	Label	X m	Y m	Z m
Basement-1	Dead	Y	2.9E-05	101	18	0	10.5
Basement-1	Live	Y	1E-05	101	18	0	10.5
Basement-1	temp Max	X	0.000505	2772	-5.4306	33.1	10.5
Basement-1	temp Max	Y	0.000279	70	-9.775	33.1	10.5
Basement-1	temp Min	X	0.000505	2772	-5.4306	33.1	10.5
Basement-1	temp Min	Y	0.000279	70	-9.775	33.1	10.5
Basement-1	Service	X	0.000495	2772	-5.4306	33.1	10.5
Basement-1	Service	Y	0.000262	70	-9.775	33.1	10.5
Basement-1	1.2DL+1.6LL+1.2 Temp	X	0.000592	2772	-5.4306	33.1	10.5
Basement-1	1.2DL+1.6LL+1.2 Temp	Y	0.000313	70	-9.775	33.1	10.5
Basement-2	Dead	X	7E-06	88	-9.775	-5.65	7
Basement-2	Dead	Y	1.3E-05	102	18	-5.65	7
Basement-2	Live	X	2E-06	88	-9.775	-5.65	7
Basement-2	Live	Y	4E-06	102	18	-5.65	7
Basement-2	temp Max	X	0.001001	2766	-6.5167	33.1	7
Basement-2	temp Max	Y	0.000538	2751	-9.775	31.0667	7
Basement-2	temp Min	X	0.001001	2766	-6.5167	33.1	7
Basement-2	temp Min	Y	0.000538	2751	-9.775	31.0667	7
Basement-2	Service	X	0.000999	2766	-6.5167	33.1	7
Basement-2	Service	Y	0.000536	2751	-9.775	31.0667	7
Basement-2	1.2DL+1.6LL+1.2 Temp	X	0.001198	2766	-6.5167	33.1	7
Basement-2	1.2DL+1.6LL+1.2 Temp	Y	0.000644	2751	-9.775	31.0667	7
Basement-3	Dead	X	1.1E-05	2662	130.775	16	3.5
Basement-3	Dead	Y	1.1E-05	70	-9.775	33.1	3.5
Basement-3	Live	X	4E-06	2661	130.775	15	3.5
Basement-3	Live	Y	3E-06	70	-9.775	33.1	3.5
Basement-3	temp Max	X	0.002551	2350	-9.775	16	3.5
Basement-3	temp Max	Y	0.002473	3595	64.8333	33.1	3.5
Basement-3	temp Min	X	0.002551	2350	-9.775	16	3.5
Basement-3	temp Min	Y	0.002473	3595	64.8333	33.1	3.5
Basement-3	Service	X	0.002565	2350	-9.775	16	3.5
Basement-3	Service	Y	0.002482	3595	64.8333	33.1	3.5
Basement-3	1.2DL+1.6LL+1.2 Temp	X	0.00308	2350	-9.775	16	3.5
Basement-3	1.2DL+1.6LL+1.2 Temp	Y	0.002979	3595	64.8333	33.1	3.5

Table B-37- Model C - Story Forces

Story	Load Case/Combo	Location	P kN	VX kN	VY kN	T kN-m	MX kN-m	MY kN-m
Basement-1	Dead	Top	48644.4304	-552.1058	-77.4141	-12095.0785	710713.524	-2910929
Basement-1	Dead	Bottom	64177.6333	-552.1058	-77.4141	-12095.0785	941997.6977	-3824409
Basement-1	Live	Top	17949.3183	-129.1354	-15.8659	-3300.0627	261614.8683	-1076452
Basement-1	Live	Bottom	17949.3183	-129.1354	-15.8659	-3300.0627	261670.399	-1076904
Basement-1	temp Max	Top	18263.0419	28936.5661	-1758.6961	-107534.8619	-78534.4792	-1397189
Basement-1	temp Max	Bottom	18263.0419	28936.5661	-1758.6961	-107534.8619	-72379.043	-1295911
Basement-1	temp Min	Top	18263.0419	28936.5661	-1758.6961	-107534.8619	-78534.4792	-1397189
Basement-1	temp Min	Bottom	18263.0419	28936.5661	-1758.6961	-107534.8619	-72379.043	-1295911
Basement-1	Service	Top	84856.7906	28255.3249	-1851.9761	-122930.003	893793.913	-5384571
Basement-1	Service	Bottom	100389.9935	28255.3249	-1851.9761	-122930.003	1131289.0537	-6197224
Basement-1	1.2DL+1.6LL+1.2 Temp	Top	109007.876	33854.7357	-2228.7177	-148836.0287	1177198.6429	-6892066
Basement-1	1.2DL+1.6LL+1.2 Temp	Bottom	127647.7195	33854.7357	-2228.7177	-148836.0287	1462215.0241	-7867431
Basement-2	Dead	Top	112428.0029	-575.6461	-23.2962	-9229.07	1654525.4571	-6708467
Basement-2	Dead	Bottom	127961.2058	-575.6461	-23.2962	-9229.07	1885620.218	-7622029
Basement-2	Live	Top	35862.1754	-134.7478	-2.8635	-2685.1075	523473.7157	-2151086
Basement-2	Live	Bottom	35862.1754	-134.7478	-2.8635	-2685.1075	523483.7378	-2151558
Basement-2	temp Max	Top	26099.0178	51318.6407	-11945.1247	-898810.3455	-109812.7804	-1801518
Basement-2	temp Max	Bottom	26099.0178	51318.6407	-11945.1247	-898810.3455	-68004.8438	-1621903
Basement-2	temp Min	Top	26099.0178	51318.6407	-11945.1247	-898810.3455	-109812.7804	-1801518
Basement-2	temp Min	Bottom	26099.0178	51318.6407	-11945.1247	-898810.3455	-68004.8438	-1621903
Basement-2	Service	Top	174389.1961	50608.2468	-11971.2844	-910724.523	2068186.3924	-10661072
Basement-2	Service	Bottom	189922.399	50608.2468	-11971.2844	-910724.523	2341099.112	-11395490
Basement-2	1.2DL+1.6LL+1.2 Temp	Top	223611.9055	60675.9971	-14366.6866	-1093943	2691213.1571	-13653721
Basement-2	1.2DL+1.6LL+1.2 Temp	Bottom	242251.7489	60675.9971	-14366.6866	-1093943	3018712.4296	-14535212
Basement-3	Dead	Top	176422.7734	-384.0742	27.2777	-4893.4725	2597184.3382	-10519816
Basement-3	Dead	Bottom	191955.9763	-384.0742	27.2777	-4893.4725	2828102.0906	-11432707
Basement-3	Live	Top	53813.2908	-92.3193	8.2064	-1705.4809	785112.5761	-3228382
Basement-3	Live	Bottom	53813.2908	-92.3193	8.2064	-1705.4809	785083.8538	-3228705
Basement-3	temp Max	Top	29355.0198	67568.9354	-40683.9268	-3199880	-83943.7652	-1826539
Basement-3	temp Max	Bottom	29355.0198	67568.9354	-40683.9268	-3199880	58449.9786	-1590048
Basement-3	temp Min	Top	29355.0198	67568.9354	-40683.9268	-3199880	-83943.7652	-1826539
Basement-3	temp Min	Bottom	29355.0198	67568.9354	-40683.9268	-3199880	58449.9786	-1590048
Basement-3	Service	Top	259591.084	67092.5418	-40648.4427	-3206479	3298353.1491	-15574737
Basement-3	Service	Bottom	275124.2869	67092.5418	-40648.4427	-3206479	3671635.923	-16251460
Basement-3	1.2DL+1.6LL+1.2 Temp	Top	333034.6171	80474.1224	-48774.8487	-3848457	4272068.8093	-19981037
Basement-3	1.2DL+1.6LL+1.2 Temp	Bottom	351674.4606	80474.1224	-48774.8487	-3848457	4719996.6491	-20793234

3.3 Modal Results

Table B-38- Model C - Modal Periods and Frequencies

Case	Mode	Period sec	Frequency cyc/sec	Circular Frequency rad/sec	Eigenvalue rad²/sec²
Modal	1	0.11	9.079	57.0466	3254.3115
Modal	2	0.081	12.404	77.9359	6074.0082
Modal	3	0.075	13.372	84.018	7059.0264
Modal	4	0.073	13.787	86.6249	7503.8817
Modal	5	0.065	15.294	96.0951	9234.2675

Case	Mode	Period sec	Frequency cyc/sec	Circular Frequency rad/sec	Eigenvalue rad²/sec²
Modal	6	0.057	17.604	110.6081	12234.1621
Modal	7	0.053	18.84	118.3777	14013.2735
Modal	8	0.051	19.561	122.903	15105.1431
Modal	9	0.051	19.757	124.1365	15409.8605
Modal	10	0.044	22.59	141.9381	20146.4167
Modal	11	0.043	23.38	146.9034	21580.595
Modal	12	0.043	23.515	147.7479	21829.4393

Table B-39- Model C Modal Participating Mass Ratios (Part 1 of 2)

Case	Mode	Period sec	UX	UY	UZ	Sum UX	Sum UY	Sum UZ
Modal	1	0.11	0.0164	0.6062	0	0.0164	0.6062	0
Modal	2	0.081	0.034	0.1421	0	0.0504	0.7483	0
Modal	3	0.075	0.652	0.0244	0	0.7024	0.7727	0
Modal	4	0.073	0.0008	0.0678	0	0.7033	0.8405	0
Modal	5	0.065	0.0186	0.0659	0	0.7218	0.9063	0
Modal	6	0.057	0.0972	0.0228	0	0.8191	0.9291	0
Modal	7	0.053	0.0006	0.0011	0	0.8197	0.9302	0
Modal	8	0.051	0.0001	0.0113	0	0.8198	0.9415	0
Modal	9	0.051	0.0305	0.0022	0	0.8503	0.9437	0
Modal	10	0.044	0.0005	0.0166	0	0.8508	0.9603	0
Modal	11	0.043	2.404E-05	0.0044	0	0.8508	0.9647	0
Modal	12	0.043	0.0539	5.83E-06	0	0.9046	0.9647	0

Table B-40- Model C Modal Participating Mass Ratios (Part 2 of 2)

Case	Mode	RX	RY	RZ	Sum RX	Sum RY	Sum RZ
Modal	1	0.1654	0.0036	0.1702	0.1654	0.0036	0.1702
Modal	2	0.0192	0.006	0.4573	0.1846	0.0095	0.6275
Modal	3	0.0028	0.1352	0.0072	0.1874	0.1447	0.6347
Modal	4	0.5111	0.0002	0.0061	0.6985	0.1449	0.6407
Modal	5	0.0036	0.0039	0.1253	0.7021	0.1488	0.766
Modal	6	0.0027	0.0182	0.003	0.7048	0.167	0.769
Modal	7	0.0048	0.0034	0.0657	0.7095	0.1703	0.8347
Modal	8	0.0386	2.018E-06	0.0001	0.7482	0.1704	0.8349
Modal	9	0.0001	0.0067	0.0745	0.7483	0.177	0.9093
Modal	10	0.1407	0.0028	0.0021	0.889	0.1798	0.9114
Modal	11	0.0001	0.0442	0.0047	0.8891	0.224	0.9161
Modal	12	0.0064	0.3775	0.0006	0.8955	0.6015	0.9167

Table B-41- Model C - Modal Load Participation Ratios

Case	Item Type	Item	Static %	Dynamic %
Modal	Acceleration	UX	98.34	90.46
Modal	Acceleration	UY	99.77	96.47
Modal	Acceleration	UZ	0	0

Table B-42- Model C - Modal Direction Factors

Case	Mode	Period sec	UX	UY	UZ	RZ
Modal	1	0.11	0.025	0.951	0	0.024
Modal	2	0.081	0.197	0.8	0	0.003
Modal	3	0.075	0.953	0.034	0	0.013
Modal	4	0.073	0.002	0.997	0	0.002
Modal	5	0.065	0.132	0.431	0	0.436
Modal	6	0.057	0.06	0.013	0	0.927

Case	Mode	Period sec	UX	UY	UZ	RZ
Modal	7	0.053	0.007	0.022	0	0.971
Modal	8	0.051	0	0.972	0	0.028
Modal	9	0.051	0.023	0.005	0	0.972
Modal	10	0.044	0.017	0.772	0	0.211
Modal	11	0.043	0.376	0.035	0	0.59
Modal	12	0.043	0.943	0.014	0	0.043

Appendix C

Table C-1 Creep and Shrinkage Strains, Millionths in./in.

Concrete release strength = 3500 psi Average prestress = 600 psi Relative humidity = 70% Volume-to-surface ratio = 1.5 in.				
Time, days	Creep		Shrinkage	
	Normalweight	Lightweight	Moist Cure	Accelerated Cure
1	29	43	16	9
3	51	76	44	26
5	65	97	70	43
7	76	114	93	58
9	86	127	115	72
10	90	133	124	78
20	118	176	204	136
30	137	204	258	180
40	150	224	299	215
50	161	239	329	243
60	169	252	354	266
70	177	263	373	286
80	183	272	390	302
90	188	280	403	317
100	193	287	415	329
200	222	331	477	400
1 year	244	363	511	443
3 year	273	407	543	486
5 year	283	422	549	495
Final	315	468	560	510

Table C-2 Correction Factors for Relative Humidity (RH)

Average ambient RH (from Design Aid 4.11.12)	Creep	Shrinkage
40	1.25	1.43
50	1.17	1.29
60	1.08	1.14
70	1.00	1.00
80	0.92	0.86
90	0.83	0.43
100	0.75	0.00

Appendix D

D-1 Model A

D-1-1 Column M22

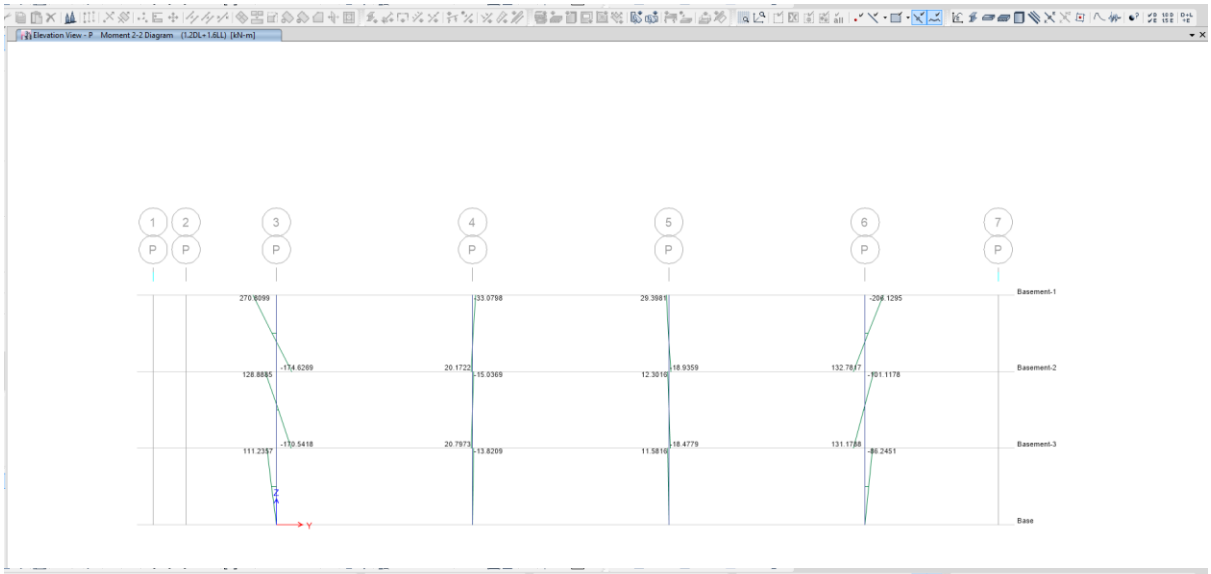

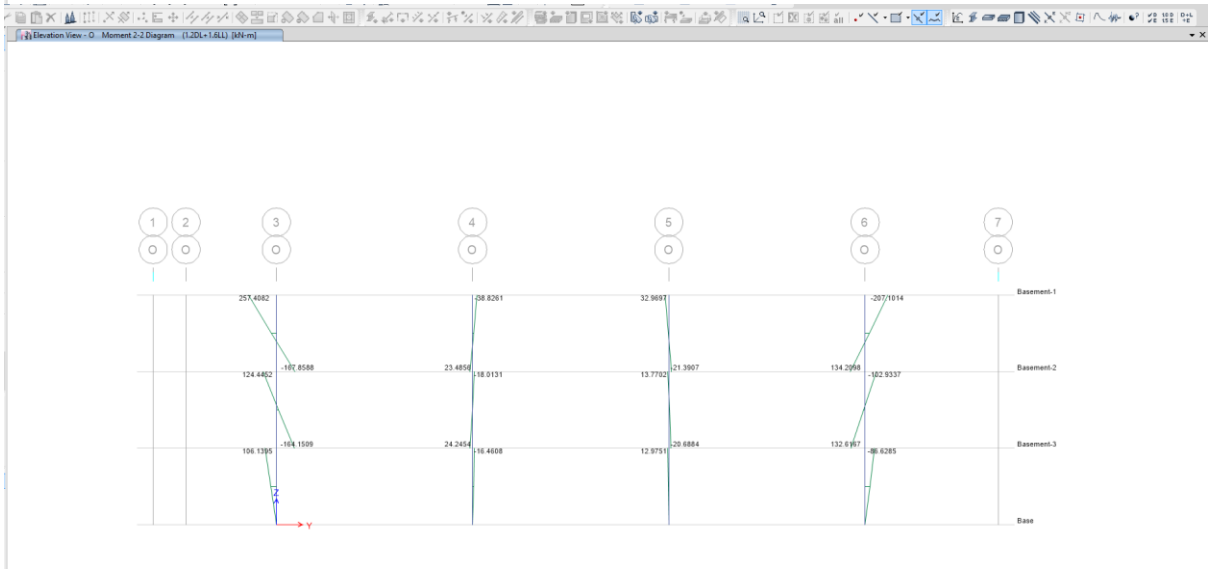

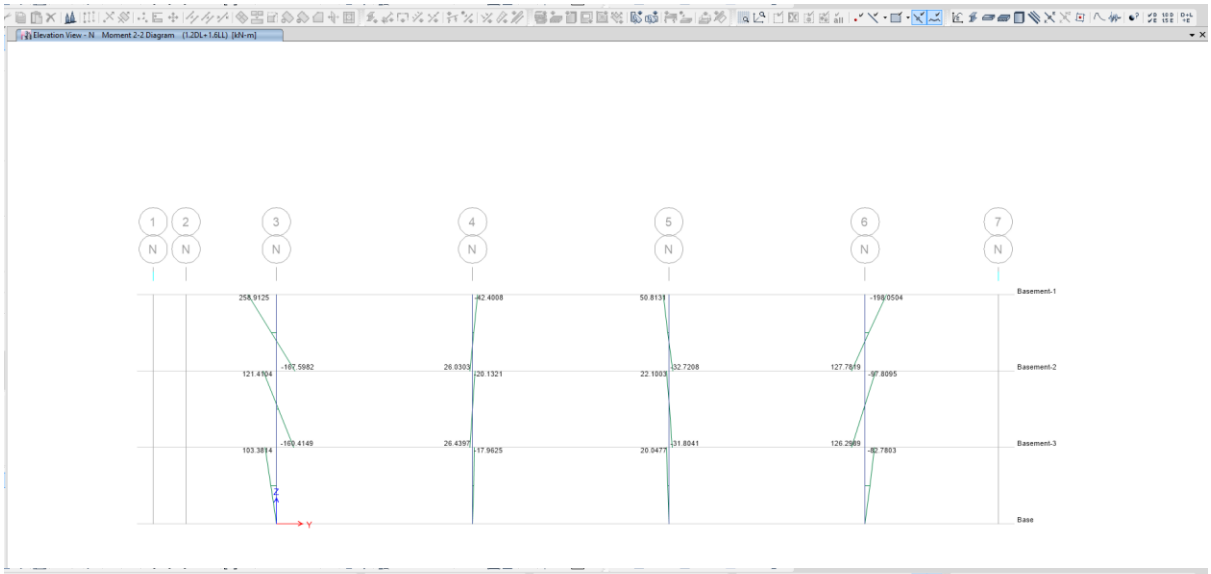
Elevation View - N Moment 2-2 Diagram (1.2DL+1.6LL) [kN-m]
1 2 3 4 5 6 7
N N N N N N N
Basement-1
Basement-2
Basement-3
Base

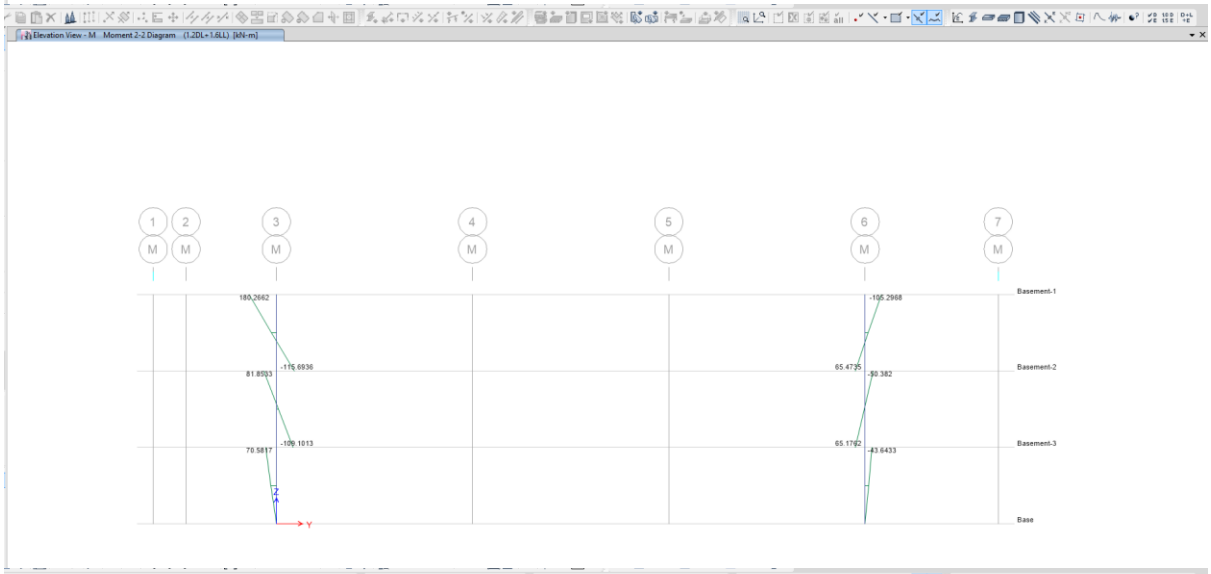
Elevation View - M Moment 2-2 Diagram (1.2DL+1.6LL) [kN-m]
1 2 3 4 5 6 7
M M M M M M M
Basement-1
Basement-2
Basement-3
Base

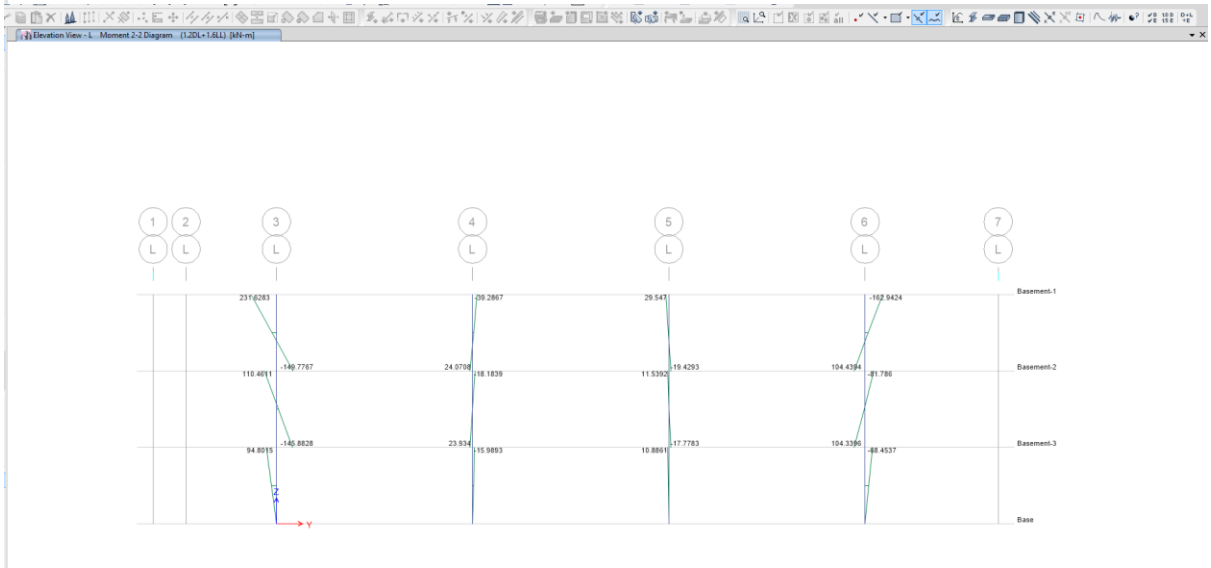
Elevation View - L Moment 2-2 Diagram (1.2DL+1.6LL) [kN-m]
1 2 3 4 5 6 7
L L L L L L L
Basement-1
Basement-2
Basement-3
Base

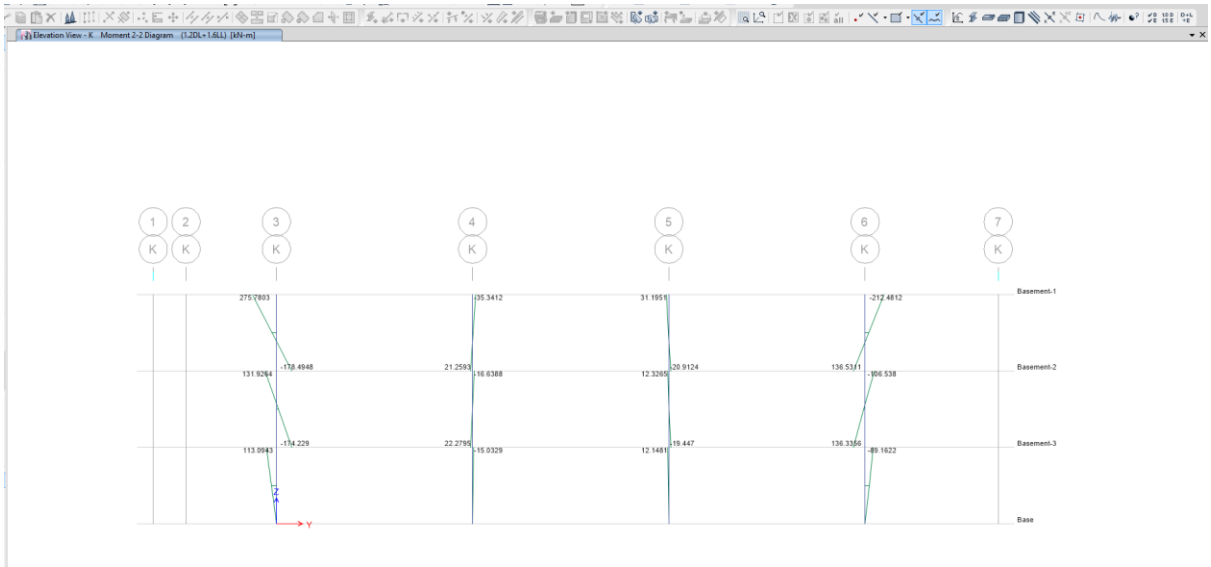
Elevation View - K Moment 2-2 Diagram (1.2DL+1.6LL) [kN-m]
1 2 3 4 5 6 7
K K K K K K K
Basement-1
Basement-2
Basement-3
Base

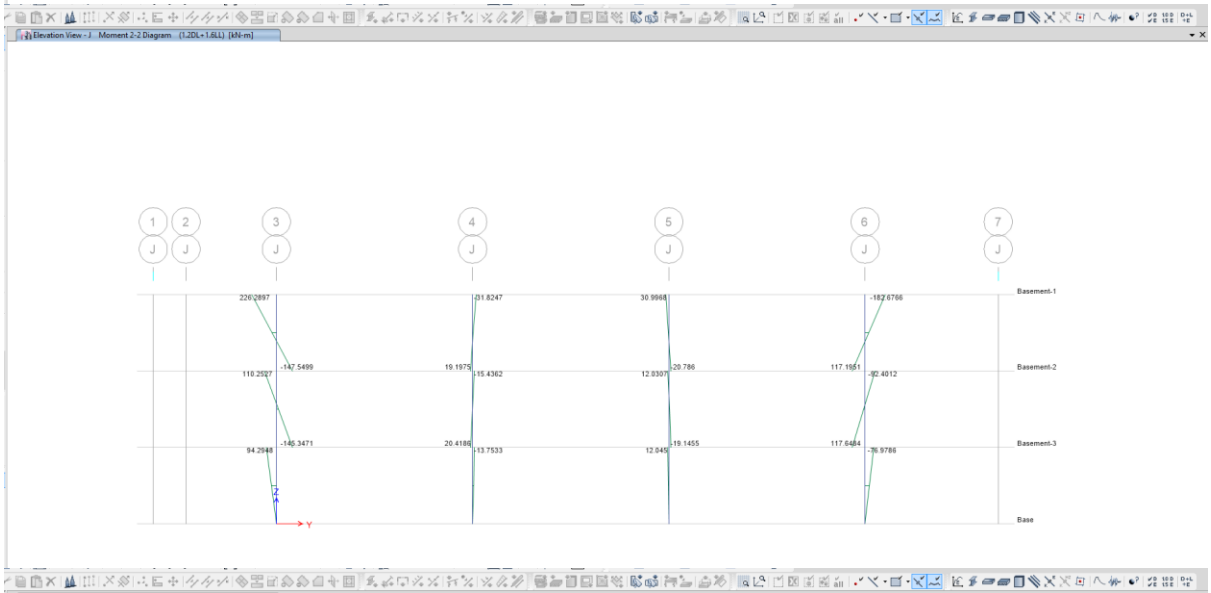
Elevation View - J Moment 2-2 Diagram (1.2DL+1.6LL) [kN-m]
1 2 3 4 5 6 7
J J J J J J J
Basement-1
Basement-2
Basement-3
Base

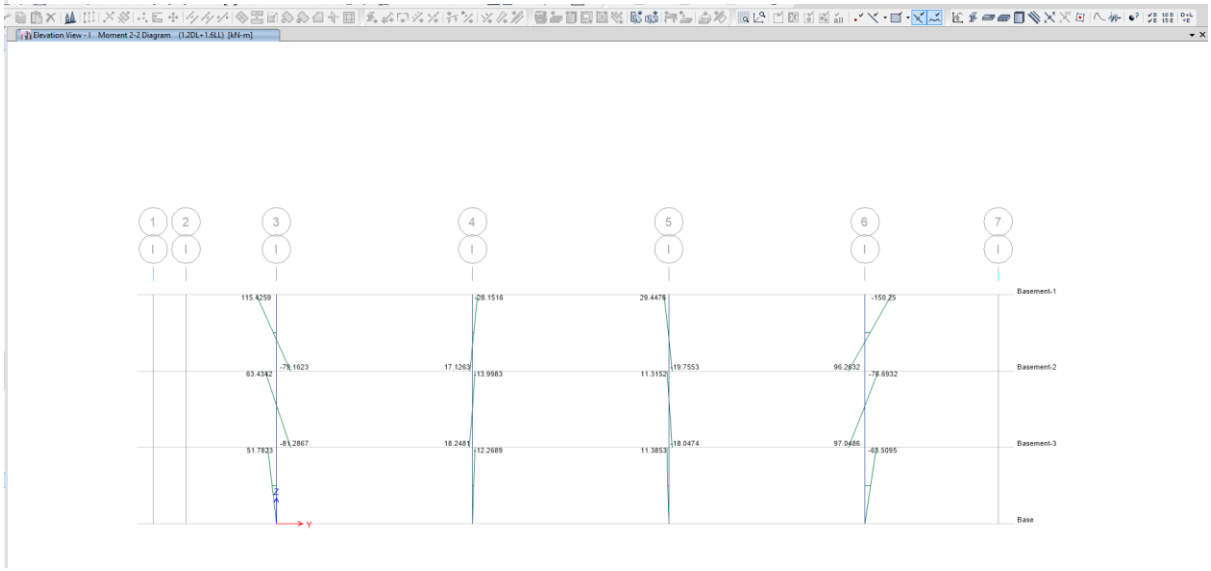
Elevation View - I Moment 2-2 Diagram (1.2DL+1.6LL) [kN-m]
1 2 3 4 5 6 7
I I I I I I I
Basement-1
Basement-2
Basement-3
Base

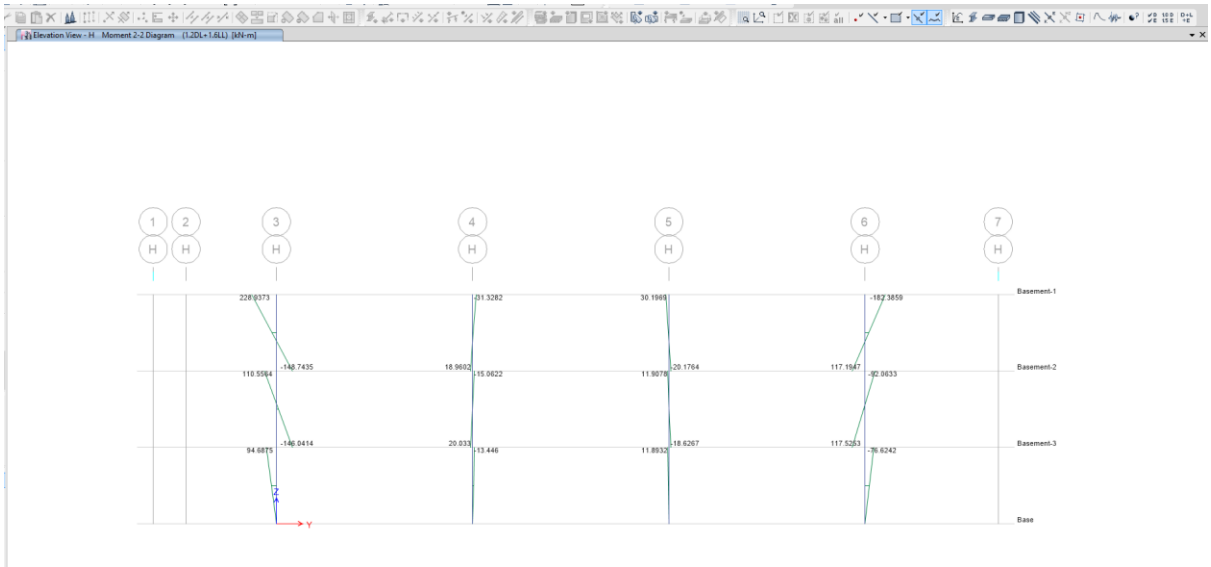
Elevation View - H Moment 2-2 Diagram (1.2DL+1.6LL) [kN-m]
1 2 3 4 5 6 7
H H H H H H H
228.0373
110.5564
94.6875
-148.7435
-146.0414
31.3282
18.9602
20.033
-115.0622
-113.446
30.1969
11.9078
11.8932
-20.1764
-18.6267
-182.3859
117.1947
117.5253
-82.0833
-76.6242
Basement-1
Basement-2
Basement-3
Base

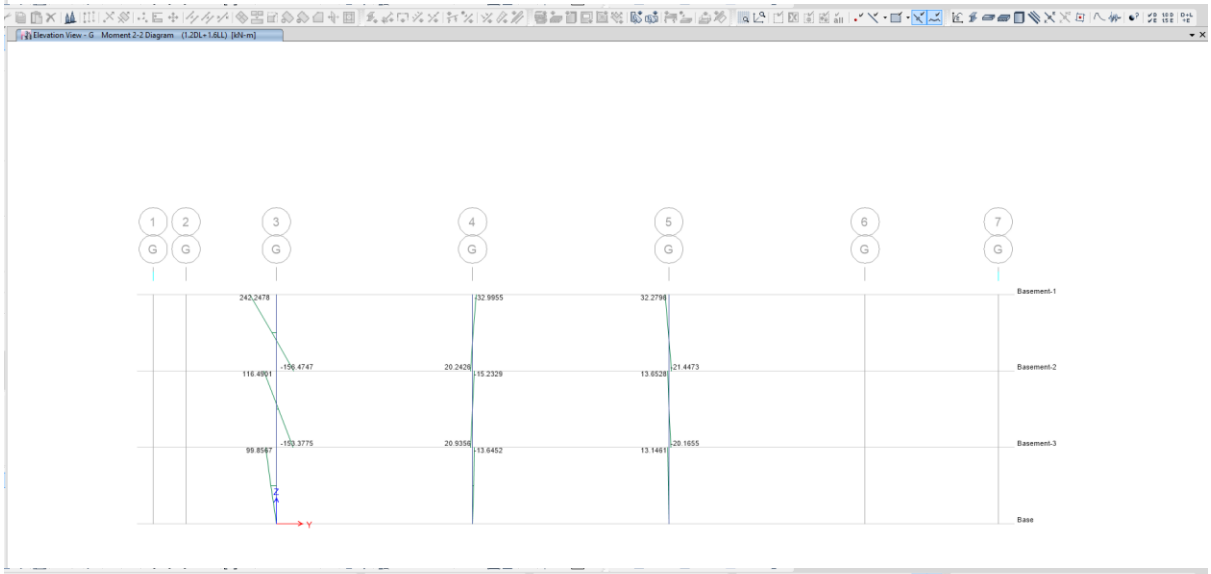
Elevation View - G Moment 2-2 Diagram (1.2DL+1.6LL) [kN-m]
1 2 3 4 5 6 7
G G G G G G G
242.2478
116.4901
99.8567
-156.4747
-150.3775
32.9955
20.2426
20.9359
-115.2329
-113.6452
32.2798
13.6528
13.1481
-21.4473
-20.1655
Basement-1
Basement-2
Basement-3
Base

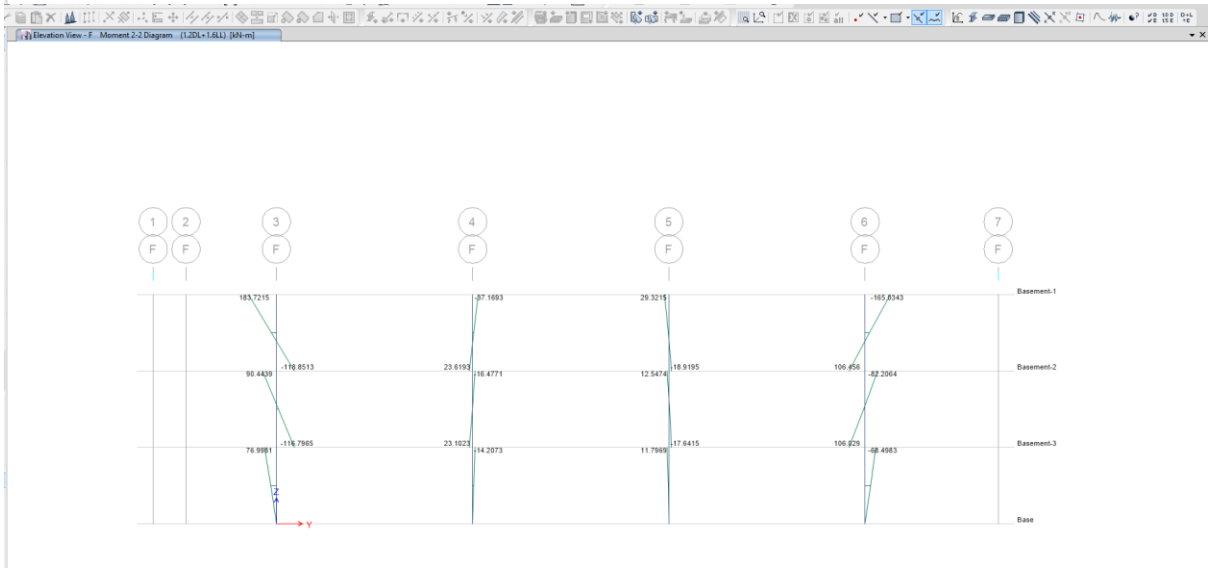
Elevation View - F Moment 2-2 Diagram (1.2DL+1.6LL) [kN-m]
1 2 3 4 5 6 7
F F F F F F F
183.7215
90.4439
76.9981
-118.8513
-116.7965
37.1693
23.6193
23.1023
-116.4771
-114.2073
29.3215
12.5474
11.7969
-18.9195
-17.6415
-165.0343
106.858
106.829
-82.2064
-78.4983
Basement-1
Basement-2
Basement-3
Base

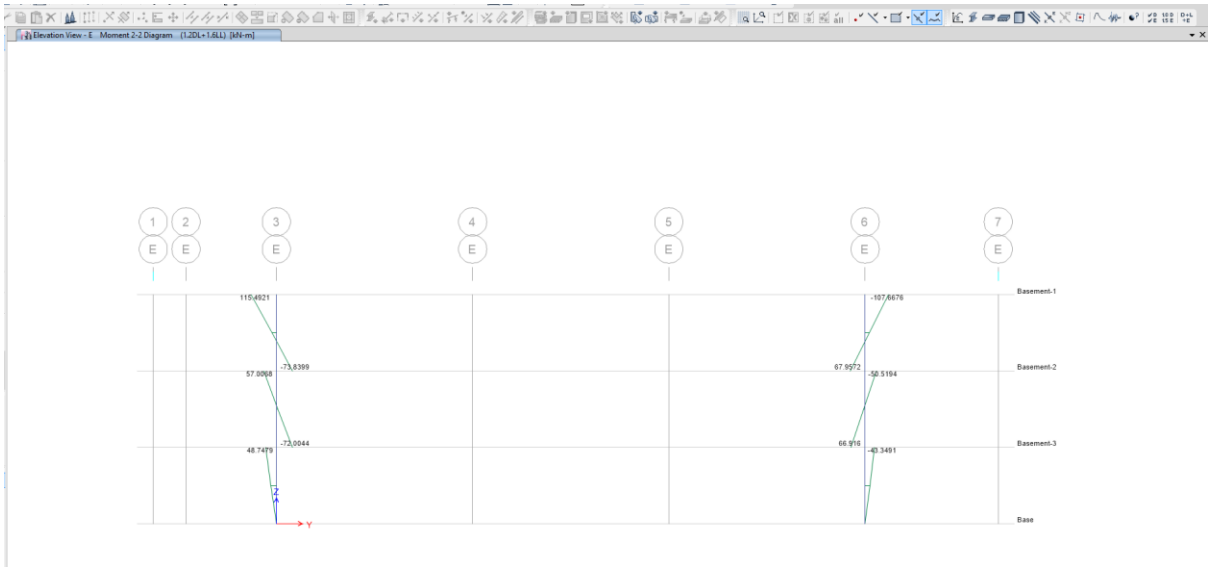
Elevation View - E Moment 2-2 Diagram (1.2DL+1.6LL) [kN-m]
1 2 3 4 5 6 7
E E E E E E E
115.4921
-73.8399
57.0068
-72.0044
48.7479
-107.6676
67.9572
-50.5194
66.916
-49.3491
Basement-1
Basement-2
Basement-3
Base

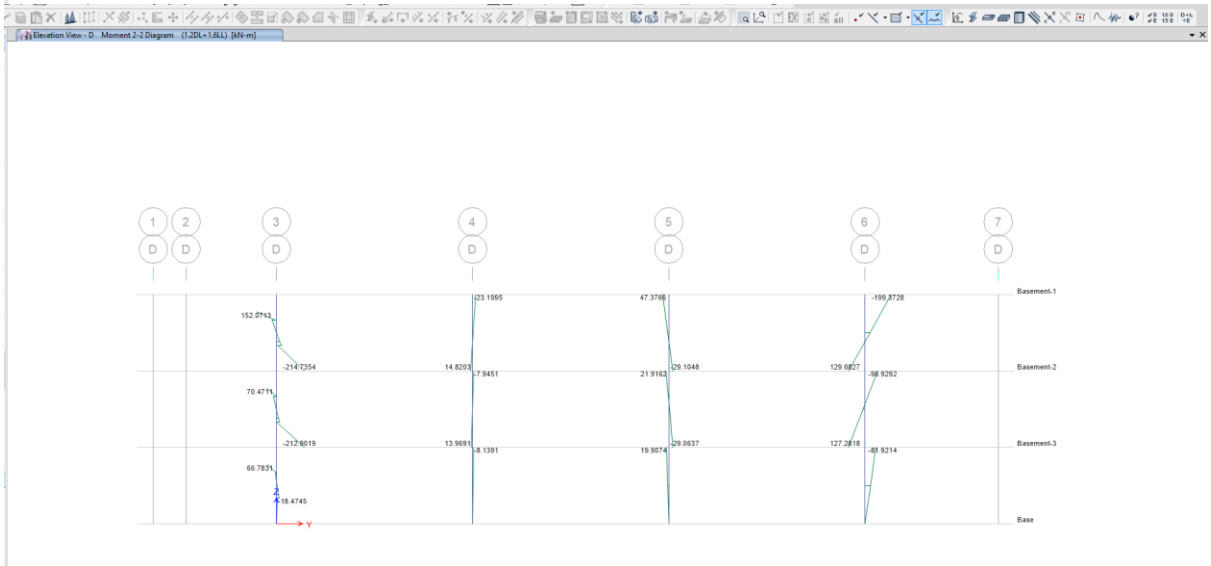
Elevation View - D Moment 2-2 Diagram (1.2DL+1.6LL) [kN-m]
1 2 3 4 5 6 7
D D D D D D D
152.0743
-214.7354
70.4771
-212.9019
66.7831
-18.4745
23.1995
-7.9451
14.8203
-8.1391
13.9691
47.3766
-29.1048
21.9162
-29.0637
19.9874
-199.8728
129.6827
-88.9292
127.2818
-88.9214
Basement-1
Basement-2
Basement-3
Base

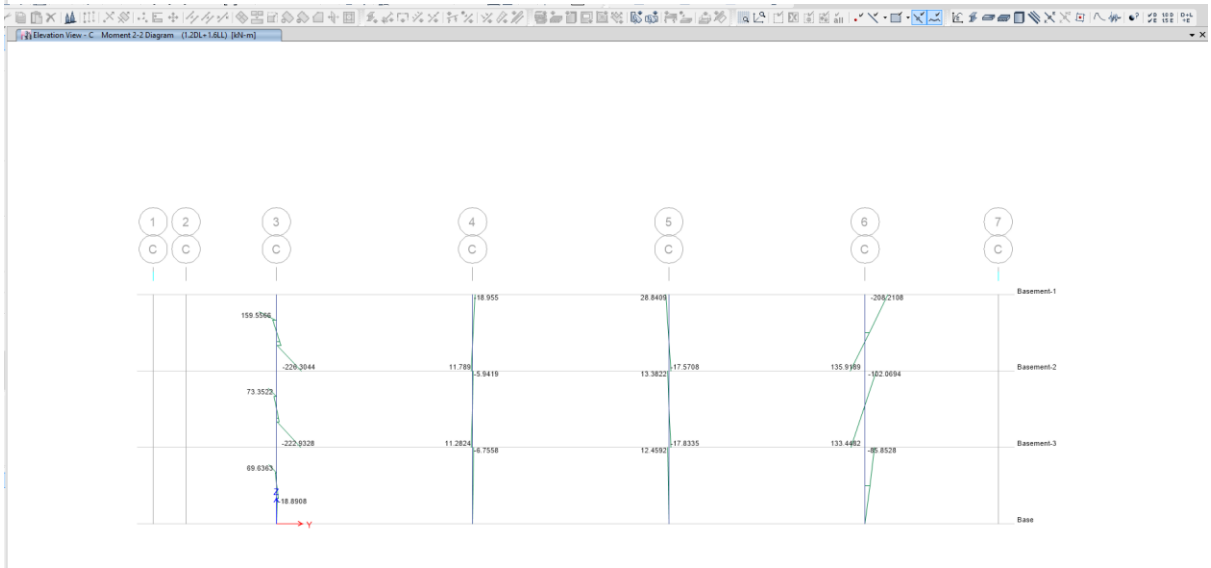
Elevation View - C Moment 2-2 Diagram (1.2DL+1.6LL) [kN-m]
1 2 3 4 5 6 7
C C C C C C C
159.5566
-220.3044
73.3523
-222.0328
69.6363
-18.8908
18.955
-5.9419
11.789
-6.7558
11.2824
28.8409
-17.5708
13.3822
-17.8335
12.4592
-208.2108
135.9189
-102.0694
133.4482
-85.8528
Basement-1
Basement-2
Basement-3
Base

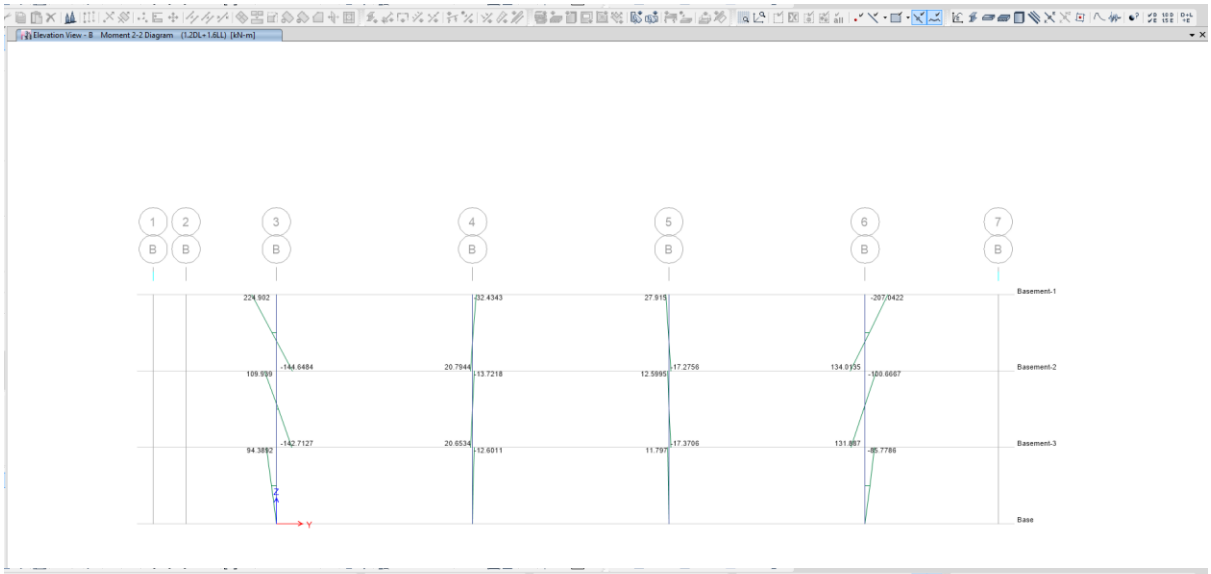
Elevation View - B Moment 2-2 Diagram (1.2DL+1.6LL) [kN-m]
1
2
3
4
5
6
7
B
224.902
-144.6484
109.9109
-142.7127
94.3892
-52.4343
20.7944
113.7218
20.6534
112.6011
27.915
-17.2756
12.5995
-17.3706
11.797
-207.0422
134.0135
-100.6667
131.867
-85.7786
Basement-1
Basement-2
Basement-3
Base

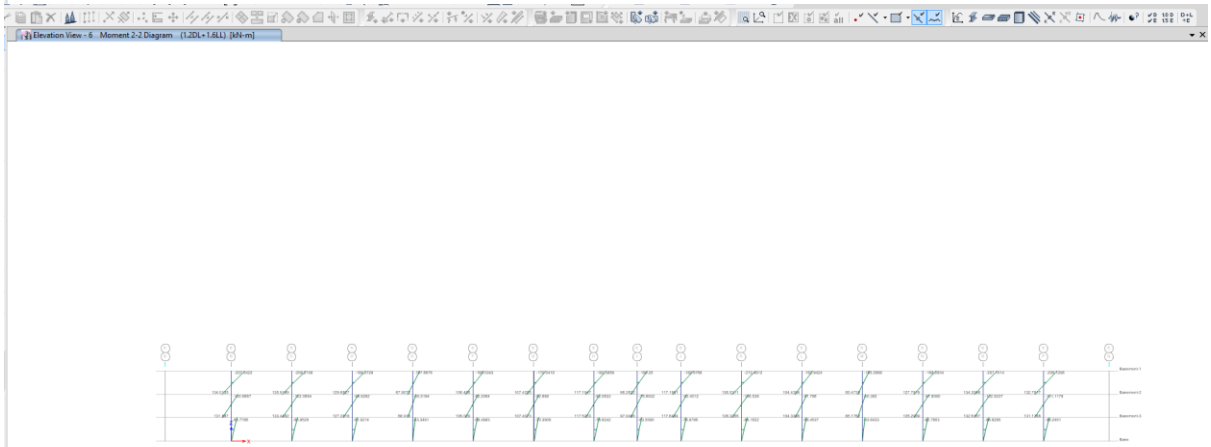
Elevation View - 6 Moment 2-2 Diagram (1.2DL+1.6LL) [kN-m]

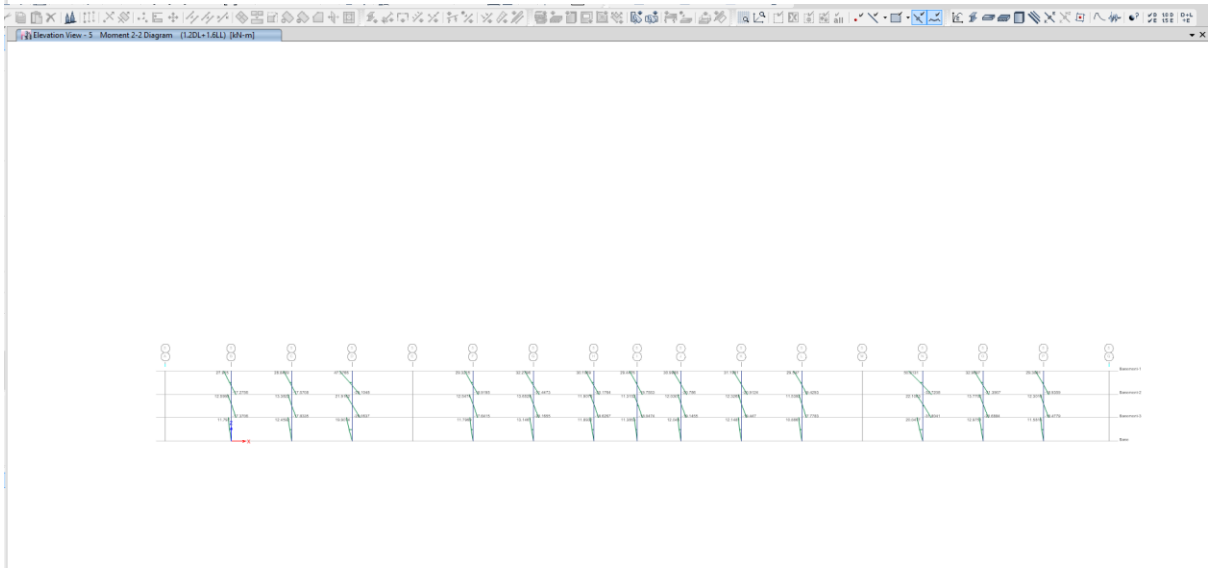
Elevation View - 5 Moment 2-2 Diagram (1.2DL+1.6LL) [kN-m]

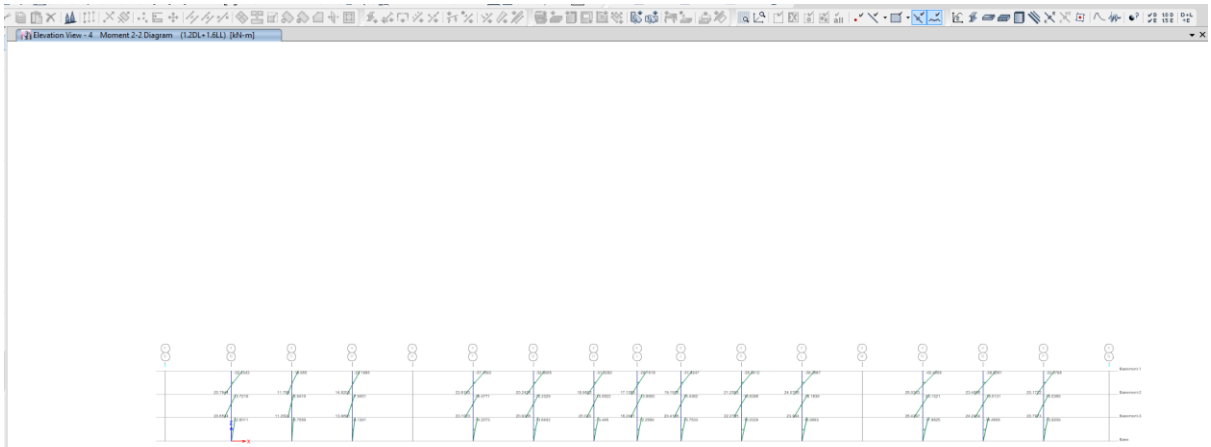

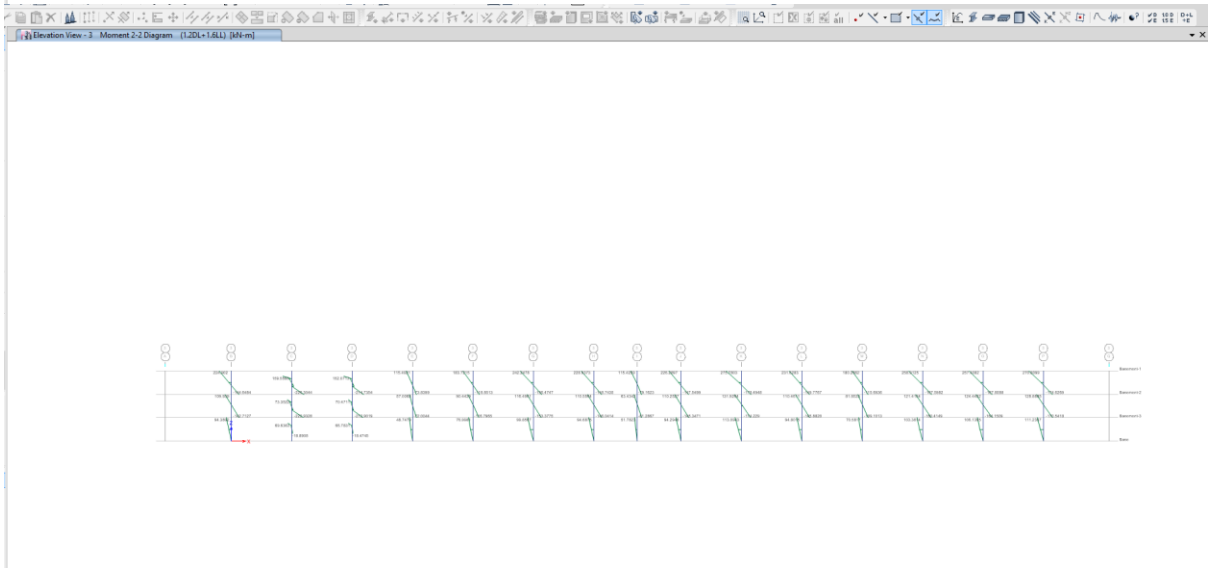

D-1-2 Column M33

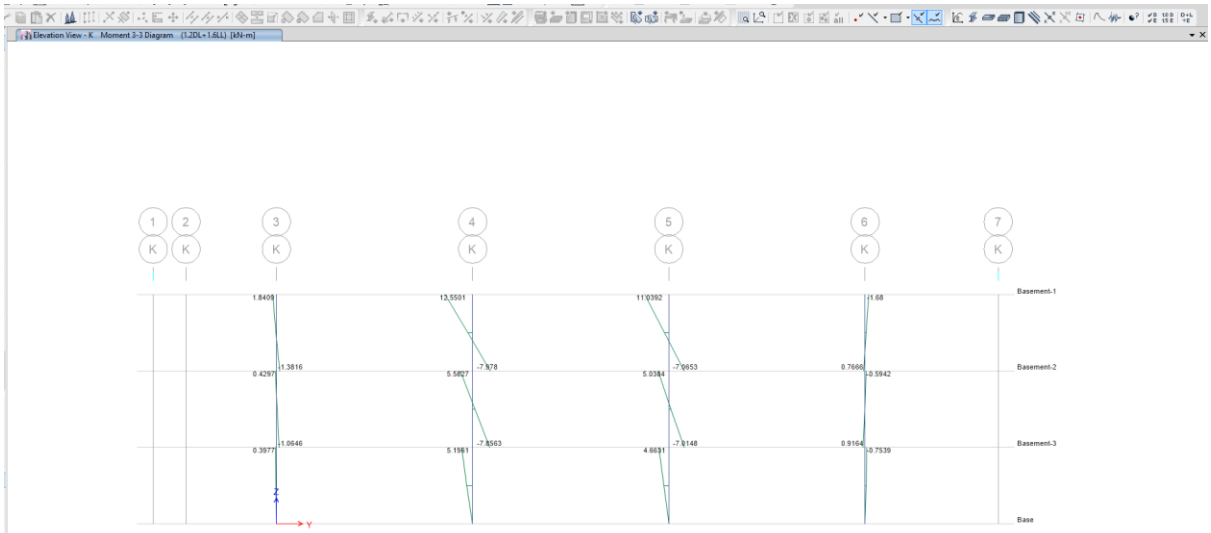
Elevation View - K Moment 3-3 Diagram (1.2DL+1.6LL) [kN-m]
1 2 3 4 5 6 7
K K K K K K K
1.8409
-1.3816
0.4297
-1.0646
0.3977
12.5501
-7.878
5.5827
-7.8563
5.1961
11.0392
-7.0853
5.0384
-7.0148
4.6631
1.68
-0.5942
0.7666
-0.7539
0.9164
Basement-1
Basement-2
Basement-3
Base

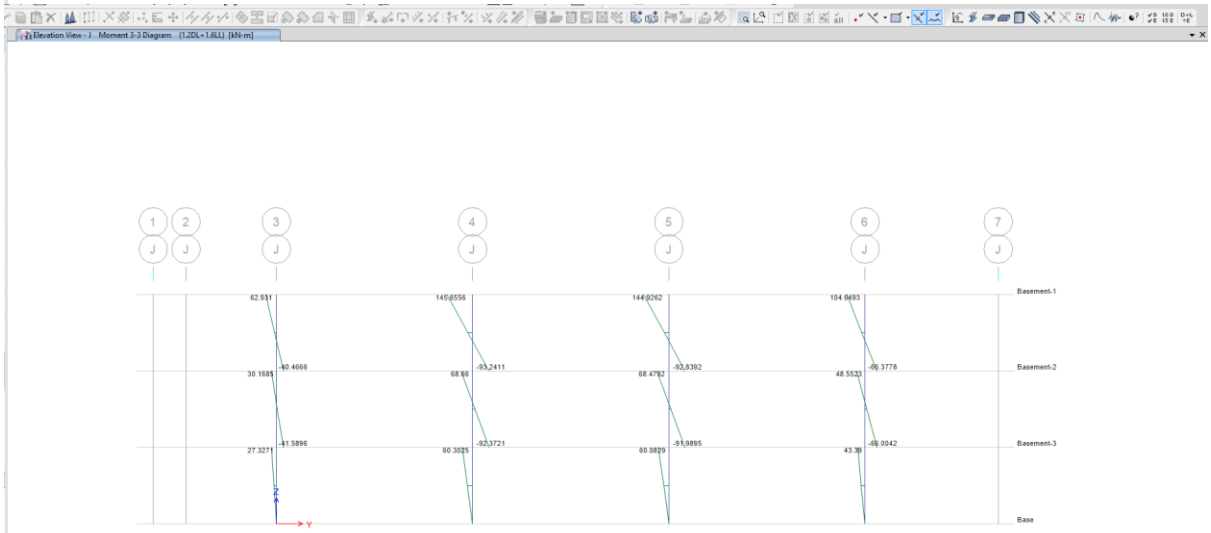
Elevation View - J Moment 3-3 Diagram (1.2DL+1.6LL) [kN-m]
1 2 3 4 5 6 7
J J J J J J J
62.931
-40.4666
30.1685
-41.5896
27.3271
145.6556
-93.2411
68.66
-92.3721
60.3025
144.0262
-92.8392
68.4792
-91.9895
60.0829
104.8493
-66.3778
48.5523
-66.0042
43.39
Basement-1
Basement-2
Basement-3
Base

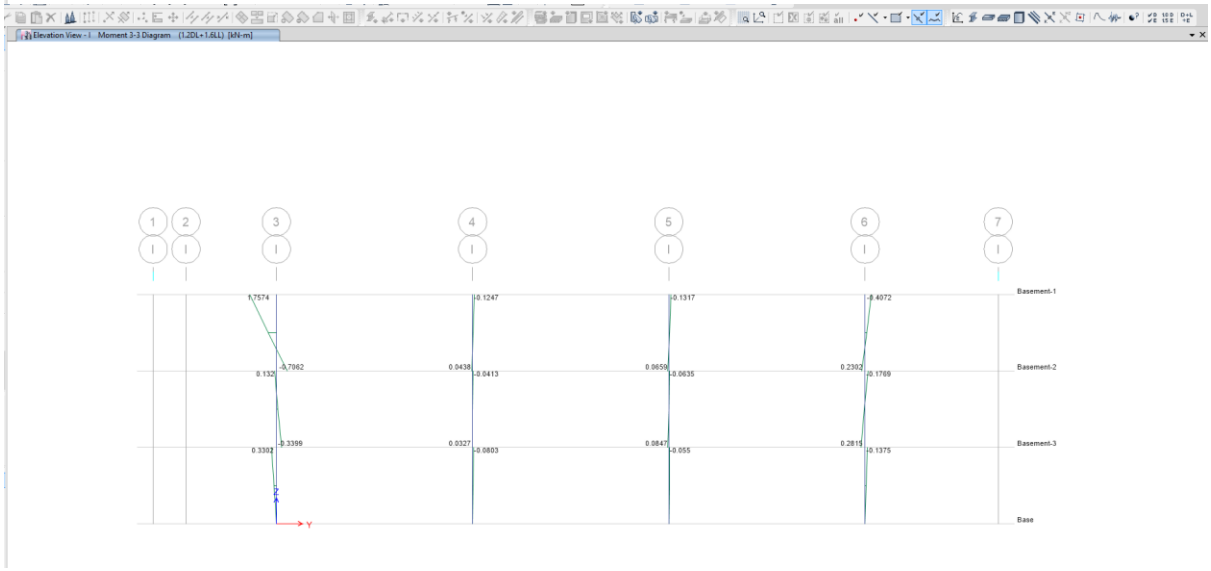
Elevation View - I Moment 3-3 Diagram (1.2DL+1.6LL) [kN-m]
1 2 3 4 5 6 7
I I I I I I I
1.7574
-0.7062
0.132
-0.3399
0.3302
0.1247
-0.0413
0.0438
-0.0803
0.0327
0.1317
-0.0635
0.0659
-0.055
0.0847
0.4072
-0.1769
0.2302
-0.1375
0.2815
Basement-1
Basement-2
Basement-3
Base

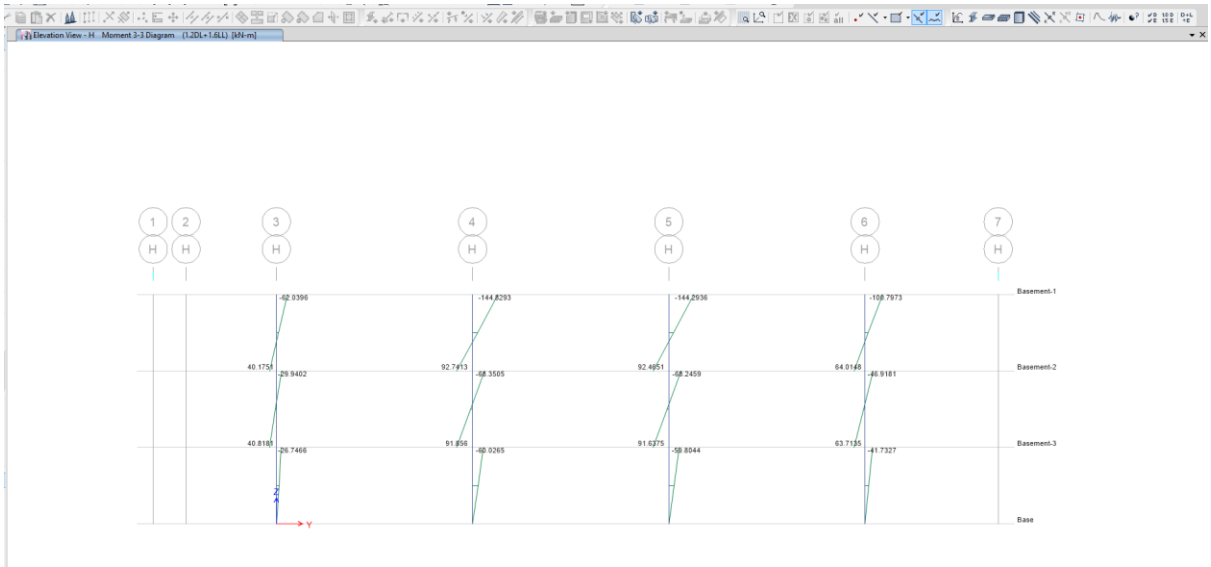
Elevation View - H Moment 3-3 Diagram (1.2DL+1.6LL) [kN-m]
1 2 3 4 5 6 7
H H H H H H H
-82.0396
-144.8293
-144.2936
-108.7973
40.1751
-29.9402
92.7913
-68.3505
92.4951
-68.2459
64.0148
-46.9181
40.8188
-29.7466
91.856
-68.0265
91.6375
-58.8044
63.7135
-41.7327
Basement-1
Basement-2
Basement-3
Base

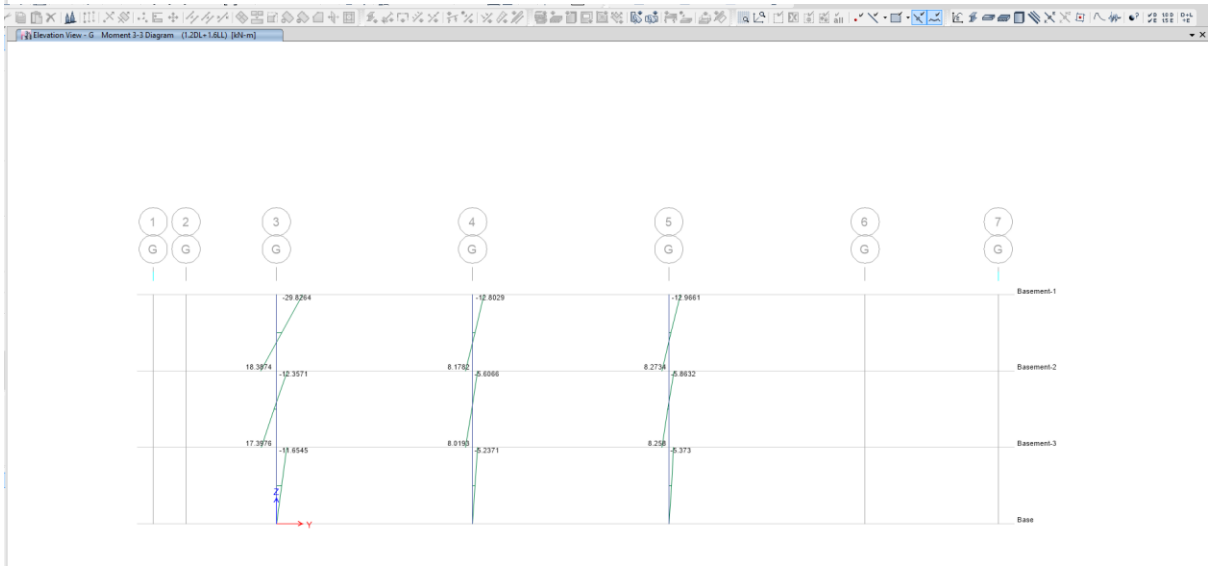
Elevation View - G Moment 3-3 Diagram (1.2DL+1.6LL) [kN-m]
1 2 3 4 5 6 7
G G G G G G G
-29.8264
-12.8029
-12.9661
18.3874
-12.3571
8.1782
-5.6066
8.2734
-5.8632
17.3978
-11.6545
8.0193
-5.2371
8.258
-5.373
Basement-1
Basement-2
Basement-3
Base

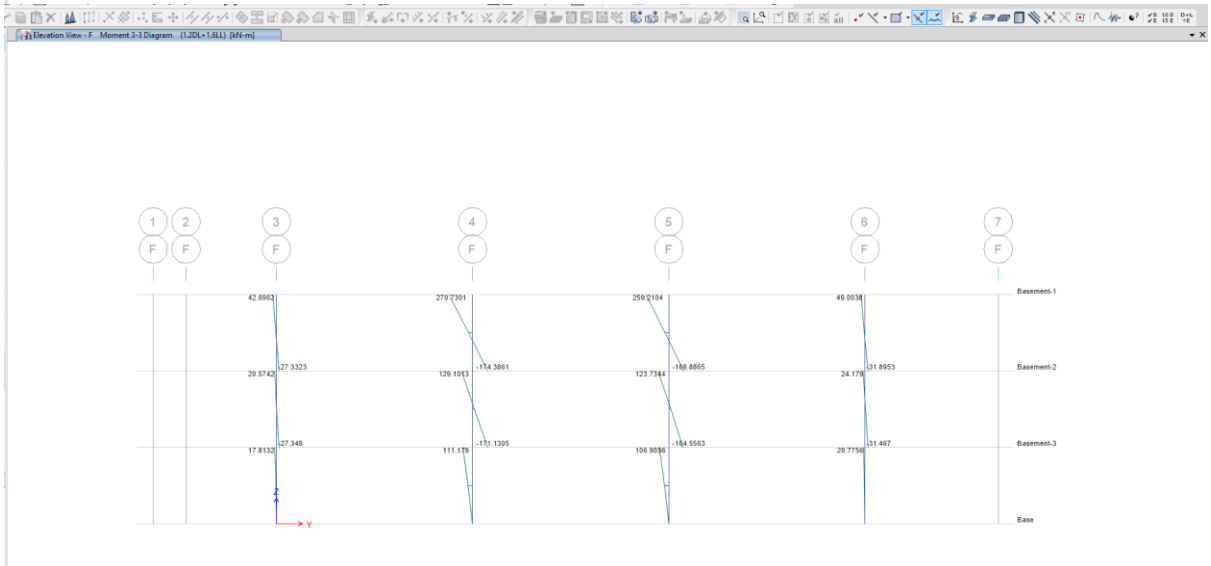
Elevation View - F Moment 3-3 Diagram (1.2DL+1.6LL) [kN-m]
1 2 3 4 5 6 7
F F F F F F F
42.8962
270.7301
259.2104
49.9038
20.5742
-27.3323
129.1013
-174.3861
123.7344
-166.8865
24.178
-31.8953
17.8132
-27.349
111.179
-171.1305
106.9056
-164.5563
20.7756
-31.467
Basement-1
Basement-2
Basement-3
Base

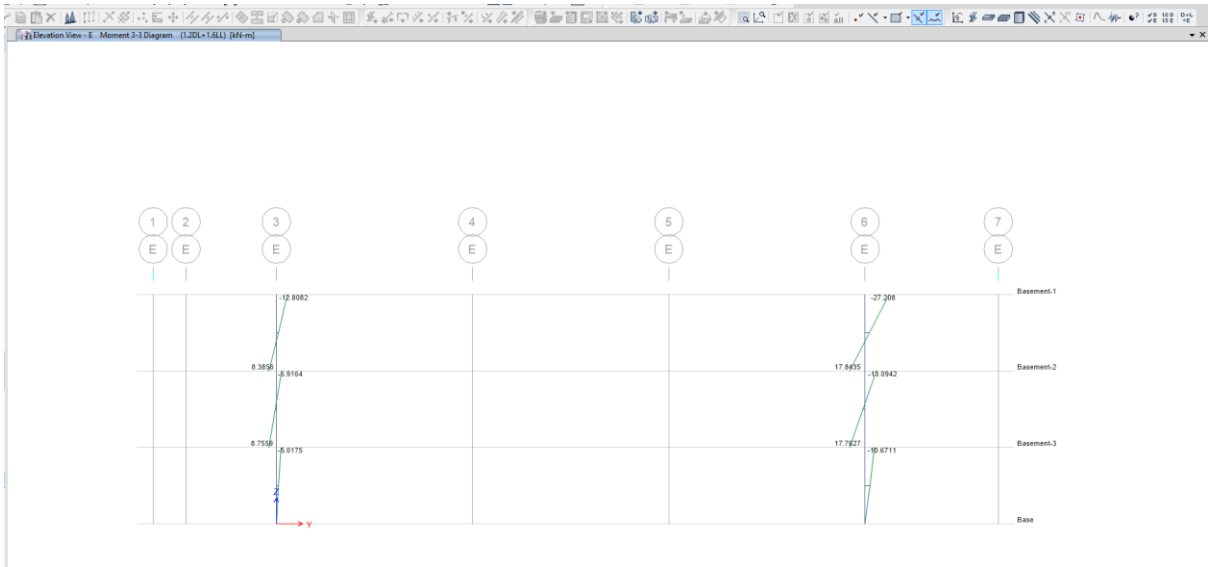
Elevation View - E Moment 3-3 Diagram (1.2DL+1.6LL) [kN-m]
1 2 3 4 5 6 7
E E E E E E E
-12.8082
8.3858
-8.9164
8.7558
-9.0175
-27.208
17.8435
-18.0942
17.7927
-18.0711
Basement-1
Basement-2
Basement-3
Base

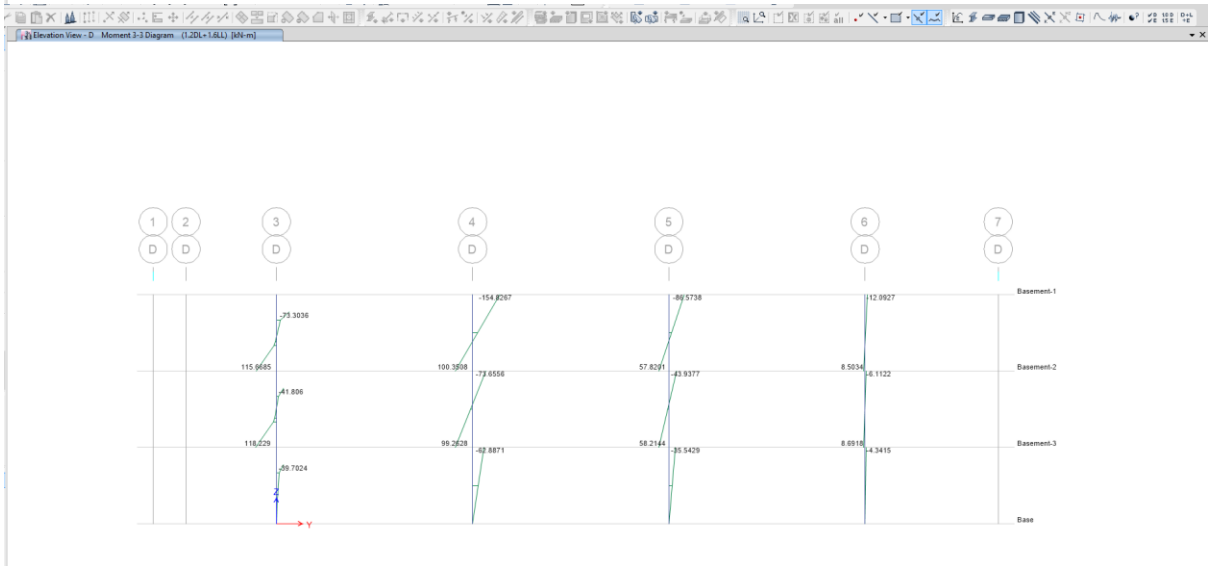
Elevation View - D Moment 3-3 Diagram (1.2DL+1.6LL) [kN-m]
1 2 3 4 5 6 7
D D D D D D D
-75.3036
115.9685
-41.806
118.229
-89.7024
-154.8267
100.3598
-73.6556
99.2628
-82.8871
-89.5738
57.8291
-43.9377
58.2144
-35.5429
12.0927
8.5034
-6.1122
8.6918
-4.3415
Basement-1
Basement-2
Basement-3
Base

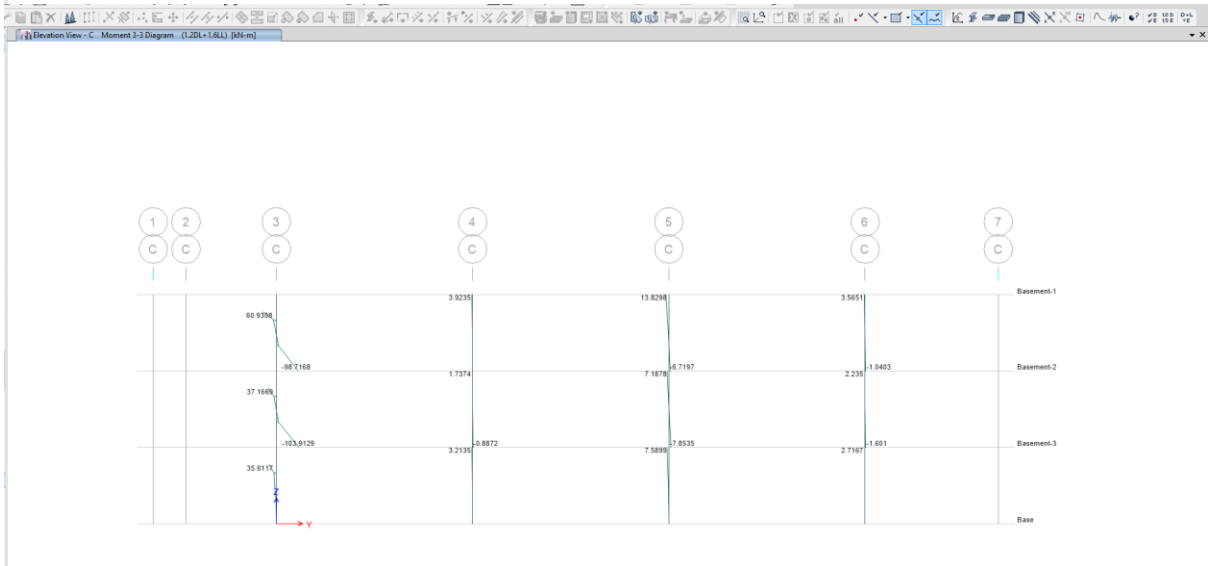
Elevation View - C Moment 3-3 Diagram (1.2DL+1.6LL) [kN-m]
1 2 3 4 5 6 7
C C C C C C C
60.9398
-88.7168
37.1669
-103.9129
35.6117
3.9235
1.7374
-0.8872
3.2135
13.8298
7.1878
-6.7197
7.5899
-7.8535
3.5651
2.235
-1.9403
2.7167
-1.691
Basement-1
Basement-2
Basement-3
Base

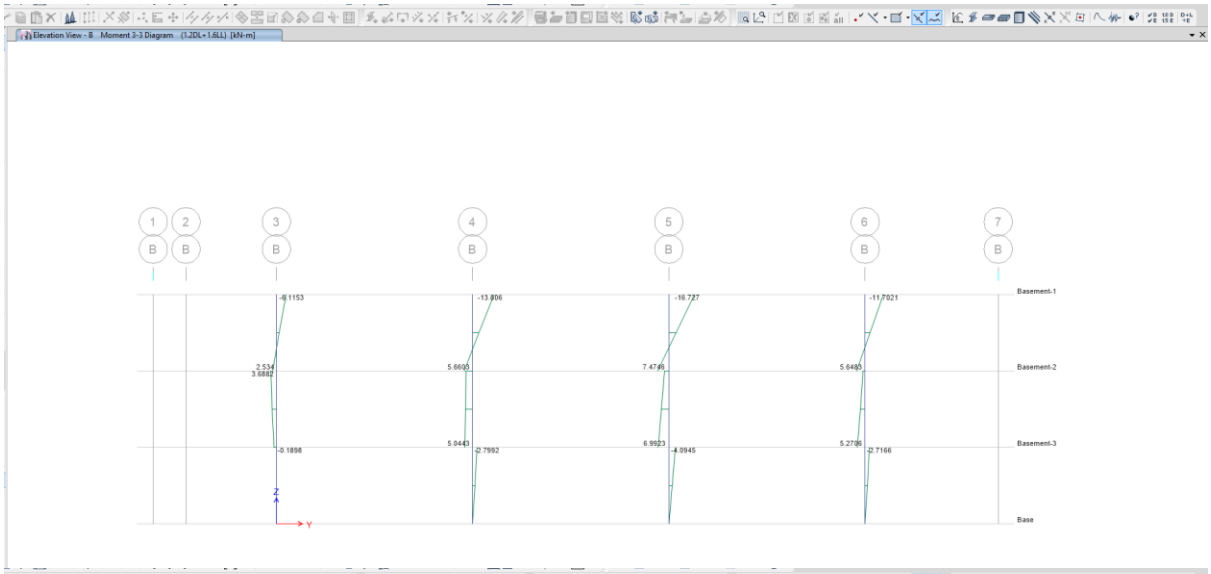
Elevation View - B Moment 3-3 Diagram (1.2DL+1.6LL) [kN-m]
1
2
3
4
5
6
7
B
-8.1153
-13.806
-16.727
-11.7021
2.534
3.6882
5.6605
7.4749
5.6485
-0.1898
5.9443
-2.7992
6.9923
-4.0945
5.2736
-2.7166
Basement-1
Basement-2
Basement-3
Base

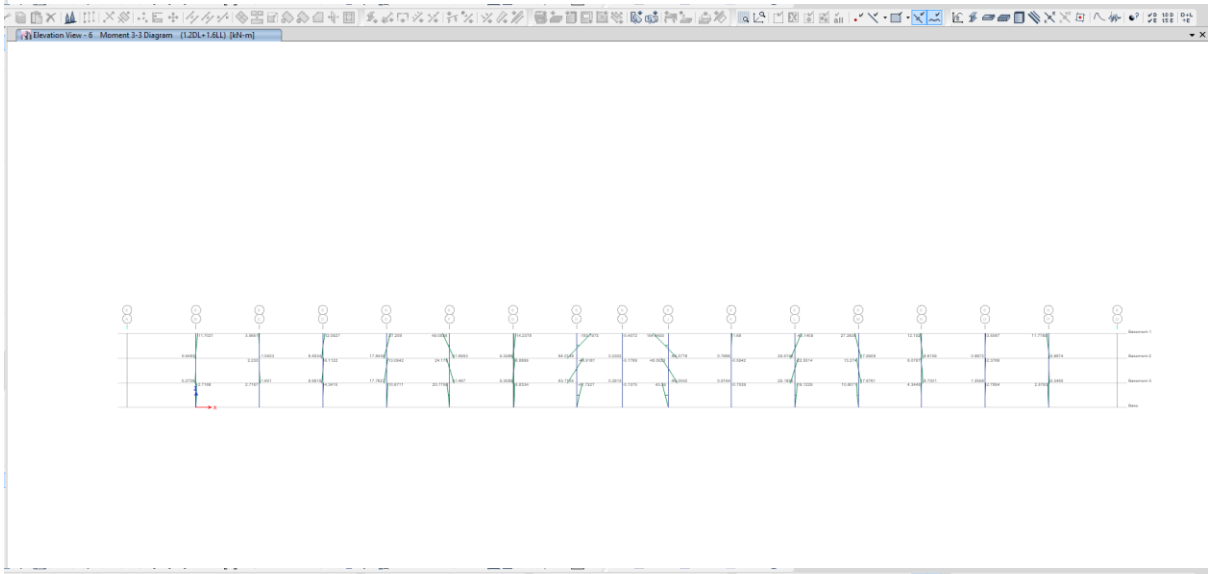
Elevation View - 6 Moment 3-3 Diagram (1.2DL+1.6LL) [kN-m]

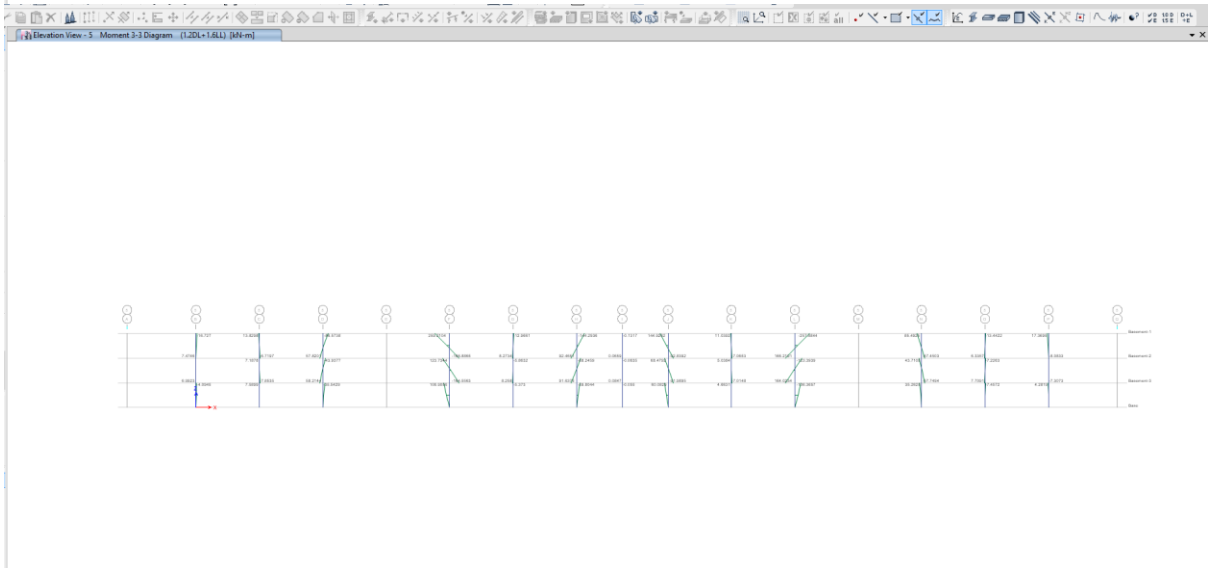
Elevation View - 5 Moment 3-3 Diagram (1.2DL+1.6LL) [kN-m]

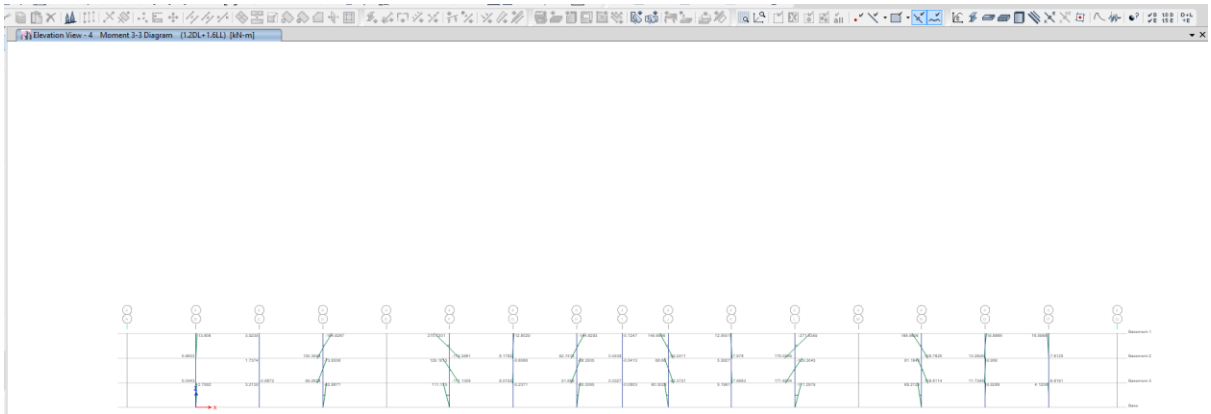

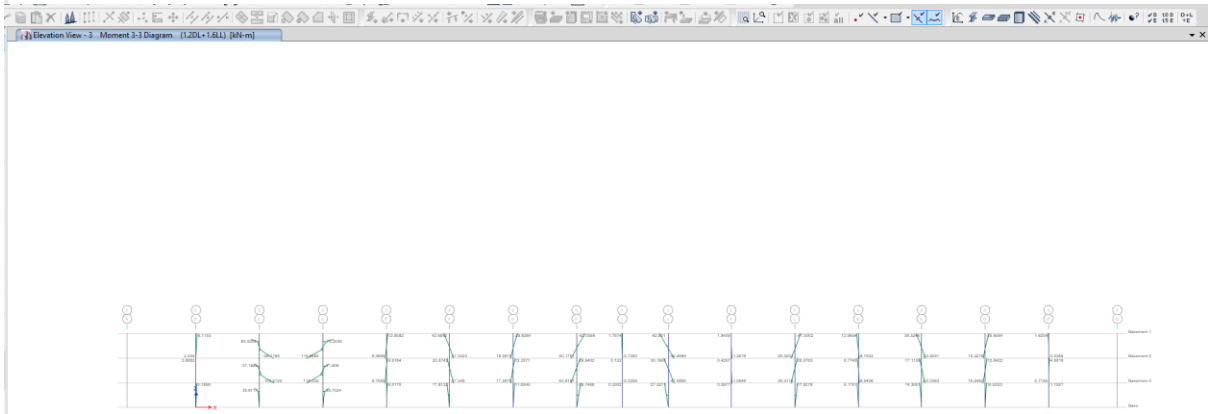

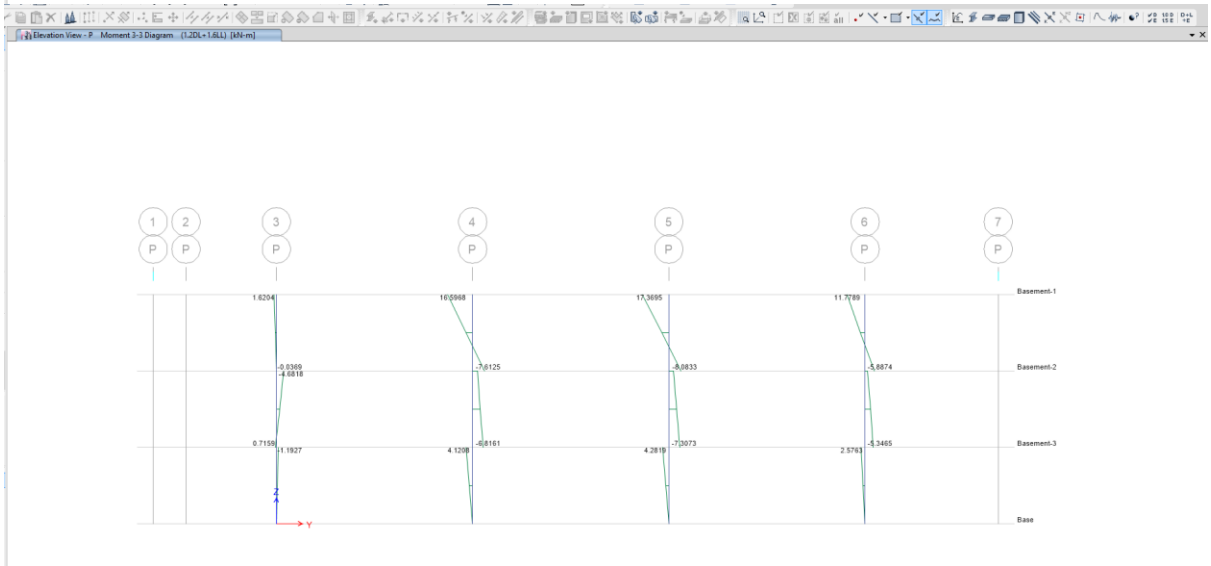
1
2
3
4
5
6
7
P
1.6204
-0.0369
-4.6818
0.7159
-1.1927
16.0968
-7.6125
-6.8161
4.1208
17.3695
-8.0833
-7.3073
4.2819
11.7789
-5.8874
-5.3465
2.5763
Basement-1
Basement-2
Basement-3
Base

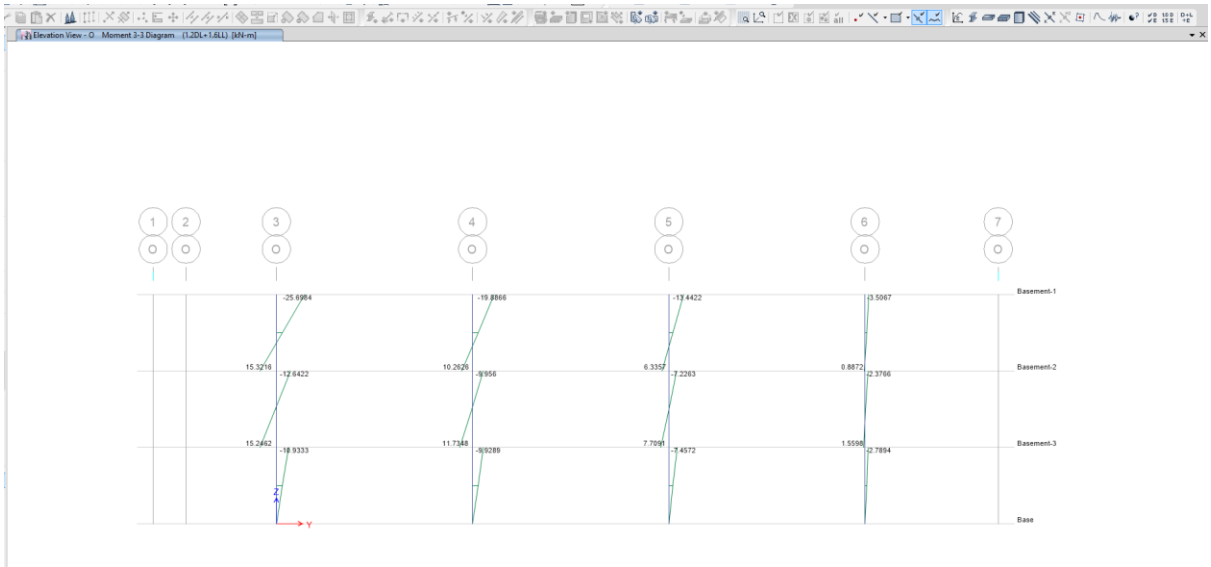
Elevation View - O Moment 3-3 Diagram (1.2DL+1.6LL) [kN-m]
1
2
3
4
5
6
7
O
-25.6984
15.3216
-17.6422
15.2462
-18.9333
-19.8866
10.2629
-8.956
11.7348
-9.9289
-17.4422
6.3357
-7.2263
7.7098
-7.4572
3.5067
0.8872
2.3766
1.5598
2.7894
Basement-1
Basement-2
Basement-3
Base

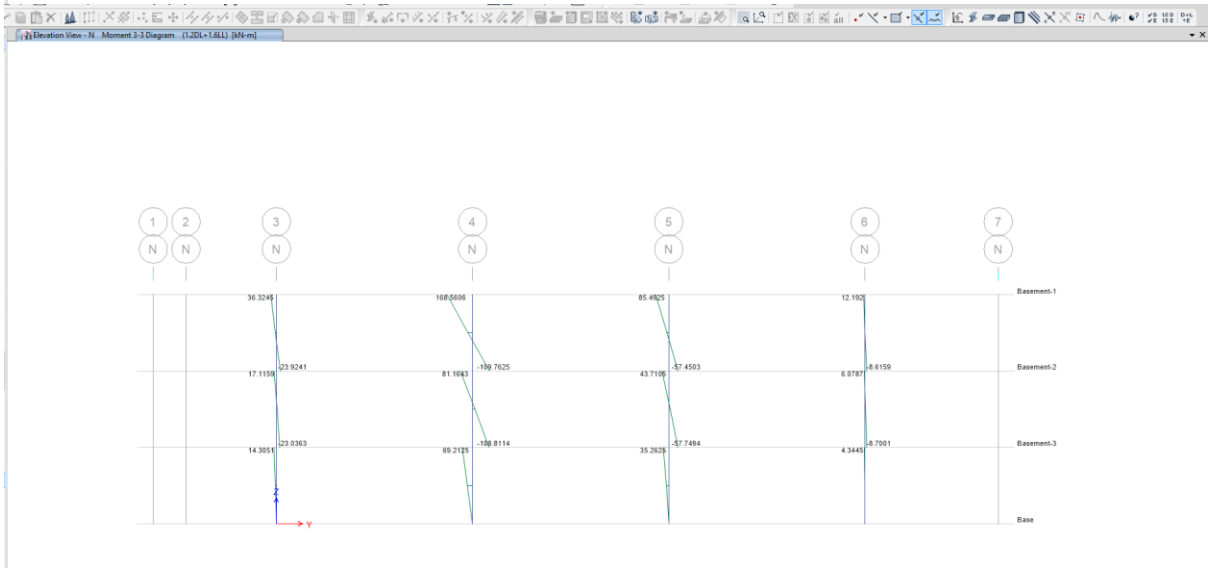
Elevation View - N Moment 3-3 Diagram (1.2DL+1.6LL) [kN-m]
1
2
3
4
5
6
7
N
36.3245
17.1159
23.9241
14.3051
23.0363
168.5606
81.1643
-109.7625
69.2125
-109.8114
85.4925
43.7105
-57.4503
35.2625
-57.7494
12.1925
6.0787
-8.6159
4.3445
-8.7001
Basement-1
Basement-2
Basement-3
Base

D-1-3 Slab Forces

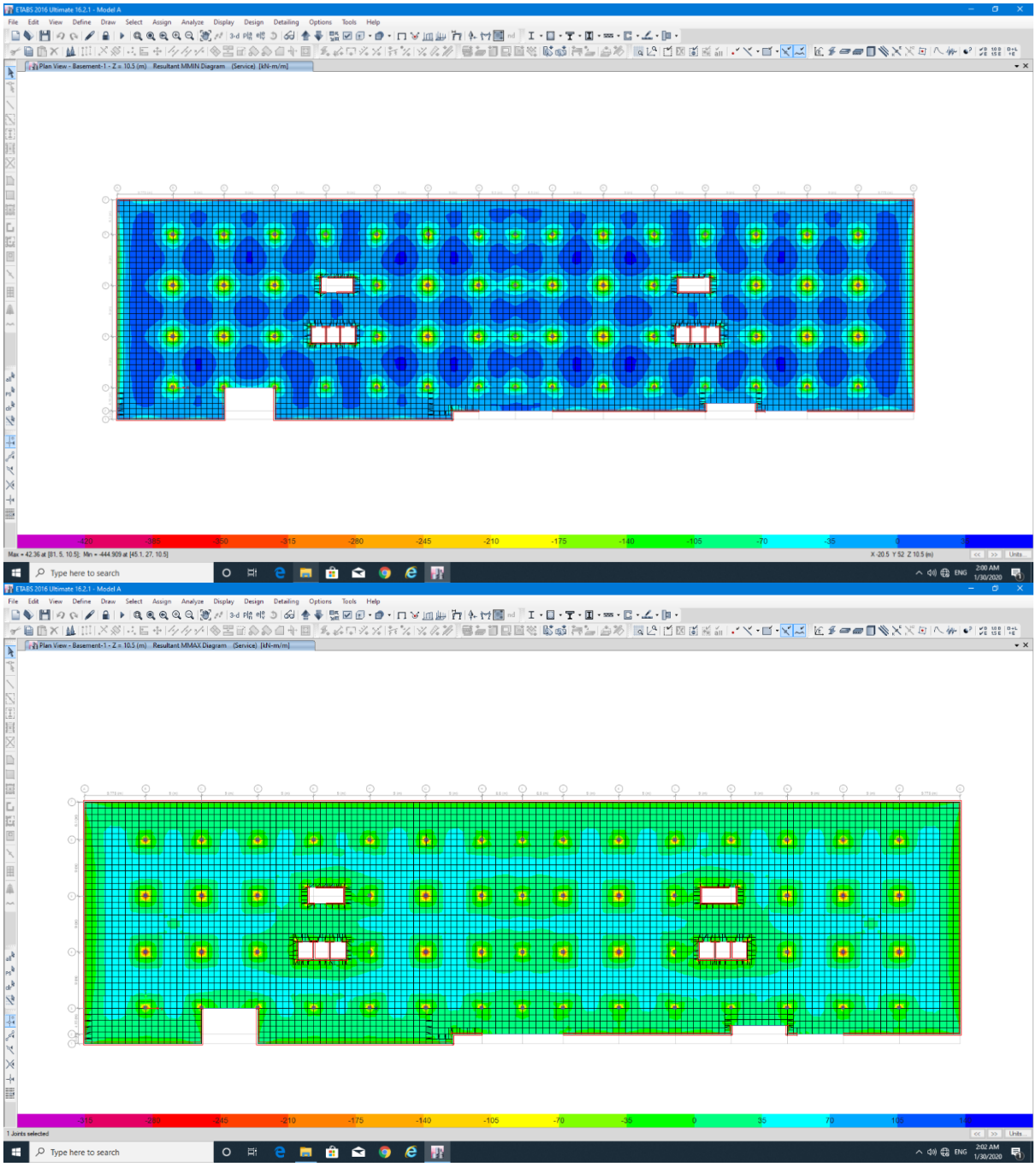
ETABS 2016 Ultimate 16.2.1 - Model A
Plan View - Basement-1 - Z = 10.5 (m) Resultant MMIN Diagram (Service) [kN-m/m]
-420 -385 -350 -315 -280 -245 -210 -175 -140 -105 -70 -35 0 35
Max = 42.36 at [81.5, 10.5]; Min = -444.909 at [45.1, 27, 10.5]
X -20.5 Y 52 Z 10.5 (m)
Type here to search
2:00 AM 1/30/2020
ETABS 2016 Ultimate 16.2.1 - Model A
Plan View - Basement-1 - Z = 10.5 (m) Resultant MMAX Diagram (Service) [kN-m/m]
-315 -280 -245 -210 -175 -140 -105 -70 -35 0 35 70 105 140
1 Joints selected
Type here to search
2:02 AM 1/30/2020

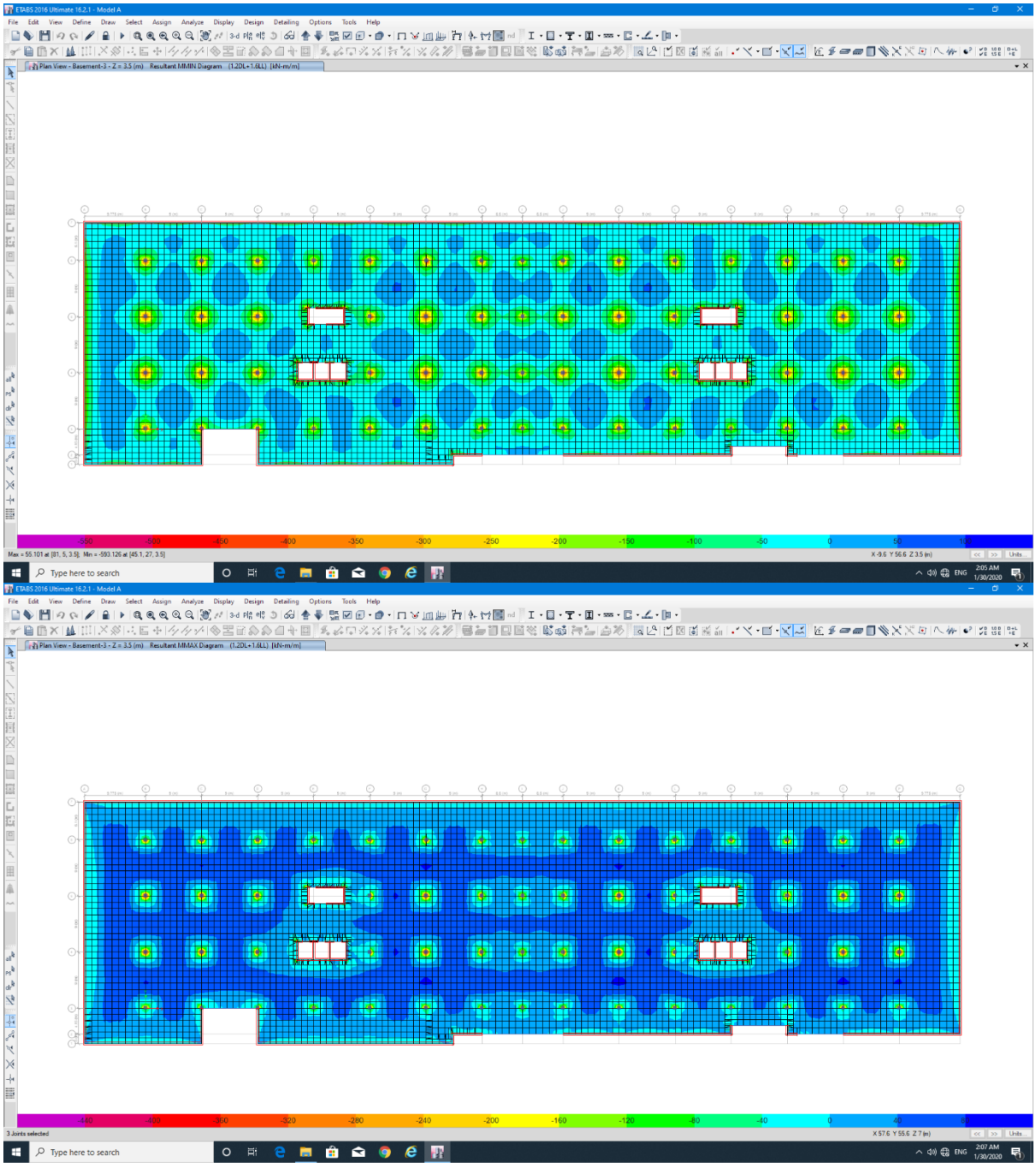
ETABS 2016 Ultimate 16.2.1 - Model A
Plan View - Basement-3 - Z = 3.5 (m) Resultant MMIN Diagram (1.2DL+1.6LL) [kN-m/m]
Type here to search
2:05 AM
1/30/2020
ETABS 2016 Ultimate 16.2.1 - Model A
Plan View - Basement-3 - Z = 3.5 (m) Resultant MMAX Diagram (1.2DL+1.6LL) [kN-m/m]
Type here to search
2:07 AM
1/30/2020

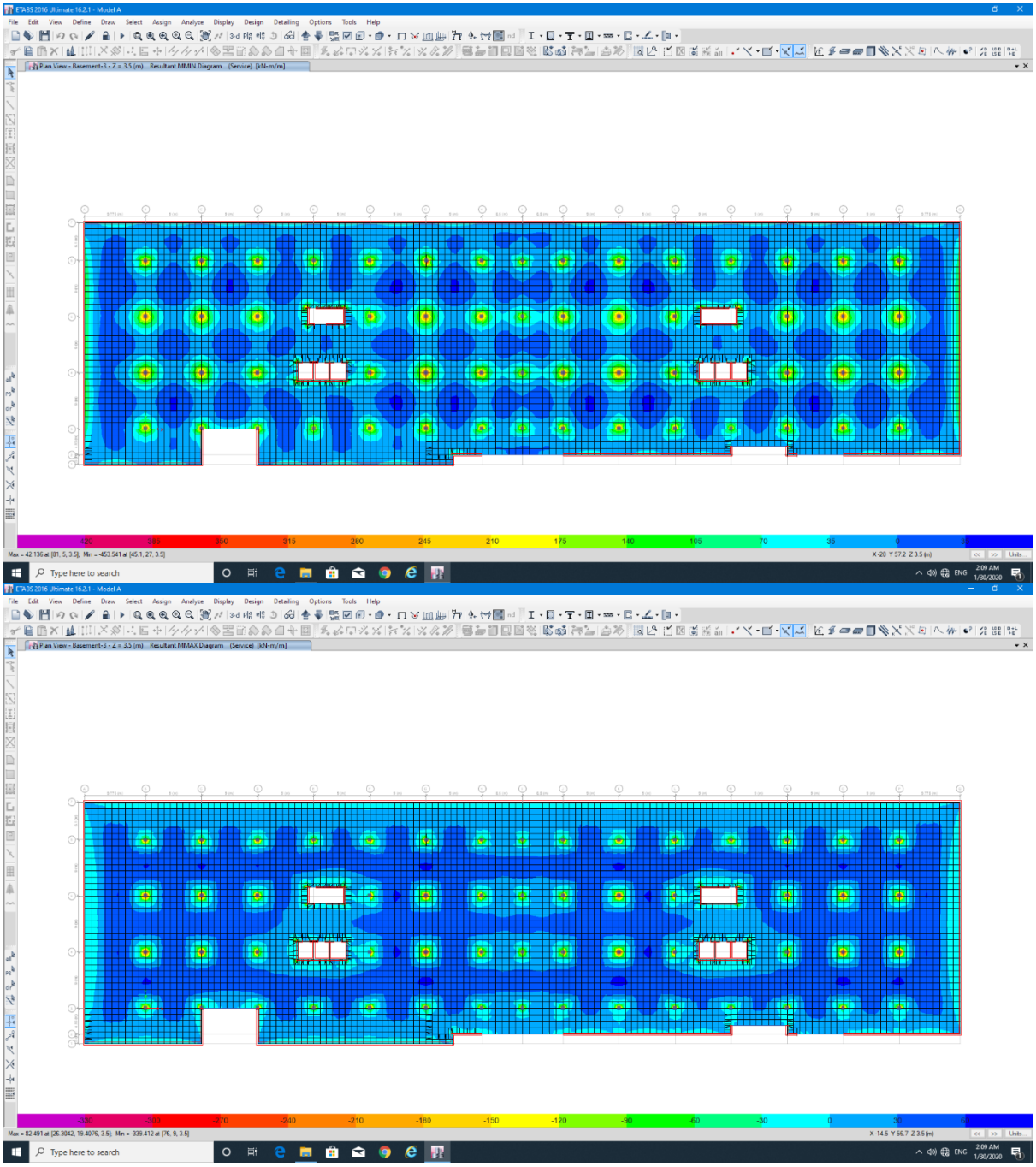
ETABS 2016 Ultimate 16.2.1 - Model A
Plan View - Basement-3 - Z = 3.5 (m) Resultant MMIN Diagram (Service) (kN-m/m)
-420 -385 -350 -315 -280 -245 -210 -175 -140 -105 -70 -35 0 35
Type here to search
2:09 AM 1/30/2020
ETABS 2016 Ultimate 16.2.1 - Model A
Plan View - Basement-3 - Z = 3.5 (m) Resultant MMAX Diagram (Service) (kN-m/m)
-330 -300 -270 -240 -210 -180 -150 -120 -90 -60 -30 0 30 60
Type here to search
2:09 AM 1/30/2020

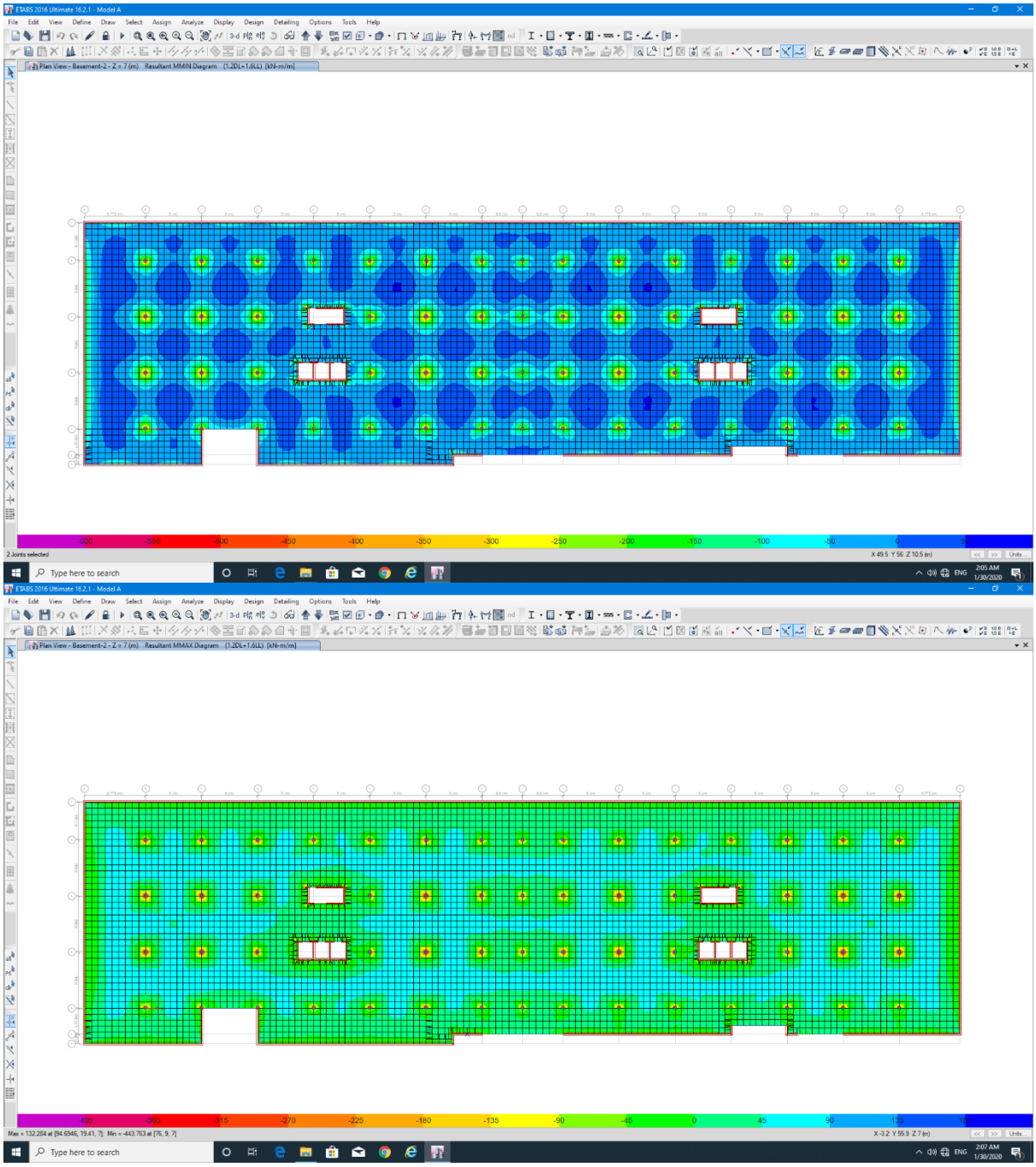
ETABS 2016 Ultimate 16.2.1 - Model A
Plan View - Basement-2 - Z = 7 (m) Resultant MMIN Diagram (1.2DL+1.6LL) (kN-m/m)
-600 -550 -500 -450 -400 -350 -300 -250 -200 -150 -100 -50 0 50
2 Joints selected
X 49.5 Y 56 Z 10.5 (m)
Units
Type here to search
2:05 AM
1/30/2020
ETABS 2016 Ultimate 16.2.1 - Model A
Plan View - Basement-2 - Z = 7 (m) Resultant MMAX Diagram (1.2DL+1.6LL) (kN-m/m)
-405 -360 -315 -270 -225 -180 -135 -90 -45 0 45 90 135 180
Max = 132.284 at [94.6946, 19.41, 7]; Min = -443.763 at [76, 9, 7]
X -3.2 Y 55.9 Z 7 (m)
Units
Type here to search
2:07 AM
1/30/2020

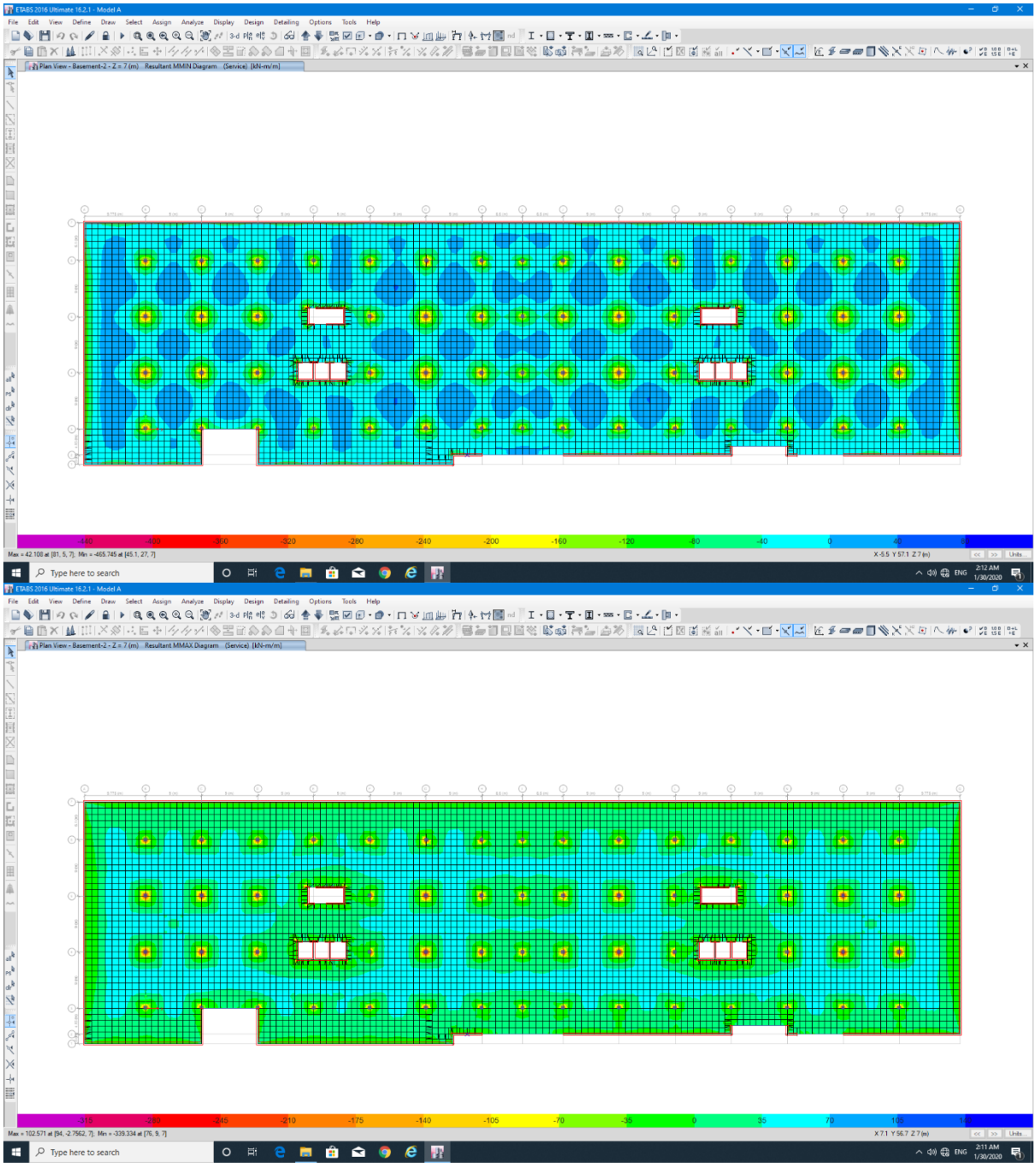
ETABS 2016 Ultimate 16.2.1 - Model A
Plan View - Basement-2 - Z = 7 (m) Resultant MMIN Diagram (Service) [kN-m/m]
-440 -400 -360 -320 -280 -240 -200 -160 -120 -80 -40 0 40 80
Max = 42.108 at [81, 5, 7]; Min = -465.745 at [45.1, 27, 7]
X -5.5 Y 57.1 Z 7 (m)
Units
Type here to search
2:12 AM
1/30/2020
ETABS 2016 Ultimate 16.2.1 - Model A
Plan View - Basement-2 - Z = 7 (m) Resultant MMAX Diagram (Service) [kN-m/m]
-315 -280 -245 -210 -175 -140 -105 -70 -35 0 35 70 105 140
Max = 102.571 at [84, -2.7562, 7]; Min = -339.334 at [76, 9, 7]
X 7.1 Y 56.7 Z 7 (m)
Units
Type here to search
2:11 AM
1/30/2020

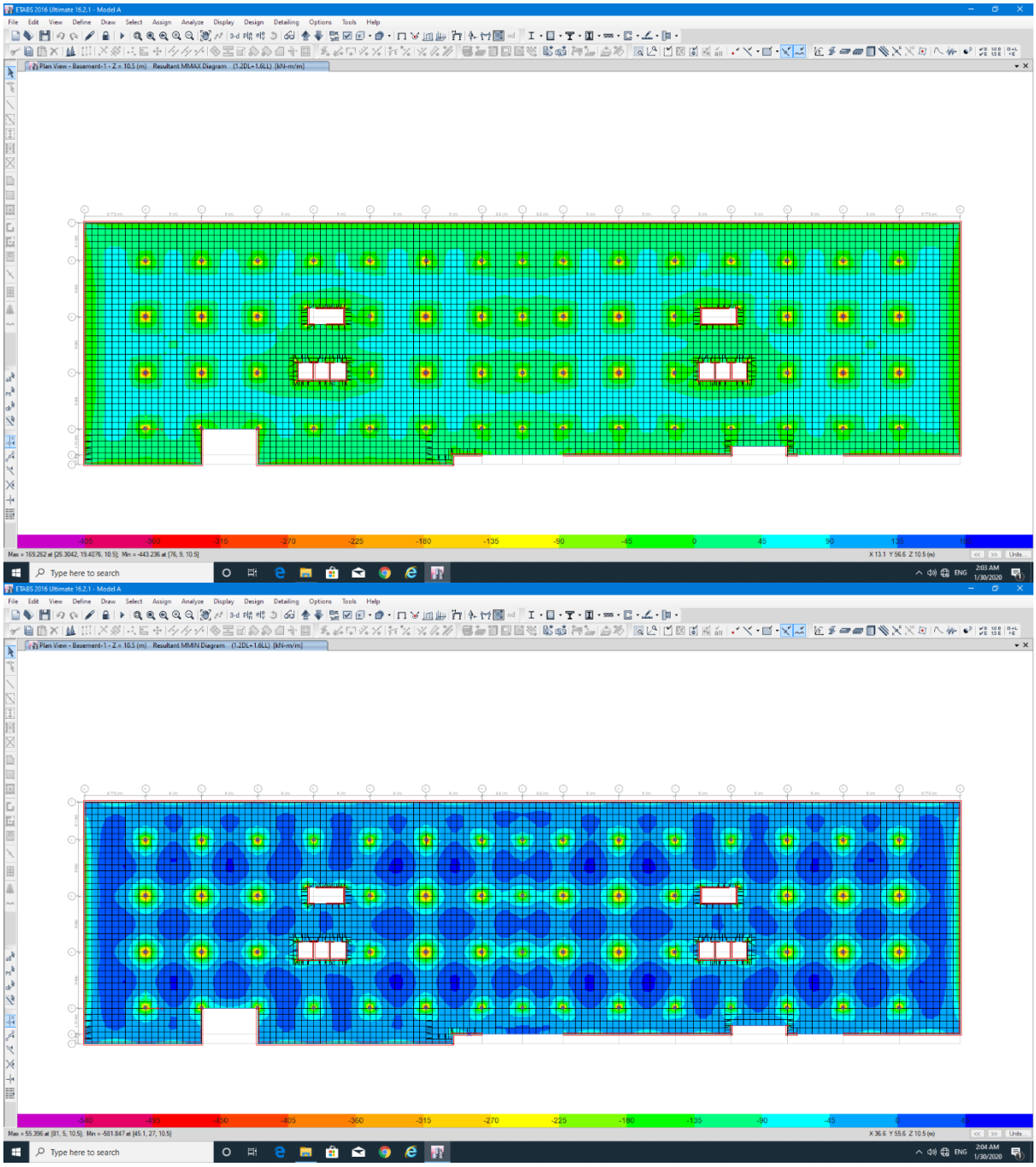

D-1-4 Walls Forces

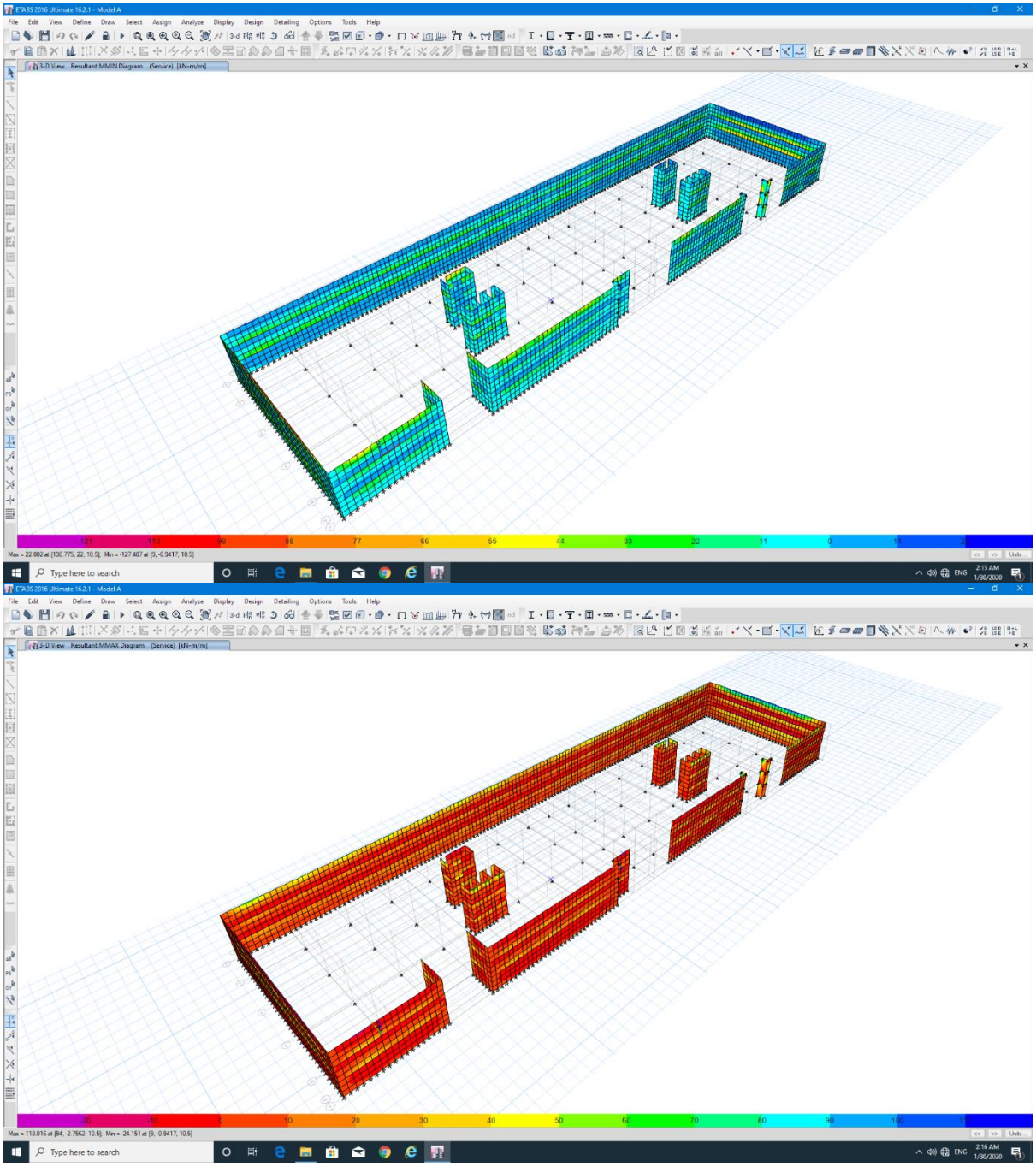
ETABS 2016 Ultimate 16.2.1 - Model A
3-D View Resultant MMIN Diagram (Service) [kN-m/m]
Type here to search
ETABS 2016 Ultimate 16.2.1 - Model A
3-D View Resultant MMAX Diagram (Service) [kN-m/m]
Type here to search

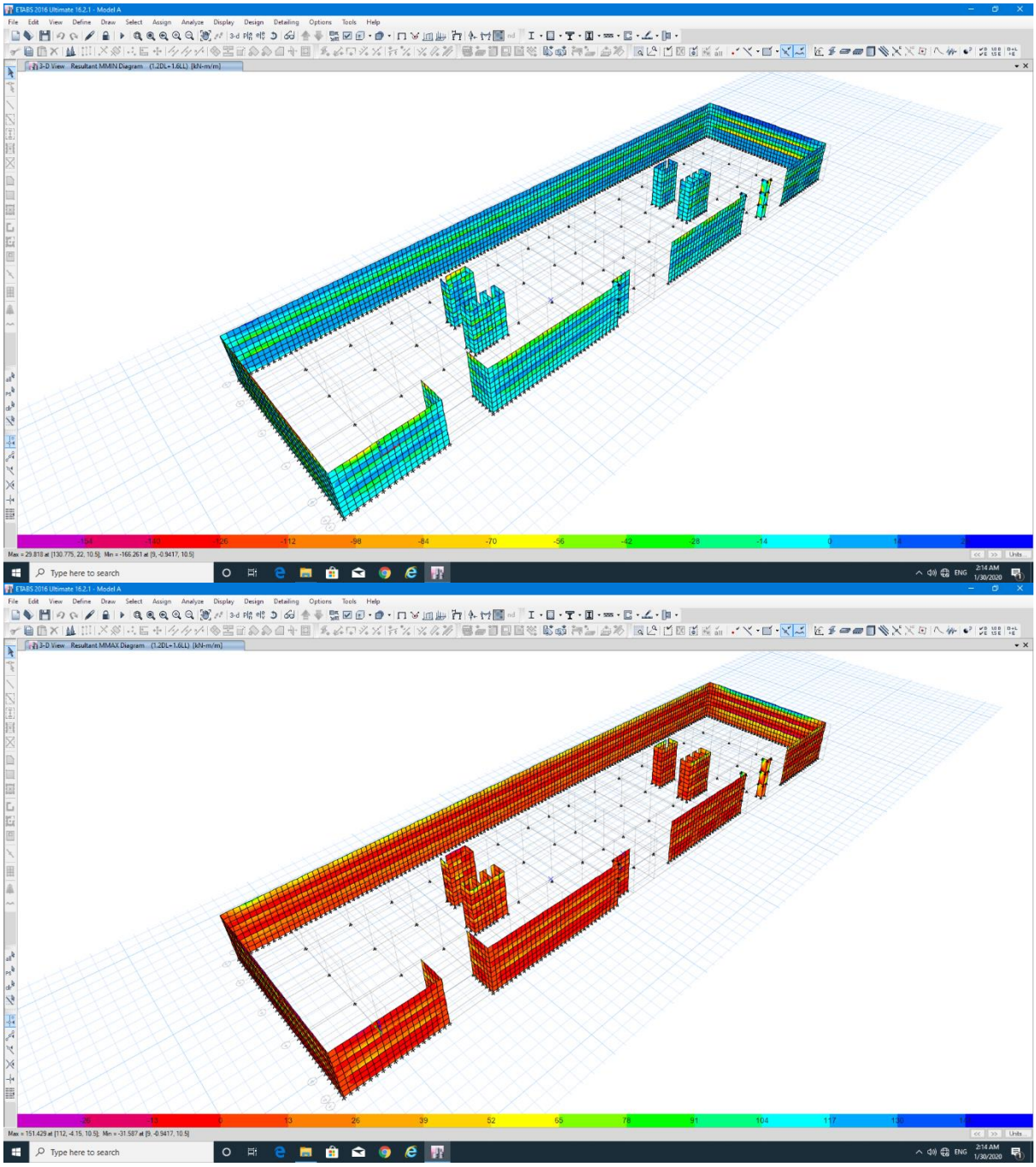

D-2 Model B
D-2-1 Column M22

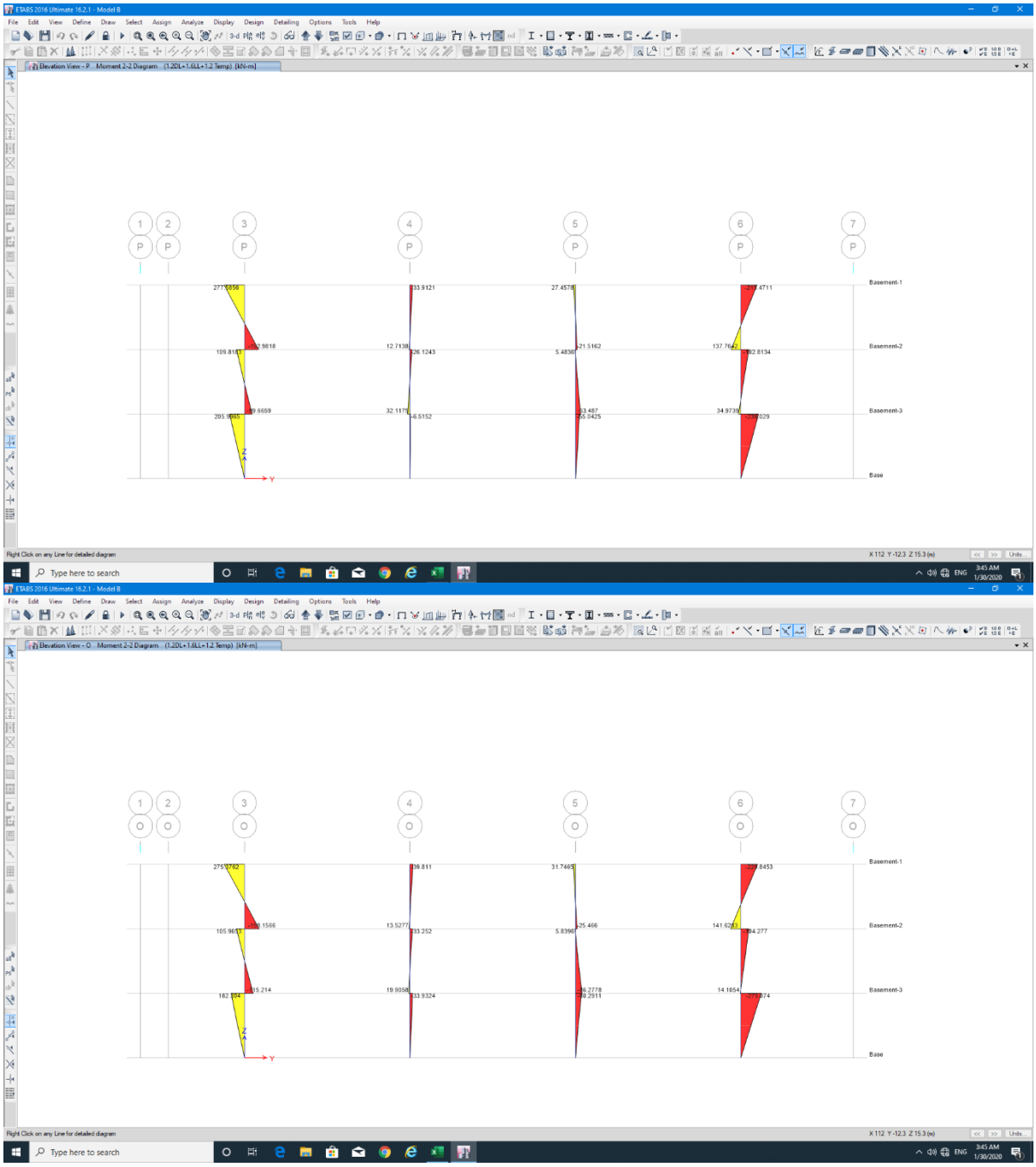
ETABS 2016 Ultimate 16.2.1 - Model B
Elevation View - P Moment 2-2 Diagram (1.2DL+1.6LL+1.2 Temp) [kN-m]
1 2 3 4 5 6 7
P P P P P P P
277.6856
109.8147
205.9005
33.9121
12.7138
32.1171
27.4578
5.4836
137.7642
34.9739
Basement-1
Basement-2
Basement-3
Base
Right Click on any Line for detailed diagram
X 112 Y -12.3 Z 15.3 (m)
Type here to search
3:45 AM
1/30/2020

ETABS 2016 Ultimate 16.2.1 - Model B
Elevation View - O Moment 2-2 Diagram (1.2DL+1.6LL+1.2 Temp) [kN-m]
1 2 3 4 5 6 7
O O O O O O O
275.0742
105.9613
182.294
39.811
13.5277
19.9058
31.7465
5.8396
141.6283
14.1054
Basement-1
Basement-2
Basement-3
Base
Right Click on any Line for detailed diagram
X 112 Y -12.3 Z 15.3 (m)
Type here to search
3:45 AM
1/30/2020

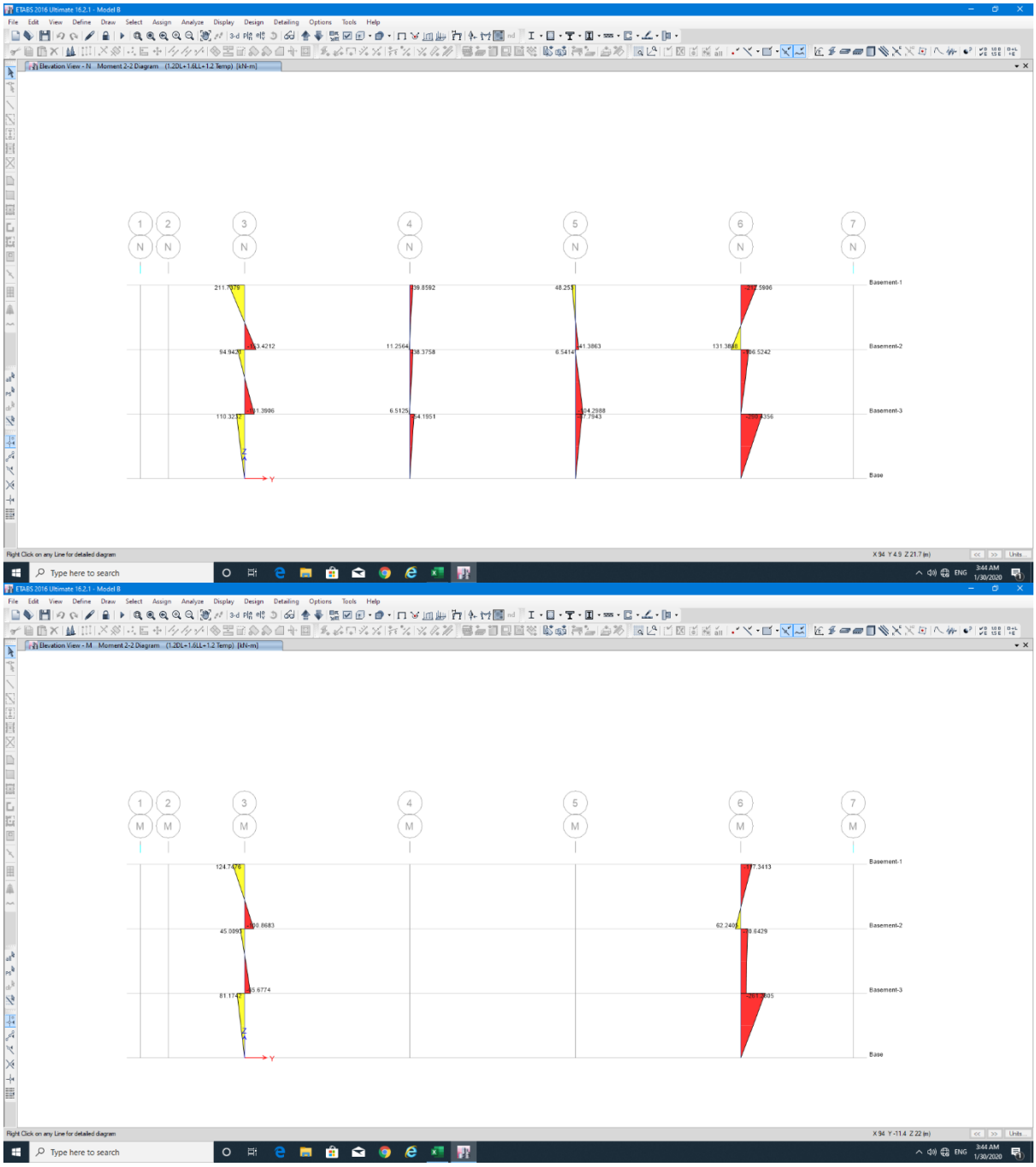
ETABS 2016 Ultimate 16.2.1 - Model B
Elevation View - N Moment 2-2 Diagram (1.2DL+1.6LL+1.2 Temp) [kN-m]
1 2 3 4 5 6 7
N N N N N N N
Basement-1
Basement-2
Basement-3
Base
211.7076
94.9430
110.3212
11.2564
6.5125
48.2511
6.5414
131.3868
Right Click on any Line for detailed diagram
Type here to search
3:44 AM
1/30/2020
ETABS 2016 Ultimate 16.2.1 - Model B
Elevation View - M Moment 2-2 Diagram (1.2DL+1.6LL+1.2 Temp) [kN-m]
1 2 3 4 5 6 7
M M M M M M M
Basement-1
Basement-2
Basement-3
Base
124.7476
45.0891
81.1744
62.2491
Right Click on any Line for detailed diagram
Type here to search
3:44 AM
1/30/2020

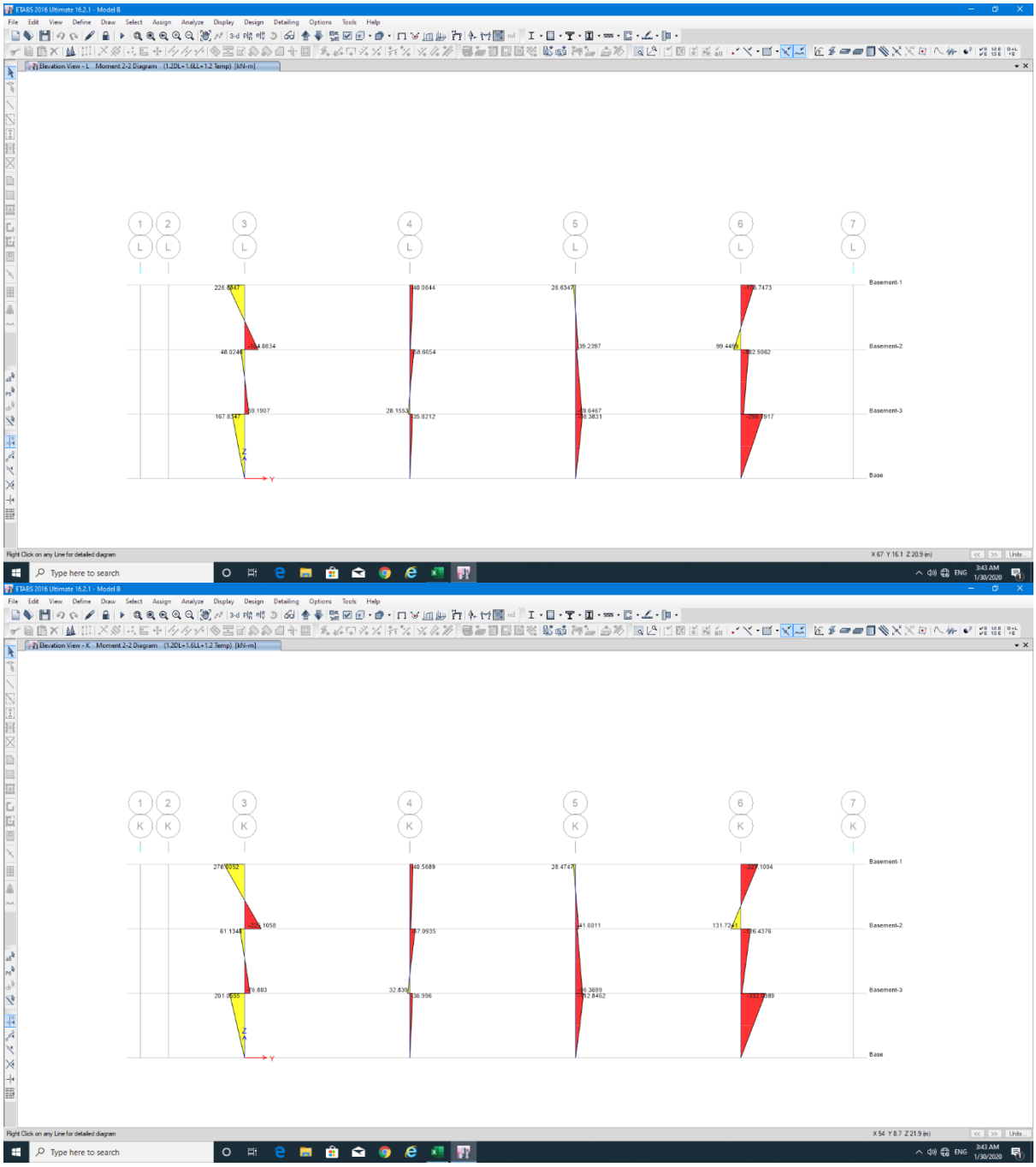
ETABS 2016 Ultimate 16.2.1 - Model B
Elevation View - L Moment 2-2 Diagram (1.2DL+1.6LL+1.2 Temp) (kN-m)
1 2 3 4 5 6 7
L L L L L L L
Basement-1
Basement-2
Basement-3
Base
Right Click on any Line for detailed diagram
Type here to search
3:43 AM
1/30/2020

ETABS 2016 Ultimate 16.2.1 - Model B
Elevation View - K Moment 2-2 Diagram (1.2DL+1.6LL+1.2 Temp) (kN-m)
1 2 3 4 5 6 7
K K K K K K K
Basement-1
Basement-2
Basement-3
Base
Right Click on any Line for detailed diagram
Type here to search
3:43 AM
1/30/2020

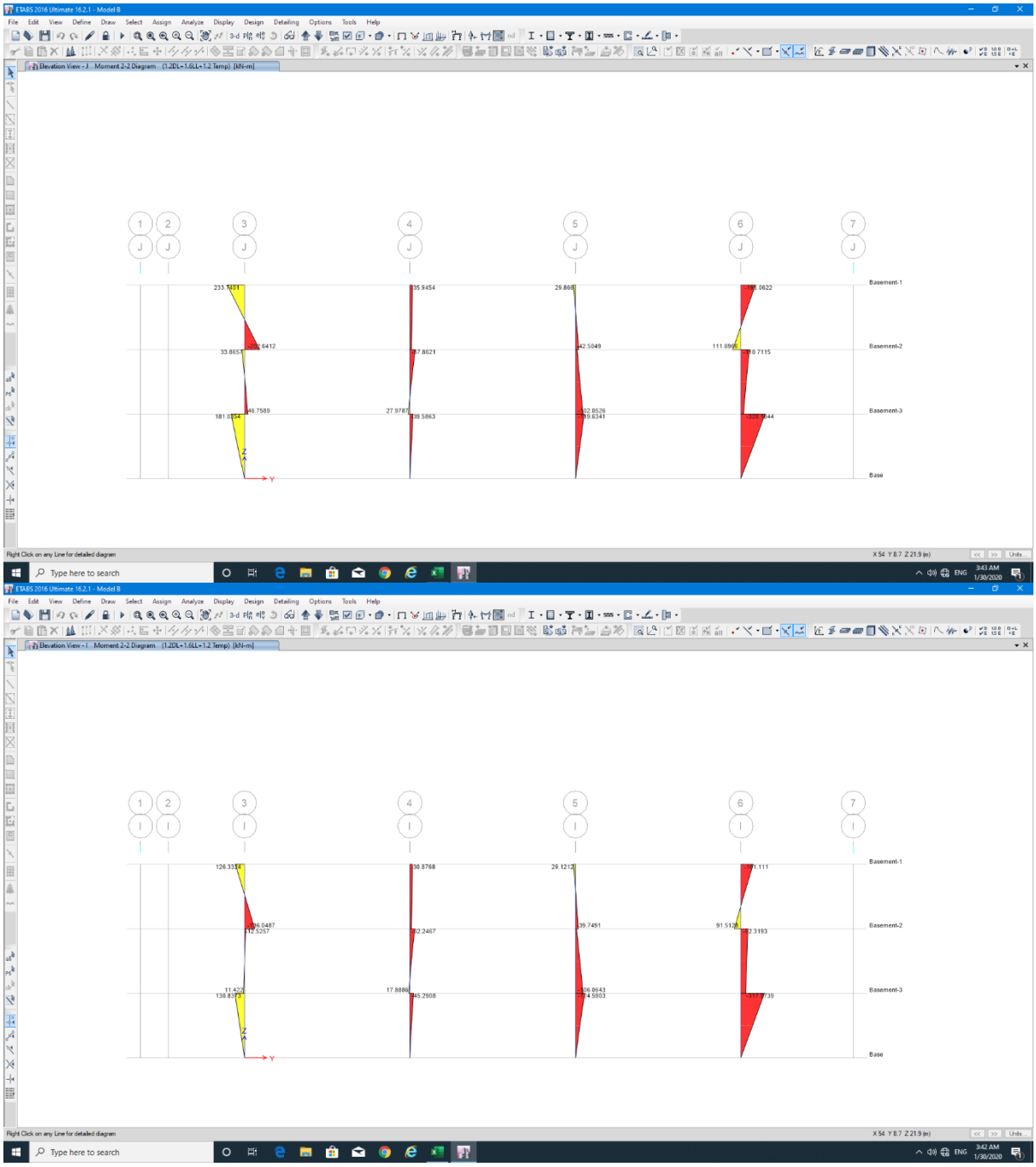
ETABS 2016 Ultimate 16.2.1 - Model B
Elevation View - J Moment 2-2 Diagram (1.2DL+1.6LL+1.2 Temp) [kN-m]
1 2 3 4 5 6 7
J J J J J J J
Basement-1
Basement-2
Basement-3
Base
Right Click on any Line for detailed diagram
X 54 Y 8.7 Z 21.9 (in)
Type here to search
3:43 AM
1/30/2020

ETABS 2016 Ultimate 16.2.1 - Model B
Elevation View - I Moment 2-2 Diagram (1.2DL+1.6LL+1.2 Temp) [kN-m]
1 2 3 4 5 6 7
I I I I I I I
Basement-1
Basement-2
Basement-3
Base
Right Click on any Line for detailed diagram
X 54 Y 8.7 Z 21.9 (in)
Type here to search
3:42 AM
1/30/2020

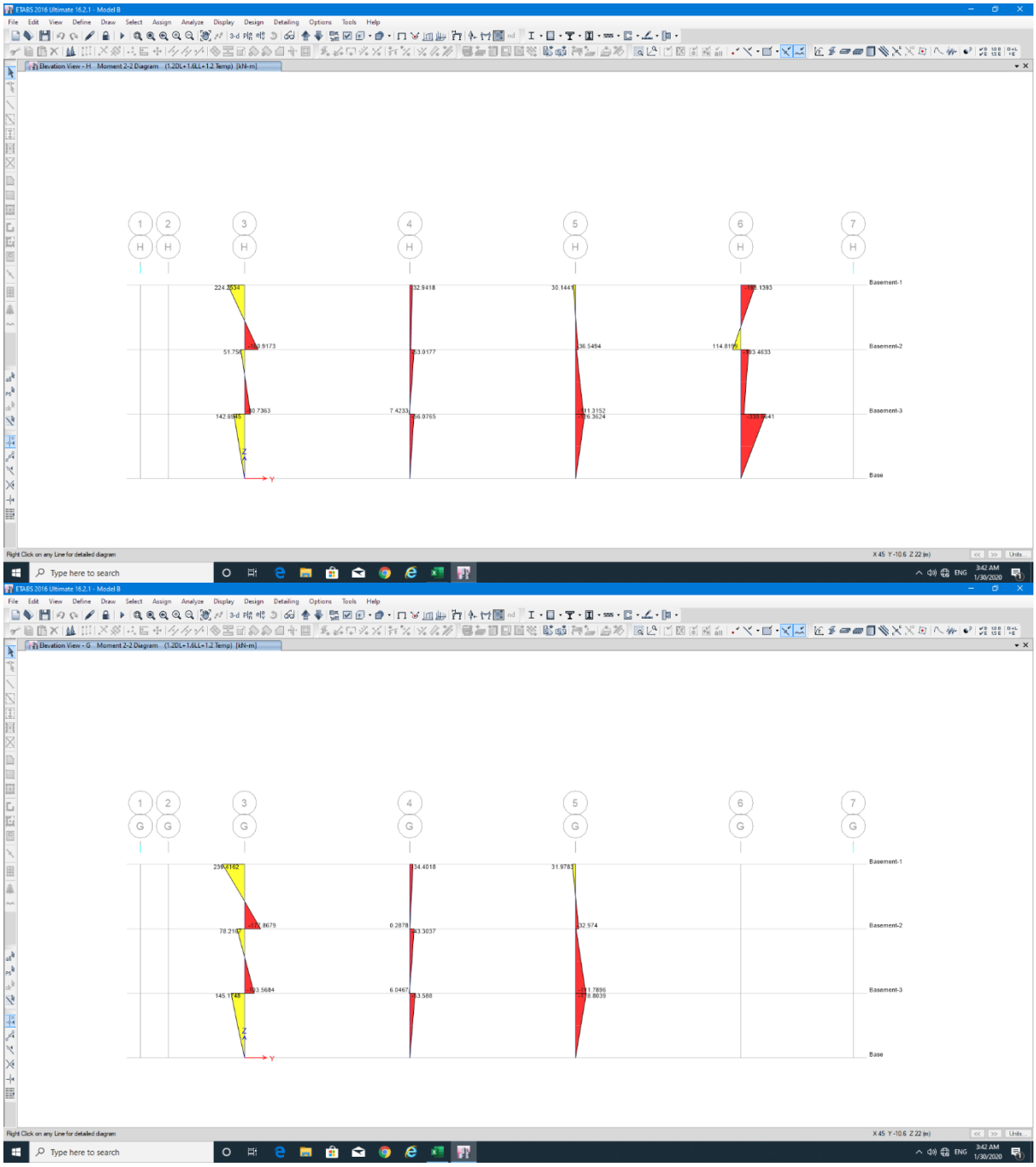
ETABS 2016 Ultimate 16.2.1 - Model B
Elevation View - H Moment 2-2 Diagram (1.2DL+1.6LL+1.2 Temp) [kN-m]
1 2 3 4 5 6 7
H H H H H H H
Basement-1
Basement-2
Basement-3
Base
Right Click on any Line for detailed diagram
Type here to search
3:42 AM
1/30/2020

ETABS 2016 Ultimate 16.2.1 - Model B
Elevation View - G Moment 2-2 Diagram (1.2DL+1.6LL+1.2 Temp) [kN-m]
1 2 3 4 5 6 7
G G G G G G G
Basement-1
Basement-2
Basement-3
Base
Right Click on any Line for detailed diagram
Type here to search
3:42 AM
1/30/2020

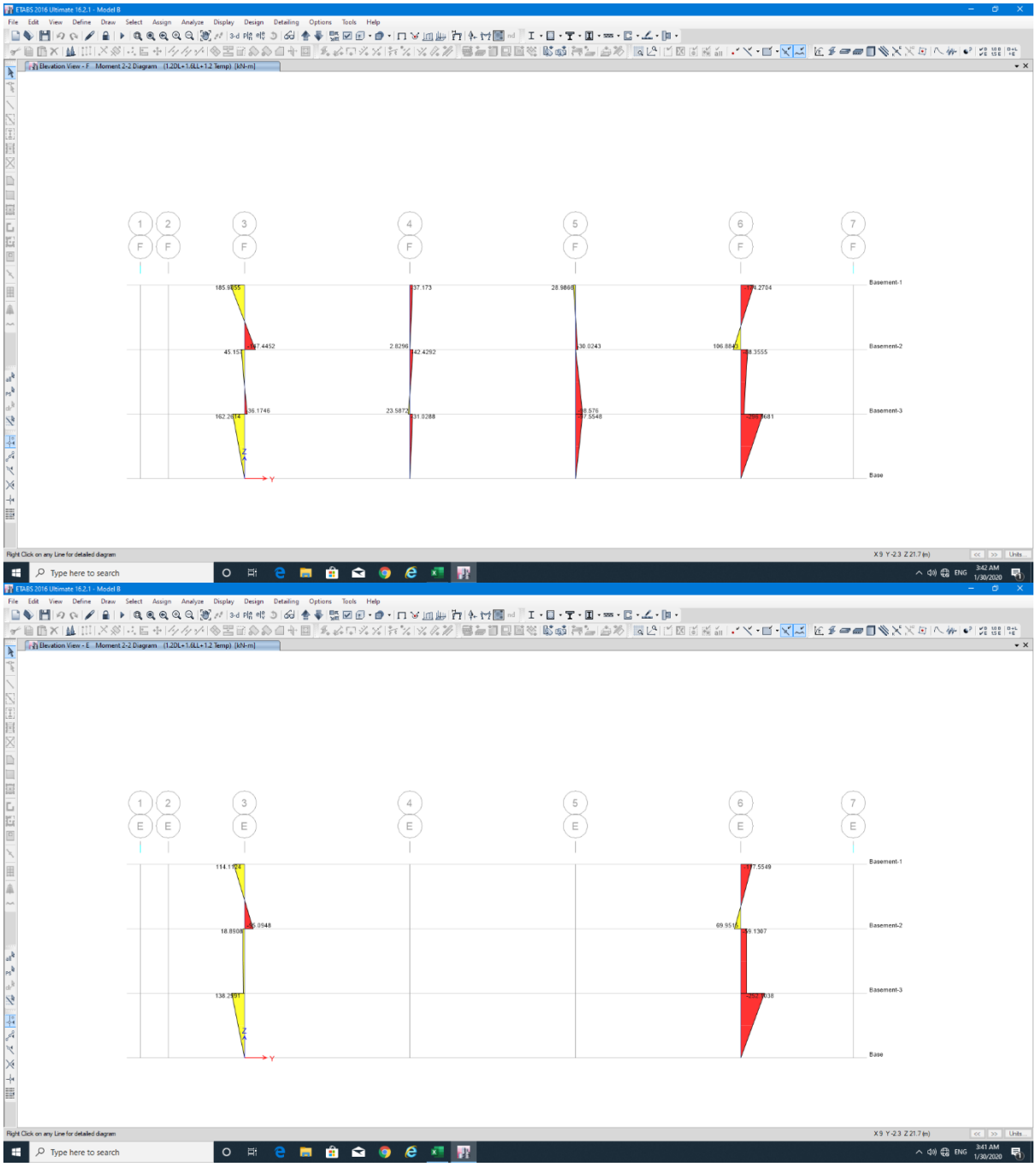
ETABS 2016 Ultimate 16.2.1 - Model B
Elevation View - F Moment 2-2 Diagram (1.2DL+1.6LL+1.2 Temp) [kN-m]
1 2 3 4 5 6 7
F F F F F F F
Basement-1
Basement-2
Basement-3
Base
185.9855
45.1511
162.2014
36.1746
37.173
2.8296
42.4292
23.5872
31.0288
28.9866
30.0243
8.576
7.5548
106.8844
8.3555
Right Click on any Line for detailed diagram
X 9 Y -2.3 Z 21.7 (m)
Type here to search
3:42 AM
1/30/2020

ETABS 2016 Ultimate 16.2.1 - Model B
Elevation View - E Moment 2-2 Diagram (1.2DL+1.6LL+1.2 Temp) [kN-m]
1 2 3 4 5 6 7
E E E E E E E
Basement-1
Basement-2
Basement-3
Base
114.1124
18.8908
138.2491
7.5549
69.9516
Right Click on any Line for detailed diagram
X 9 Y -2.3 Z 21.7 (m)
Type here to search
3:41 AM
1/30/2020

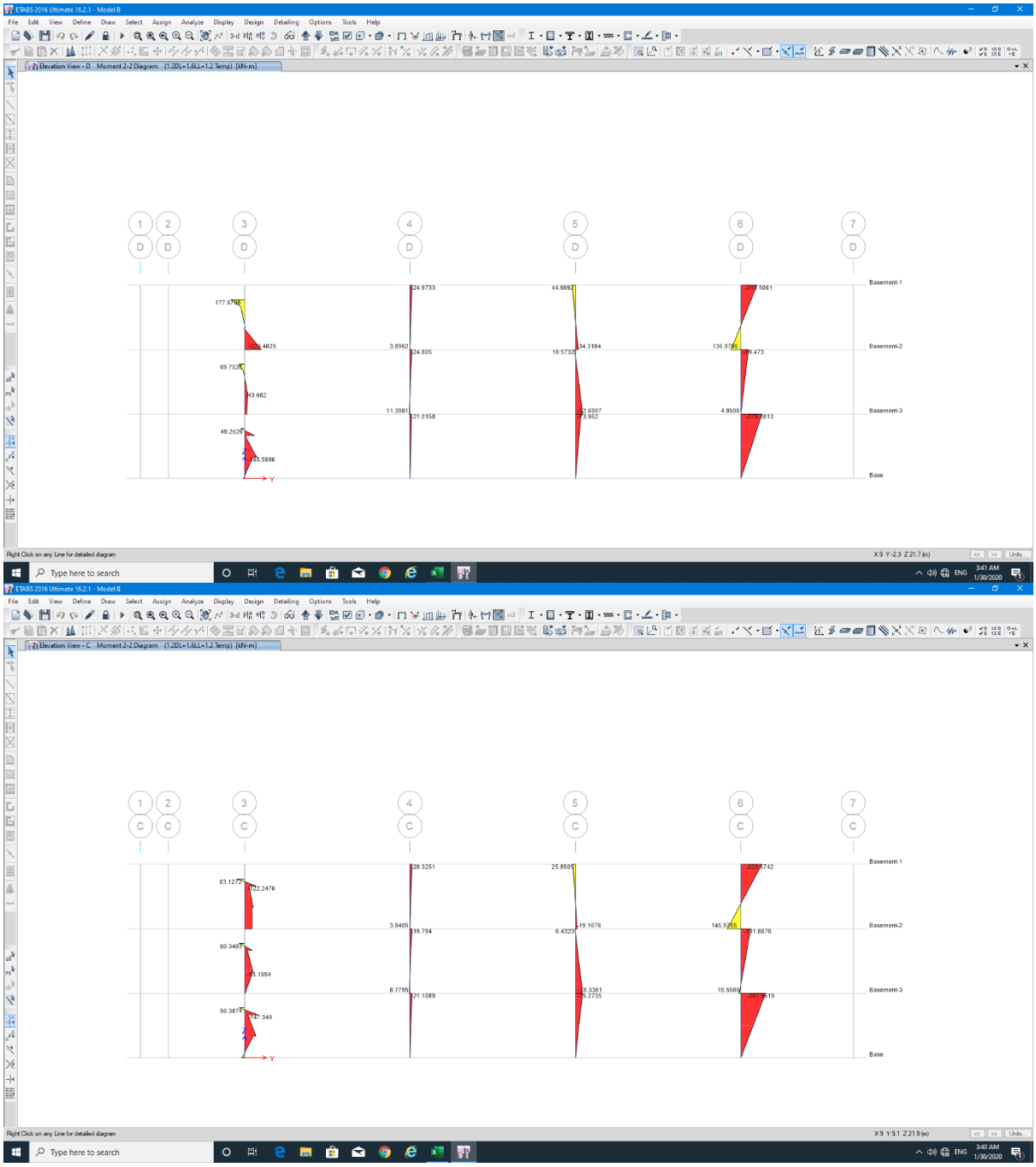
ETABS 2016 Ultimate 16.2.1 - Model B
Elevation View - D Moment 2-2 Diagram (1.2DL+1.6LL+1.2 Temp) [kN-m]
1 2 3 4 5 6 7
D D D D D D D
Basement-1
Basement-2
Basement-3
Base
177.9798
324.9733
44.6692
3.8962
124.805
10.5735
134.3184
136.5798
69.7525
43.682
11.3981
121.0158
4.8508
49.2626
Right Click on any Line for detailed diagram
X 9 Y -2.3 Z 21.7 (m)
Type here to search
3:41 AM
1/30/2020

ETABS 2016 Ultimate 16.2.1 - Model B
Elevation View - C Moment 2-2 Diagram (1.2DL+1.6LL+1.2 Temp) [kN-m]
1 2 3 4 5 6 7
C C C C C C C
Basement-1
Basement-2
Basement-3
Base
83.1272
320.3251
25.8505
3.8405
119.754
6.4323
145.9265
60.0407
8.7795
121.1089
56.3874
Right Click on any Line for detailed diagram
X 9 Y 9.1 Z 21.9 (m)
Type here to search
3:40 AM
1/30/2020

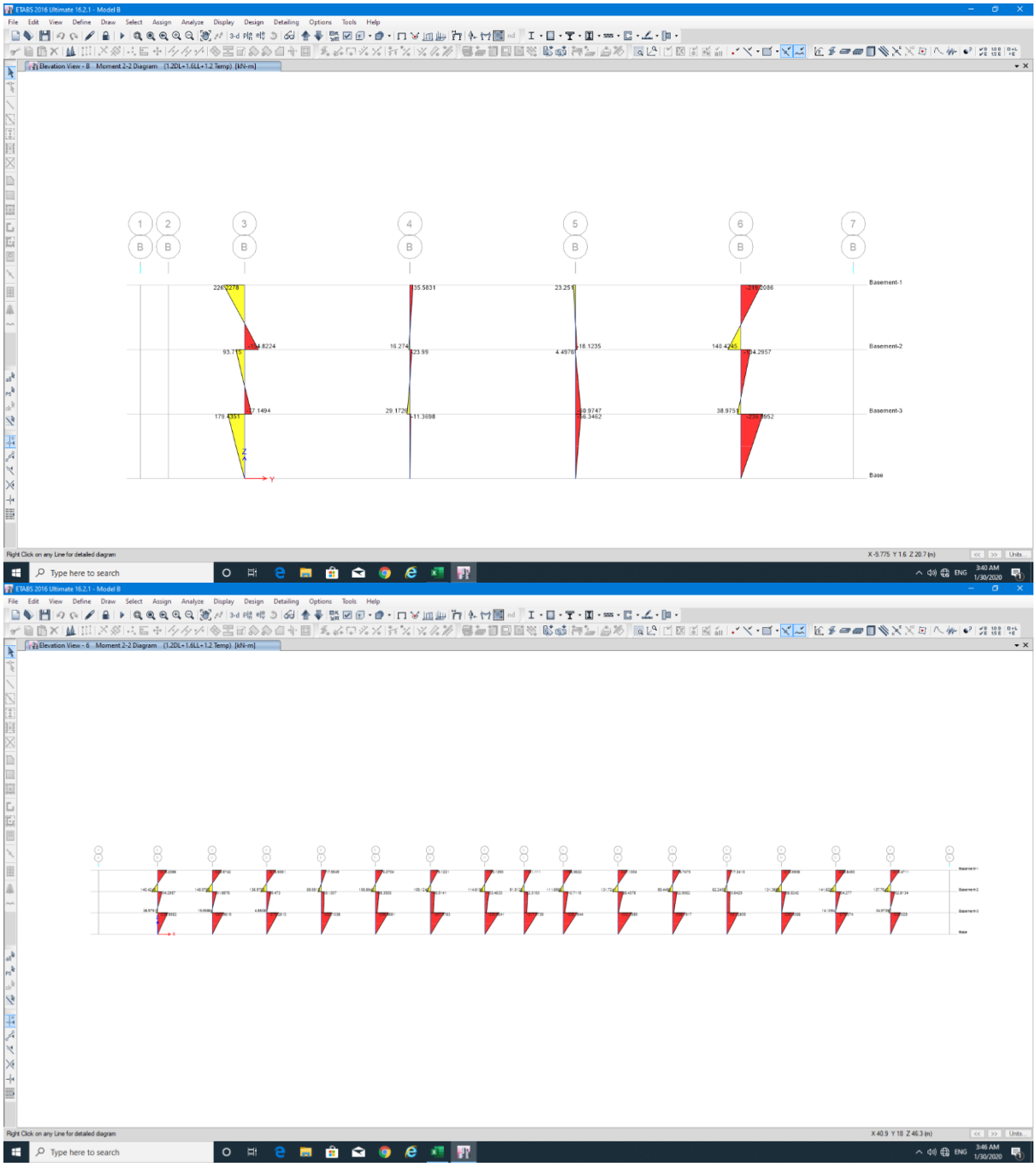
ETABS 2016 Ultimate 16.2.1 - Model B
Elevation View - B Moment 2-2 Diagram (1.2DL+1.6LL+1.2 Temp) [kN-m]
1
2
3
4
5
6
7
B
Basement-1
Basement-2
Basement-3
Base
Right Click on any Line for detailed diagram
Type here to search
3:40 AM
1/30/2020
ETABS 2016 Ultimate 16.2.1 - Model B
Elevation View - 6 Moment 2-2 Diagram (1.2DL+1.6LL+1.2 Temp) [kN-m]
Right Click on any Line for detailed diagram
Type here to search
3:46 AM
1/30/2020

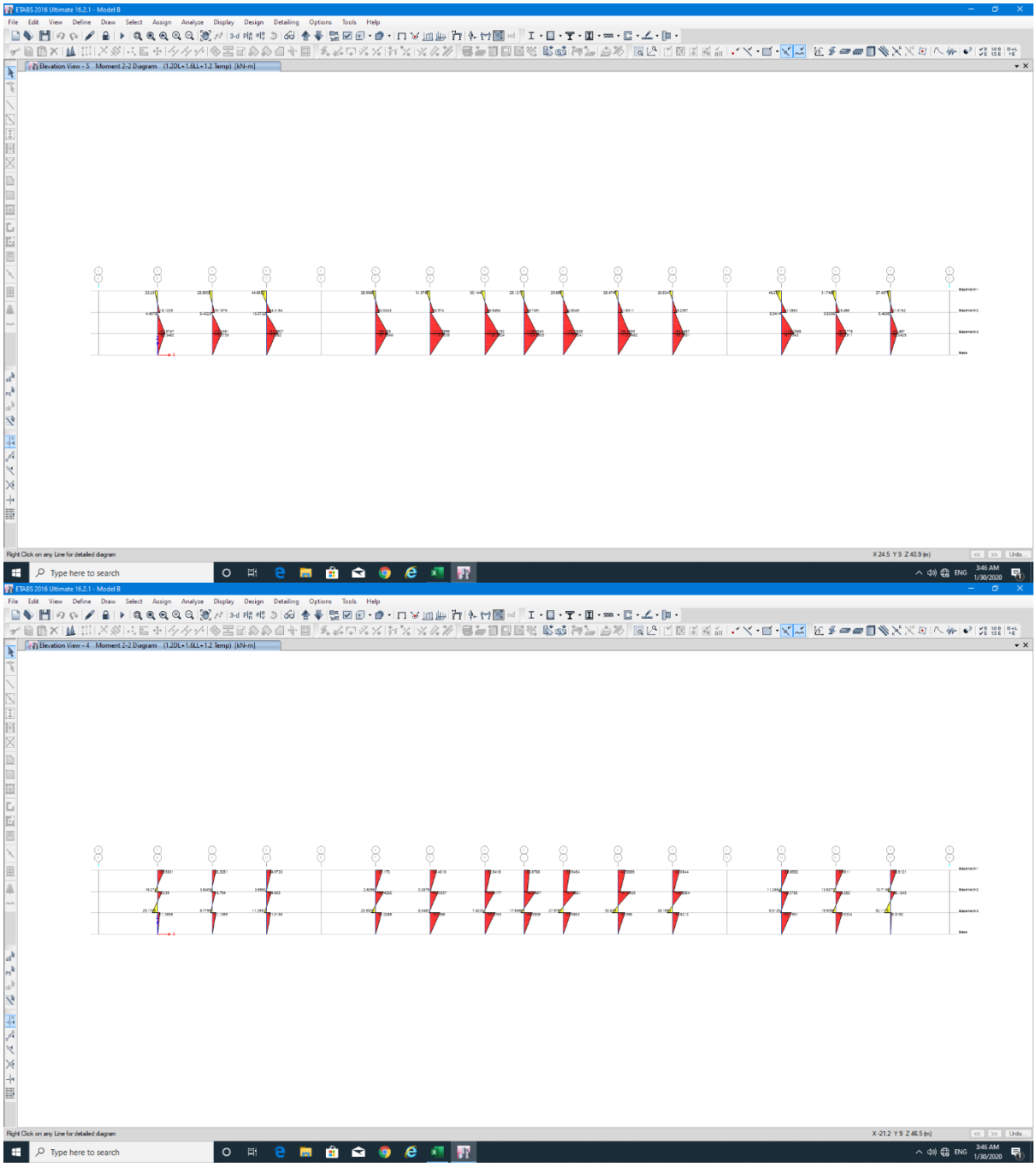
ETABS 2016 Ultimate 16.2.1 - Model 8
Elevation View - 5 Moment 2-2 Diagram (1.2DL+1.6LL+1.2 Temp) [kN-m]
Right Click on any Line for detailed diagram
Type here to search
ETABS 2016 Ultimate 16.2.1 - Model 8
Elevation View - 4 Moment 2-2 Diagram (1.2DL+1.6LL+1.2 Temp) [kN-m]
Right Click on any Line for detailed diagram
Type here to search

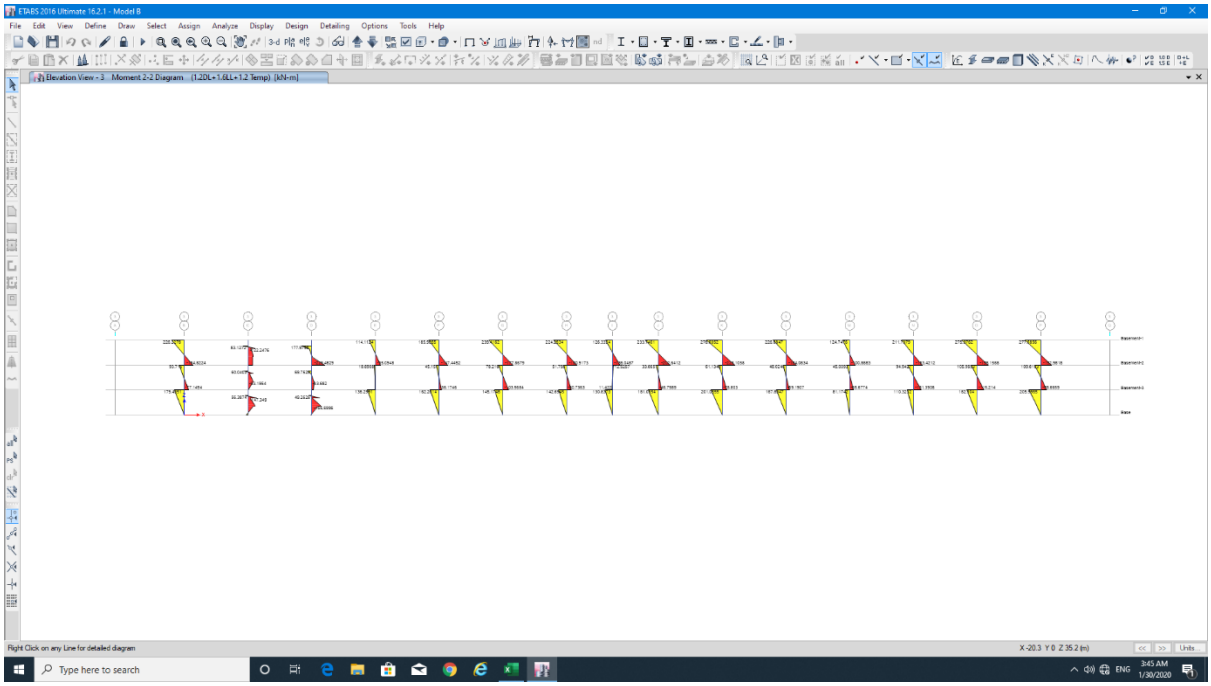

D-2-2 Column M33

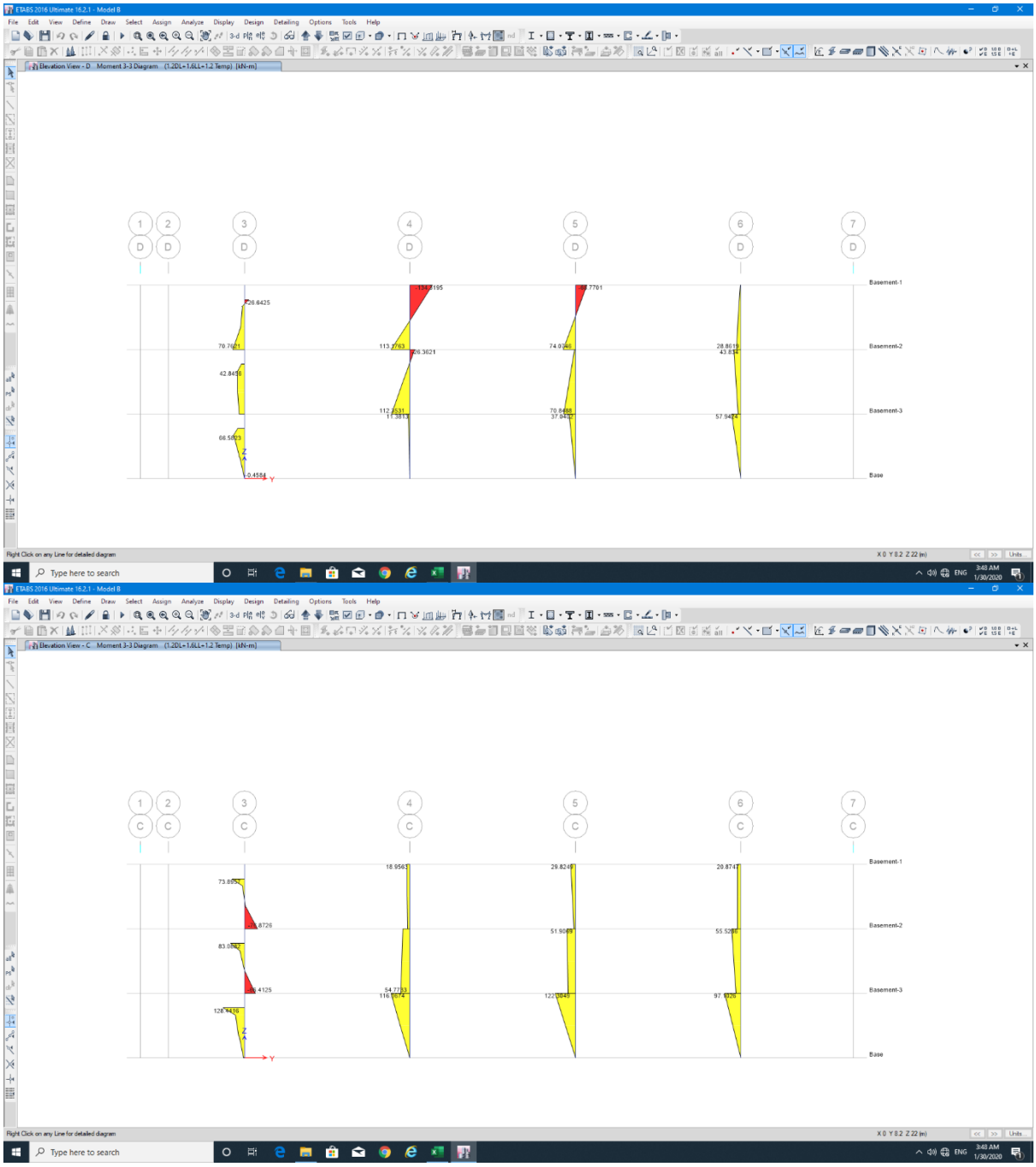
ETABS 2016 Ultimate 16.2.1 - Model B
Elevation View - D Moment 3-3 Diagram (1.2DL+1.6LL+1.2 Temp) [kN-m]
1 2 3 4 5 6 7
D D D D D D D
Basement-1
Basement-2
Basement-3
Base
Right Click on any Line for detailed diagram
Type here to search
3:48 AM
1/30/2020

ETABS 2016 Ultimate 16.2.1 - Model B
Elevation View - C Moment 3-3 Diagram (1.2DL+1.6LL+1.2 Temp) [kN-m]
1 2 3 4 5 6 7
C C C C C C C
Basement-1
Basement-2
Basement-3
Base
Right Click on any Line for detailed diagram
Type here to search
3:48 AM
1/30/2020

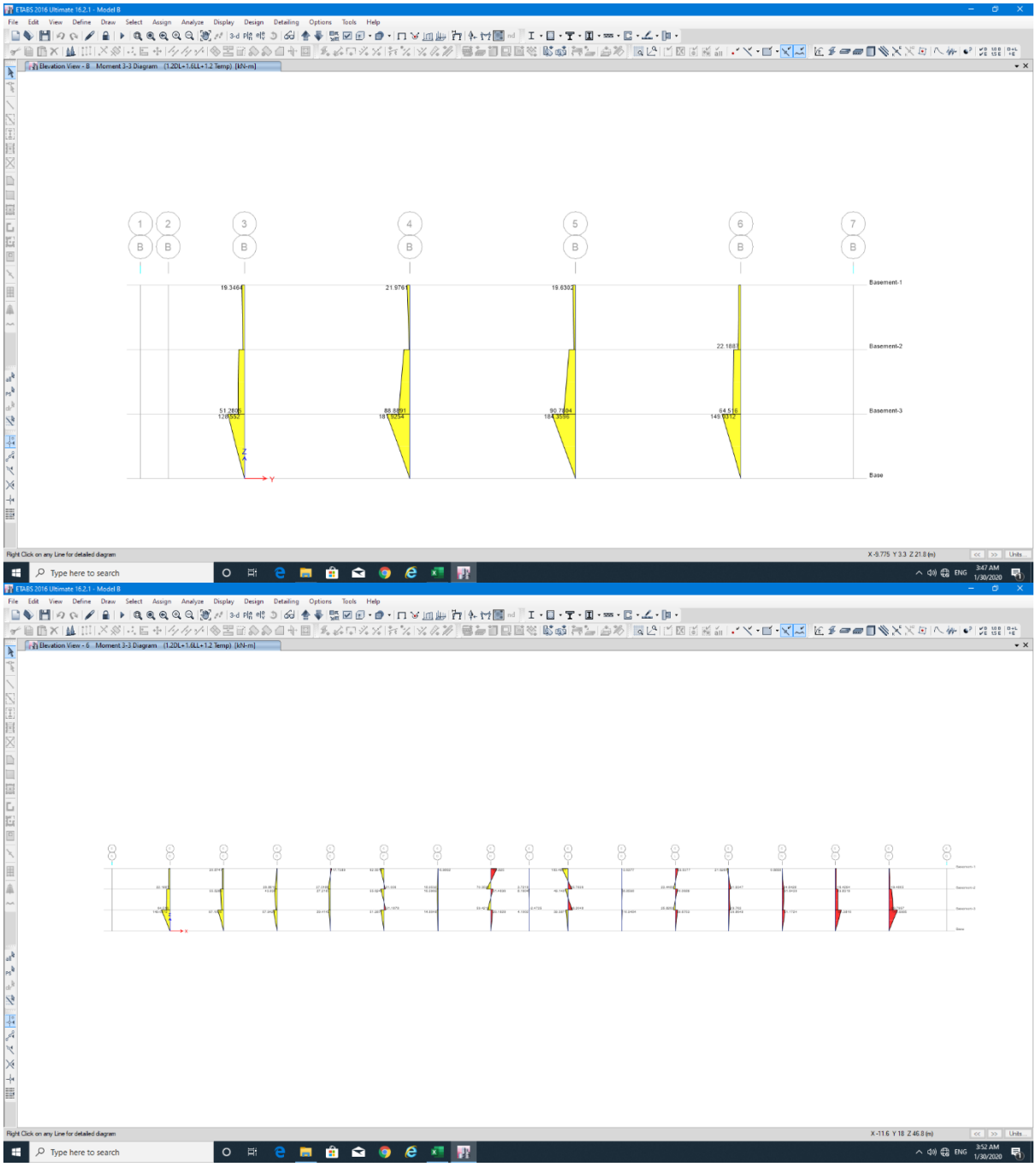
ETABS 2016 Ultimate 16.2.1 - Model B
Elevation View - B Moment 3-3 Diagram (1.2DL+1.6LL+1.2 Temp) [kN-m]
1 2 3 4 5 6 7
B B B B B B B
19.3464
21.9761
19.6302
22.1883
Basement-1
Basement-2
Basement-3
Base
Right Click on any Line for detailed diagram
Type here to search
3:47 AM
1/30/2020

ETABS 2016 Ultimate 16.2.1 - Model B
Elevation View - 6 Moment 3-3 Diagram (1.2DL+1.6LL+1.2 Temp) [kN-m]
Right Click on any Line for detailed diagram
Type here to search
3:52 AM
1/30/2020

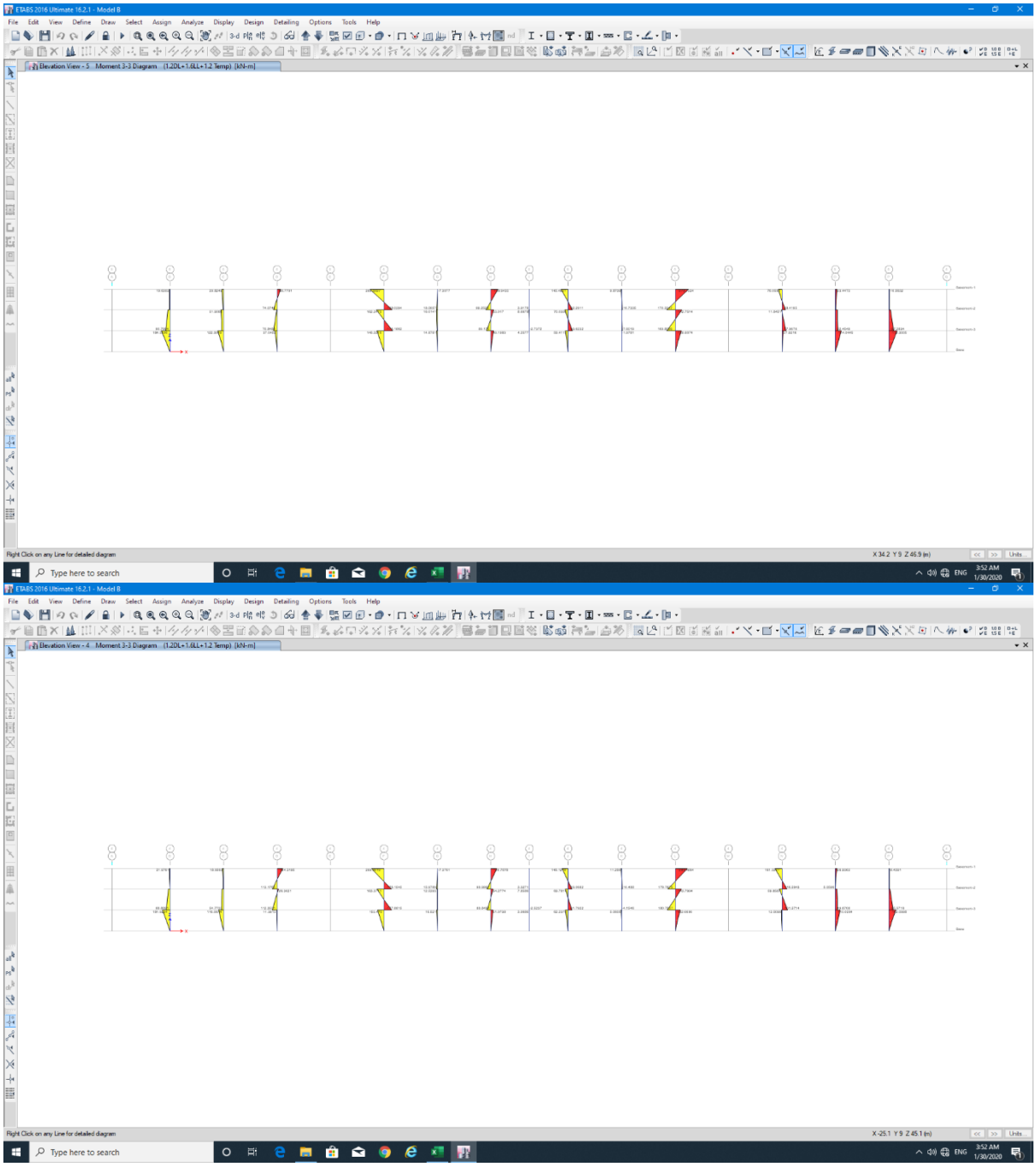
ETABS 2016 Ultimate 16.2.1 - Model 8
File Edit View Define Draw Select Assign Analyze Display Design Detailing Options Tools Help
Elevation View - 5 Moment 3-3 Diagram (1.2DL+1.6LL+1.2 Temp) [kN-m]
Right Click on any Line for detailed diagram
X 34.2 Y 9 Z 46.9 (m)
Units
Type here to search
ENG
3:52 AM
1/30/2020
ETABS 2016 Ultimate 16.2.1 - Model 8
File Edit View Define Draw Select Assign Analyze Display Design Detailing Options Tools Help
Elevation View - 4 Moment 3-3 Diagram (1.2DL+1.6LL+1.2 Temp) [kN-m]
Right Click on any Line for detailed diagram
X -25.1 Y 9 Z 45.1 (m)
Units
Type here to search
ENG
3:52 AM
1/30/2020

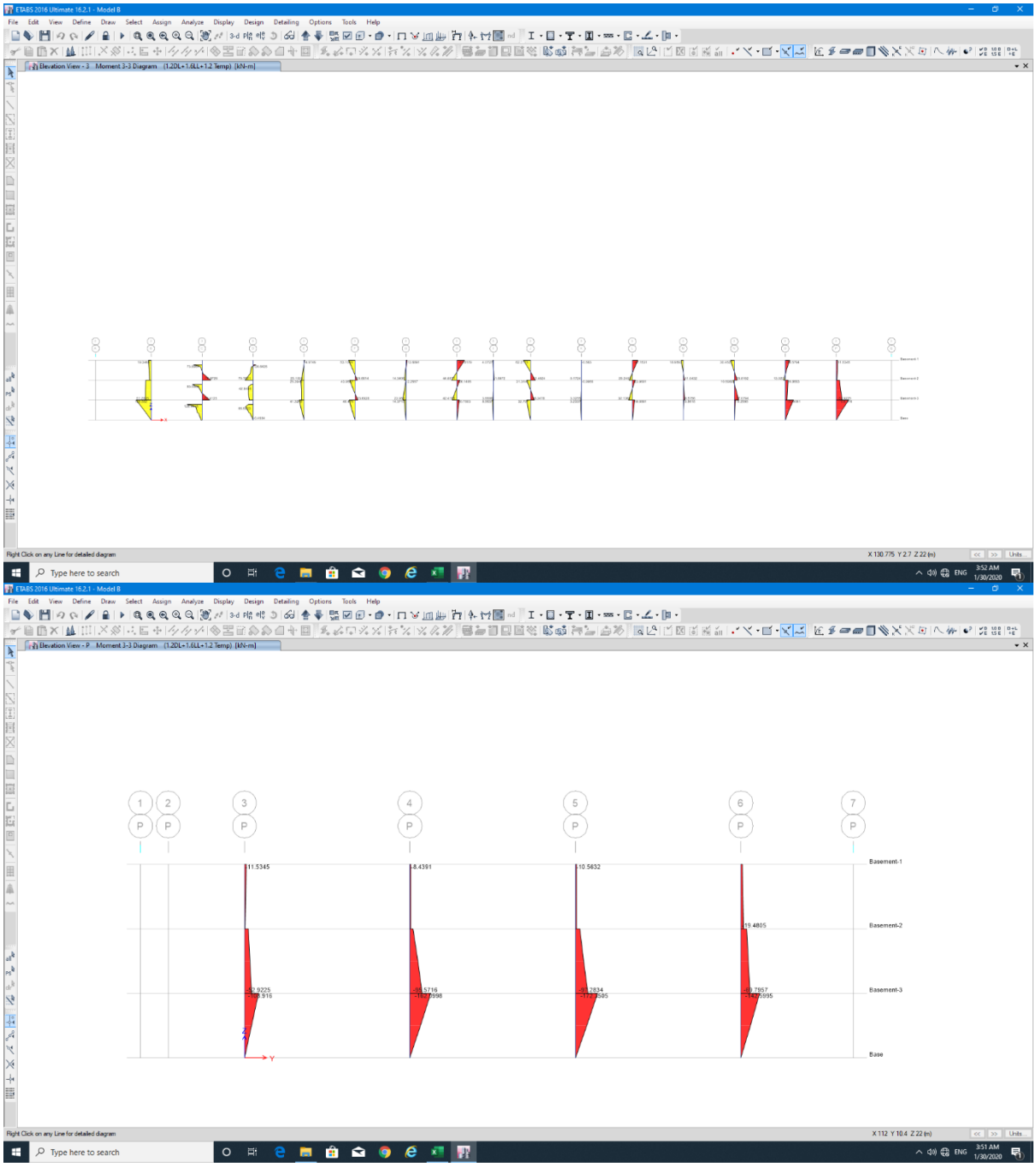
ETABS 2016 Ultimate 16.2.1 - Model B
Elevation View - 3 Moment 3-3 Diagram (1.2DL+1.6LL+1.2 Temp) (kN-m)
Right Click on any Line for detailed diagram
Type here to search
ETABS 2016 Ultimate 16.2.1 - Model B
Elevation View - P Moment 3-3 Diagram (1.2DL+1.6LL+1.2 Temp) (kN-m)
1
2
3
4
5
6
7
P
11.5345
8.4391
10.5632
19.4805
Basement-1
Basement-2
Basement-3
Base
Right Click on any Line for detailed diagram
Type here to search

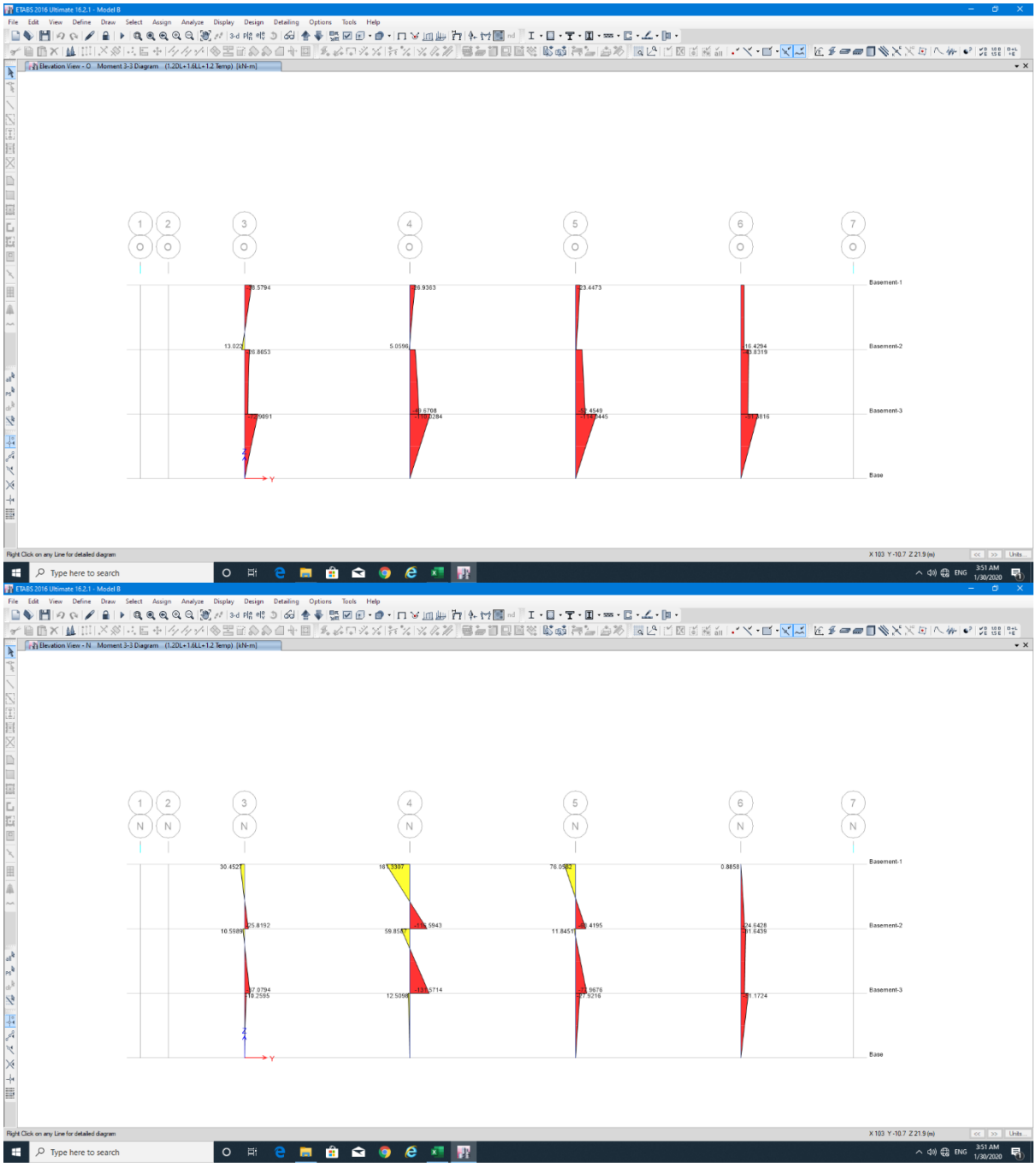
ETABS 2016 Ultimate 16.2.1 - Model B
Elevation View - O Moment 3-3 Diagram (1.2DL+1.6LL+1.2 Temp) [kN-m]
1 2 3 4 5 6 7
O O O O O O O
Basement-1
Basement-2
Basement-3
Base
Right Click on any Line for detailed diagram
Type here to search
3:51 AM
1/30/2020

ETABS 2016 Ultimate 16.2.1 - Model B
Elevation View - N Moment 3-3 Diagram (1.2DL+1.6LL+1.2 Temp) [kN-m]
1 2 3 4 5 6 7
N N N N N N N
30.4527
10.5589
59.8587
12.5098
76.0582
11.8451
0.8858
Basement-1
Basement-2
Basement-3
Base
Right Click on any Line for detailed diagram
Type here to search
3:51 AM
1/30/2020

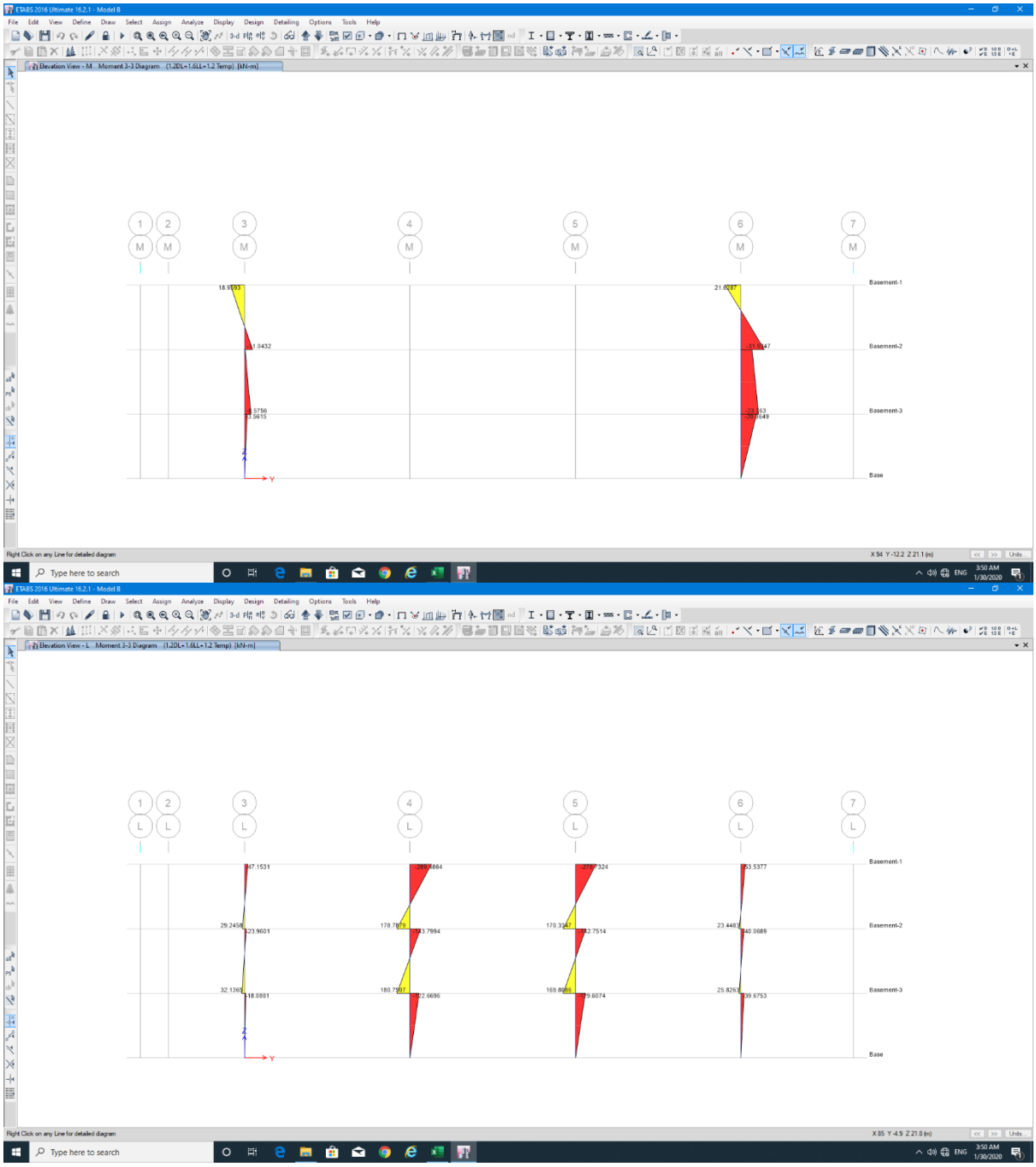
ETABS 2016 Ultimate 16.2.1 - Model B
Elevation View - M Moment 3-3 Diagram (1.2DL+1.6LL+1.2 Temp) [kN-m]
1 2 3 4 5 6 7
M M M M M M M
Basement-1
Basement-2
Basement-3
Base
Right Click on any Line for detailed diagram
Type here to search
3:50 AM
1/30/2020
ETABS 2016 Ultimate 16.2.1 - Model B
Elevation View - L Moment 3-3 Diagram (1.2DL+1.6LL+1.2 Temp) [kN-m]
1 2 3 4 5 6 7
L L L L L L L
Basement-1
Basement-2
Basement-3
Base
Right Click on any Line for detailed diagram
Type here to search
3:50 AM
1/30/2020

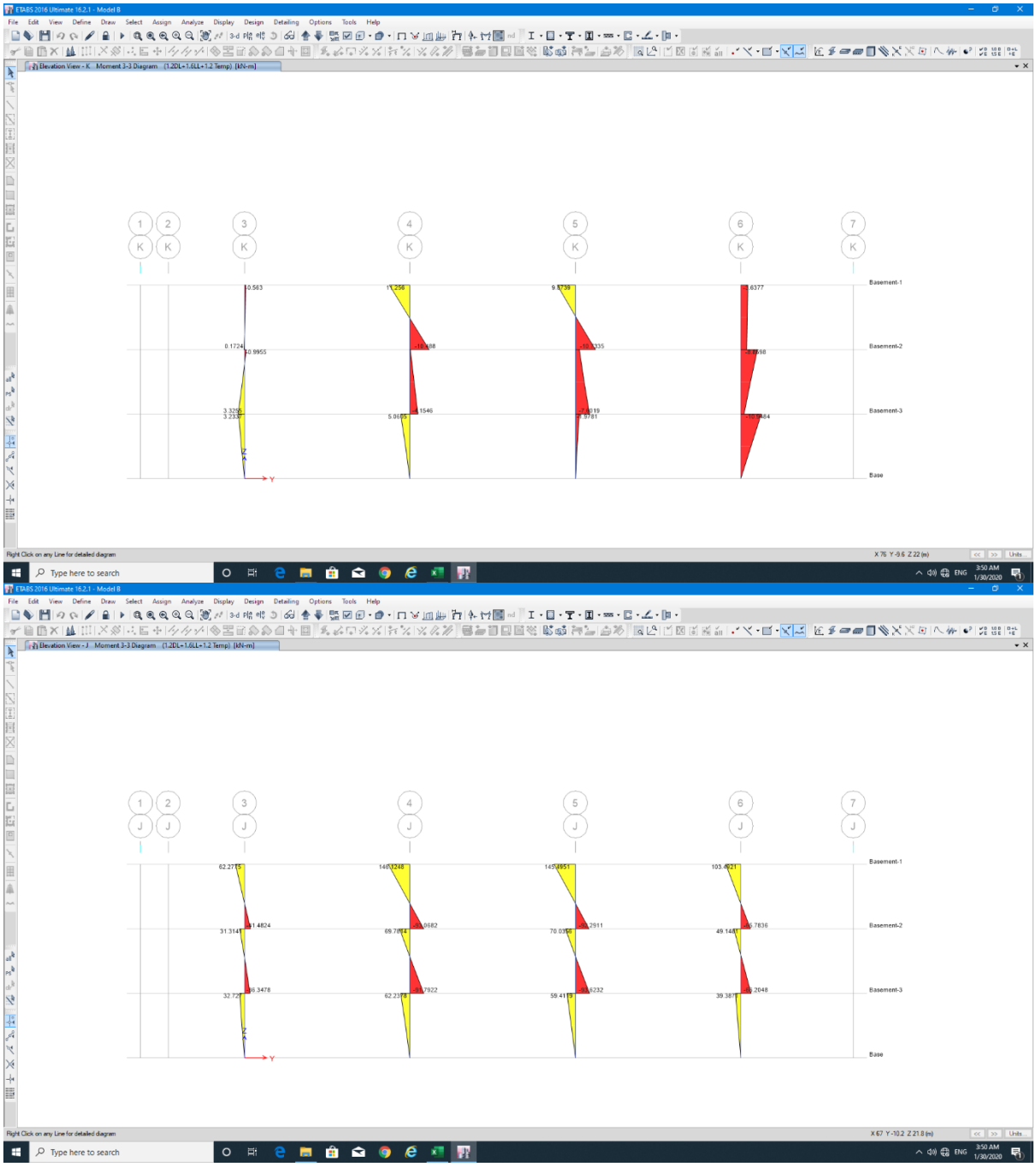
ETABS 2016 Ultimate 16.2.1 - Model B
Elevation View - K Moment 3-3 Diagram (1.2DL+1.6LL+1.2 Temp) [kN-m]
1 2 3 4 5 6 7
K K K K K K K
Basement-1
Basement-2
Basement-3
Base
Right Click on any Line for detailed diagram
Type here to search
3:50 AM
1/30/2020

ETABS 2016 Ultimate 16.2.1 - Model B
Elevation View - J Moment 3-3 Diagram (1.2DL+1.6LL+1.2 Temp) [kN-m]
1 2 3 4 5 6 7
J J J J J J J
Basement-1
Basement-2
Basement-3
Base
Right Click on any Line for detailed diagram
Type here to search
3:50 AM
1/30/2020

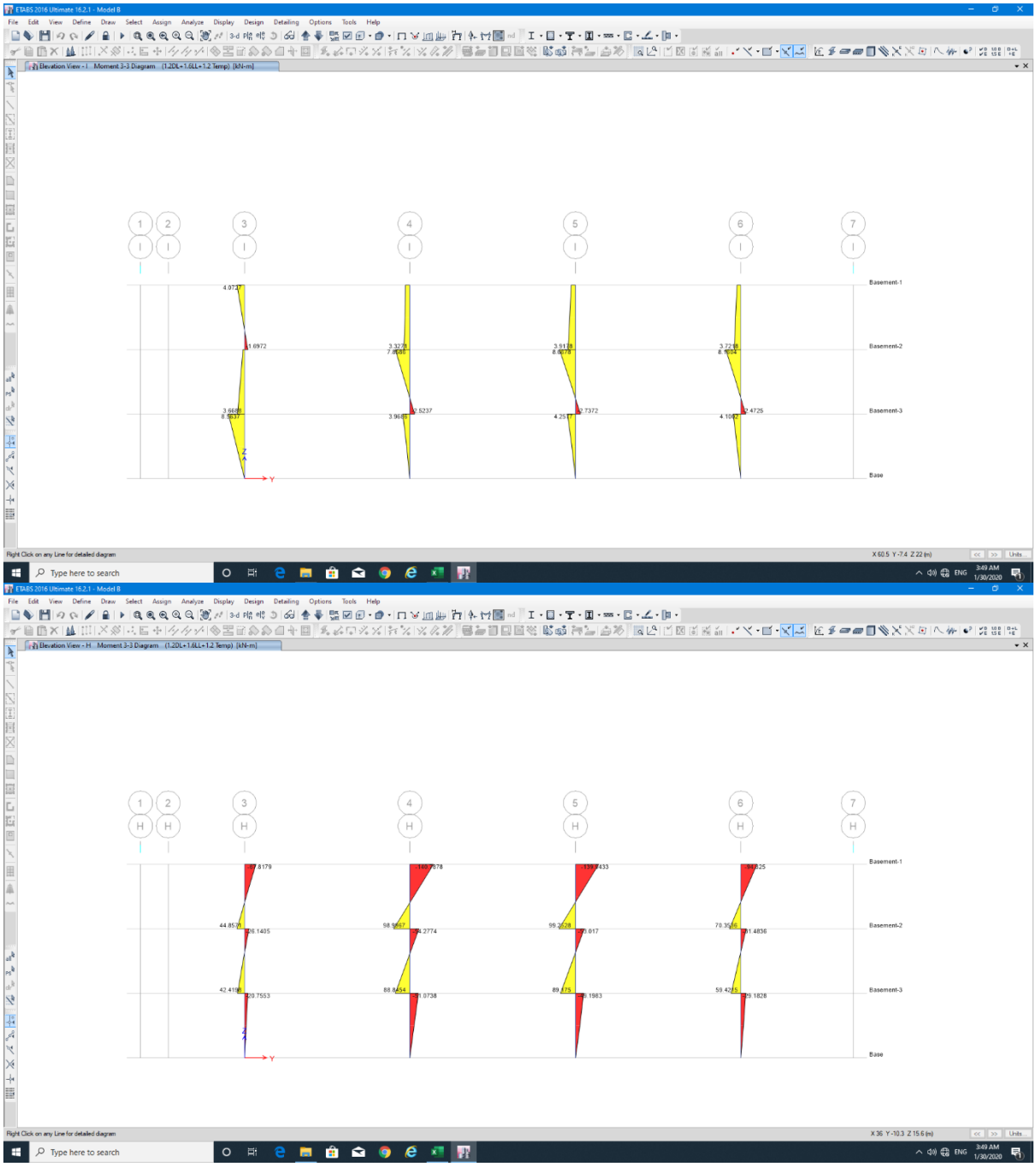
ETABS 2016 Ultimate 16.2.1 - Model B
Elevation View - I Moment 3-3 Diagram (1.2DL+1.6LL+1.2 Temp) [kN-m]
1
2
3
4
5
6
7
I
Basement-1
Basement-2
Basement-3
Base
Right Click on any Line for detailed diagram
Type here to search
3:49 AM
1/30/2020

ETABS 2016 Ultimate 16.2.1 - Model B
Elevation View - H Moment 3-3 Diagram (1.2DL+1.6LL+1.2 Temp) [kN-m]
1
2
3
4
5
6
7
H
Basement-1
Basement-2
Basement-3
Base
Right Click on any Line for detailed diagram
Type here to search
3:49 AM
1/30/2020

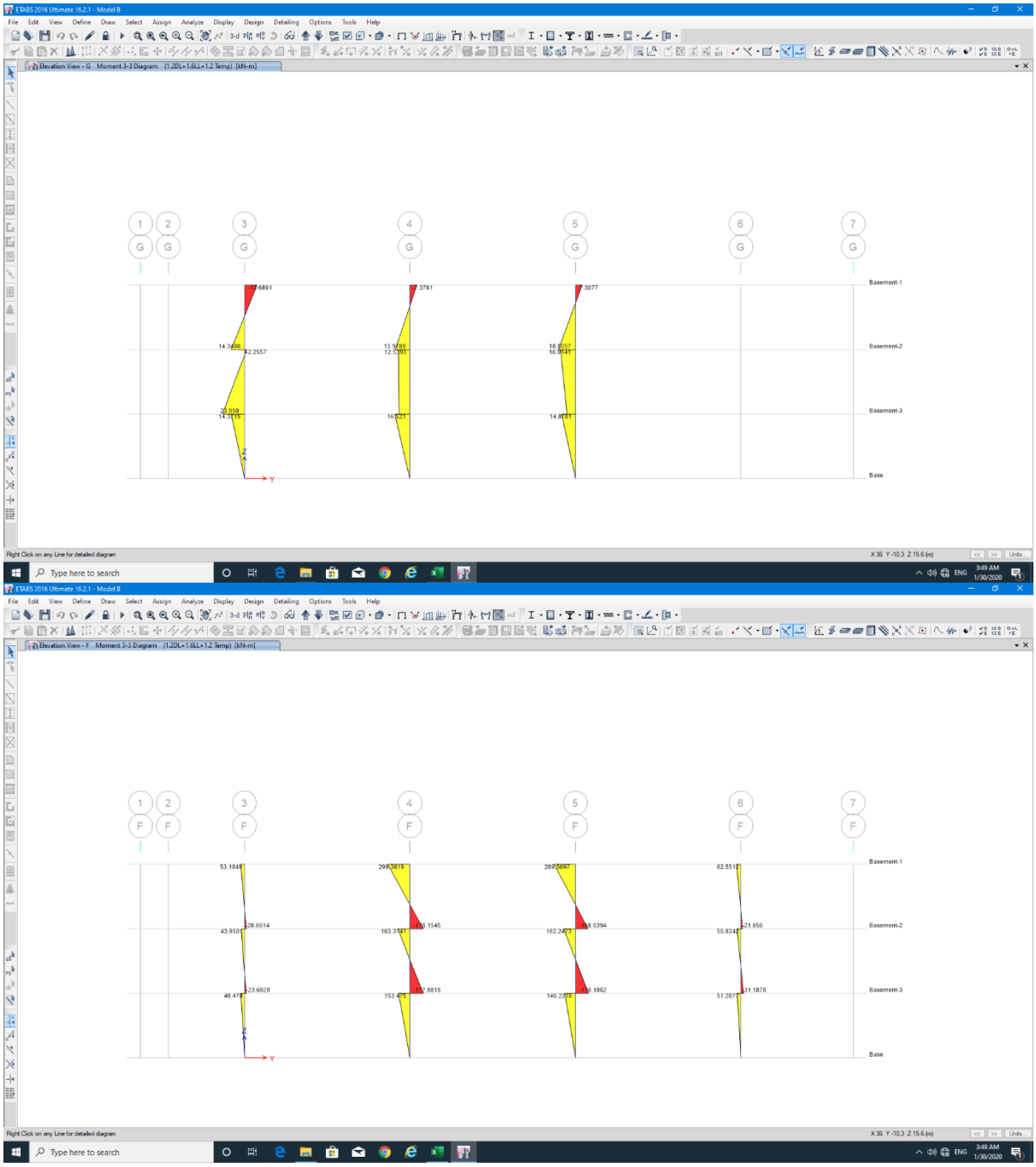
ETABS 2016 Ultimate 16.2.1 - Model B
Elevation View - G Moment 3-3 Diagram (1.2DL+1.6LL+1.2 Temp) [kN-m]
1 2 3 4 5 6 7
G G G G G G G
Basement-1
Basement-2
Basement-3
Base
Right Click on any Line for detailed diagram
Type here to search
3:49 AM
1/30/2020

ETABS 2016 Ultimate 16.2.1 - Model B
Elevation View - F Moment 3-3 Diagram (1.2DL+1.6LL+1.2 Temp) [kN-m]
1 2 3 4 5 6 7
F F F F F F F
53.1048
43.9501
48.4781
299.3619
163.3741
153.4743
289.5697
162.2473
146.2278
62.5518
55.6243
51.2871
Basement-1
Basement-2
Basement-3
Base
Right Click on any Line for detailed diagram
Type here to search
3:49 AM
1/30/2020

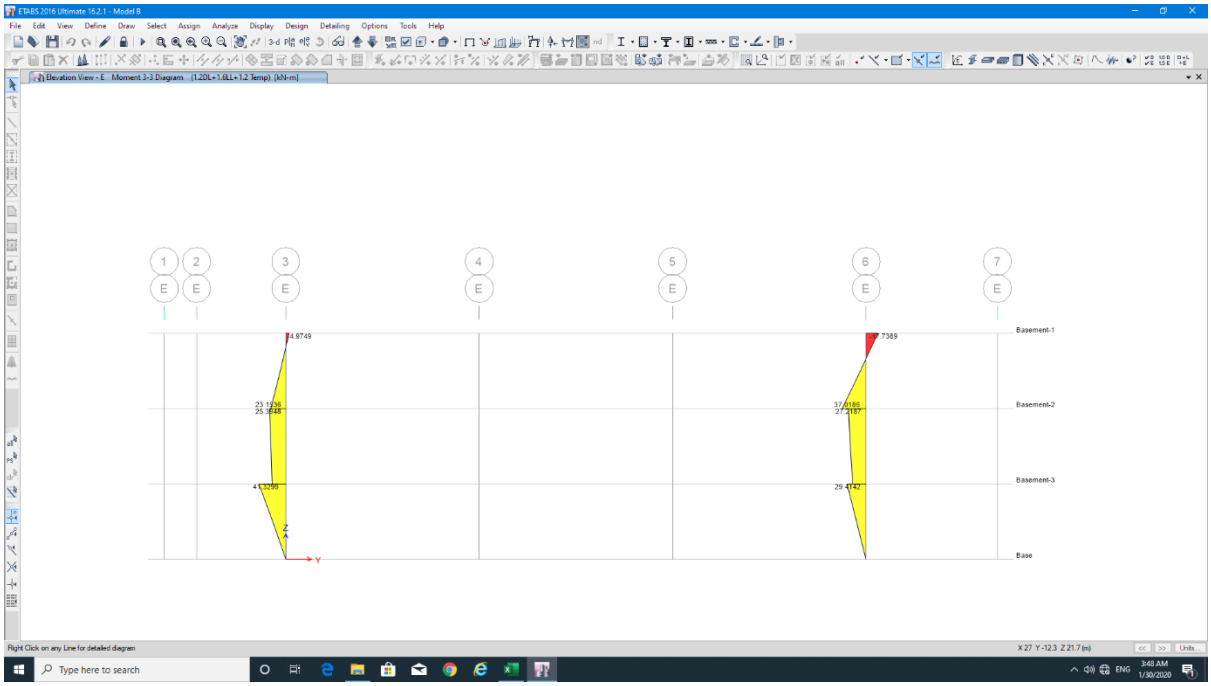

D-2-3 Slab Forces

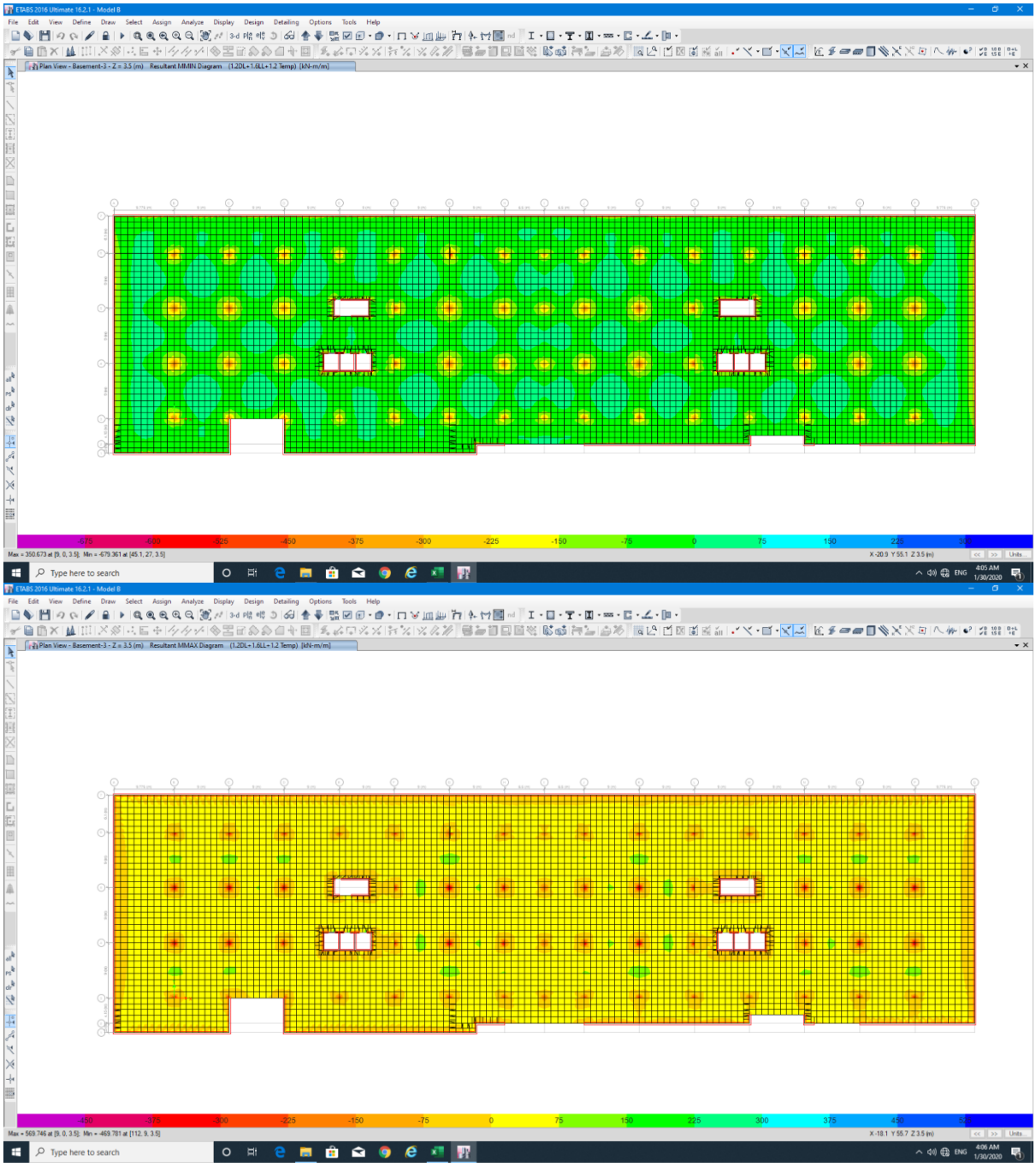
ETABS 2016 Ultimate 16.2.1 - Model B
Plan View - Basement-3 - Z = 3.5 (m) Resultant MMIN Diagram (1.2DL+1.6LL+1.2 Temp) [kN-m/m]
-675 -600 -525 -450 -375 -300 -225 -150 -75 0 75 150 225 300
Max = 350.673 at [9, 0, 3.5], Min = -679.361 at [45.1, 27, 3.5]
X -20.9 Y 55.1 Z 3.5 (m)
Units
Type here to search
4:05 AM
1/30/2020

ETABS 2016 Ultimate 16.2.1 - Model B
Plan View - Basement-3 - Z = 3.5 (m) Resultant MMAX Diagram (1.2DL+1.6LL+1.2 Temp) [kN-m/m]
-450 -375 -300 -225 -150 -75 0 75 150 225 300 375 450 525
Max = 563.746 at [9, 0, 3.5], Min = -469.781 at [112, 9, 3.5]
X -18.1 Y 55.7 Z 3.5 (m)
Units
Type here to search
4:06 AM
1/30/2020

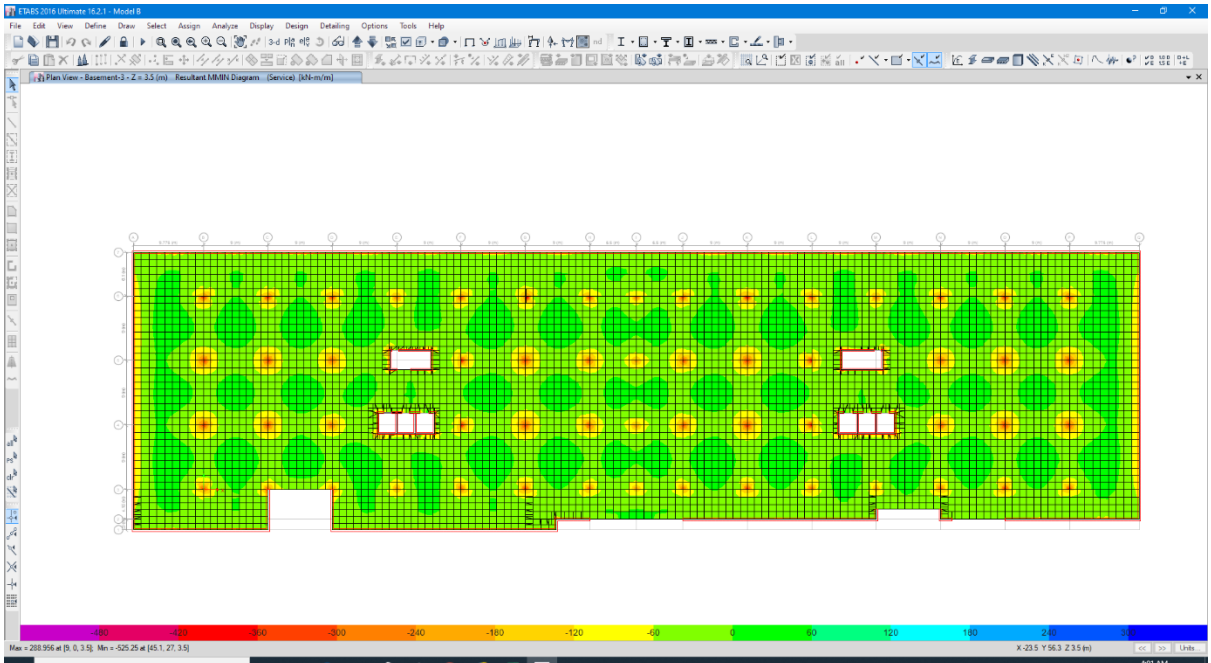
ETABS 2016 Ultimate 16.2.1 - Model B
Plan View - Basement-3 - Z = 3.5 (m) Resultant MMIN Diagram (Service) (kN-m/m)
-480 -420 -360 -300 -240 -180 -120 -60 0 60 120 180 240 300
Type here to search
4:01 AM
1/30/2020

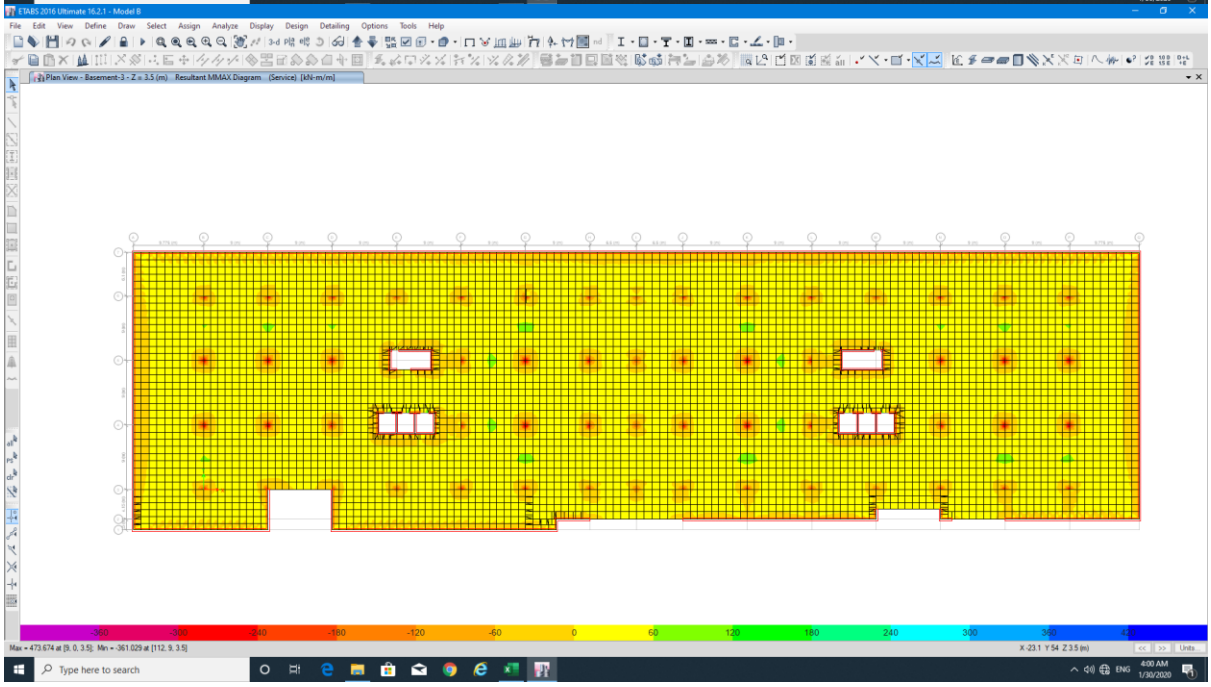
ETABS 2016 Ultimate 16.2.1 - Model B
Plan View - Basement-3 - Z = 3.5 (m) Resultant MMAX Diagram (Service) (kN-m/m)
-360 -300 -240 -180 -120 -60 0 60 120 180 240 300 360 420
Type here to search
4:00 AM
1/30/2020

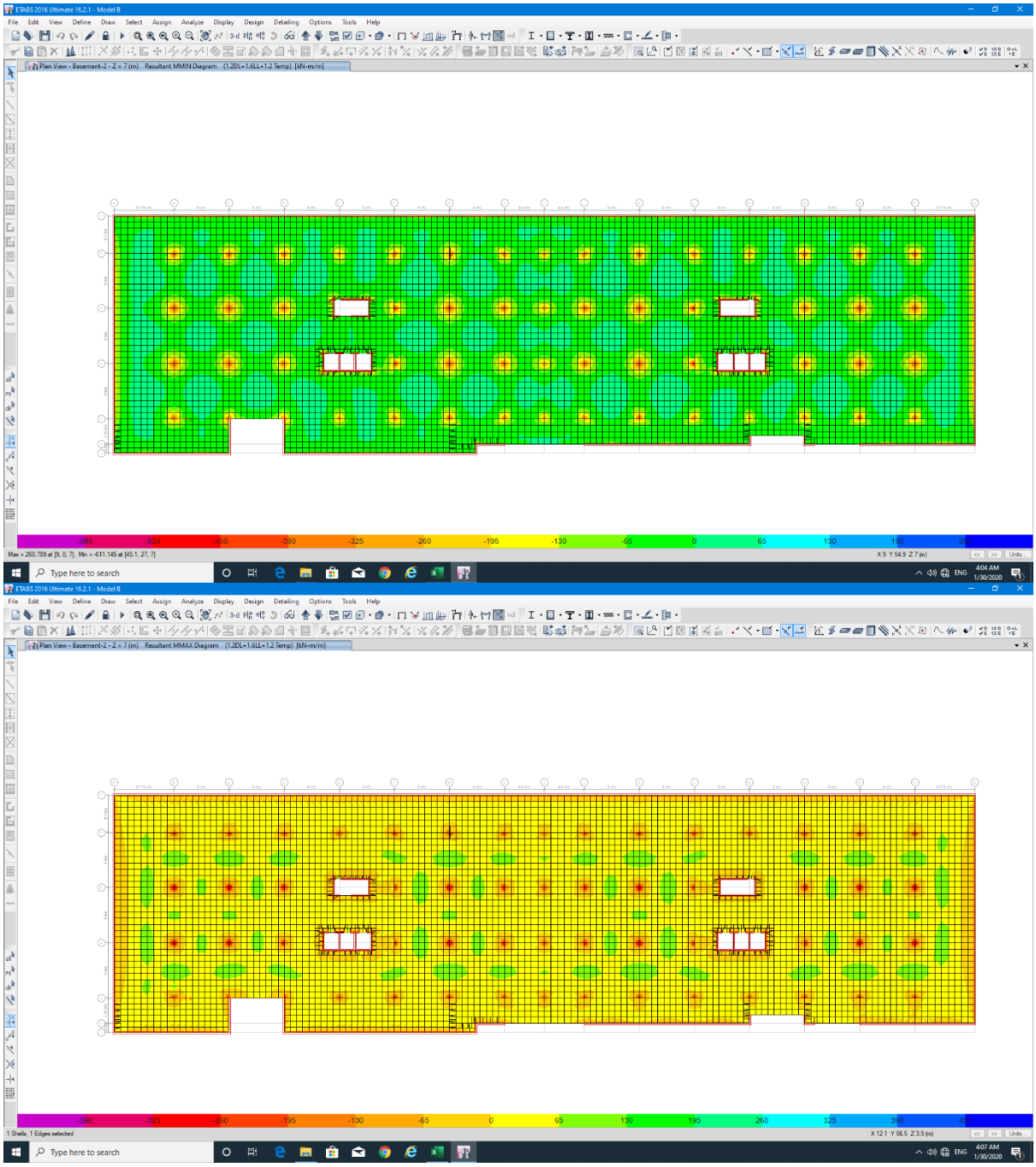
ETABS 2016 Ultimate 16.2.1 - Model B
Plan View - Basement-2 - Z = 7 (m) Resultant MMIN Diagram (1.2DL+1.6LL+1.2 Temp) [kN-m/m]
-585 -520 -455 -390 -325 -260 -195 -130 -65 0 65 130 195 260
Max = 260.789 at [9, 0, 7]; Min = -611.145 at [45.1, 27, 7]
X 9 Y 54.9 Z 7 (m)
Units
Type here to search
4:04 AM
1/30/2020
ETABS 2016 Ultimate 16.2.1 - Model B
Plan View - Basement-2 - Z = 7 (m) Resultant MMAX Diagram (1.2DL+1.6LL+1.2 Temp) [kN-m/m]
-390 -325 -260 -195 -130 -65 0 65 130 195 260 325 390 455
1 Shells, 1 Edges selected
X 12.1 Y 56.5 Z 3.5 (m)
Units
Type here to search
4:07 AM
1/30/2020

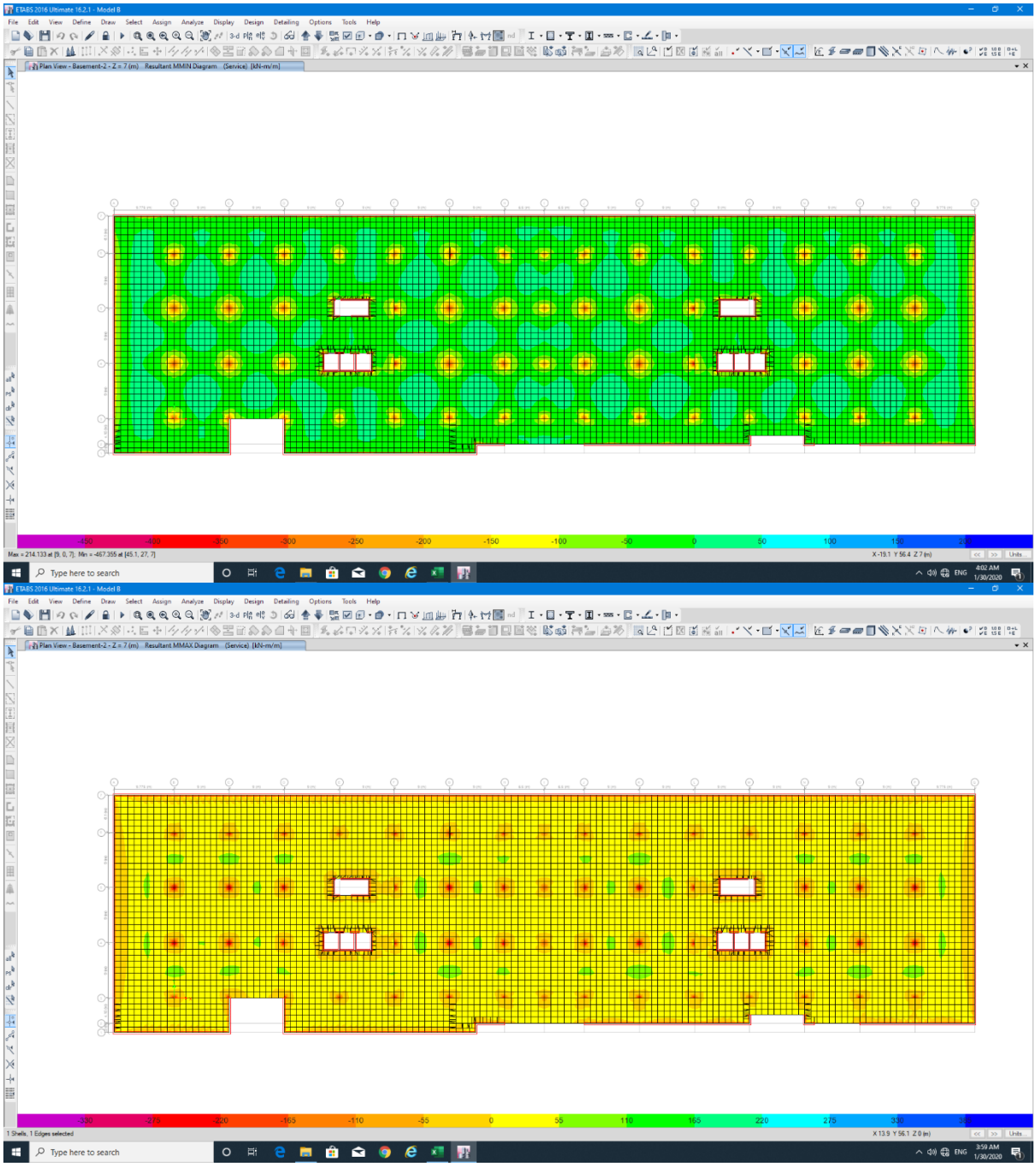
ETABS 2016 Ultimate 16.2.1 - Model B
Plan View - Basement-2 - Z = 7 (m) Resultant MMIN Diagram (Service) [kN-m/m]
-450 -400 -350 -300 -250 -200 -150 -100 -50 0 50 100 150 200
Max = 214.133 at [9, 0, 7]; Min = -467.355 at [45.1, 27, 7]
X -19.1 Y 56.4 Z 7 (in)
Type here to search
4:02 AM 1/30/2020
ETABS 2016 Ultimate 16.2.1 - Model B
Plan View - Basement-2 - Z = 7 (m) Resultant MMAX Diagram (Service) [kN-m/m]
-330 -275 -220 -165 -110 -55 0 55 110 165 220 275 330
1 Shells, 1 Edges selected
X 13.9 Y 56.1 Z 0 (in)
Type here to search
3:59 AM 1/30/2020

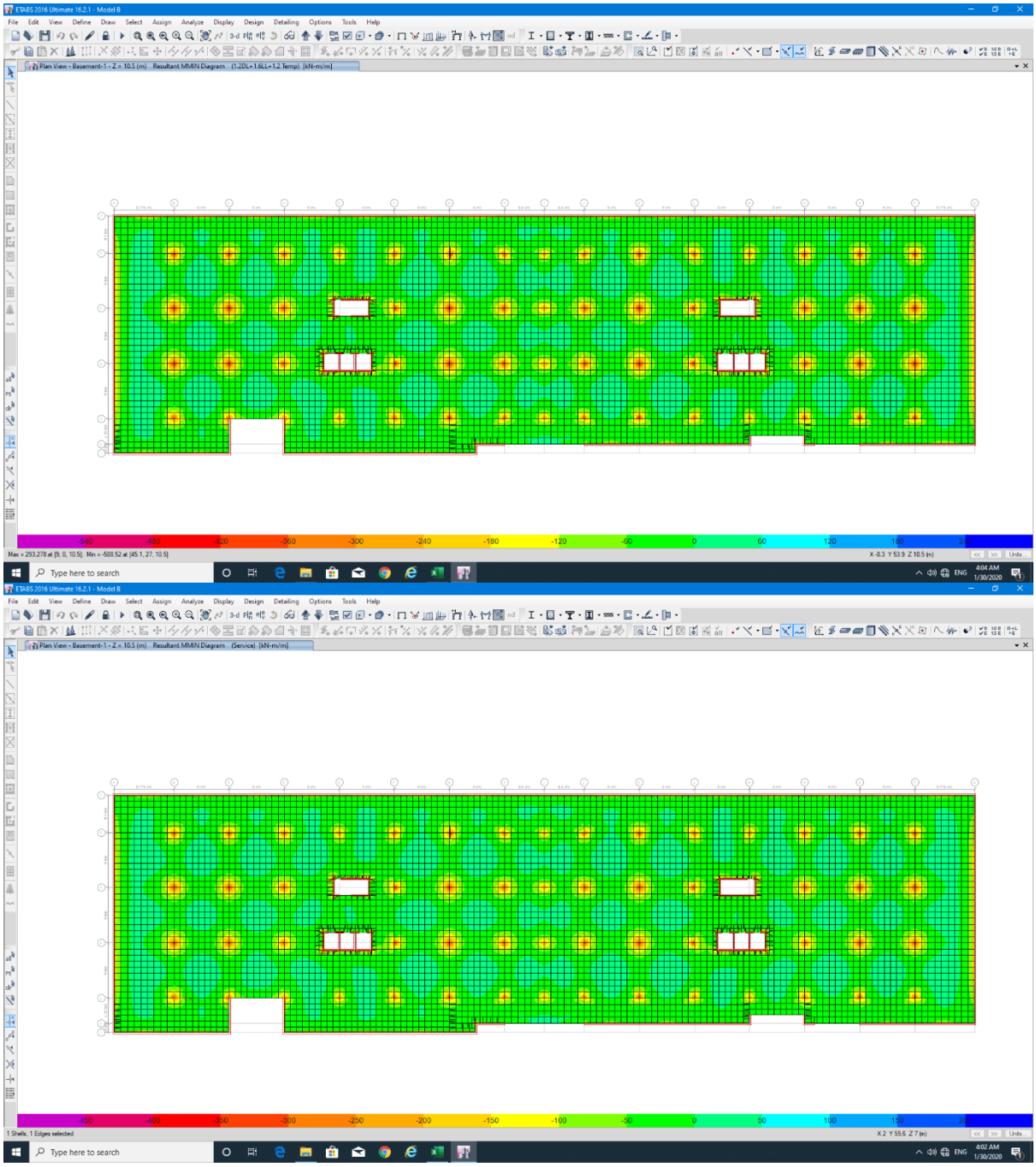
ETABS 2016 Ultimate 16.2.1 - Model B
Plan View - Basement-1 - Z = 10.5 (m) Resultant MMIN Diagram (1.2DL+1.6LL+1.2 Temp) [kN-m/m]
-540 -480 -420 -360 -300 -240 -180 -120 -60 0 60 120 180 240
Type here to search
4:04 AM
1/30/2020
ETABS 2016 Ultimate 16.2.1 - Model B
Plan View - Basement-1 - Z = 10.5 (m) Resultant MMIN Diagram (Service) [kN-m/m]
-450 -400 -350 -300 -250 -200 -150 -100 -50 0 50 100 150 200
1 Shells, 1 Edges selected
Type here to search
4:02 AM
1/30/2020

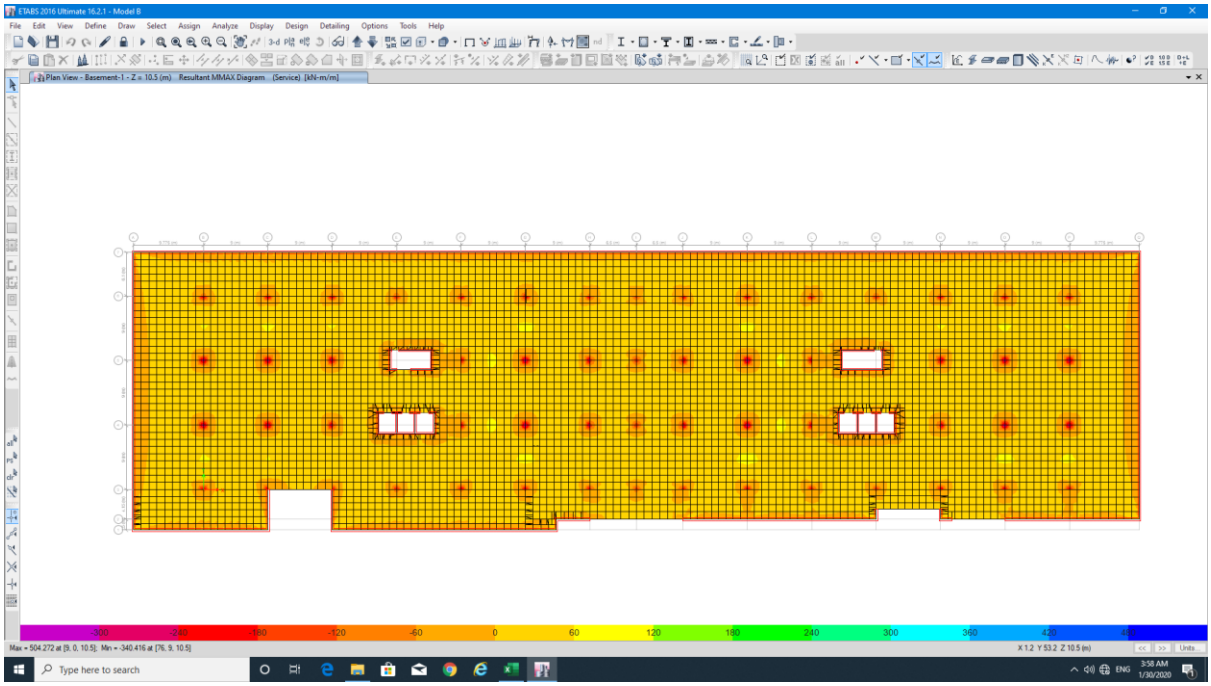

D-2-4 Walls Forces

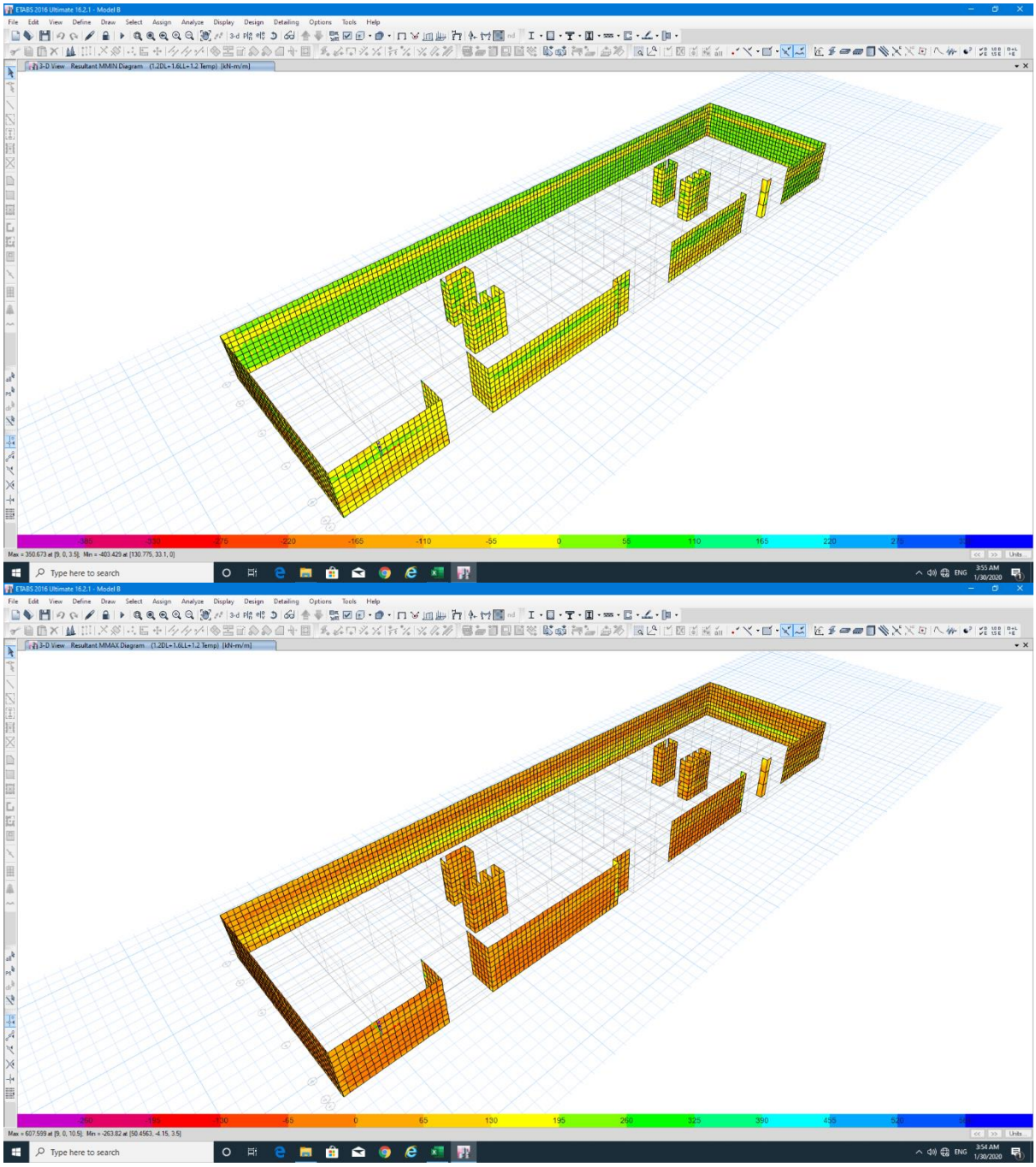
ETABS 2016 Ultimate 16.2.1 - Model 8
3-D View Resultant MMIN Diagram (1.2DL+1.6LL+1.2 Temp) [kN-m/m]
Type here to search
ETABS 2016 Ultimate 16.2.1 - Model 8
3-D View Resultant MMAX Diagram (1.2DL+1.6LL+1.2 Temp) [kN-m/m]
Type here to search

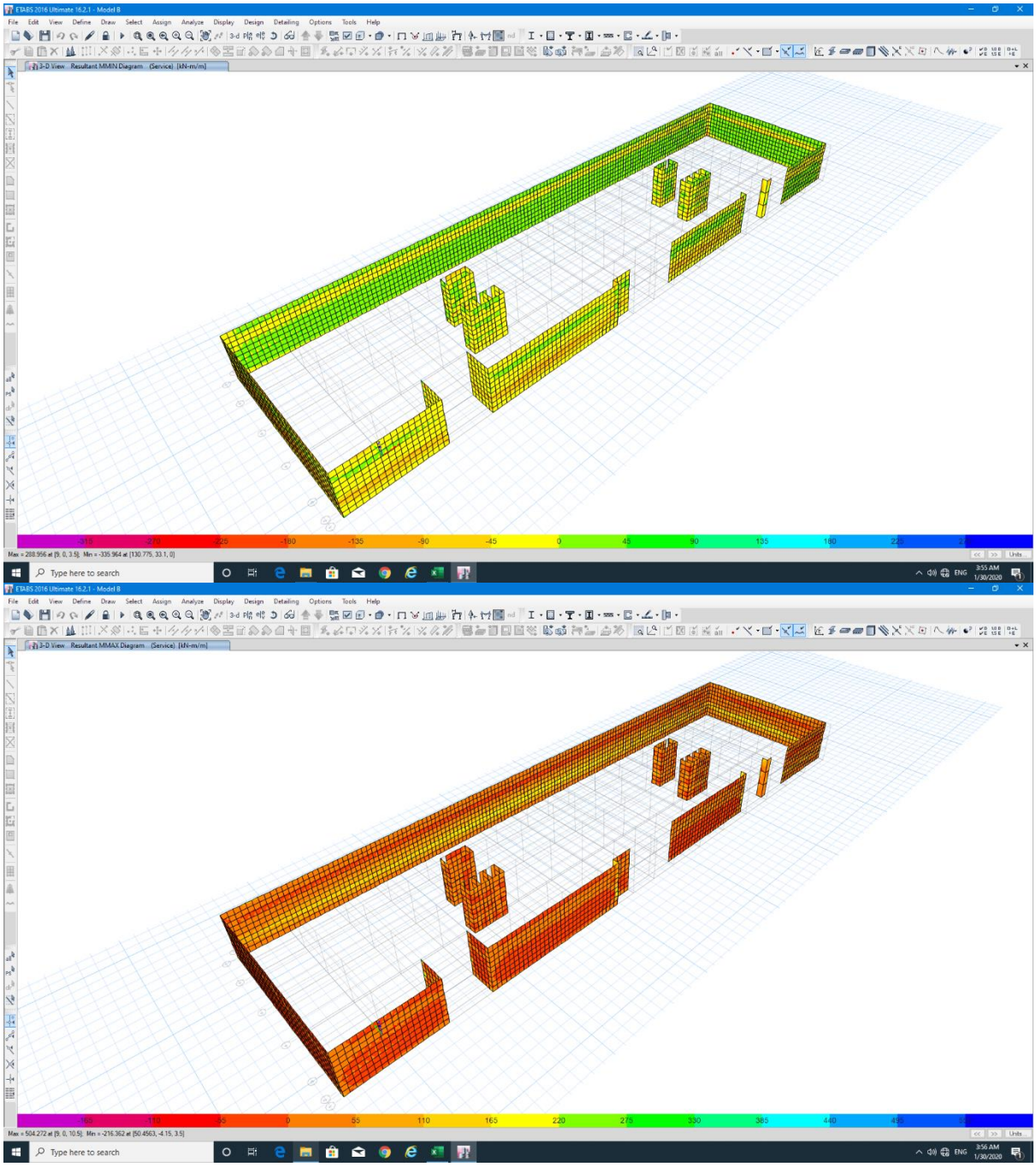

D-3 Model C
D-3-1 Column M22

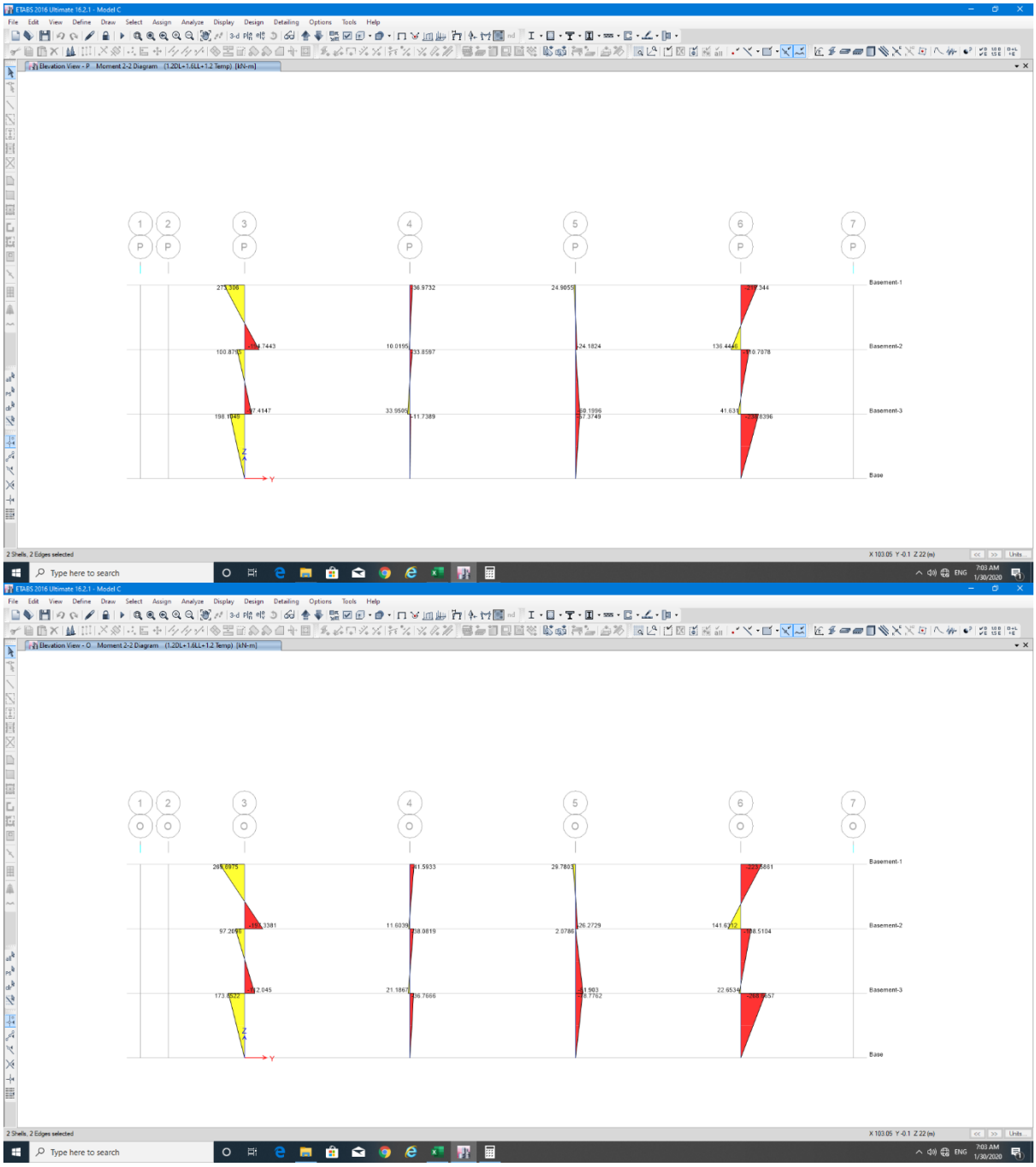
ETABS 2016 Ultimate 16.2.1 - Model C
Elevation View - P Moment 2-2 Diagram (1.2DL+1.6LL+1.2 Temp) [kN-m]
1 2 3 4 5 6 7
P P P P P P P
Basement-1
Basement-2
Basement-3
Base
2 Shells, 2 Edges selected
X 103.05 Y -0.1 Z 22 (m)
Type here to search
7:03 AM
1/30/2020

ETABS 2016 Ultimate 16.2.1 - Model C
Elevation View - O Moment 2-2 Diagram (1.2DL+1.6LL+1.2 Temp) [kN-m]
1 2 3 4 5 6 7
O O O O O O O
Basement-1
Basement-2
Basement-3
Base
2 Shells, 2 Edges selected
X 103.05 Y -0.1 Z 22 (m)
Type here to search
7:03 AM
1/30/2020

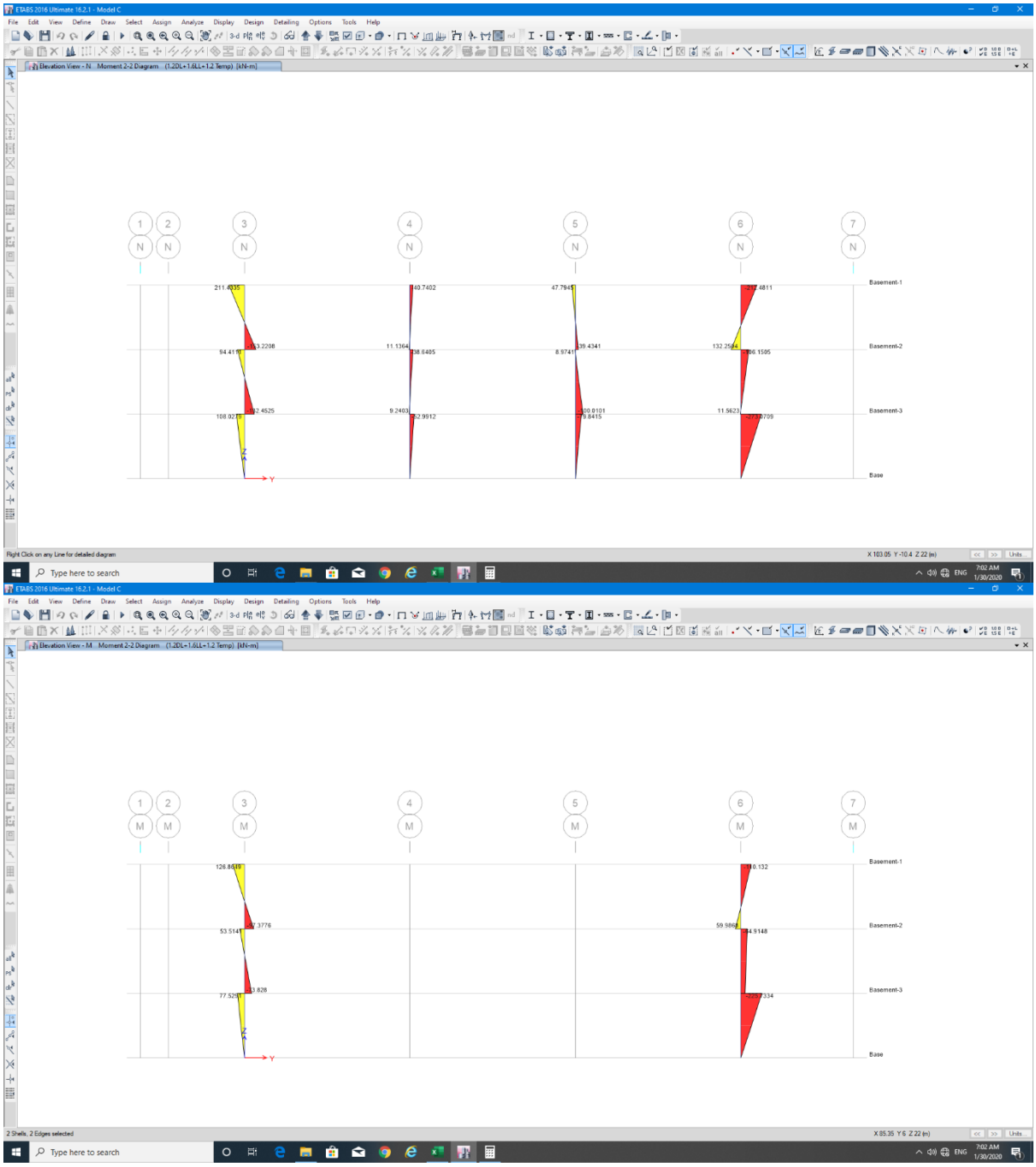
ETABS 2016 Ultimate 16.2.1 - Model C
Elevation View - N Moment 2-2 Diagram (1.2DL+1.6LL+1.2 Temp) [kN-m]
1 2 3 4 5 6 7
N N N N N N N
Basement-1
Basement-2
Basement-3
Base
Right Click on any Line for detailed diagram
Type here to search
ETABS 2016 Ultimate 16.2.1 - Model C
Elevation View - M Moment 2-2 Diagram (1.2DL+1.6LL+1.2 Temp) [kN-m]
1 2 3 4 5 6 7
M M M M M M M
Basement-1
Basement-2
Basement-3
Base
2 Shells, 2 Edges selected
Type here to search

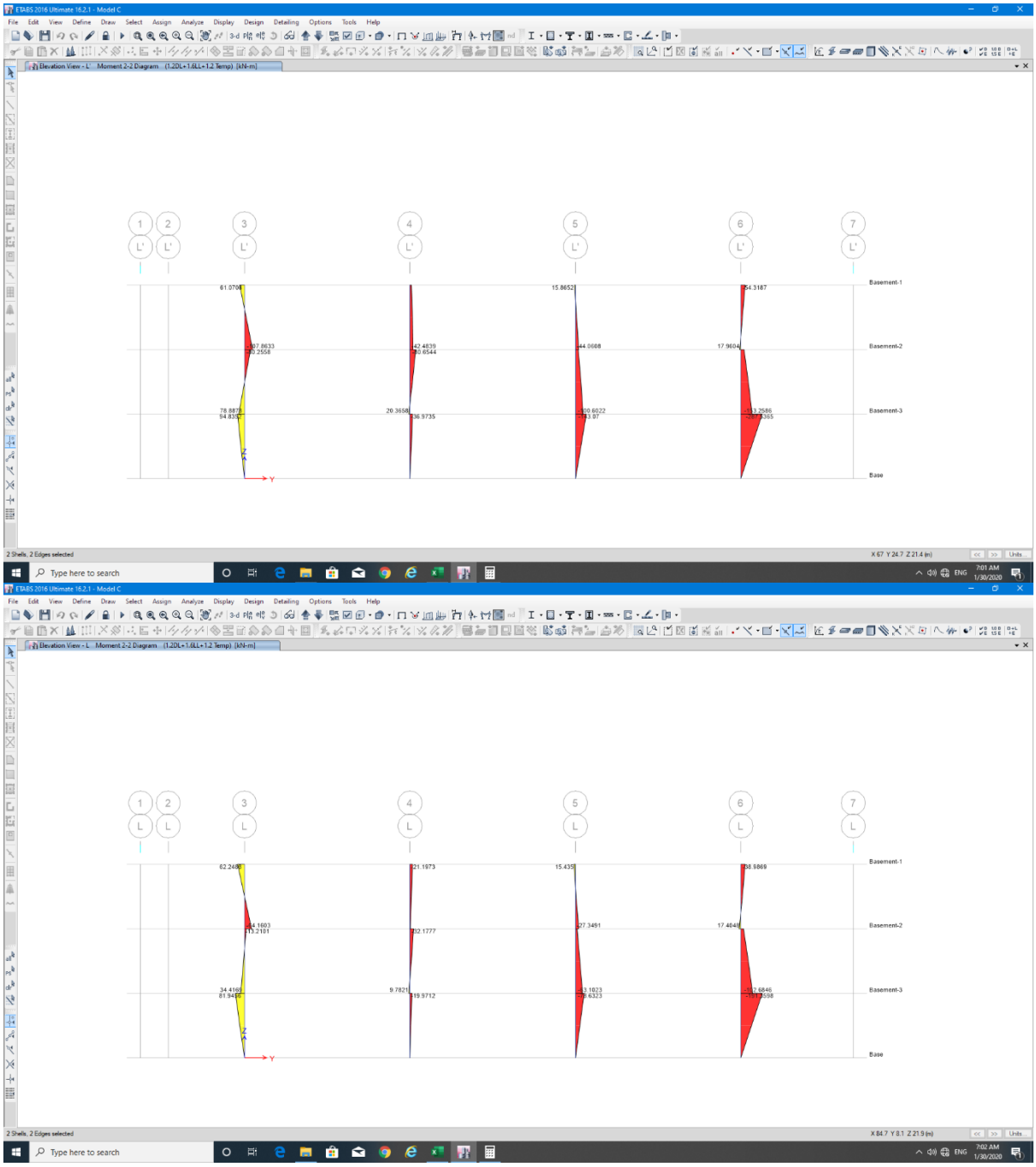
ETABS 2016 Ultimate 16.2.1 - Model C
Elevation View - L Moment 2-2 Diagram (1.2DL+1.6LL+1.2 Temp) [kN-m]
1 2 3 4 5 6 7
L' L' L' L' L' L' L'
61.0708
15.8652
54.3187
17.9604
Basement-1
Basement-2
Basement-3
Base
2 Shells, 2 Edges selected
Type here to search
7:01 AM
1/30/2020

ETABS 2016 Ultimate 16.2.1 - Model C
Elevation View - L Moment 2-2 Diagram (1.2DL+1.6LL+1.2 Temp) [kN-m]
1 2 3 4 5 6 7
L L L L L L L
62.2400
15.4351
17.4048
Basement-1
Basement-2
Basement-3
Base
2 Shells, 2 Edges selected
Type here to search
7:02 AM
1/30/2020

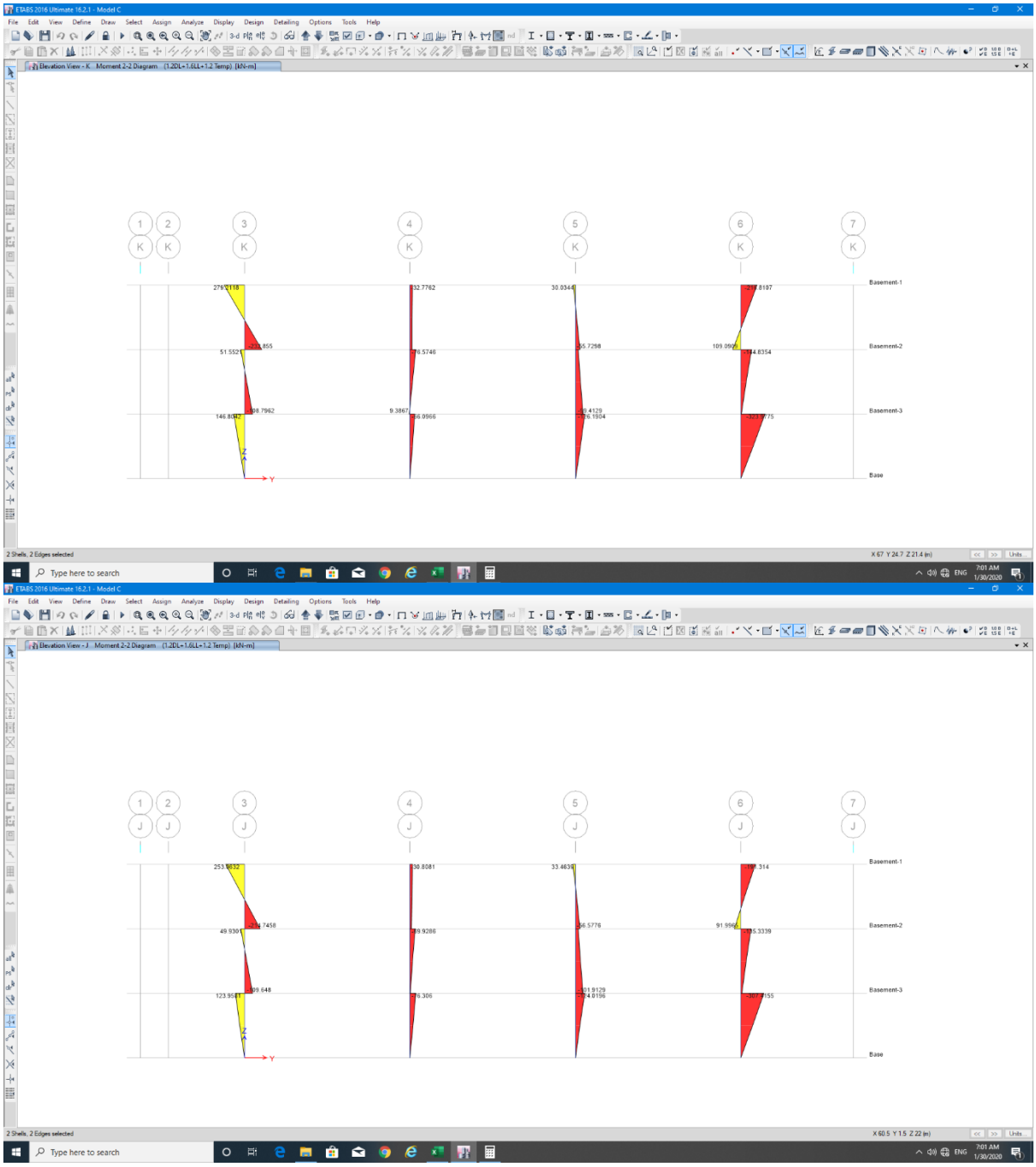
ETABS 2016 Ultimate 16.2.1 - Model C
Elevation View - K Moment 2-2 Diagram (1.2DL+1.6LL+1.2 Temp) [kN-m]
1 2 3 4 5 6 7
K K K K K K K
Basement-1
Basement-2
Basement-3
Base
2 Shells, 2 Edges selected
Type here to search
7:01 AM
1/30/2020
ETABS 2016 Ultimate 16.2.1 - Model C
Elevation View - J Moment 2-2 Diagram (1.2DL+1.6LL+1.2 Temp) [kN-m]
1 2 3 4 5 6 7
J J J J J J J
Basement-1
Basement-2
Basement-3
Base
2 Shells, 2 Edges selected
Type here to search
7:01 AM
1/30/2020

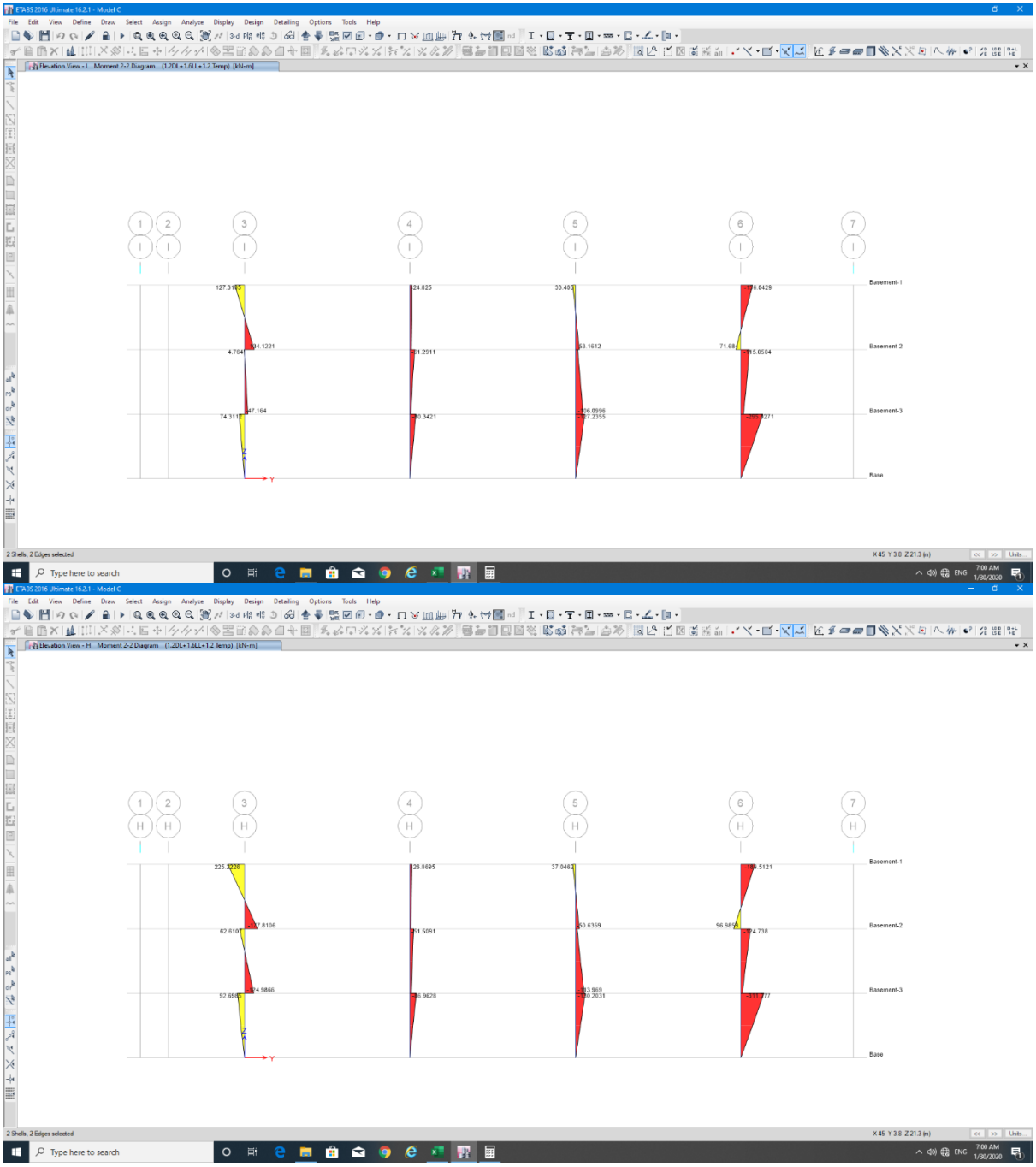
ETABS 2016 Ultimate 16.2.1 - Model C
Elevation View - I Moment 2-2 Diagram (1.2DL+1.6LL+1.2 Temp) [kN-m]
1 2 3 4 5 6 7
I I I I I I I
127.3145
4.764
74.3117
124.825
51.2911
30.3421
33.405
83.1612
71.684
Basement-1
Basement-2
Basement-3
Base
2 Shells, 2 Edges selected
X 45 Y 3.8 Z 21.3 (in)
Type here to search
7:00 AM
1/30/2020

ETABS 2016 Ultimate 16.2.1 - Model C
Elevation View - H Moment 2-2 Diagram (1.2DL+1.6LL+1.2 Temp) [kN-m]
1 2 3 4 5 6 7
H H H H H H H
225.2226
62.6107
92.6943
126.0695
51.5091
37.0463
96.9892
Basement-1
Basement-2
Basement-3
Base
2 Shells, 2 Edges selected
X 45 Y 3.8 Z 21.3 (in)
Type here to search
7:00 AM
1/30/2020

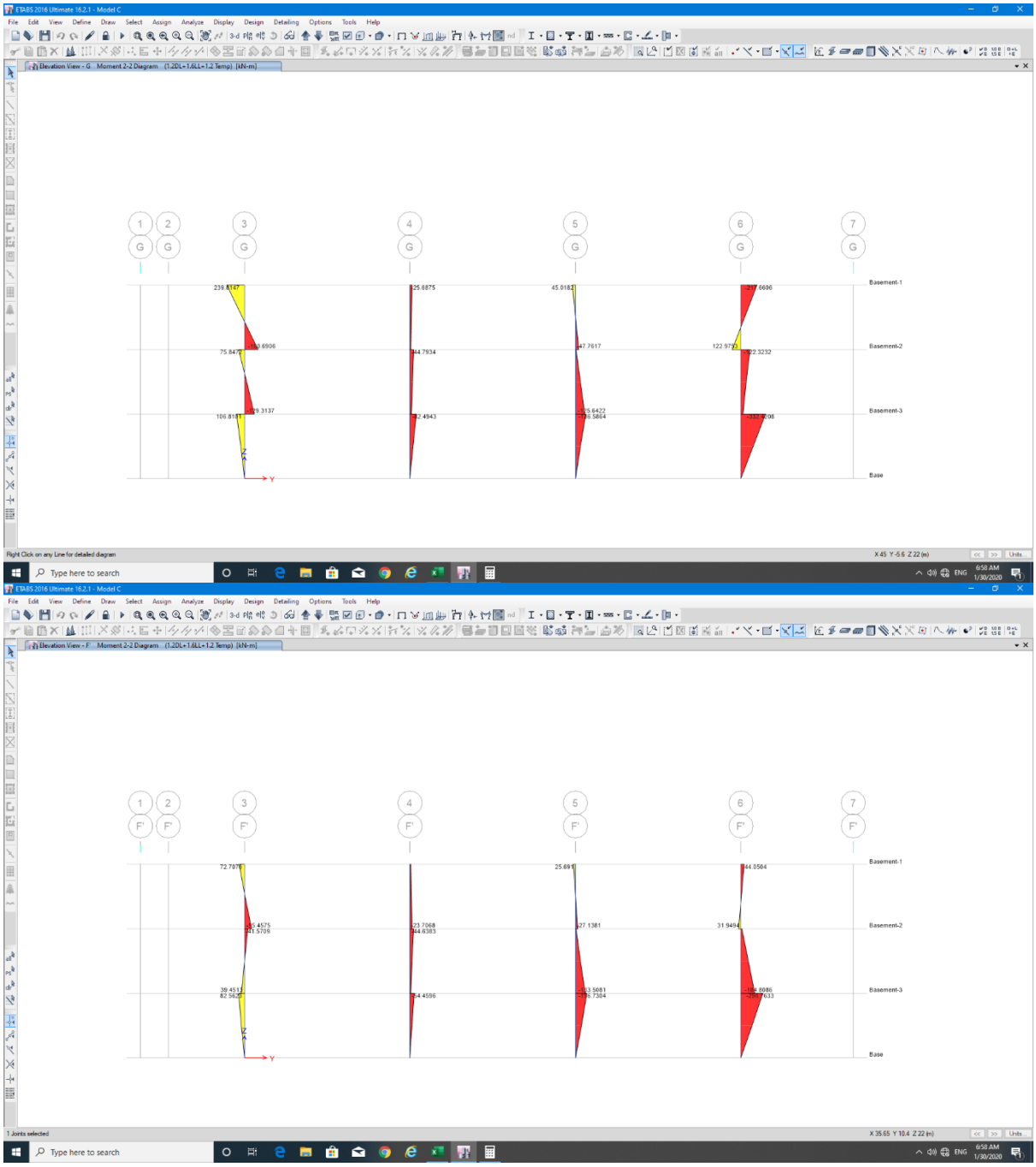
ETABS 2016 Ultimate 16.2.1 - Model C
Elevation View - G Moment 2-2 Diagram (1.2DL+1.6LL+1.2 Temp) [kN-m]
1 2 3 4 5 6 7
G G G G G G G
Basement-1
Basement-2
Basement-3
Base
Right Click on any Line for detailed diagram
Type here to search
6:58 AM
1/30/2020

ETABS 2016 Ultimate 16.2.1 - Model C
Elevation View - F Moment 2-2 Diagram (1.2DL+1.6LL+1.2 Temp) [kN-m]
1 2 3 4 5 6 7
F' F' F' F' F' F' F'
Basement-1
Basement-2
Basement-3
Base
1 Joints selected
Type here to search
6:58 AM
1/30/2020

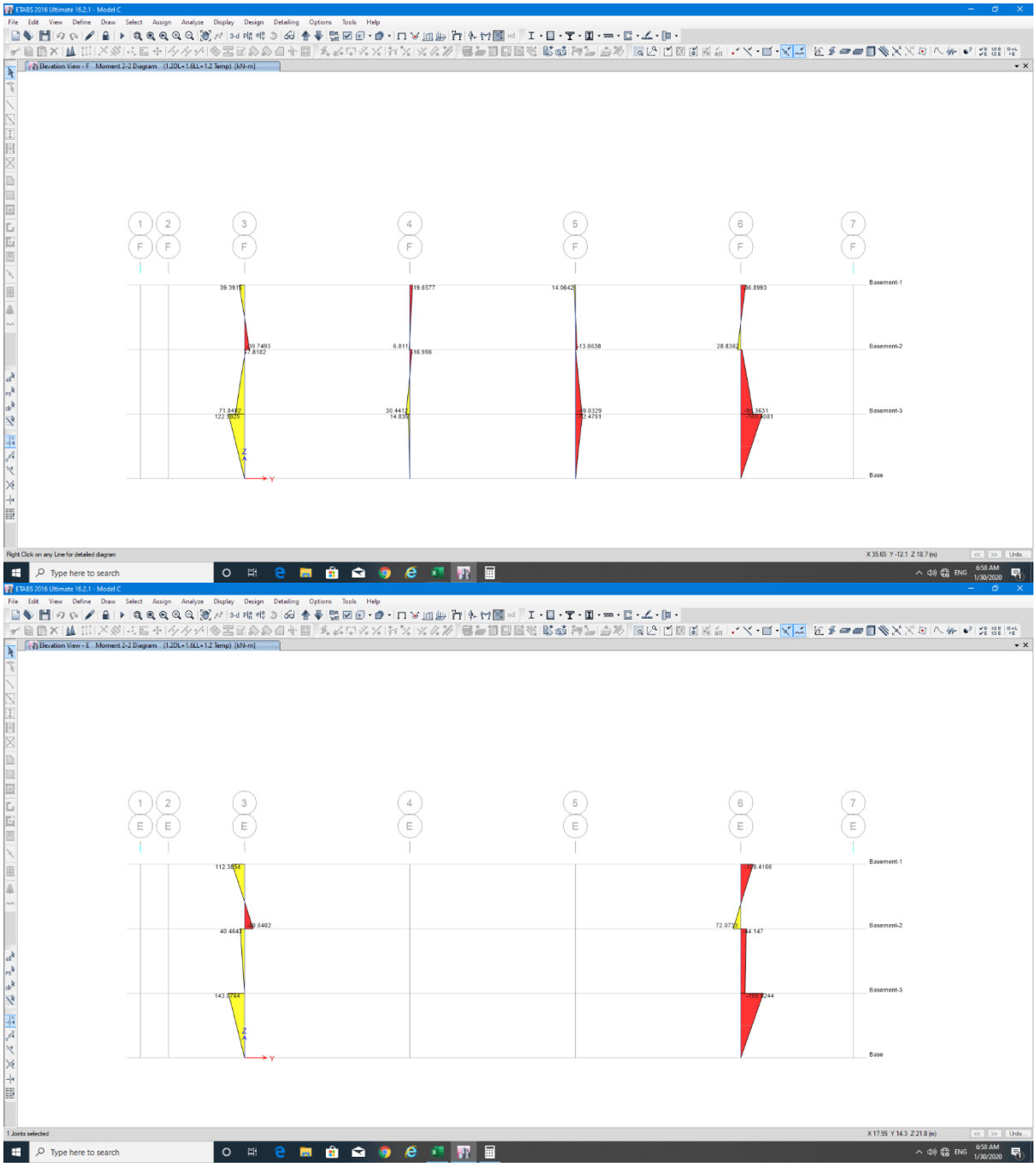
ETABS 2016 Ultimate 16.2.1 - Model C
Elevation View - F Moment 2-2 Diagram (1.2DL+1.6LL+1.2 Temp) [kN-m]
1 2 3 4 5 6 7
F F F F F F F
Basement-1
Basement-2
Basement-3
Base
Right Click on any Line for detailed diagram
Type here to search
ETABS 2016 Ultimate 16.2.1 - Model C
Elevation View - E Moment 2-2 Diagram (1.2DL+1.6LL+1.2 Temp) [kN-m]
1 2 3 4 5 6 7
E E E E E E E
Basement-1
Basement-2
Basement-3
Base
1 Joints selected
Type here to search

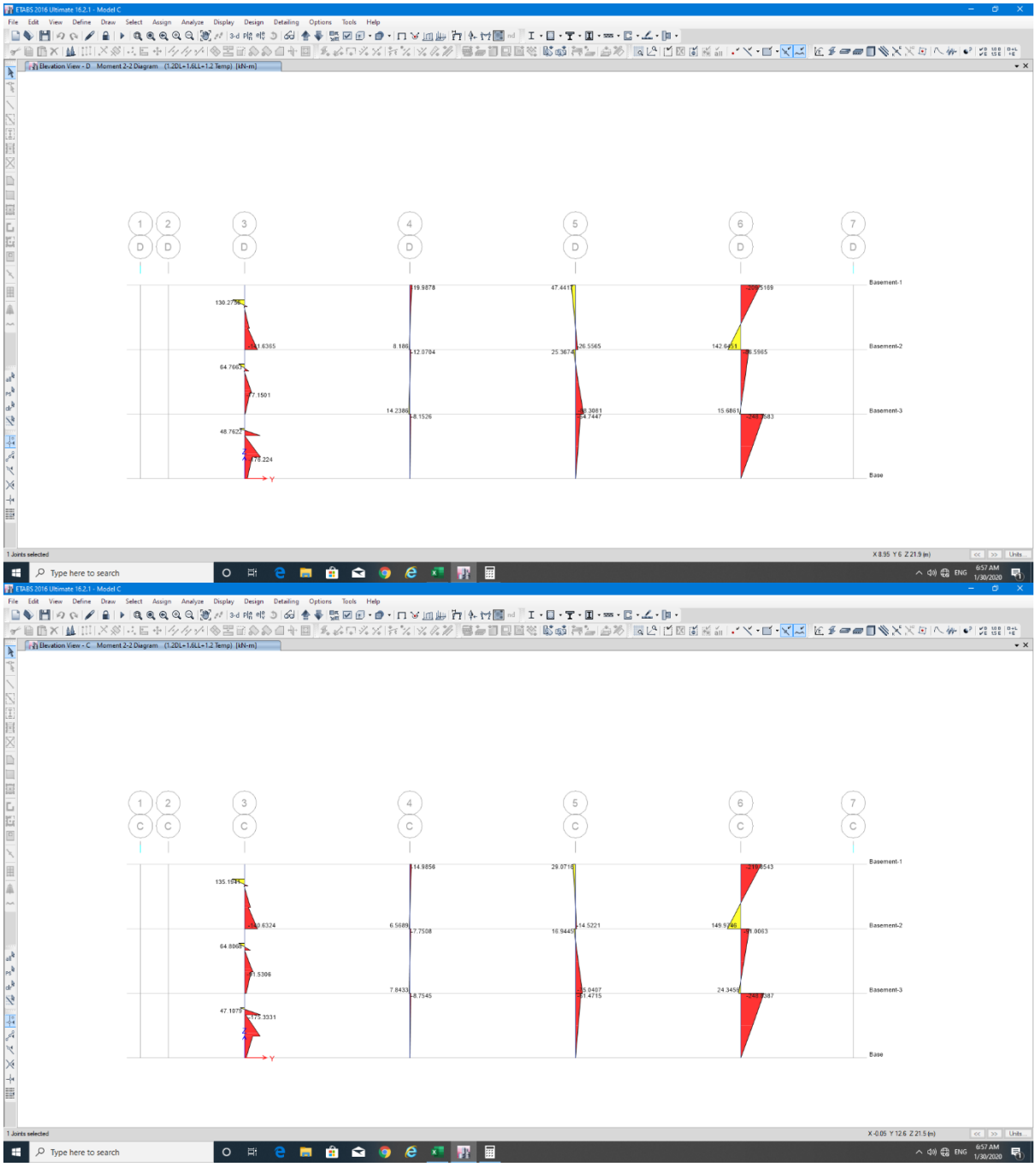
ETABS 2016 Ultimate 16.2.1 - Model C
Elevation View - D Moment 2-2 Diagram (1.2DL+1.6LL+1.2 Temp) [kN-m]
1 2 3 4 5 6 7
D
Basement-1
Basement-2
Basement-3
Base
1 Joints selected
Type here to search
ETABS 2016 Ultimate 16.2.1 - Model C
Elevation View - C Moment 2-2 Diagram (1.2DL+1.6LL+1.2 Temp) [kN-m]
1 2 3 4 5 6 7
C
Basement-1
Basement-2
Basement-3
Base
1 Joints selected
Type here to search

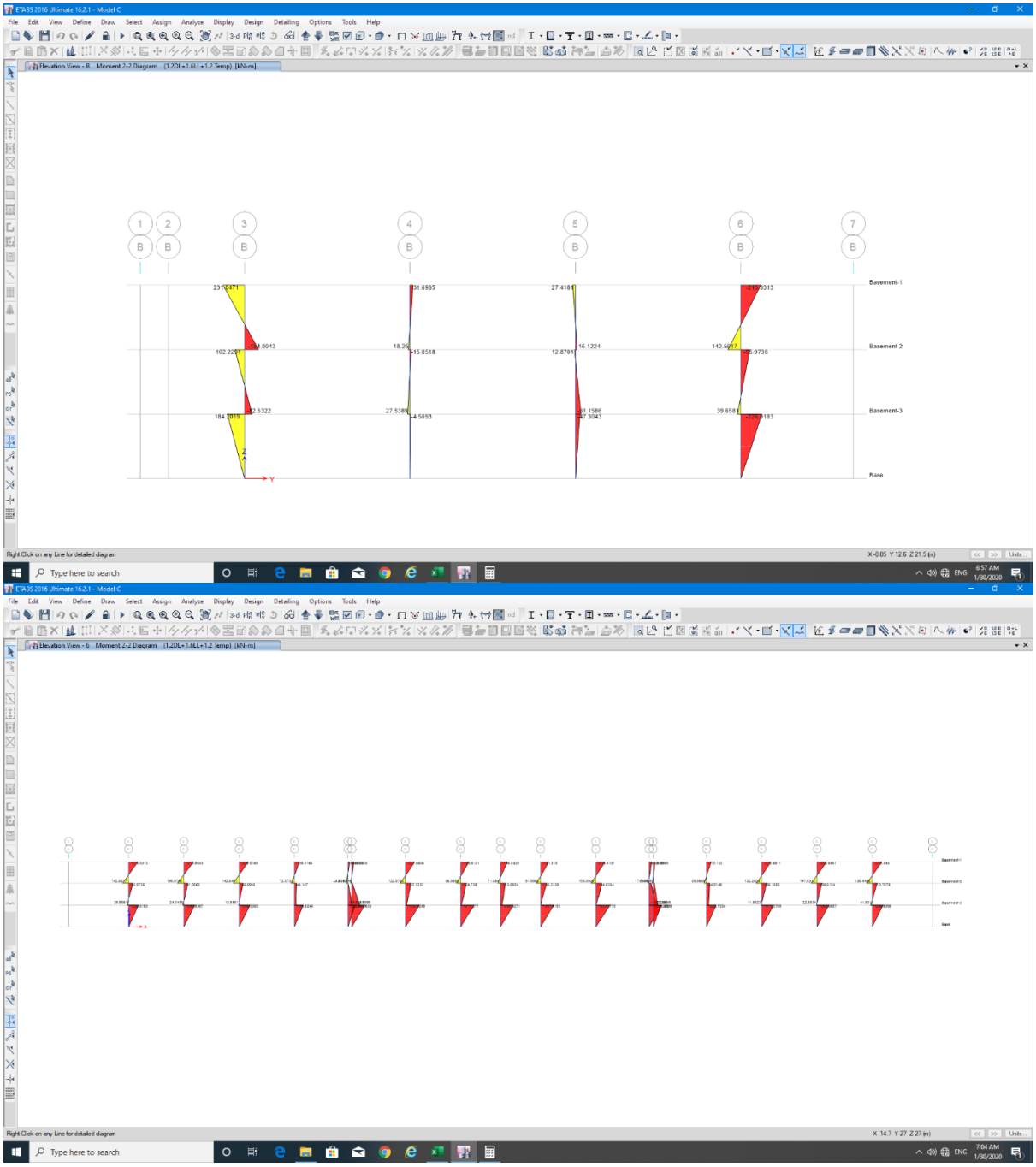
ETABS 2016 Ultimate 16.2.1 - Model C
Elevation View - B Moment 2-2 Diagram (1.2DL+1.6LL+1.2 Temp) [kN-m]
1 2 3 4 5 6 7
B B B B B B B
Basement-1
Basement-2
Basement-3
Base
Right Click on any Line for detailed diagram
Type here to search
6:57 AM
1/30/2020

ETABS 2016 Ultimate 16.2.1 - Model C
Elevation View - 6 Moment 2-2 Diagram (1.2DL+1.6LL+1.2 Temp) [kN-m]
Right Click on any Line for detailed diagram
Type here to search
7:04 AM
1/30/2020

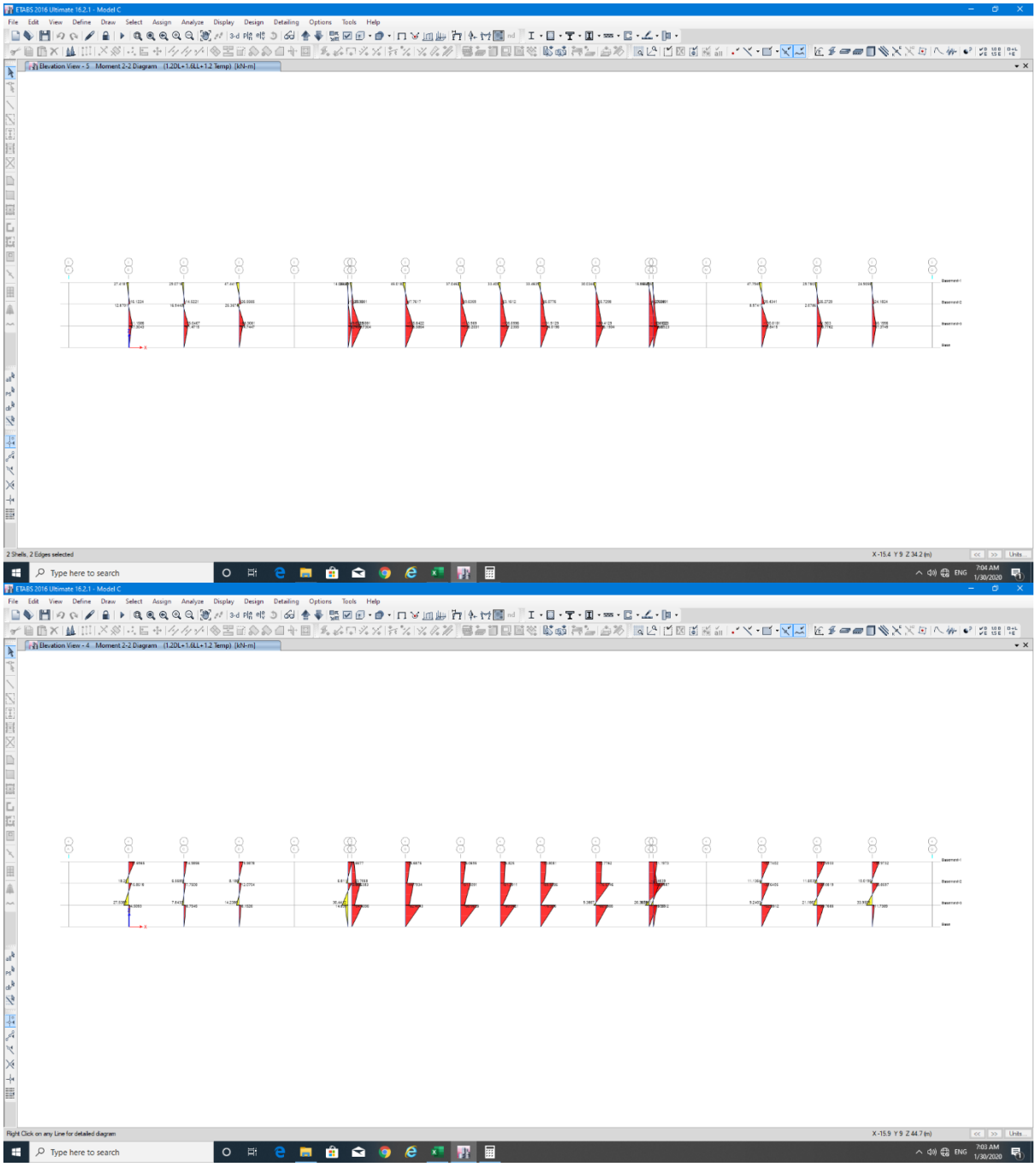
ETABS 2016 Ultimate 16.2.1 - Model C
Elevation View - 5 Moment 2-2 Diagram (1.2DL+1.6LL+1.2 Temp) [kN-m]
2 Shells, 2 Edges selected
Type here to search
ETABS 2016 Ultimate 16.2.1 - Model C
Elevation View - 4 Moment 2-2 Diagram (1.2DL+1.6LL+1.2 Temp) [kN-m]
Right Click on any Line for detailed diagram
Type here to search

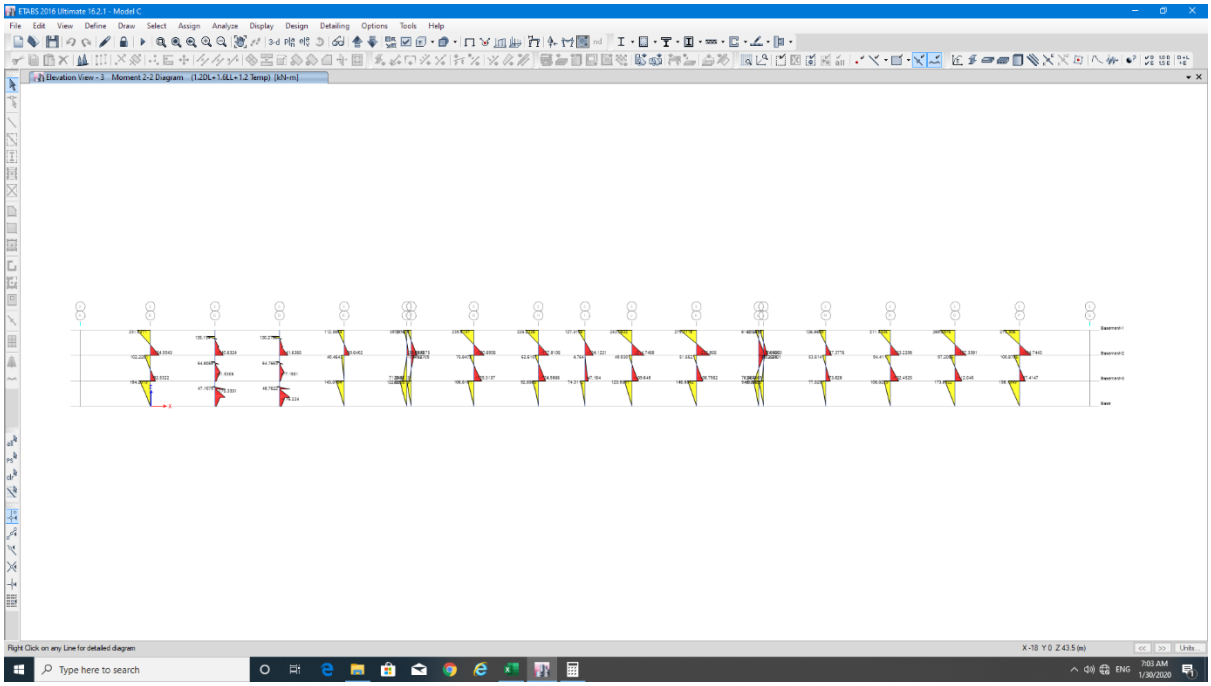

D-3-2 Column M33

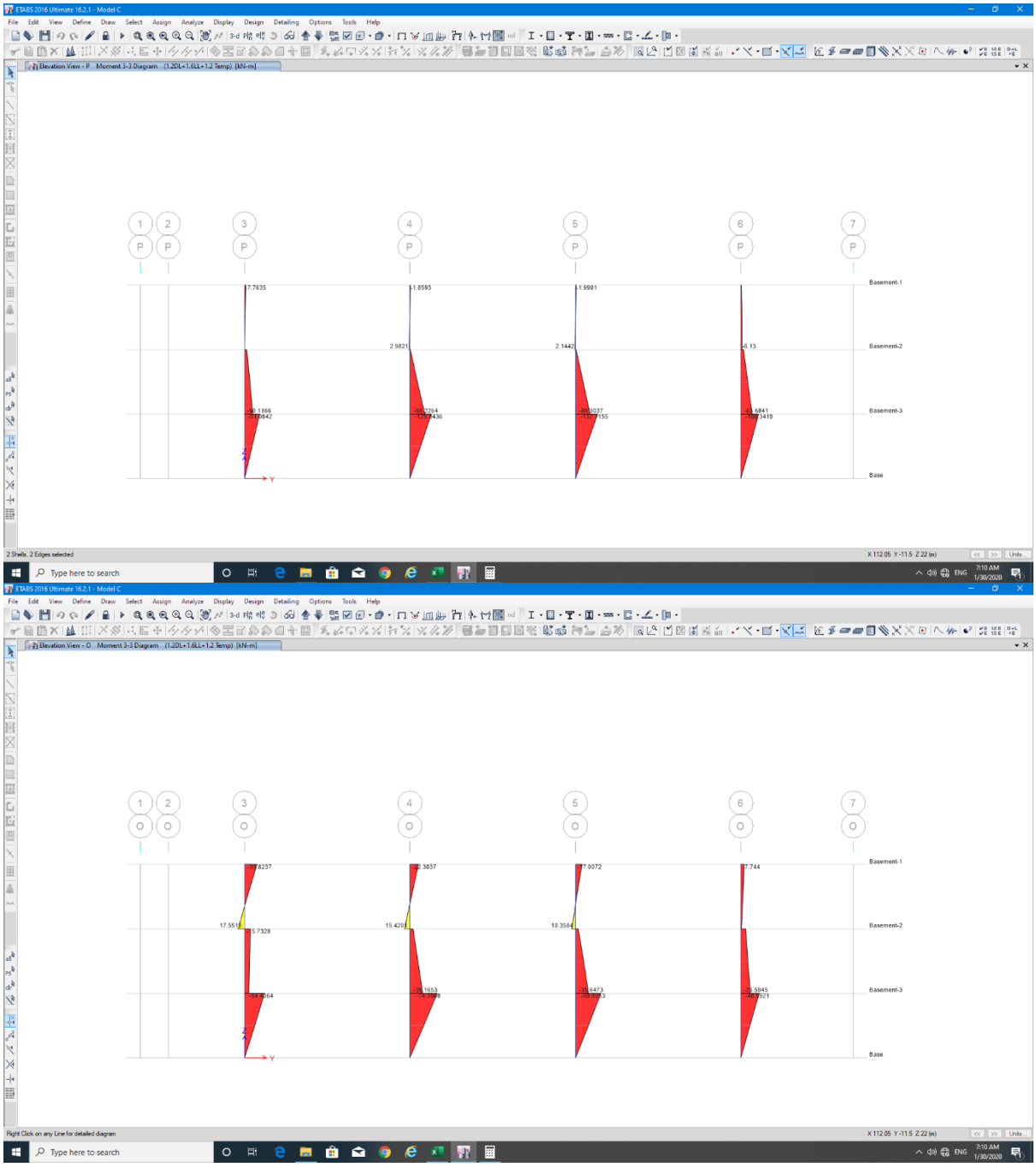
ETABS 2016 Ultimate 16.2.1 - Model C
Elevation View - P Moment 3-3 Diagram (1.2DL+1.6LL+1.2 Temp) [kN-m]
1
2
3
4
5
6
7
P
Basement-1
Basement-2
Basement-3
Base
Type here to search
ENG
7:10 AM
1/30/2020

ETABS 2016 Ultimate 16.2.1 - Model C
Elevation View - O Moment 3-3 Diagram (1.2DL+1.6LL+1.2 Temp) [kN-m]
1
2
3
4
5
6
7
O
Basement-1
Basement-2
Basement-3
Base
Right Click on any Line for detailed diagram
Type here to search
ENG
7:10 AM
1/30/2020

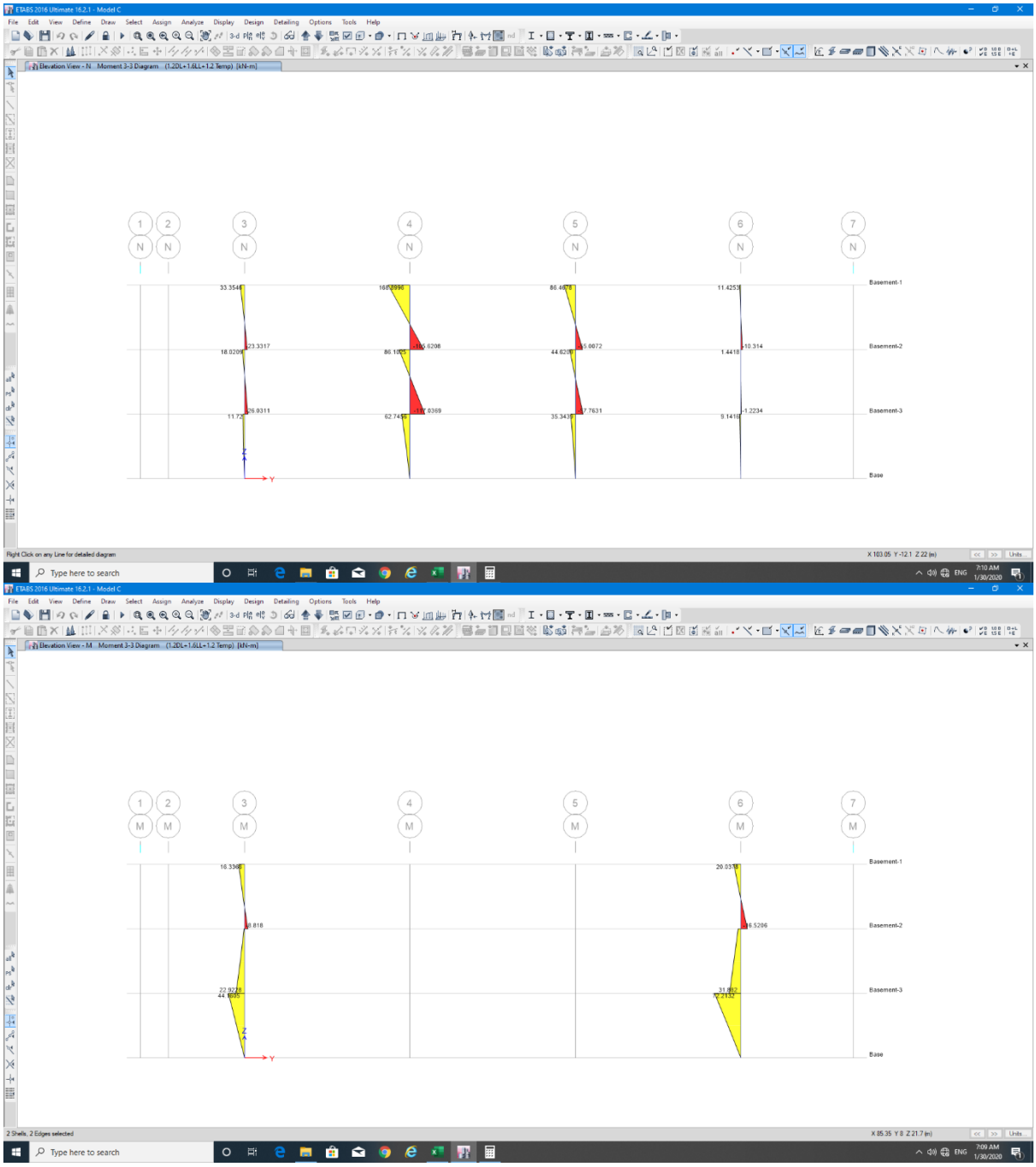
ETABS 2016 Ultimate 16.2.1 - Model C
Elevation View - N Moment 3-3 Diagram (1.2DL+1.6LL+1.2 Temp) [kN-m]
1 2 3 4 5 6 7
N N N N N N N
Basement-1
Basement-2
Basement-3
Base
Right Click on any Line for detailed diagram
Type here to search
7:10 AM
1/30/2020
ETABS 2016 Ultimate 16.2.1 - Model C
Elevation View - M Moment 3-3 Diagram (1.2DL+1.6LL+1.2 Temp) [kN-m]
1 2 3 4 5 6 7
M M M M M M M
Basement-1
Basement-2
Basement-3
Base
2 Shells, 2 Edges selected
Type here to search
7:09 AM
1/30/2020

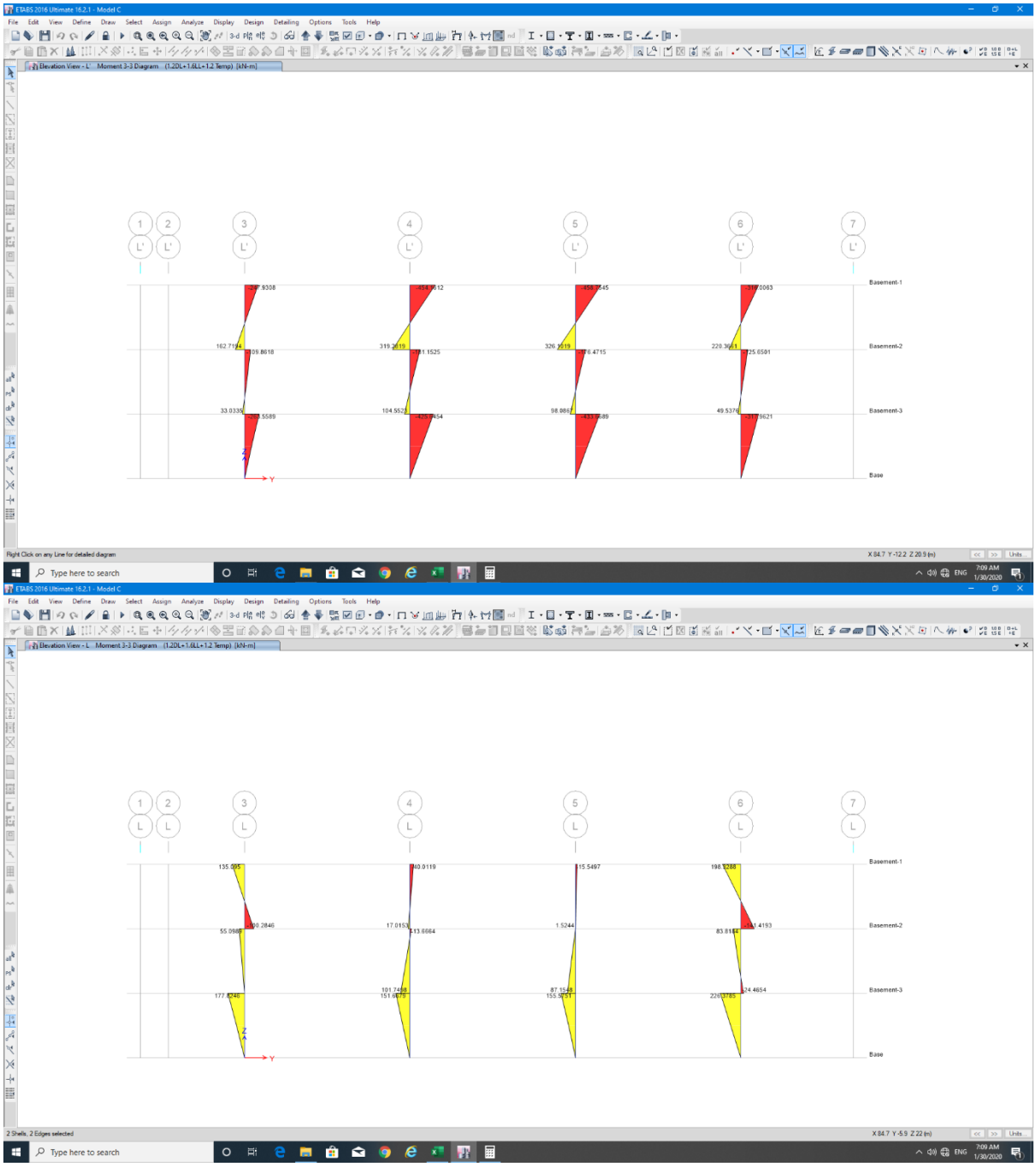
ETABS 2016 Ultimate 16.2.1 - Model C
Elevation View - L Moment 3-3 Diagram (1.2DL+1.6LL+1.2 Temp) [kN-m]
1
2
3
4
5
6
7
L'
Basement-1
Basement-2
Basement-3
Base
Right Click on any Line for detailed diagram
Type here to search
7:09 AM
1/30/2020
ETABS 2016 Ultimate 16.2.1 - Model C
Elevation View - L Moment 3-3 Diagram (1.2DL+1.6LL+1.2 Temp) [kN-m]
L
135.095
55.0508
177.8246
40.0119
17.0153
101.7488
15.5497
1.5244
87.3548
198.1288
83.8164
124.4654
Basement-1
Basement-2
Basement-3
Base
2 Shells, 2 Edges selected
Type here to search
7:09 AM
1/30/2020

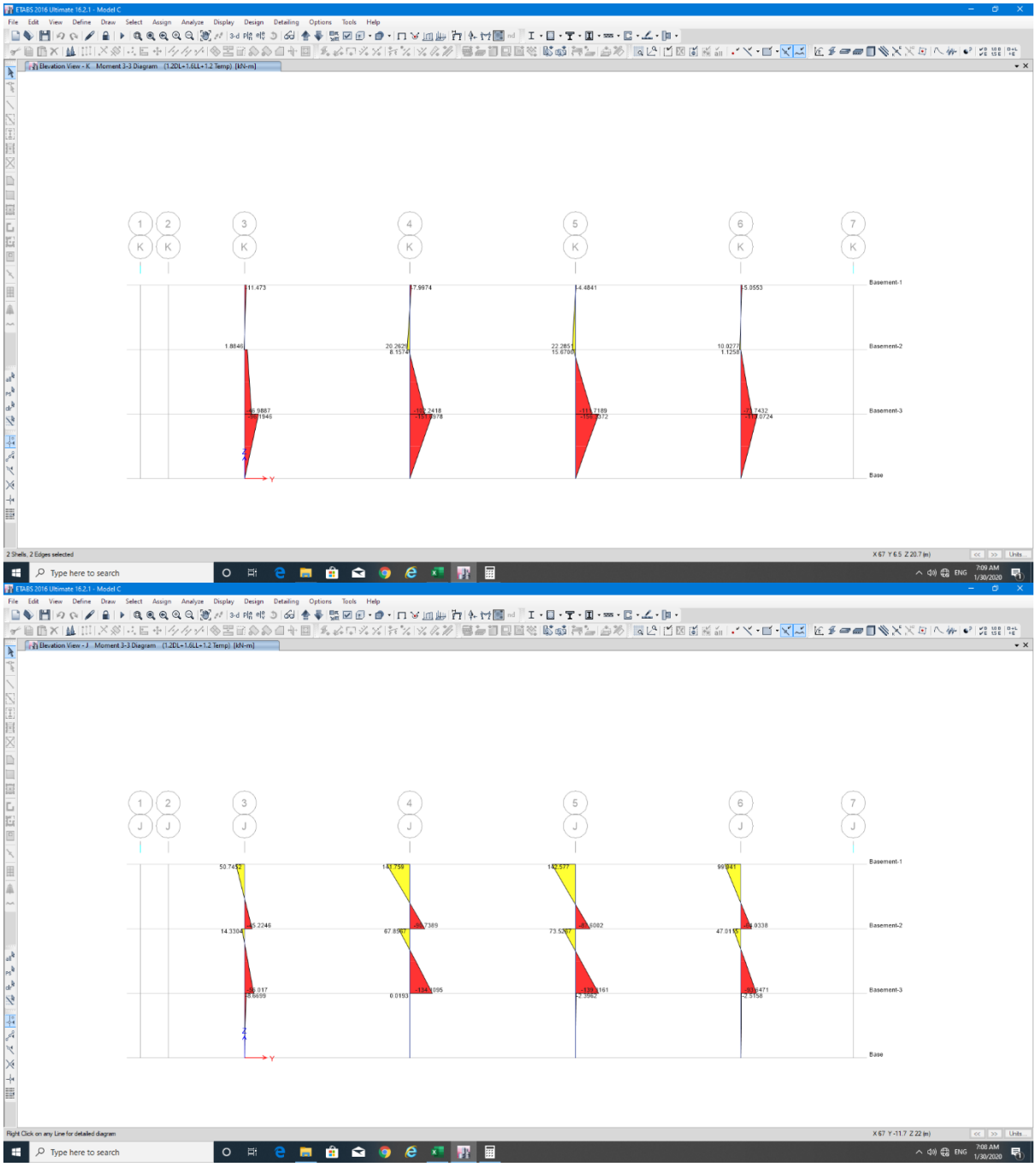
ETABS 2016 Ultimate 16.2.1 - Model C
Elevation View - K Moment 3-3 Diagram (1.2DL+1.6LL+1.2 Temp) [kN-m]
1 2 3 4 5 6 7
K K K K K K K
Basement-1
Basement-2
Basement-3
Base
2 Shells, 2 Edges selected
X 67 Y 6.5 Z 20.7 in
Type here to search
7:09 AM
1/30/2020
ETABS 2016 Ultimate 16.2.1 - Model C
Elevation View - J Moment 3-3 Diagram (1.2DL+1.6LL+1.2 Temp) [kN-m]
1 2 3 4 5 6 7
J J J J J J J
Basement-1
Basement-2
Basement-3
Base
Right Click on any Line for detailed diagram
X 67 Y -11.7 Z 22 in
Type here to search
7:08 AM
1/30/2020

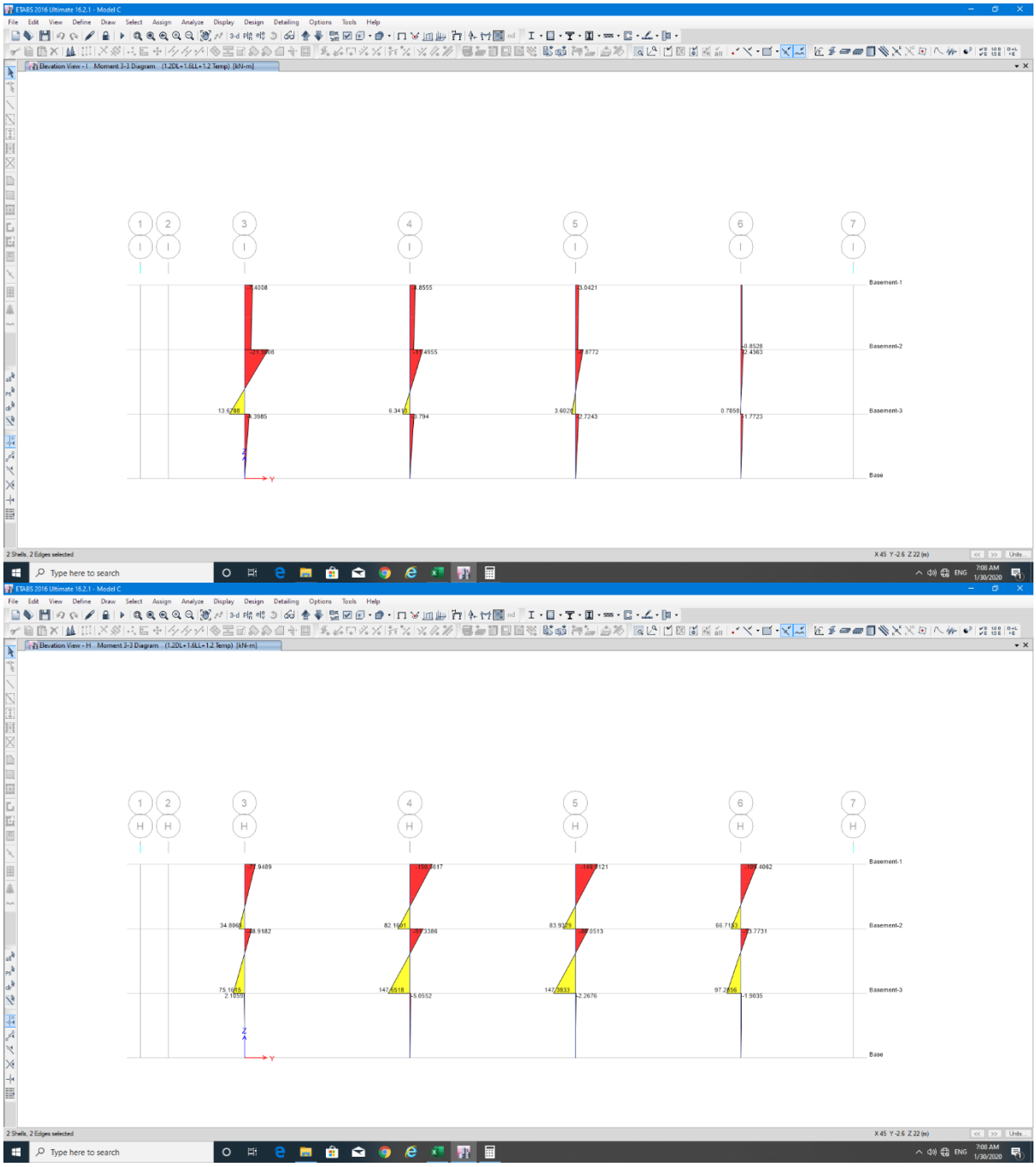
ETABS 2016 Ultimate 16.2.1 - Model C
Elevation View - I Moment 3-3 Diagram (1.2DL+1.6LL+1.2 Temp) [kN-m]
1 2 3 4 5 6 7
I I I I I I I
Basement-1
Basement-2
Basement-3
Base
2 Shells, 2 Edges selected
Type here to search
7:08 AM
1/30/2020
ETABS 2016 Ultimate 16.2.1 - Model C
Elevation View - H Moment 3-3 Diagram (1.2DL+1.6LL+1.2 Temp) [kN-m]
1 2 3 4 5 6 7
H H H H H H H
Basement-1
Basement-2
Basement-3
Base
2 Shells, 2 Edges selected
Type here to search
7:08 AM
1/30/2020

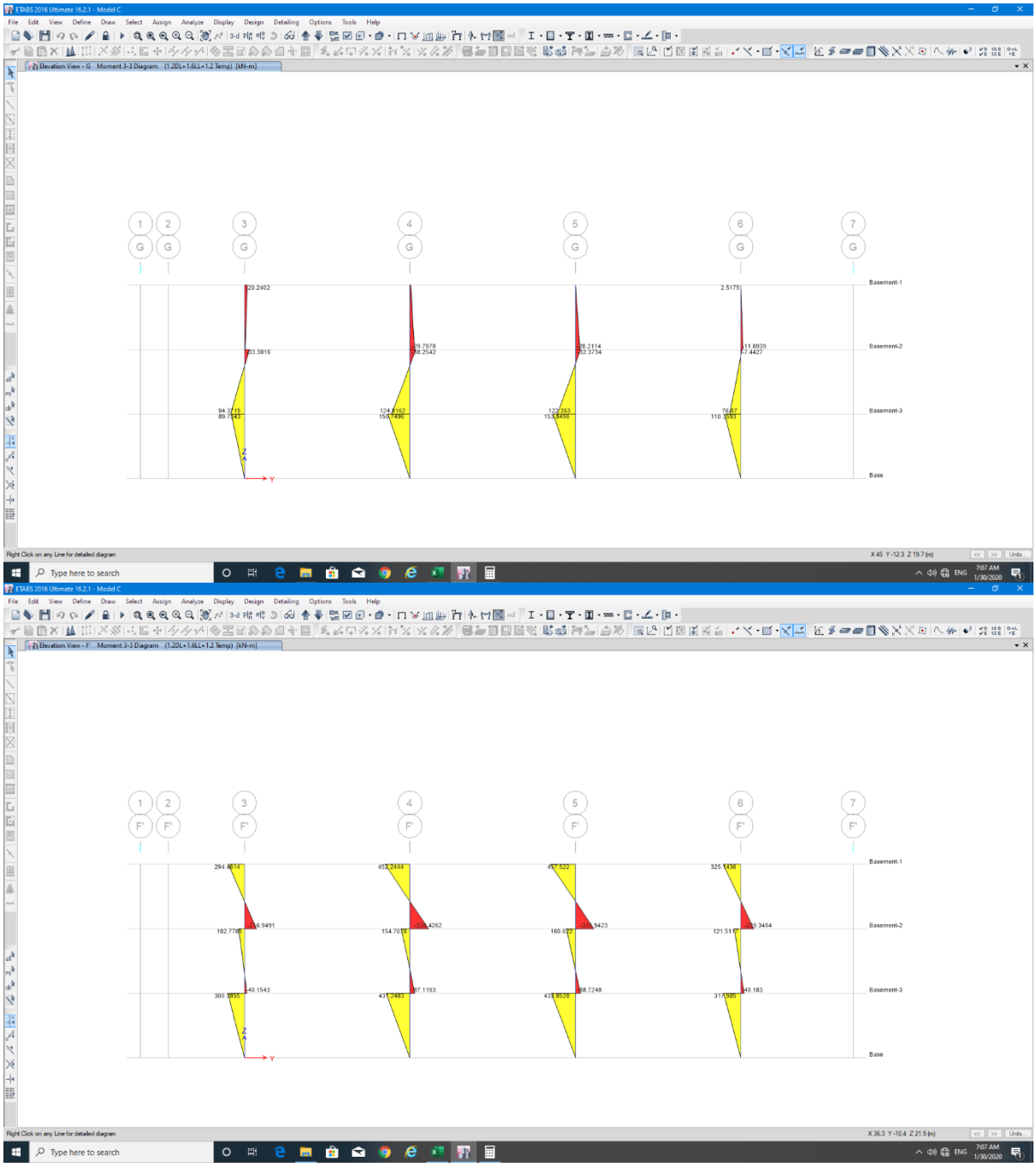
ETABS 2016 Ultimate 16.2.1 - Model C
Elevation View - G Moment 3-3 Diagram (1.2DL+1.6LL+1.2 Temp) [kN-m]
1 2 3 4 5 6 7
G G G G G G G
Basement-1
Basement-2
Basement-3
Base
Right Click on any Line for detailed diagram
Type here to search
7:07 AM
1/30/2020

ETABS 2016 Ultimate 16.2.1 - Model C
Elevation View - F Moment 3-3 Diagram (1.2DL+1.6LL+1.2 Temp) [kN-m]
1 2 3 4 5 6 7
F' F' F' F' F' F' F'
Basement-1
Basement-2
Basement-3
Base
Right Click on any Line for detailed diagram
Type here to search
7:07 AM
1/30/2020

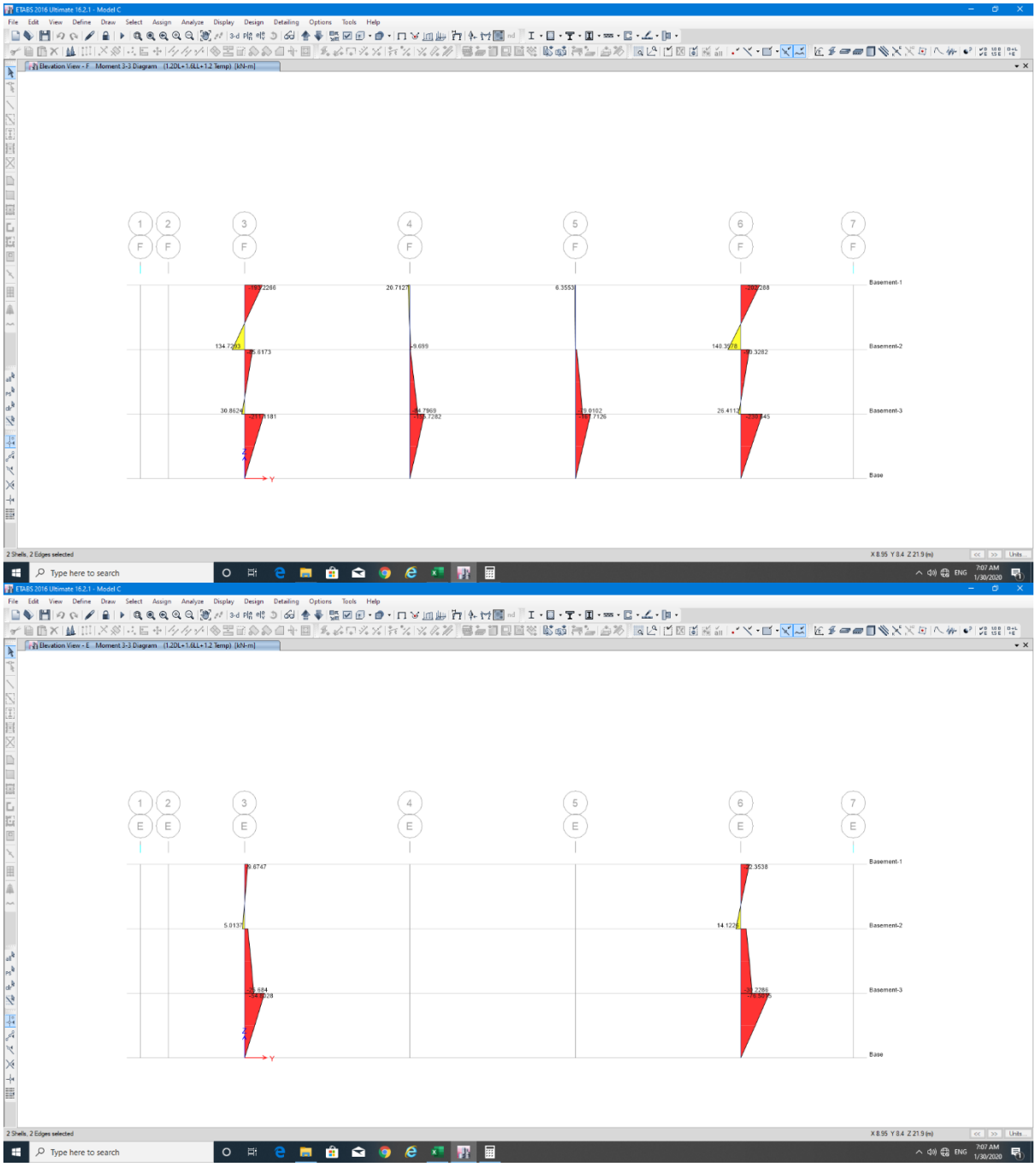
ETABS 2016 Ultimate 16.2.1 - Model C
Elevation View - F Moment 3-3 Diagram (1.2DL+1.6LL+1.2 Temp) [kN-m]
1 2 3 4 5 6 7
F F F F F F F
Basement-1
Basement-2
Basement-3
Base
2 Shells, 2 Edges selected
Type here to search

ETABS 2016 Ultimate 16.2.1 - Model C
Elevation View - E Moment 3-3 Diagram (1.2DL+1.6LL+1.2 Temp) [kN-m]
1 2 3 4 5 6 7
E E E E E E E
Basement-1
Basement-2
Basement-3
Base
2 Shells, 2 Edges selected
Type here to search

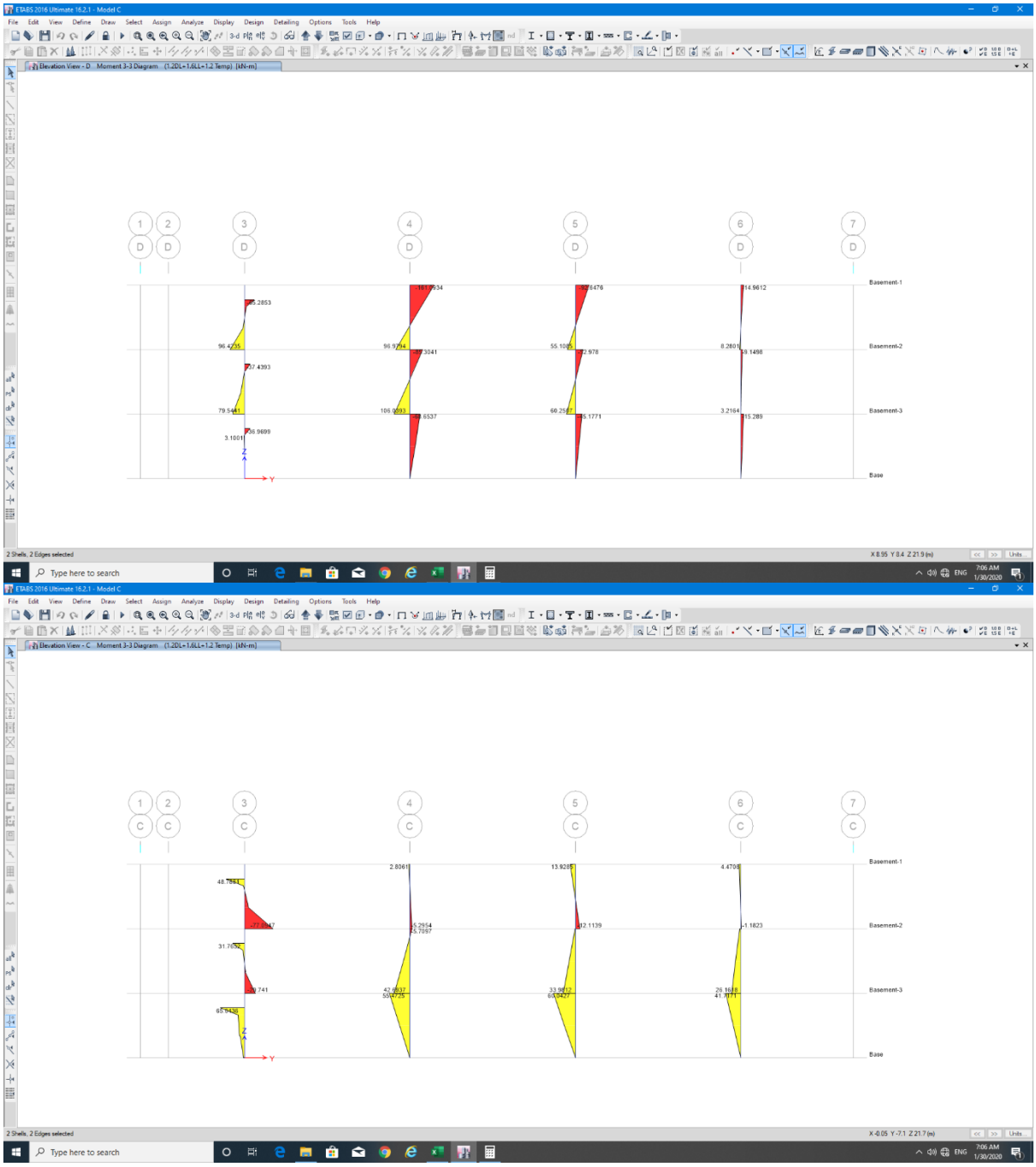
ETABS 2016 Ultimate 16.2.1 - Model C
Elevation View - D Moment 3-3 Diagram (1.2DL+1.6LL+1.2 Temp) [kN-m]
1 2 3 4 5 6 7
D D D D D D D
Basement-1
Basement-2
Basement-3
Base
2 Shells, 2 Edges selected
Type here to search
7:06 AM
1/30/2020
ETABS 2016 Ultimate 16.2.1 - Model C
Elevation View - C Moment 3-3 Diagram (1.2DL+1.6LL+1.2 Temp) [kN-m]
1 2 3 4 5 6 7
C C C C C C C
Basement-1
Basement-2
Basement-3
Base
2 Shells, 2 Edges selected
Type here to search
7:06 AM
1/30/2020

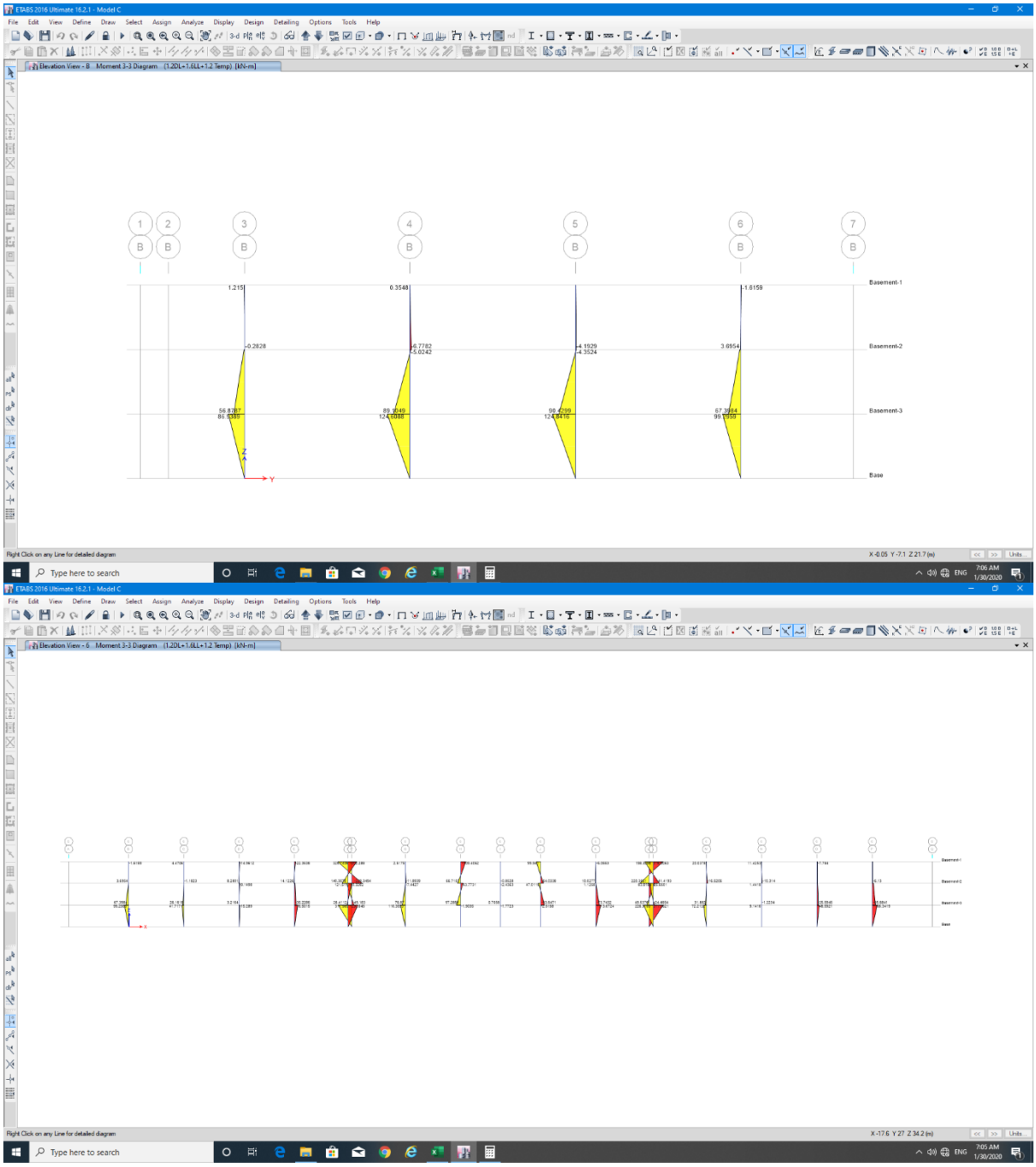
ETABS 2016 Ultimate 16.2.1 - Model C
Elevation View - B Moment 3-3 Diagram (1.2DL+1.6LL+1.2 Temp) [kN-m]
1 2 3 4 5 6 7
B B B B B B B
Basement-1
Basement-2
Basement-3
Base
Right Click on any Line for detailed diagram
Type here to search
7:06 AM
1/30/2020

ETABS 2016 Ultimate 16.2.1 - Model C
Elevation View - 6 Moment 3-3 Diagram (1.2DL+1.6LL+1.2 Temp) [kN-m]
Right Click on any Line for detailed diagram
Type here to search
7:05 AM
1/30/2020

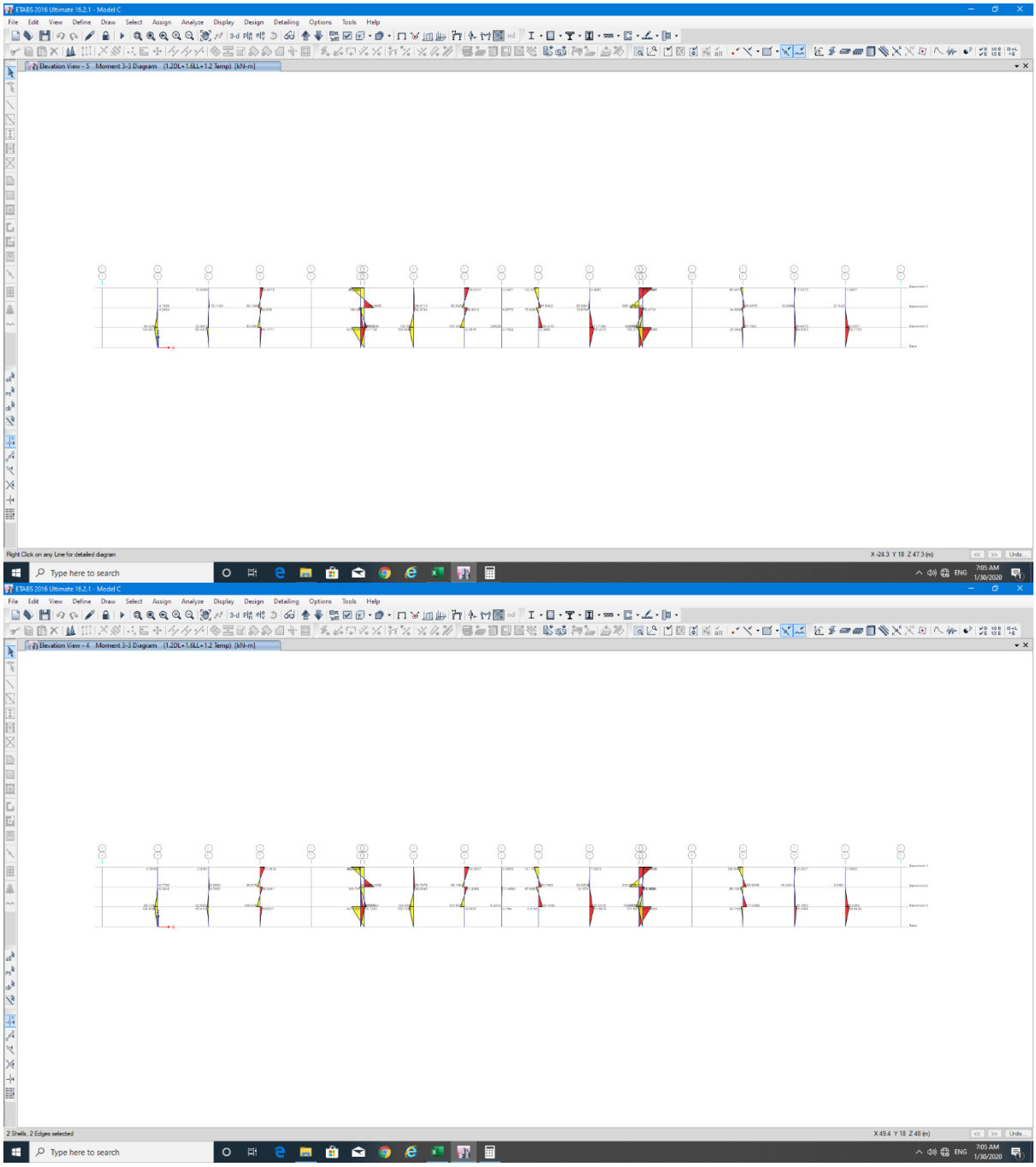
ETABS 2016 Ultimate 16.2.1 - Model C
Elevation View - 5 Moment 3-3 Diagram (1.2DL+1.6LL+1.2 Temp) [kN-m]
Right Click on any Line for detailed diagram
Type here to search
ETABS 2016 Ultimate 16.2.1 - Model C
Elevation View - 4 Moment 3-3 Diagram (1.2DL+1.6LL+1.2 Temp) [kN-m]
2 Shells, 2 Edges selected
Type here to search

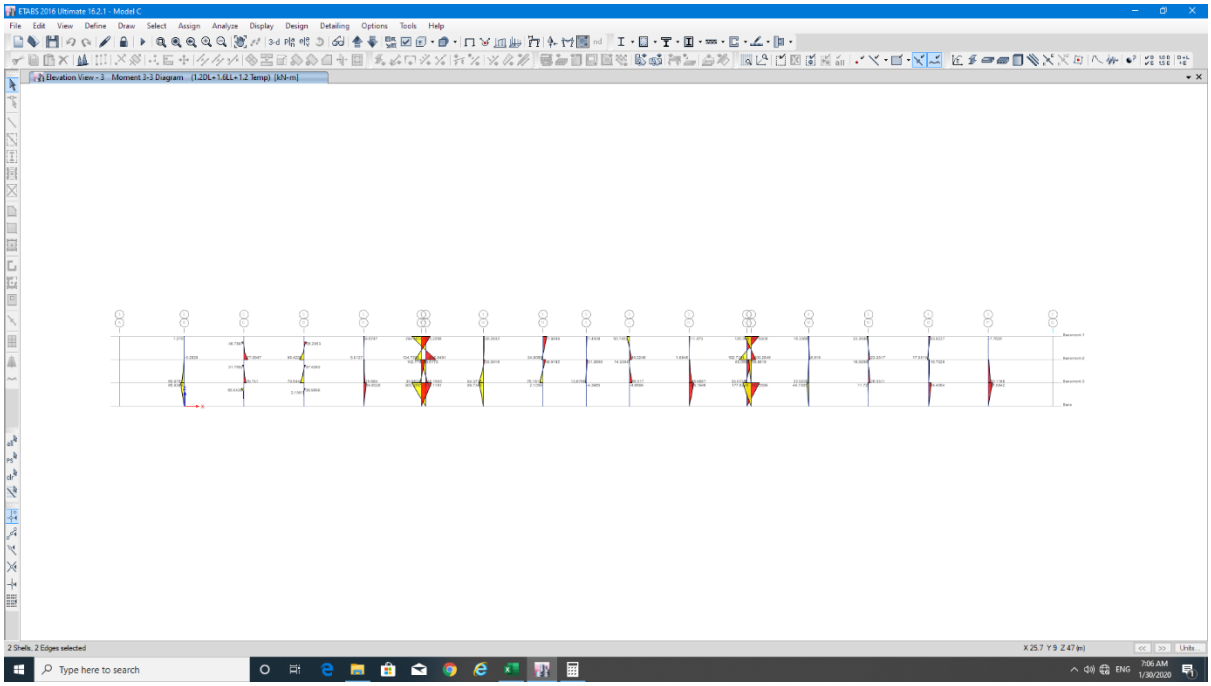

D-3-3 Slabs Forces

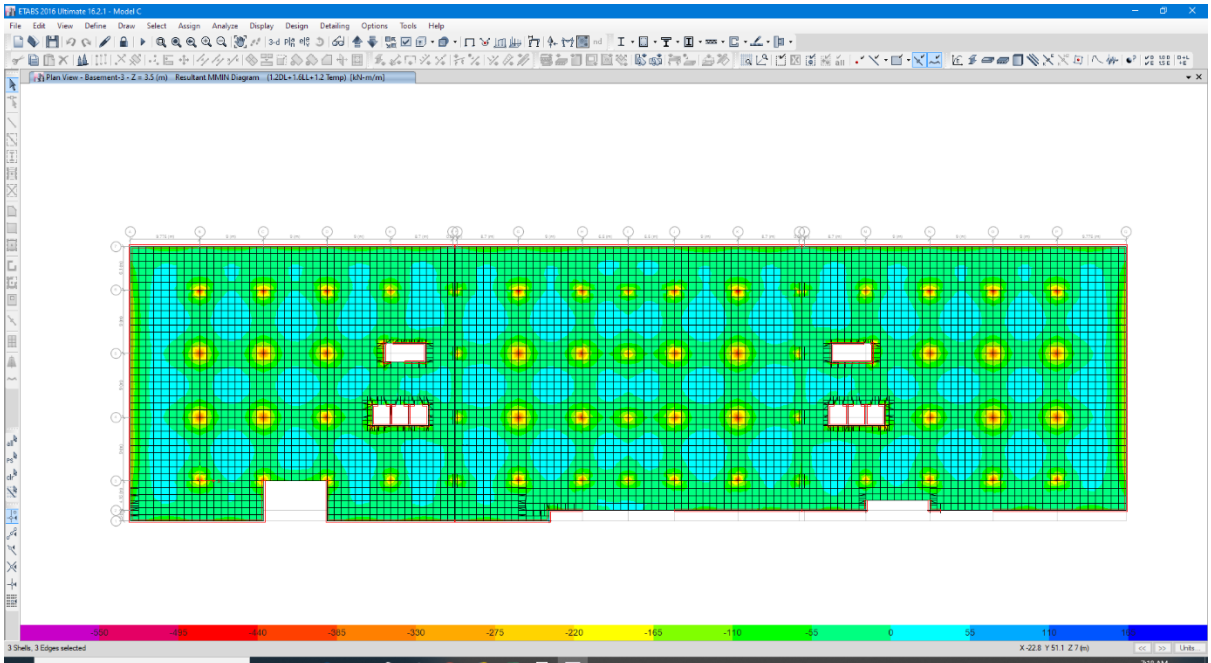
ETABS 2016 Ultimate 16.2.1 - Model C
Plan View - Basement-3 - Z = 3.5 (m) Resultant MMIN Diagram (1.2DL+1.6LL+1.2 Temp) [kN-m/m]
-550 -495 -440 -385 -330 -275 -220 -165 -110 -55 0 55 110 165
3 Shells, 3 Edges selected
X -22.8 Y 51.1 Z 7 (m)
Type here to search
7:18 AM
1/30/2020

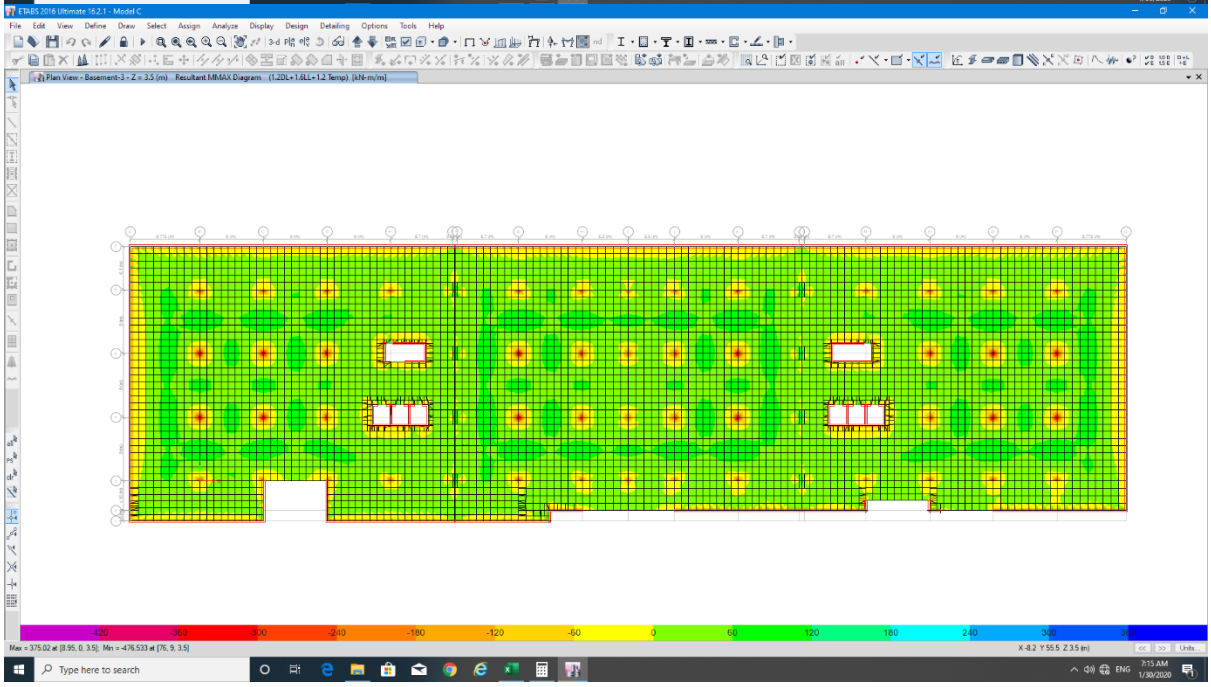
ETABS 2016 Ultimate 16.2.1 - Model C
Plan View - Basement-3 - Z = 3.5 (m) Resultant MMAX Diagram (1.2DL+1.6LL+1.2 Temp) [kN-m/m]
-420 -360 -300 -240 -180 -120 -60 0 60 120 180 240 300
Max = 375.02 at [8.95, 0, 3.5]; Min = -476.533 at [76, 9, 3.5]
X -8.2 Y 55.5 Z 3.5 (m)
Type here to search
7:15 AM
1/30/2020

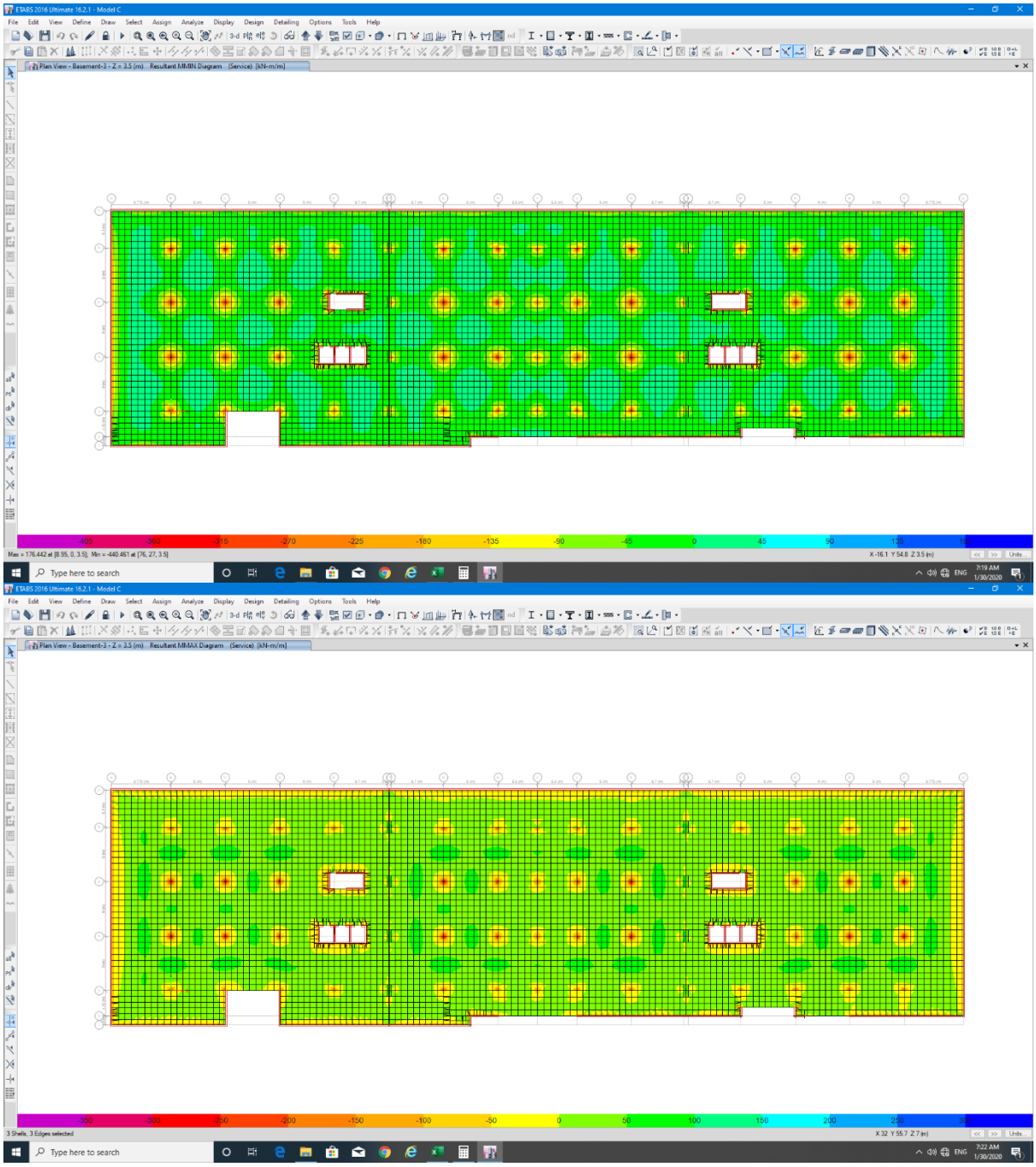
ETABS 2016 Ultimate 16.2.1 - Model C
Plan View - Basement-3 - Z = 3.5 (m) Resultant MMIN Diagram (Service) (kN-m/m)
-405 -360 -315 -270 -225 -180 -135 -90 -45 0 45 90 135 180
Type here to search
7:19 AM
1/30/2020
ETABS 2016 Ultimate 16.2.1 - Model C
Plan View - Basement-3 - Z = 3.5 (m) Resultant MMAX Diagram (Service) (kN-m/m)
-350 -300 -250 -200 -150 -100 -50 0 50 100 150 200 250 300
3 Shells, 3 Edges selected
Type here to search
7:22 AM
1/30/2020

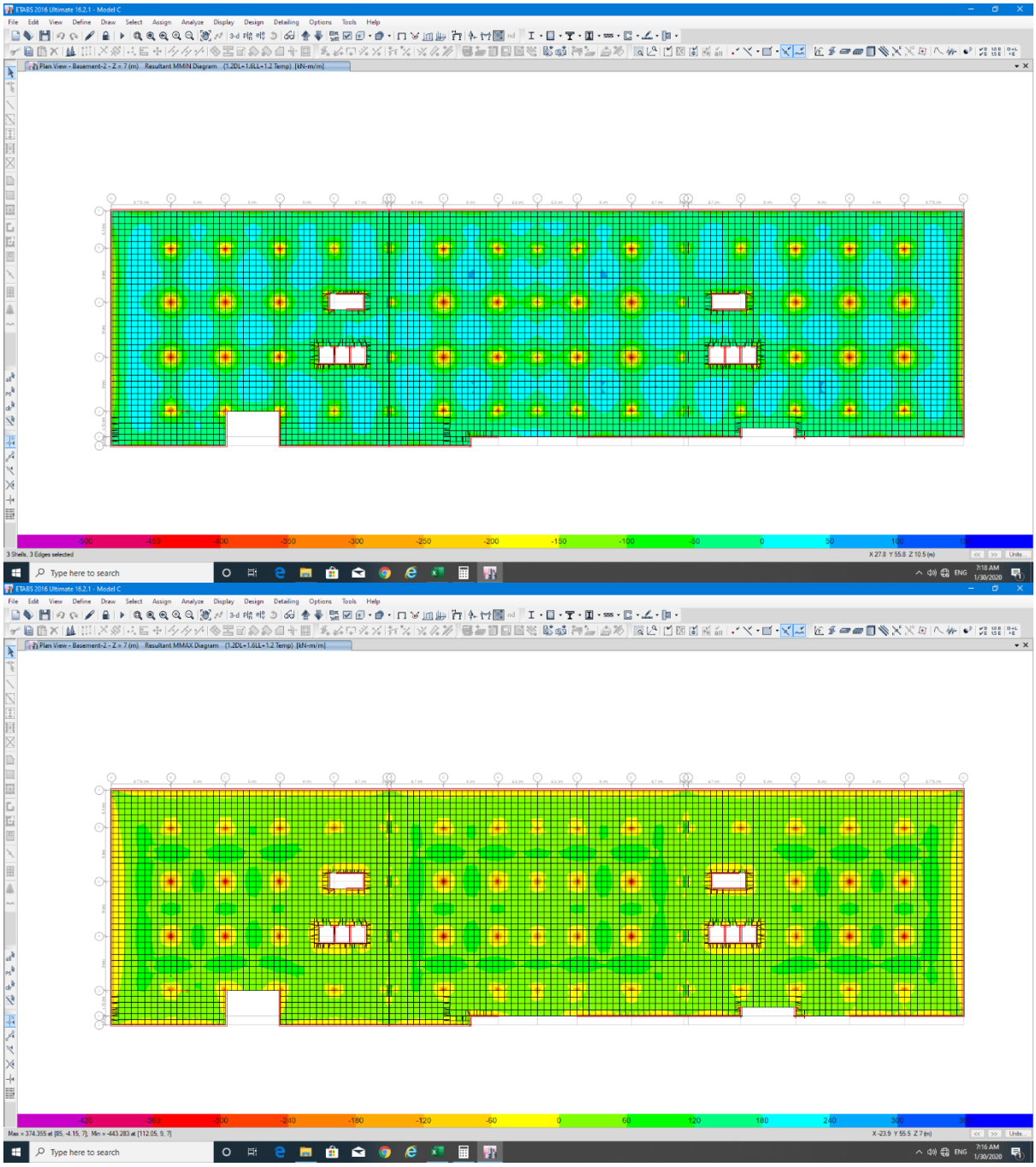
ETABS 2016 Ultimate 16.2.1 - Model C
Plan View - Basement-2 - Z = 7 (m) Resultant MMIN Diagram (1.2DL+1.6LL+1.2 Temp) [kN-m/m]
-500 -450 -400 -350 -300 -250 -200 -150 -100 -50 0 50 100 150
3 Shells, 3 Edges selected
X 27.8 Y 55.8 Z 10.5 (m)
Type here to search
7:18 AM
1/30/2020

ETABS 2016 Ultimate 16.2.1 - Model C
Plan View - Basement-2 - Z = 7 (m) Resultant MMAX Diagram (1.2DL+1.6LL+1.2 Temp) [kN-m/m]
-420 -360 -300 -240 -180 -120 -60 0 60 120 180 240 300 360
Max = 374.355 at [85, -4.15, 7]; Min = -443.283 at [112.05, 9, 7]
X -23.9 Y 55.5 Z 7 (m)
Type here to search
7:16 AM
1/30/2020

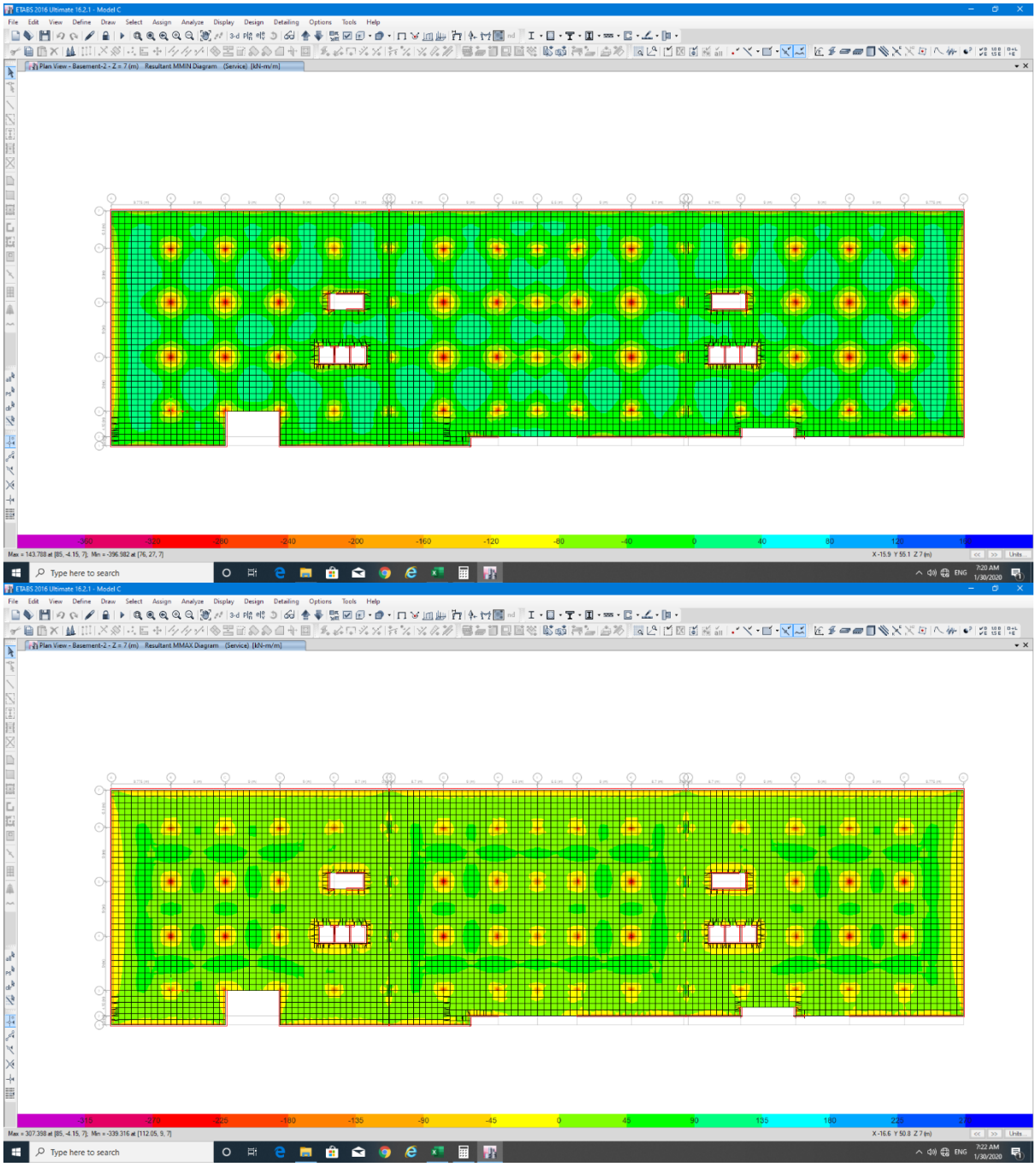
ETABS 2016 Ultimate 16.2.1 - Model C
Plan View - Basement-2 - Z = 7 (m) Resultant MMIN Diagram (Service) [kN-m/m]
Plan View - Basement-2 - Z = 7 (m) Resultant MMAX Diagram (Service) [kN-m/m]
Type here to search

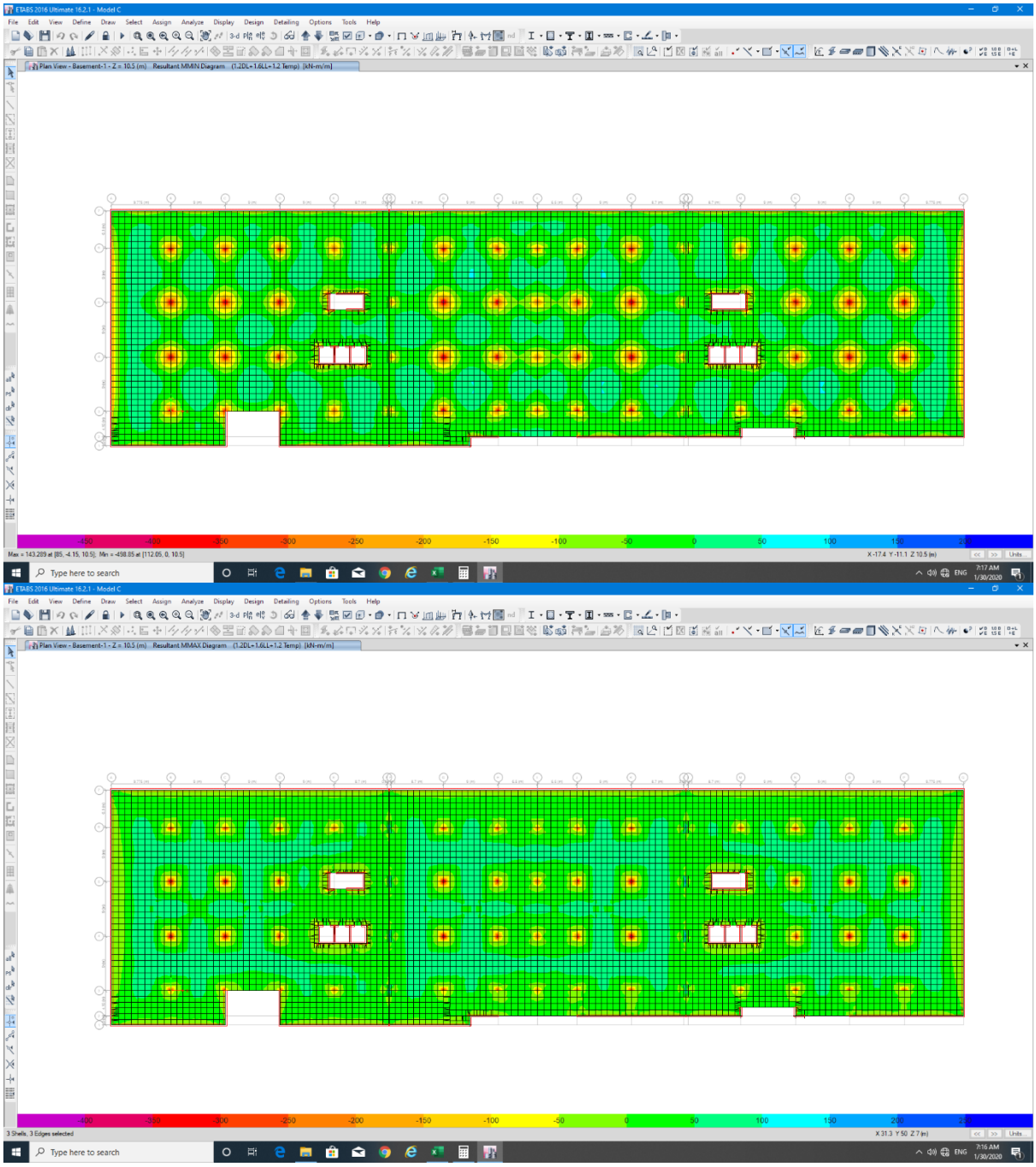
ETABS 2016 Ultimate 16.2.1 - Model C
Plan View - Basement-1 - Z = 10.5 (m) Resultant MMIN Diagram (1.2DL+1.6LL+1.2 Temp) (kN-m/m)
-450 -400 -350 -300 -250 -200 -150 -100 -50 0 50 100 150 200
Type here to search
7:17 AM
1/30/2020
ETABS 2016 Ultimate 16.2.1 - Model C
Plan View - Basement-1 - Z = 10.5 (m) Resultant MMAX Diagram (1.2DL+1.6LL+1.2 Temp) (kN-m/m)
-400 -350 -300 -250 -200 -150 -100 -50 0 50 100 150 200 250
Type here to search
7:16 AM
1/30/2020

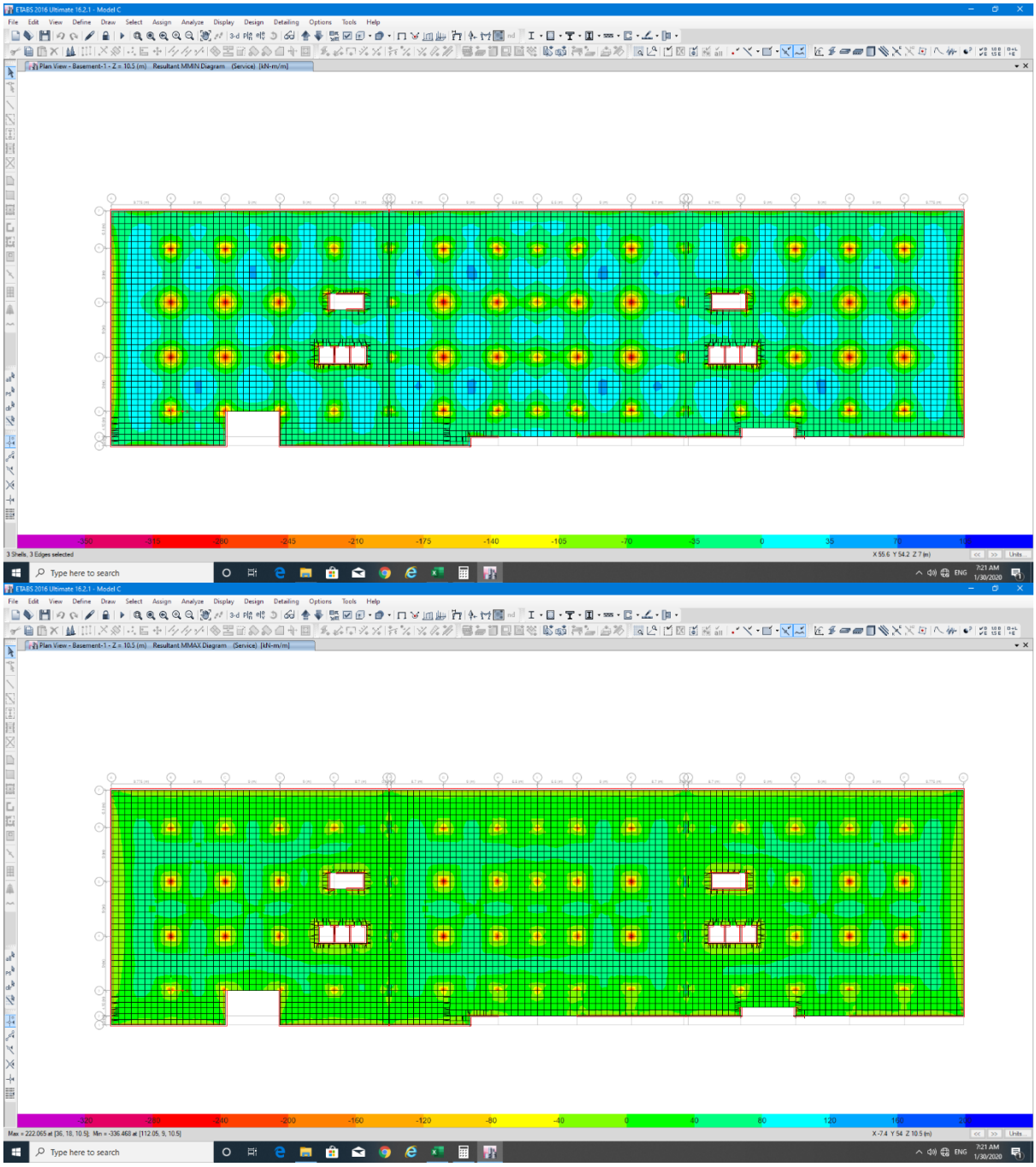

D-3-4 Walls Forces

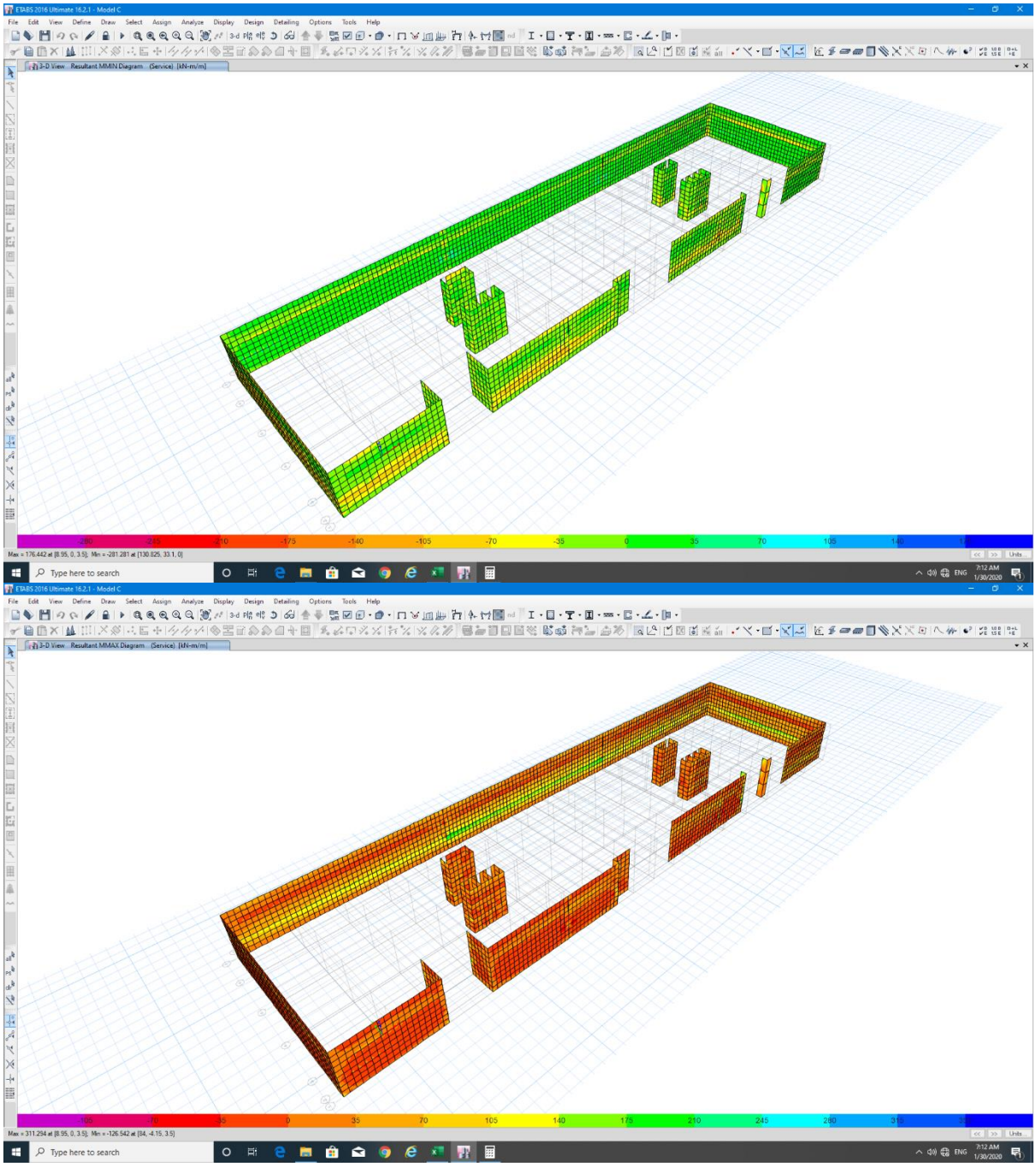
ETABS 2016 Ultimate 16.2.1 - Model C
3-D View Resultant MMIN Diagram (Service) [kN-m/m]
Type here to search

ETABS 2016 Ultimate 16.2.1 - Model C
3-D View Resultant MMAX Diagram (Service) [kN-m/m]
Type here to search

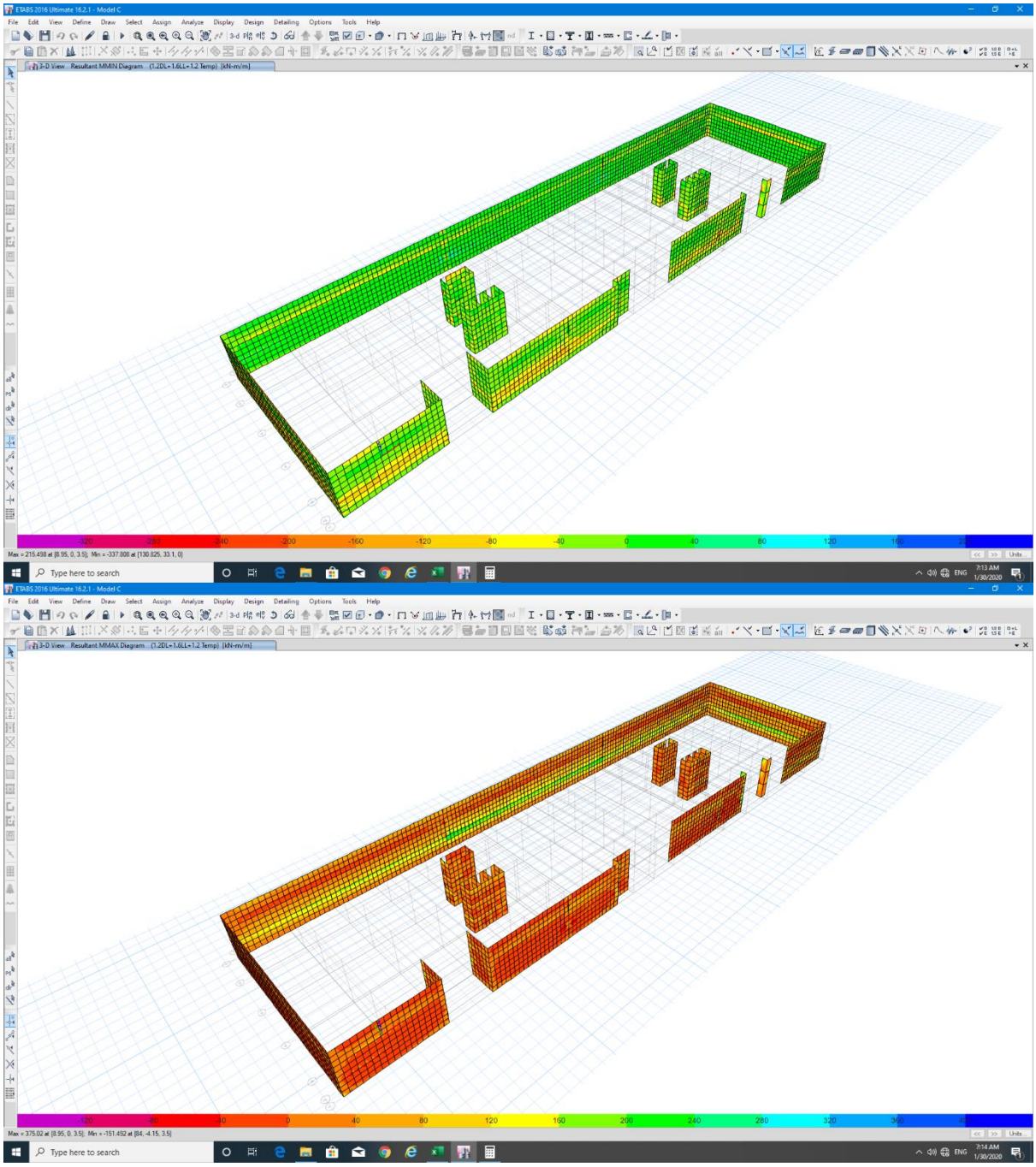
ETABS 2016 Ultimate 16.2.1 - Model C
3-D View Resultant MMIN Diagram (1.2DL+1.6LL+1.2 Temp) [kN-m/m]
-320 -280 -240 -200 -160 -120 -80 -40 0 40 80 120 160 200
Max = 215.458 at [8.95, 0, 3.5]; Min = -337.808 at [130.825, 33.1, 0]
Units
Type here to search
ENG
7:13 AM
1/30/2020

ETABS 2016 Ultimate 16.2.1 - Model C
3-D View Resultant MMAX Diagram (1.2DL+1.6LL+1.2 Temp) [kN-m/m]
-120 -80 -40 0 40 80 120 160 200 240 280 320 360 400
Max = 375.02 at [8.95, 0, 3.5]; Min = -151.452 at [84, -4.15, 3.5]
Units
Type here to search
ENG
7:14 AM
1/30/2020